SPACE SYSTEMS

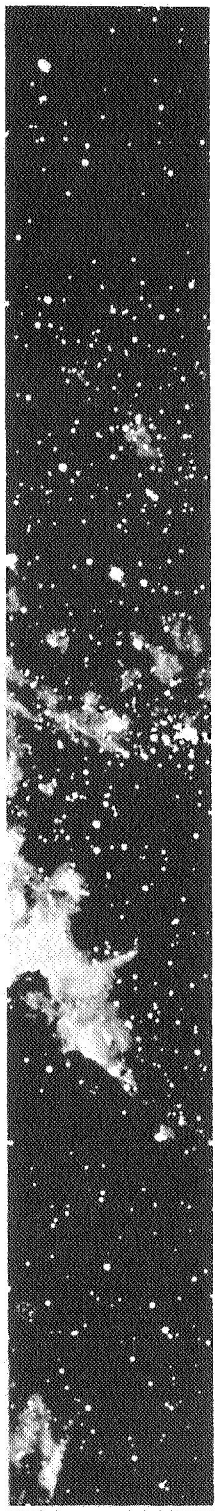

FEASIBILITY STUDY

30 WATTS PER POUND ROLL-UP SOLAR ARRAY

FINAL REPORT

Prepared For
Jet Propulsion Laboratory
California Institute of Technology

GENERAL ELECTRIC

REPORT NO. 68SD4301
21 JUNE 1968

FEASIBILITY STUDY

30 WATTS PER POUND ROLL-UP SOLAR ARRAY

FINAL REPORT

PREPARED FOR

JET PROPULSION LABORATORY
CALIFORNIA INSTITUTE OF TECHNOLOGY
4800 OAK GROVE DRIVE
PASADENA, CALIFORNIA

PREPARED UNDER
CONTRACT NO. 951970
CONTRACTING OFFICER C.E. PRICE
PROJECT MANAGER W.A. HASBACH

PREPARED BY:

N.F. SHEPARD
F.A. BLAKE
W.S. BUSCH
A. LATOUR
R.J. KYLE
P.J. DEMARTINO
D.N. MATTEO
W.C. YOUNG
R.C. FERGUSON

APPROVED BY:

K L Hanson

K.L. HANSON,
PROGRAM MANAGER

This work was performed for the Jet Propulsion Laboratory, California Institute of Technology, as sponsored by the National Aeronautics and Space Administration under Contract NAS 7-100.

GENERAL ELECTRIC

MISSILE AND SPACE DIVISION
Valley Forge Space Technology Center
P. O. Box 8555 • Philadelphia, Penna. 19101

ABSTRACT

This report summarizes the preliminary design and analysis of a 250-square-foot roll-up solar array which has a power-to-weight ratio of 32.3 watts per pound and which meets the specified requirements. The selected array configuration is presented, along with a complete description of each component within the system. The supporting design analysis and tradeoff studies are presented. A model was fabricated to demonstrate the deployability of the flight design. This model is described in detail.

TABLE OF CONTENTS

TABLE OF CONTENTS (CONT'D)

SECTION 1

INTRODUCTION

This document contains a detailed summary of the work performed under JPL Contract 951970, "Feasibility Study - 30 Watts Per Pound Roll-up Solar Array." The objective of the program was to perform a preliminary design and analysis of a 250-square-foot deployable (roll-up) solar cell array panel which shall have a specific power capability of 30 watts per pound or greater and shall be capable of meeting the environmental requirements of JPL Specification No. SS501407 Revision A (Reference 1-1). These requirements are summarized in Table 1-1. The array panel design shall utilize materials and technologies presently in existence or which can be developed to production use within 1 year after completion of this effort.

There shall be four solar array panels, each 250-ft^2, mounted on a vehicle configuration shown in Figure 1-1. The design of all four panels is identical.

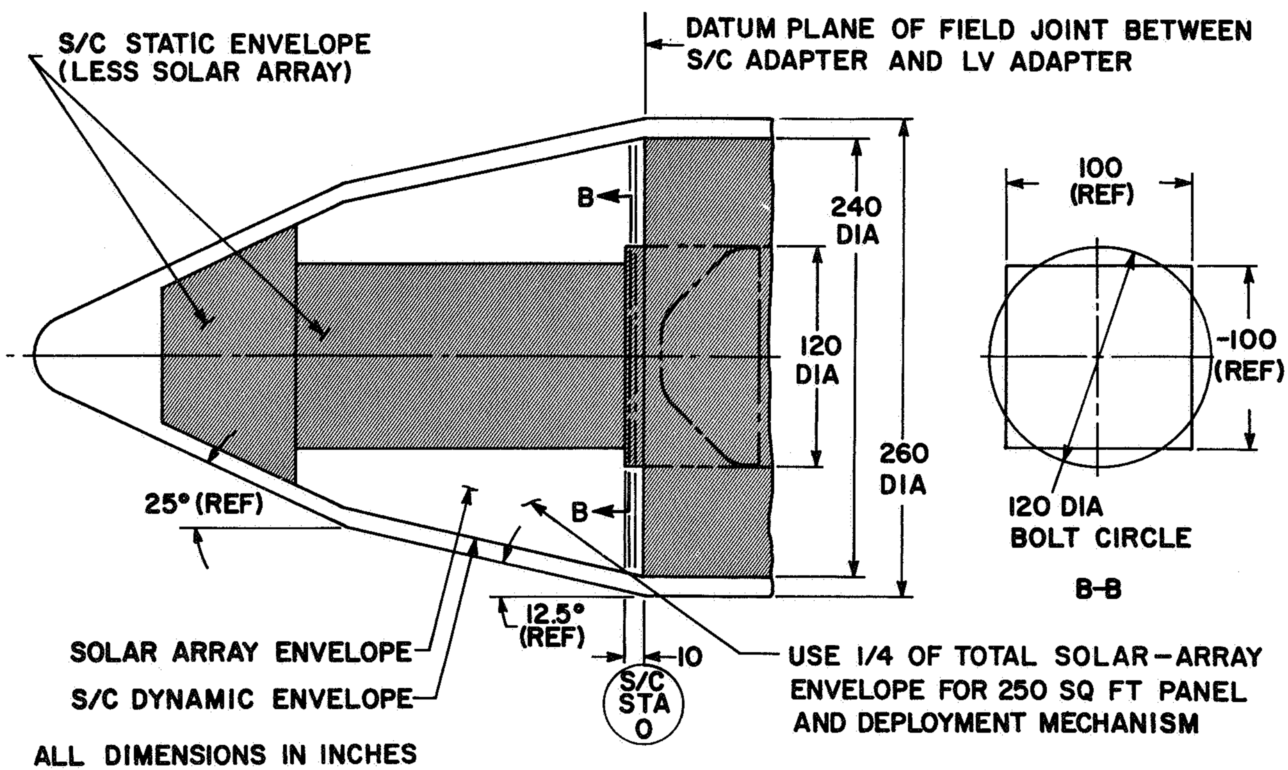

Figure 1-1. Nose Fairing and Spacecraft Envelope

Table 1-1. Summary of Environmental Requirements

- VIBRATION

SINE	0-200 Hz, 4 g(0-P), 2 OCT/MIN
RANDOM	0.1g^2/Hz, 200-600 Hz, ROLLOFF 6db/OCT, 3 MINUTES

- ACOUSTIC NOISE

  SPL = 146db OVERALL

- ACCELERATION

  +13g OR -4g LONGITUDINAL AXIS
  6 g LATERAL AXIS

- THERMAL SHOCK

  -100 TO +75°C, 30°C/MIN

- MATERIALS SELECTION CRITERIA

  95% RH AT 30°C FOR 50 HRS

  -20° TO +60°C, 150 THERMAL CYCLES

  -195° TO +140°C, 10^{-7} TORR, 10 THERMAL CYCLES

- SOLAR INTENSITY

  140 TO 260 mw/cm^2

- RADIATION DOSE

  10^7 RADS

- DEPLOYED STEP ACCELERATION

  2×10^{-5} RAD/SEC^2 PITCH ANGLE ACCELERATION,

  13 SEC TO 5 MINUTE DURATION

The power capability of the array is based on cells having an efficiency such that an electrical output of 10 watts/square foot will be achieved at air mass zero, $55^{o}C$ and 1.0 A.U. The cells to be used in the design are 0.008 inch thick, N/P protected by a 0.003-inch-thick microsheet cover glass.

In the deployed configuration, under steady-state conditions, the solar array panel shall have sufficient rigidity, so that by controlling the attitude of the spacecraft, the array can be oriented and maintained in a plane normal to the direction of the sun within ± 10 degrees. The first mode resonant frequency of the entire deployed array shall be greater than 0.04 Hz to prevent deleterious coupling with the spacecraft guidance system.

The initial tasks of this program consisted of studies of candidate arrangements and deployment concepts to sufficient depth that a basis for the selection of the system configuration was established. These system tasks were supported by two additional detailed studies, one involving deployment boom and deployment mechanism preliminary design and the other involving conversion of empirical solar cell data into forms required by the general array I-V curve computer program. These tasks were essentially completed during the first quarter.

The second major segment of the program involved the preliminary detailed design of the components making up the 30 watts per pound roll-up solar array panel. Design tradeoff studies and analyses were completed. Component specifications for the solar panel actuator (deployable boom) and the slip ring assembly were prepared.

The third phase of the program was centered around the Engineering Demonstration Model (EDM). The EDM, a contract end item, was designed and fabricated to demonstrate the deployability of the selected flight configuration. Deployment tests were performed utilizing this model. As a related activity, thermal cycling tests were conducted to verify the proposed interconnection.

This report has been organized to present a clear picture of the program results. It has been subdivided as follows:

Section 1 Introduction. An introduction to the overall program, including requirements and a chronological description of the program events.

Section 2 Summary. A summary description of the selected design, the resulting power-to-weight ratio, and a tabulation of the significant program accomplishments.

Section 3 Description of Selected System. A detailed description of the selected flight solar array configuration, including a complete description of each major component.

Section 4 Performance Analysis. A summary of all performance analyses which were performed to substantiate the selected design, including: (1) dynamics, (2) structural, (3) electrical, and (4) weight.

Section 5 Tradeoff Studies. A description of the significant tradeoff studies which were conducted to arrive at the selected configuration.

Section 6 Engineering Demonstration Model. A description of the design, fabrication, and testing of this model.

Section 7 Related Studies and Activities. A summary of various activities which were performed in support of the design, including: (1) thermal cycling tests, (2) lubrication and materials studies, and (3) GSE preliminary design.

SECTION 2
SUMMARY

The selected array design shown in Figure 2-1 deploys 250 square feet of solar cell module area with an extended length of 33.5-feet. The first mode natural frequency is maintained above 0.04 Hz by tension in the array substrate. One 1.34-inch diameter BI-STEM actuator is the only electromechanical device required to deploy or retract the array. The array blankets are mounted with a total of 55,176 2-by-2-cm, 8-mil, N/P, 2-ohm-cm solar cells. The power generated by these cells is transferred from the movable storage drums to the stationary support structure through a slip ring assembly housed in each drum. The calculated power available at the spacecraft interface (accounting for solar cell losses, bus strip I^2R losses, and slip ring losses) is 2469 watts at 55°C, 10 degrees solar angle of incidence, 1.0 A.U., and beginning-of-life. The total system weight of 76.4 pounds is made possible by the use of beryllium for the storage drums and the leading edge member. The resulting power-to-weight ratio is 32.3 watts per pound. No extensions of the existing state of the art are required to implement this design.

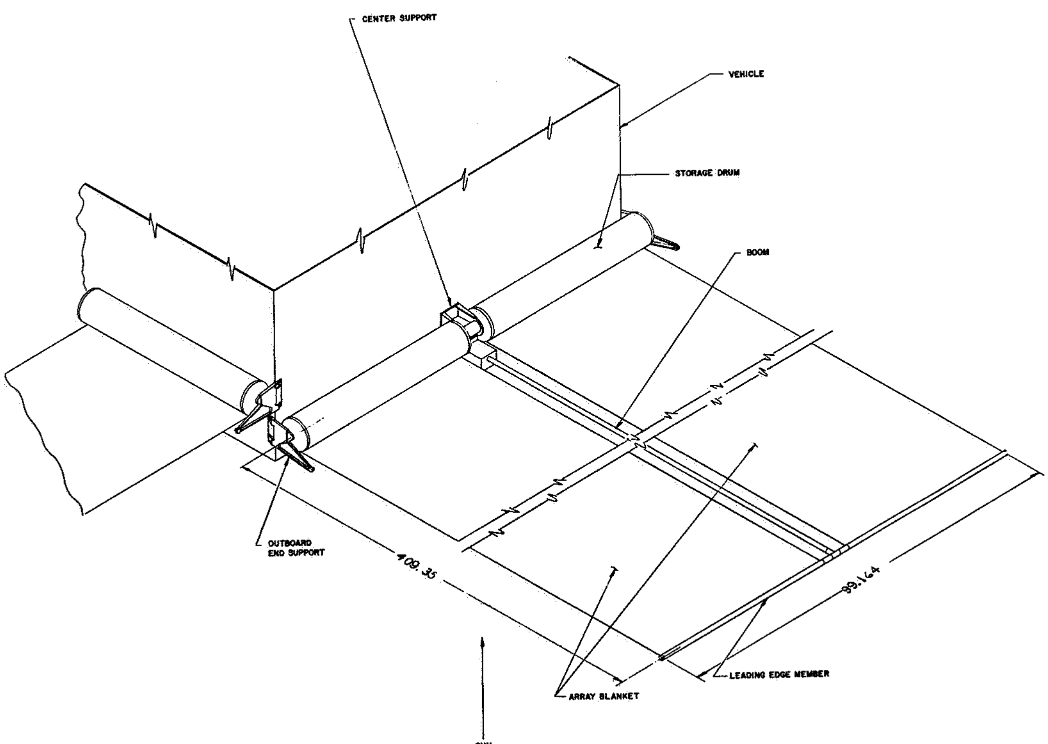

Figure 2-1. Selected Roll-up Array Configuration

An Engineering Demonstration Model (EDM) was designed and fabricated to demonstrate the deployability of the selected flight array design (see Figure 2-2). This model is capable of being deployed/retracted vertically upward, unaided, to a height of 25-feet. To enable the full extension of 33.5-feet, it is necessary to provide a counterbalancing deployment aid at the tip of the array.

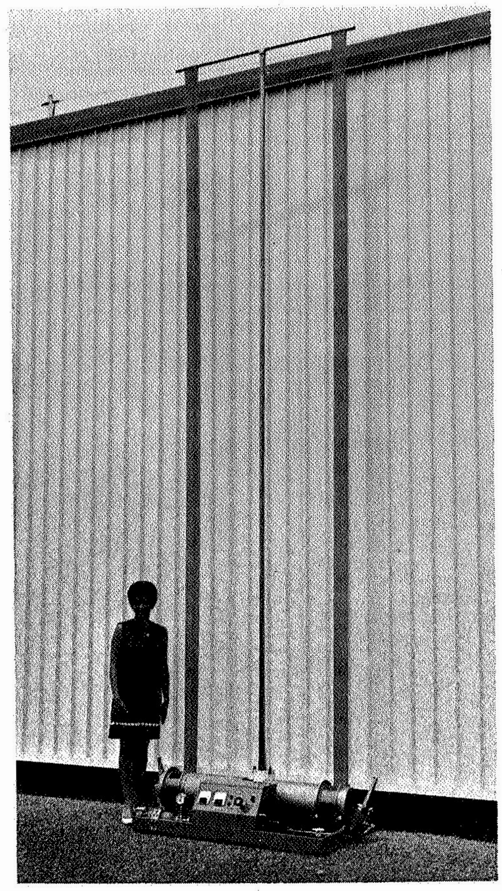

Figure 2-2. EDM Deployed 16 Feet

Thermal cycling tests were conducted on two-types of solar cell interconnections: (1) photoetched beryllium-copper and (2) silver expanded metal. The photoetched interconnection generated considerable cell cracking at the feet on the "N" contact when cycled 100 times between -200°F and +200°F*. The silver expanded metal interconnection has successfully passed this same test, but problems were encountered when the temperature range was extended from -250°F to +200°F.

*The thermal shock test specified in Reference 1-1 is between the extremes of -100°C (-148°F) and 75°C (167°F).

SECTION 3

DESCRIPTION OF SELECTED SYSTEM

3.1 GENERAL DESCRIPTION OF SELECTED SYSTEM

THE CONFIGURATION OF THE SOLAR ARRAY PANEL, ESTABLISHED ON THE BASIS OF TRADE STUDIES TO MINIMIZE WEIGHT, FEATURES:

A. TWO SUBPANELS AND THEIR ASSOCIATED STORAGE DRUMS

B. A SINGLE SOLAR PANEL DEPLOYMENT ACTUATOR

C. SOLAR PANEL NATURAL FREQUENCY REQUIREMENT (I.E., STRUCTURAL STIFFNESS) IS PROVIDED BY TENSION IN THE ARRAY SUBSTRATE.

D. A SINGLE POINT ATTACHMENT TO THE VEHICLE IN THE DEPLOYED STATE

E. MULTIPOINT ATTACHMENT TO THE VEHICLE IN THE STOWED STATE

F. BERYLLIUM STRUCTURAL ELEMENTS

G. SLIP RINGS TO TRANSFER THE ELECTRICAL POWER ACROSS THE INTERFACE BETWEEN FIXED AND MOVING PARTS

H. THE USE OF AN "OFF-THE-SHELF" ACTUATOR (DEPLOYABLE BOOM)

I. AN ARRAY MAXIMUM POWER VOLTAGE OF 102 VOLTS AT 1.0 AU AND 55°C

The solar array panel consists of the following major components:

a. Array blanket (2)

b. Storage drum (2)

c. Leading edge member

d. Outboard end support (2)

e. Center support

f. Solar panel actuator

The array blanket is attached to and rolled up on the storage drum in the stowed state (see Figure 3-1, sheet 1). Interlayer cushioning is provided by foamed RTV560 buttons which are deposited on the rear of the array blanket. The leading edge member is attached to the solar panel actuator (deployable boom) at the center, and the leading edge of each array blanket is attached to this tubular member on either side of the central boom attachment point. The attachment of the boom tip to the leading edge member is through the ball bearing joint which allows the boom to have torsional freedom as it is deployed.

Both storage drums are mounted to a center support structure through a shaft which is mounted to the center support (see Figure 3-1, sheet 2). This center support structure is the only attachment of the array to the vehicle in the deployed condition. Each storage drum is mounted to the shaft with a preloaded pair of ball bearings.* Thus, in the deployed condition, each drum is cantilevered from the center support structure.

In the stowed (launch) position, the outboard end of each drum is supported by an arm which is mounted to the vehicle structure. This outboard end support serves two additional functions: (1) that of preventing the drum from rotating about its own axis, and (2) that of supporting the outboard ends of the leading edge member. The array deployment sequence is initiated by firing electro-explosive devices which release each of the outboard end supports. These supports then swing clear of the drums and leading edge member. In addition to the end support, the leading edge member is resting in a cradle on either side of the boom attachment point. This arrangement relieves the launch loads from the retracted boom.

In order to maintain the first mode resonant frequency of the entire deployed array above 0.04 Hz, it is necessary to maintain a minimum preload of 2 pounds in each array blanket. This is accomplished by mounting a Neg'ator constant torque spring motor in each drum. Those springs are matched at final assembly to provide nearly equal forces on each blanket. The storage drum must rotate approximately 15 times to fully deploy the array. The array power is transferred from the movable drum to the stationary structure by slip rings which are housed in each drum.

---

*This method of support is used for the Nimbus solar array paddles. Bearings similar to the Nimbus design have been selected.

FOLDOUT FRAME 1

FOLDOUT FRAME 2

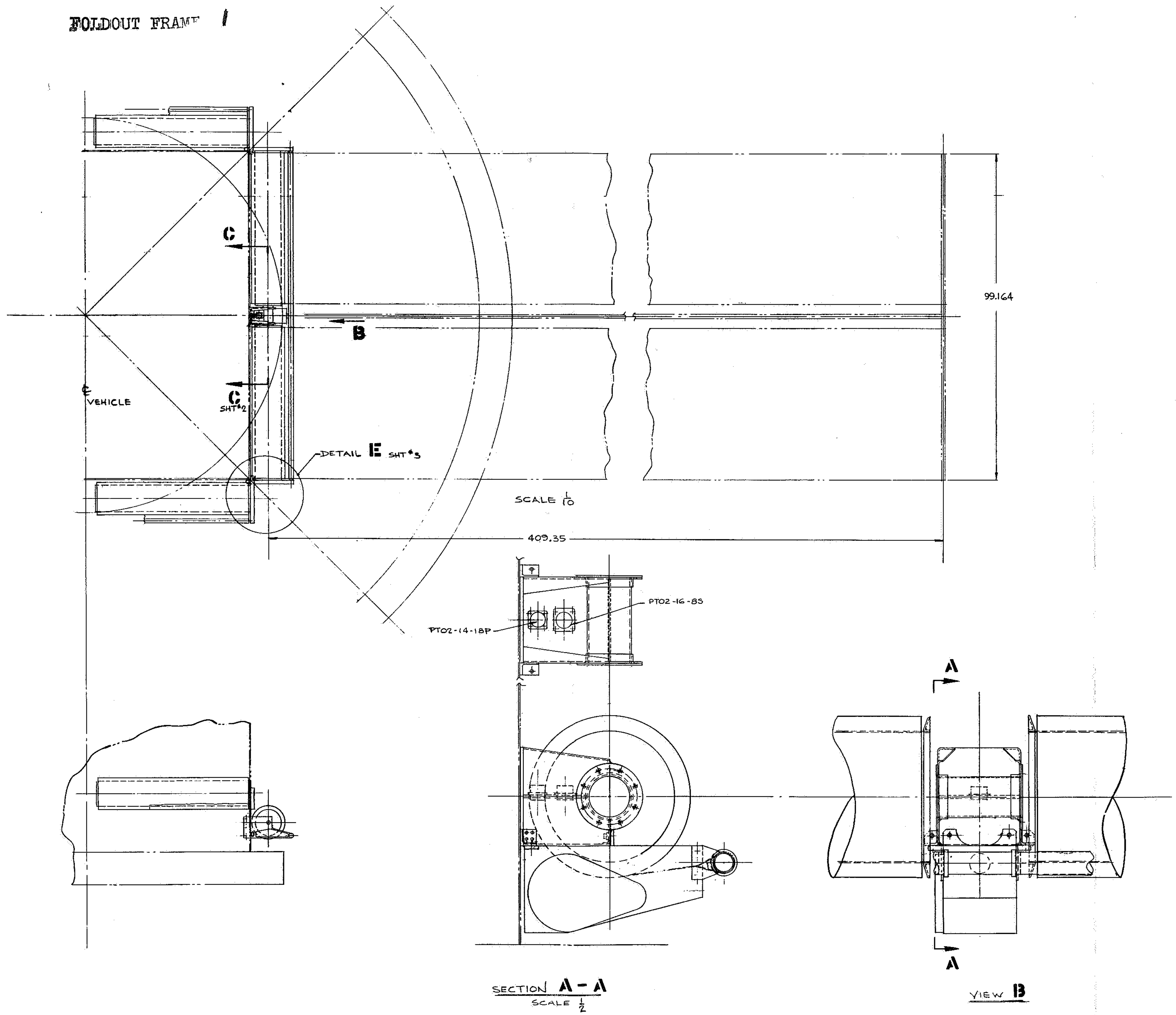

Figure 3-1. Roll-up Solar Array Configuration (Sheet 1 of 2)

FOLDOUT FRAME 1

FOLDOUT FRAME 2

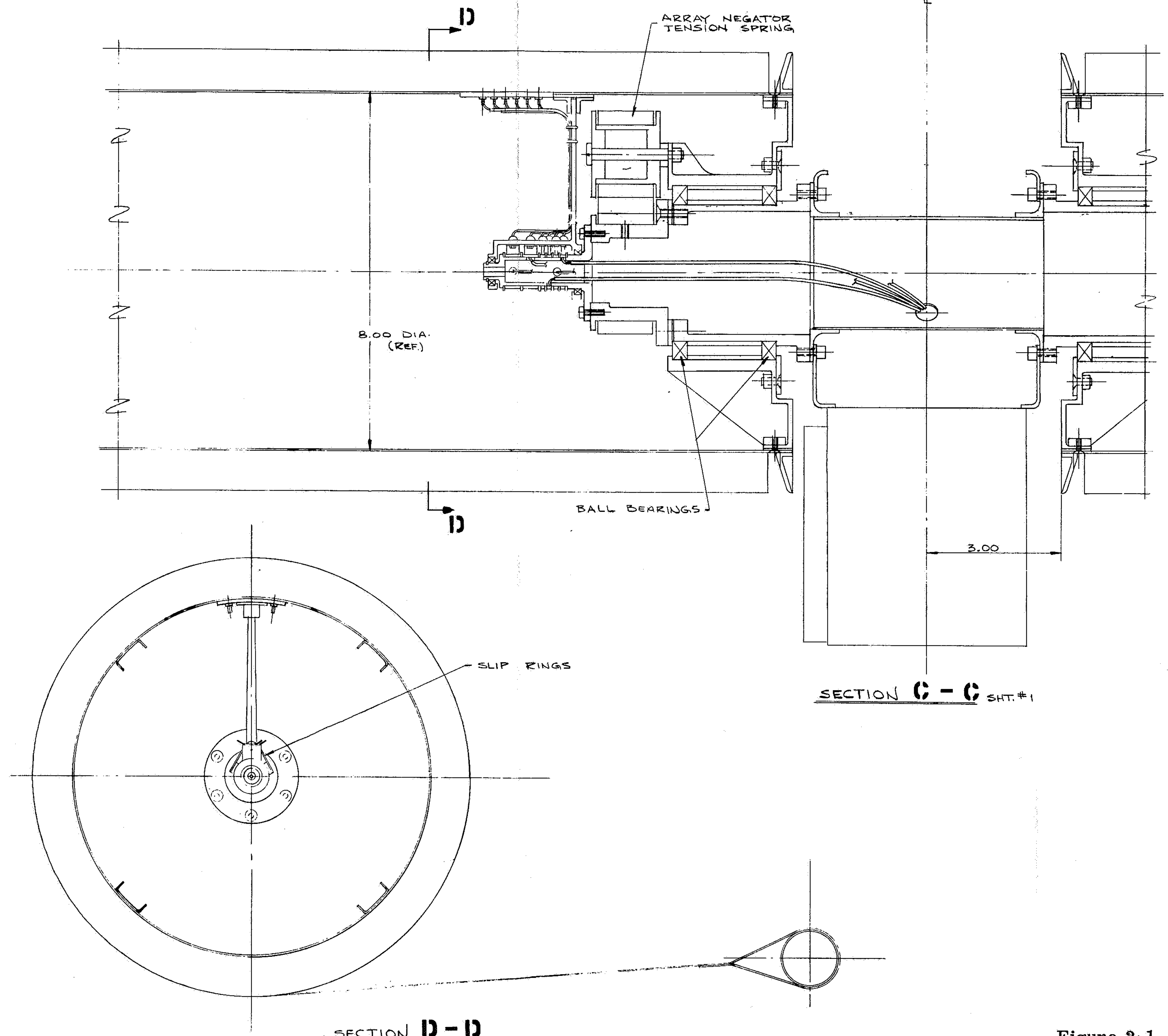

Figure 3-1. Roll-up Solar Array Configuration
(Sheet 2 of 2)

3.2 ARRAY BLANKET

THE ARRAY BLANKETS PRODUCE 2523 WATTS MAXIMUM POWER AT 1.00 A.U. AND 55°C AND WEIGH A TOTAL OF 42.0 POUNDS.

The array blanket assembly drawing is shown in Figure 3-2. Two array blanket assemblies are required for each array. A distance of 0.800 inch in the parallel direction and 0.818 inch in the series direction has been allowed for each 2-by-2-cm solar cell. The submodule is composed of 19 parallel connected solar cells, with an overall width of 15.19 inches. A string consists of 242 series-connected submodules. The basic building block within the string is a module consisting of 20 or 22 series-connected submodules. There are 12 modules per string, 11 with 20 series submodules and one with 22 series submodules. A spacing of 0.250 inch is allowed between modules. Therefore, the total length of a string is 200.35 inches. There are three adjacent strings in the parallel direction on each blanket, with 0.125 inches allowed between strings and at the edges. Therefore, the total width of each blanket is 46.06 inches. There are two adjacent strings in the series direction on each blanket, with 1.00 inch allowed between strings and 7.00 inches allowed at the outboard end as a leader. The total length of the deployed array is 409 inches (measured from the center line of the leading edge member to the center line of the drum.)

The I-V curve for the selected cell arrangement is shown in Figure 3-3 for earth's distance from the sun at a temperature of 55°C. The maximum power of 2523 watts occurs at an array voltage of 102 volts. The array utilizes 2-by-2 cm, 8-mil, 2-ohm-cm, bar contact, N/P cells. A total short-circuit current loss of 6 percent has been allowed for cover glass transmission (1.5 percent) and manufacturing and assembly (4.5 percent).

All bus strips which carry current to the drum are bonded to the rear side of the array blanket. This design minimizes the magnetic fields produced by the array, since the effects of current flow in a series string of solar cells is nullified by the same current flowing beneath the string on the rear side of the array in the reverse direction. In addition, opposite polarity bus strips run adjacent to each other on the rear side of the array blanket.

FOLDOUT FRAME 1

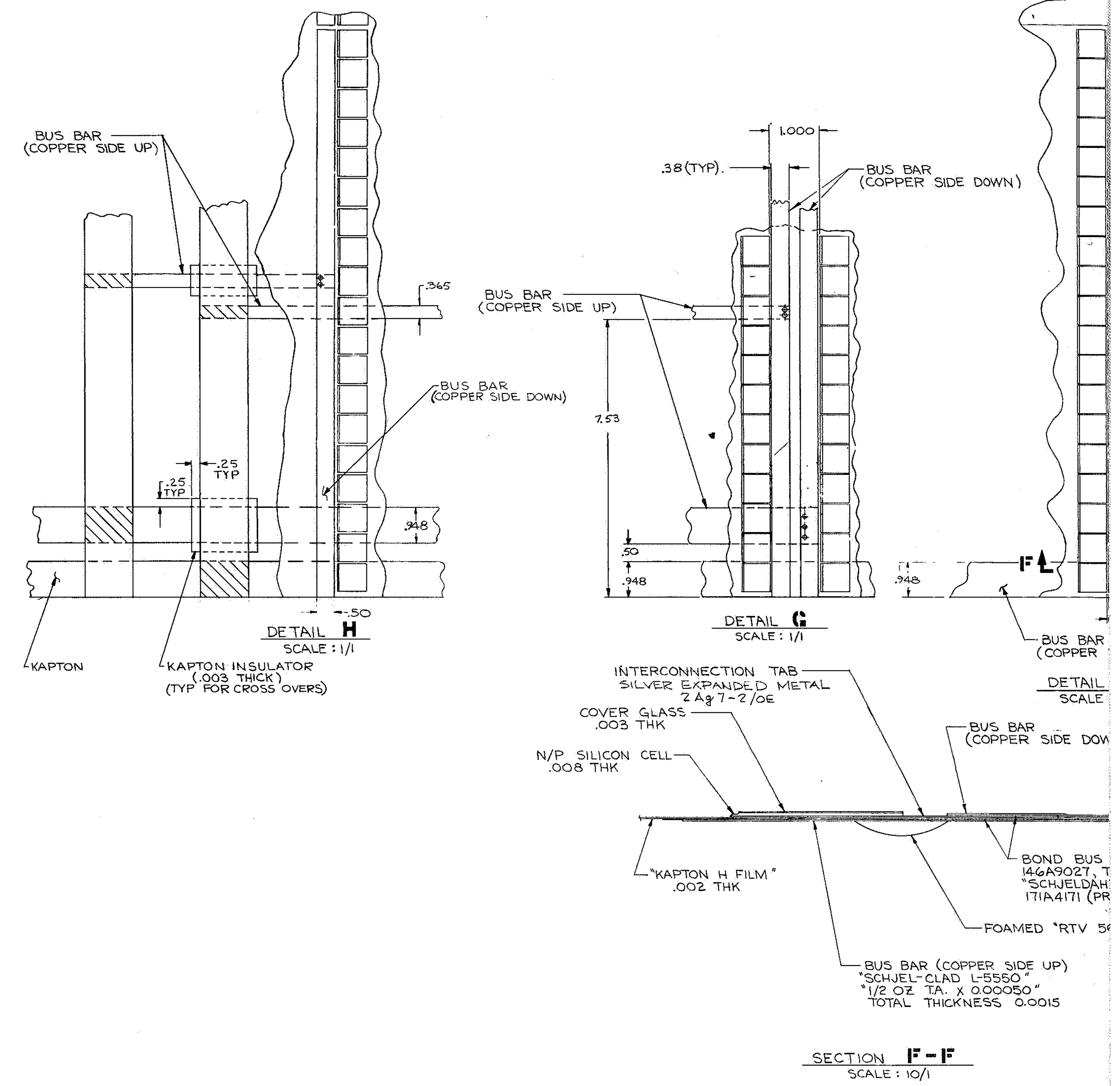

FOLDOUT FRAME 2

FOLDOUT FRAME 3

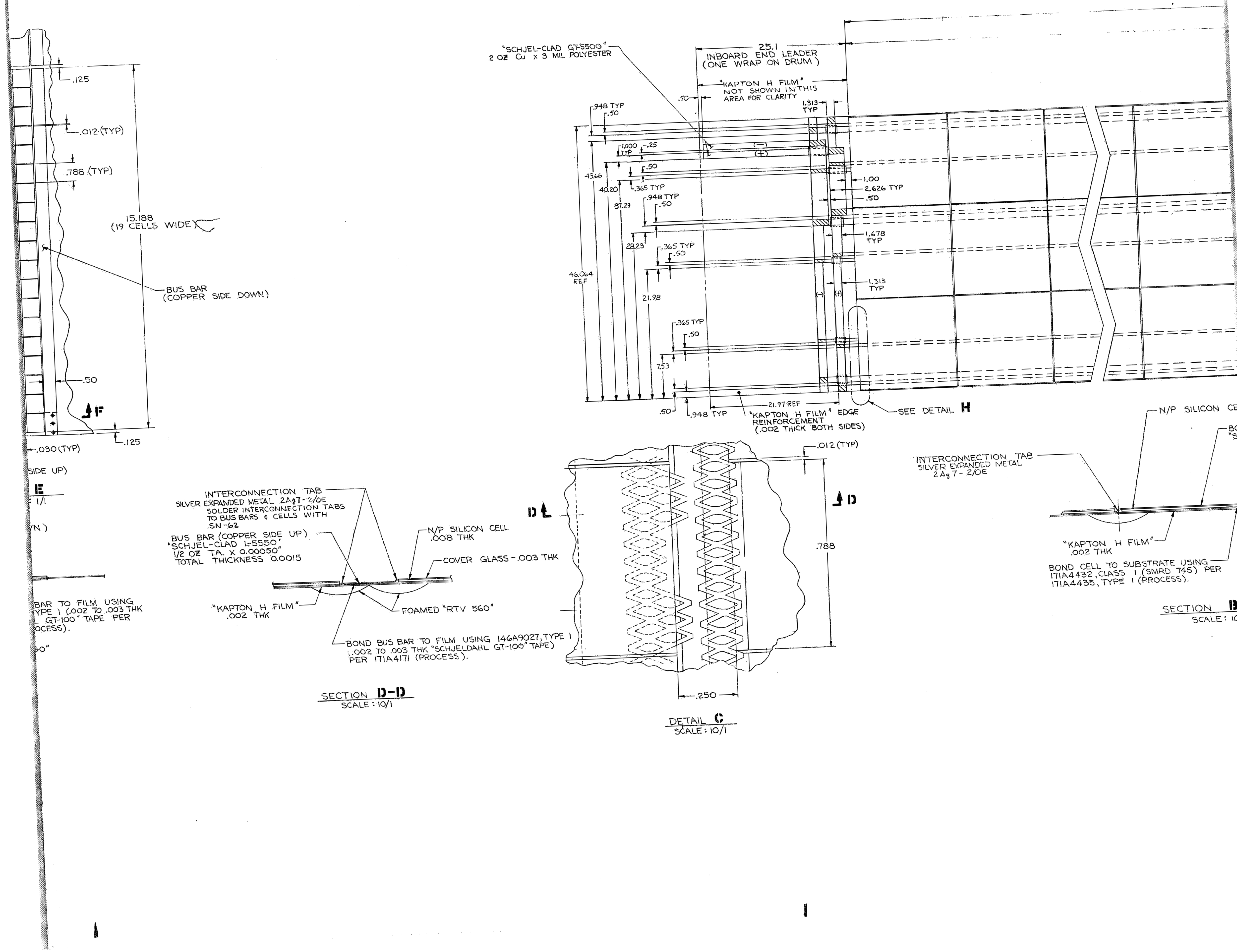

FOLDOUT FRAME 4

FOLDOUT FRAME 5

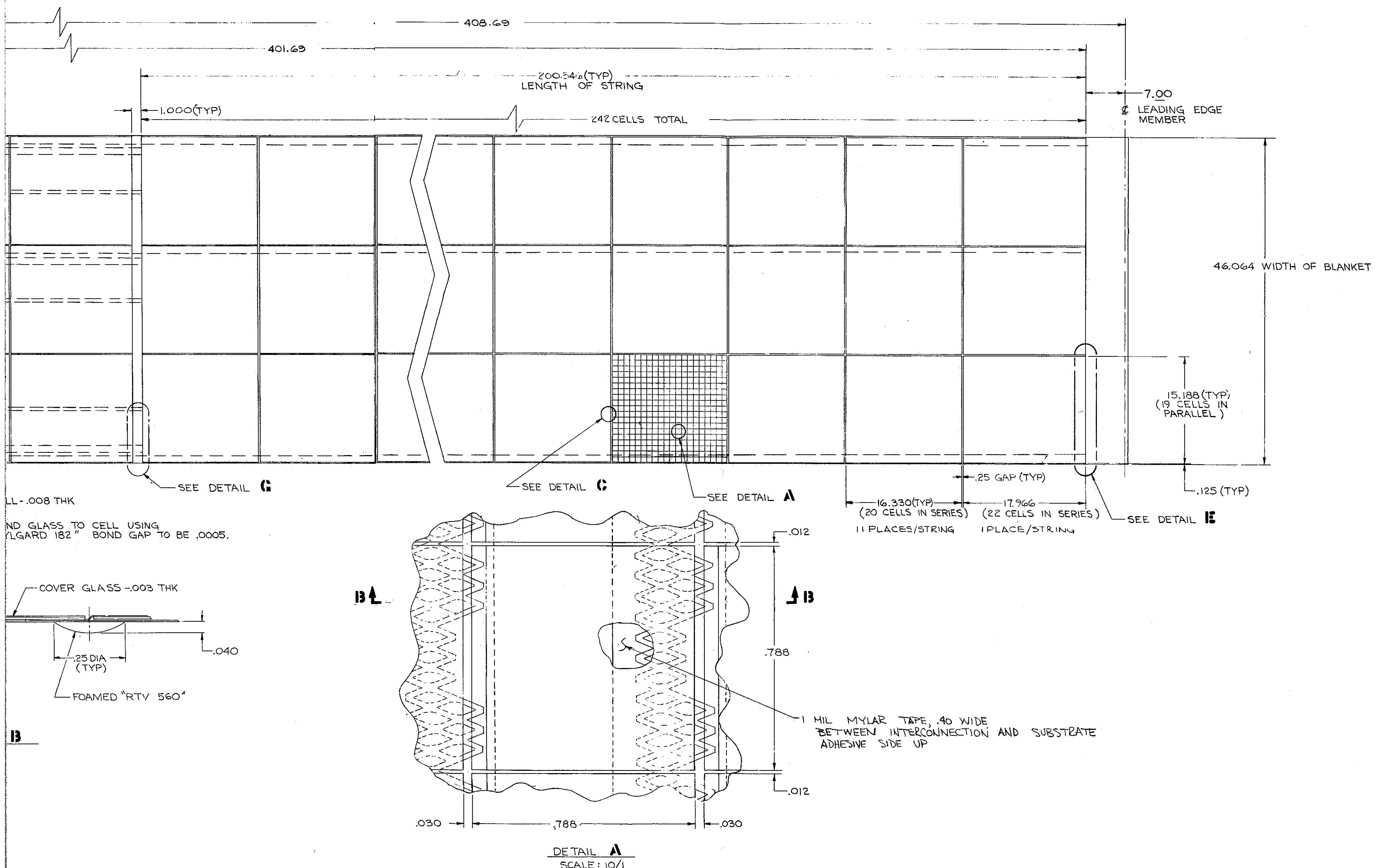

Figure 3-2. Array Blanket

The following is a description of some of the critical design areas of the array blanket assembly:

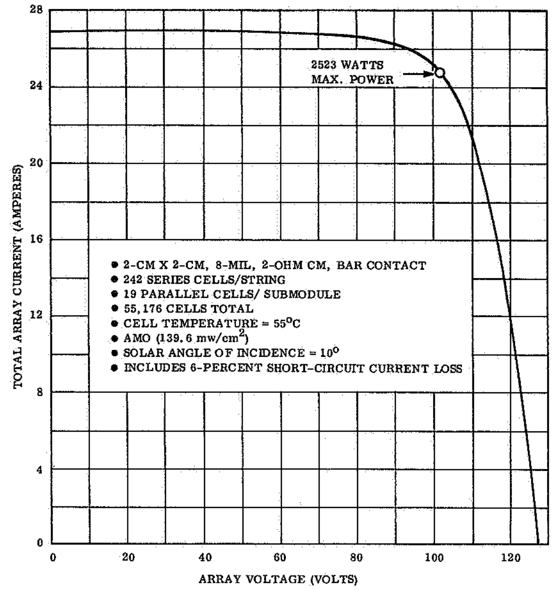

Figure 3-3. Array I-V Curve, 2-Ohm cm, 8-Mil

a. <u>Substrate Sheet - Dupont "Kapton" 0.002 inch Thick.</u> Kapton fulfills the requirements of a lightweight, (0.0148 lb/ft^2), high-strength (25,000 psi at 25°C to 17,000 psi at 200°C), temperature resistant (525°C cut through) film suitable for use as the array substrate and has demonstrated its suitability on previous engineering models built by General Electric. Its major drawback, low resistance to tear propagation (8 gm/mil), is circumvented by reinforcement of its edges by bus bars and by the reinforcement over the entire area of the cell-to-substrate bonds which limit the travel through which a puncture initiated tear could propagate. Clean-cut holes do not behave as initiated tears and may be used as needed for electrical interconnection between the cell face and the underside bus bars.

b. <u>Cell to Substrate Bond - General Electric SMRD745.</u> SMRD745 compound has been used in earlier models to perform both cell-to-Kapton and Kapton-to-Kapton bonds. Recent tests with this material bonding gold-plated copper tabs to Kapton have consistently reached or exceeded 98 psi in shear before a peeling was encountered. Stress in the Kapton at this load was 15,330 psi suggesting that yield of the base material was the probable initiator of separation.

c. <u>Bus Bars - Schjel Clad L5550.</u> This material is a lamination of 1/2 oz/ft^2 copper on 1/2-mil mylar. This material has been qualified on another program which involved physically cycling over a 1-inch radius while loaded at 8.9 lb/in. Under tensile loading, values of 98 and 115 lb/in. were carried. All of these loading conditions are well beyond the loads required for this design.

d. <u>Bus Bar-Kapton Bond - Schjeldahl GT 100.</u> GT 100 is one of the family of polyester resin thermoplastic adhesives. Recent tests have shown it to be capable of 9.8 lb/in.^{2} in shear and 3.7 lb/in. of linear edge before peeling. Although not as strong a bond as the SMRD745, it is more than adequate for the loading conditions, and is a good handling material due to practically instantaneous curing.

e. Interlayer Cushioning - Foamed RTV 560 Pads. Foamed buttons 0.250 inch in diameter by 0.040 inch thick were experimentally evaluated for their ability to provide sufficient radial and axial damping of vibration and acoustic test excitations with regard to prevention of cell of interconnection damage. This system, which adds only 0.0060 lb/ft^2 to the solar cell blanket, did provide adequate protection for the array tested (1 foot wide, 0.012-inch cells, 0.006-inch glass). It needs to be reevaluated for the lighter cells and glass as soon as possible.

f. Solar Cell Interconnections. Silver expanded metal (Exmet Corp. No. 2Ag7-2/OE) is used to fabricate the solar cell interconnection. This configuration has successfully passed 117 thermal cycles between -200 and +200°F.

A weight breakdown for the proposed array blanket is shown in Table 3-1, and a summary of the key design characteristics is shown in Table 3-2.

Table 3-1. Array Weight Breakdown

Item	Weight	
	Weight (lb)	Module Area (lb/ft^2)
Cover Glass*	7.91	0.0316
Cover Glass Adhesive	0.98	0.0039
Cells**	20.68	0.0827
Interconnections	2.04	0.0082
Interconnection Tape	0.87	0.0035
Solder	0.19	0.0008
Substrate Adhesive	2.00	0.0080
Substrate	4.14	0.0166
Buttons	1.50	0.0060
Bus Strip	1.20	0.0048
Bus Strip Adhesive	0.53	0.0021
	42.04	0.1682

*0.065 gm/cover glass
**0.17 gm/cell

Table 3-2. Array Design Characteristics

Number of Cells	55,176
Number of Parallel Cells/String	19
Number of Series Cells/String	242
Number of Parallel Strings/Array	12
Maximum Power Voltage @ +55°C	102 volts
Maximum Power @ +55°C (Includes 6% Short-circuit current loss)	2523 watts
Active Cell Area	226.03 ft^2
Gross Module Area	250.09 ft^2
Gross Array Area	261.67 ft^2

3.3 SOLAR PANEL ACTUATOR

THE SOLAR PANEL ACTUATOR (DEPLOYABLE BOOM) IS THE BI-STEM MANUFACTURED BY SPAR AEROSPACE PRODUCTS (FORMERLY deHAVILLAND AIRCRAFT)

The SPAR Aerospace BI-STEM is considered the best technical approach for the boom actuator. The 1.34-inch diameter was selected because it is an available design which is more than adequate for the orbital load requirements. As shown in Section 5.2, the use of the BI-STEM actuator results in the minimum weight system when compared to the 180-degree overlapped STEM and the interlocked rod.

Figure 3-4 is a photograph of a unit which is similar to the one proposed for the 30 Watt Per Pound Roll-up Solar Array. The outline drawing for the actuator which is proposed is shown in Figure 3-5. The unit will be equipped with an extension limit switch which stops the motor when the array has deployed to its full length. A retraction limit switch will stop the motor when the array has retracted to within approximately 1 foot of its initial launch stowed position.

The pertinent design characteristics for the BI-STEM actuator are shown in Table 3-3.

A component specification for the solar panel actuator has been prepared and is included as Appendix A of this report.

Table 3-3. BI-STEM Design Characteristics

Extended Boom Length	33.5 ft $\pm$ 2.0 in.
Boom Diameter	1.34 in. nominal
Boom Material	301 stainless steel (silver plated)
Boom Material Thickness	0.007 in.
Boom Material Width	4.000 in.
Motor Voltage	27 vdc
Current	0.5 amperes (approx)
Extension/Retraction Rate	2.2 in/sec (nominal)

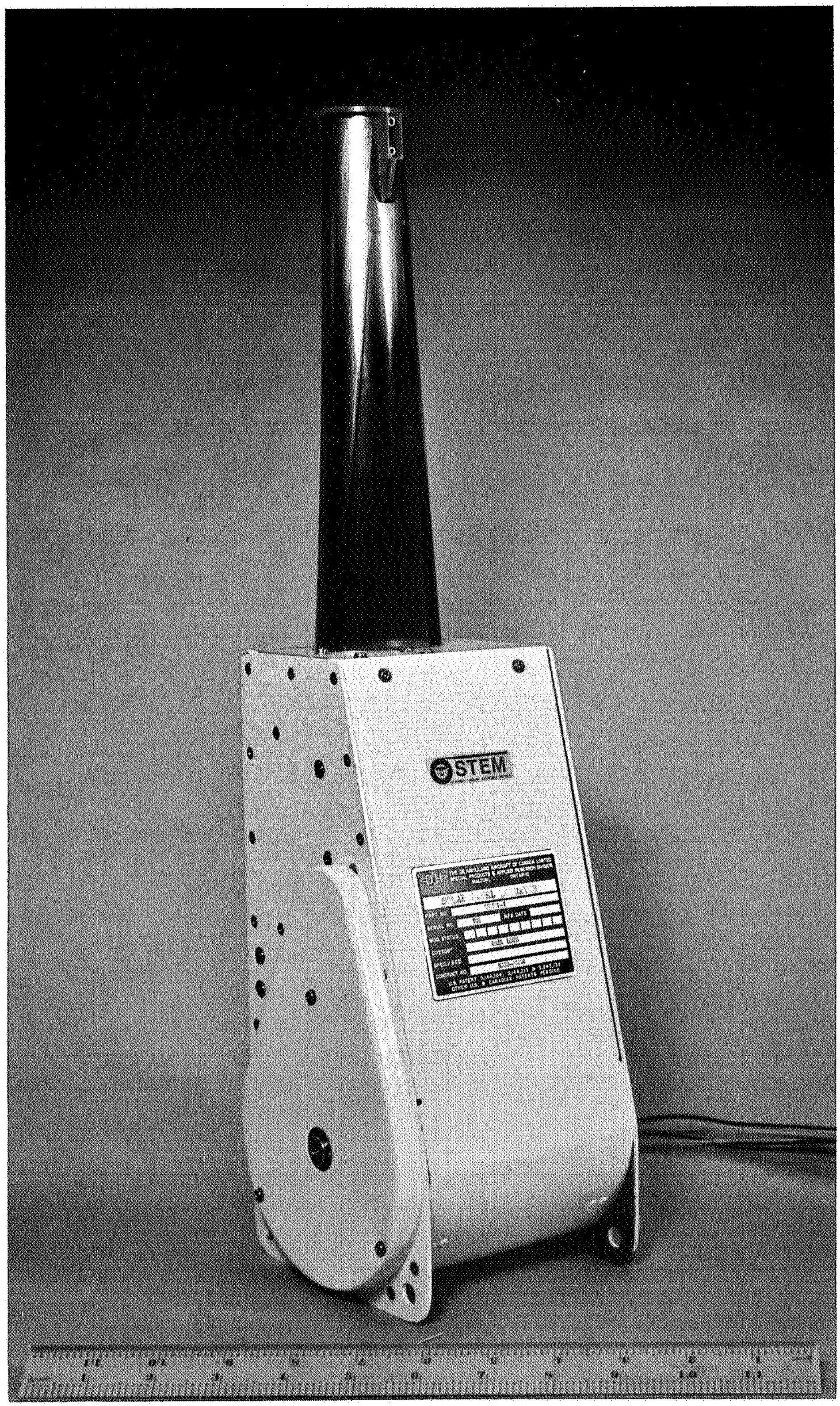

Figure 3-4. Photograph of a BI-STEM Actuator

FOLDOUT FRAME 1

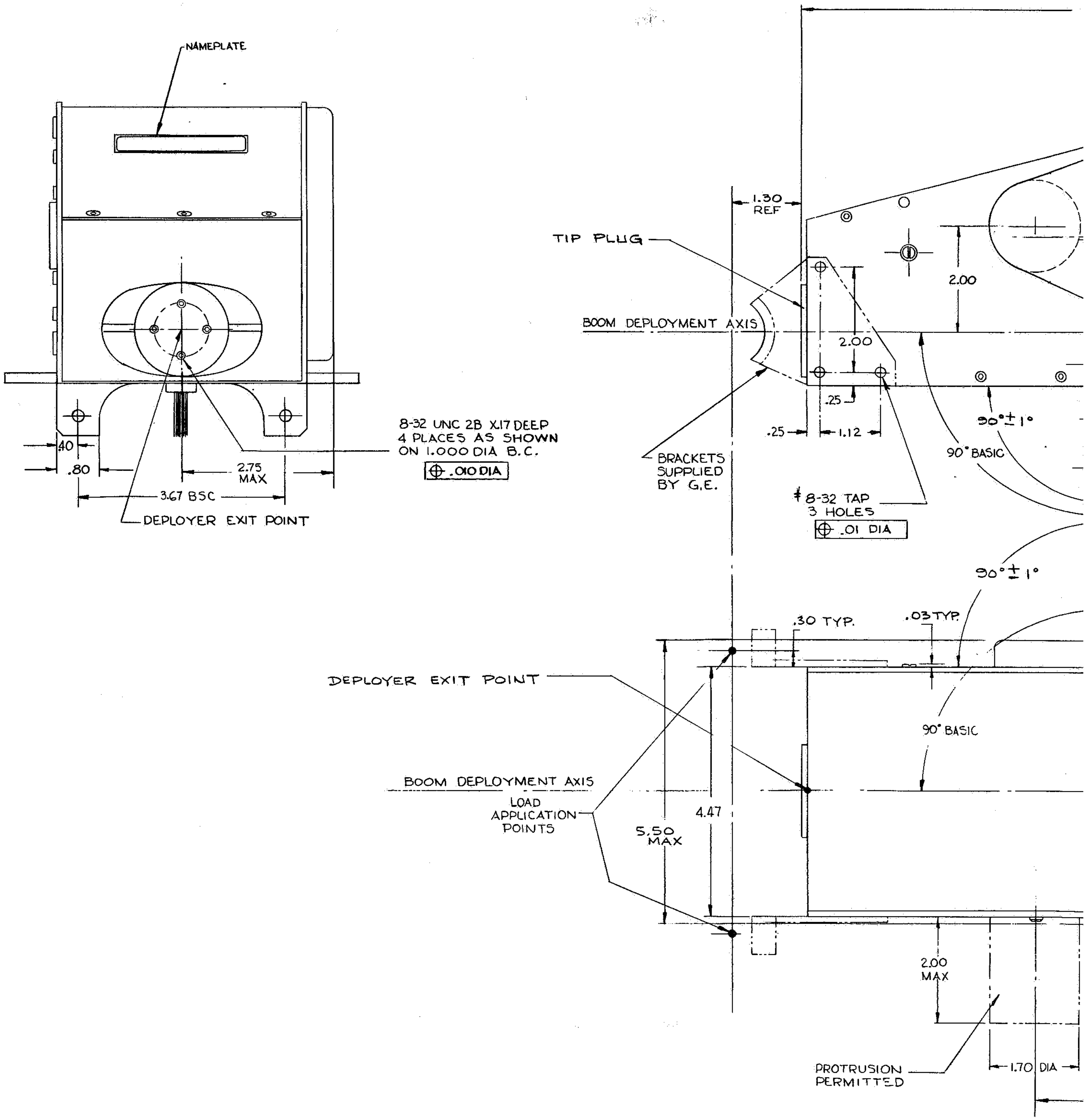

FOLDOUT FRAME 2

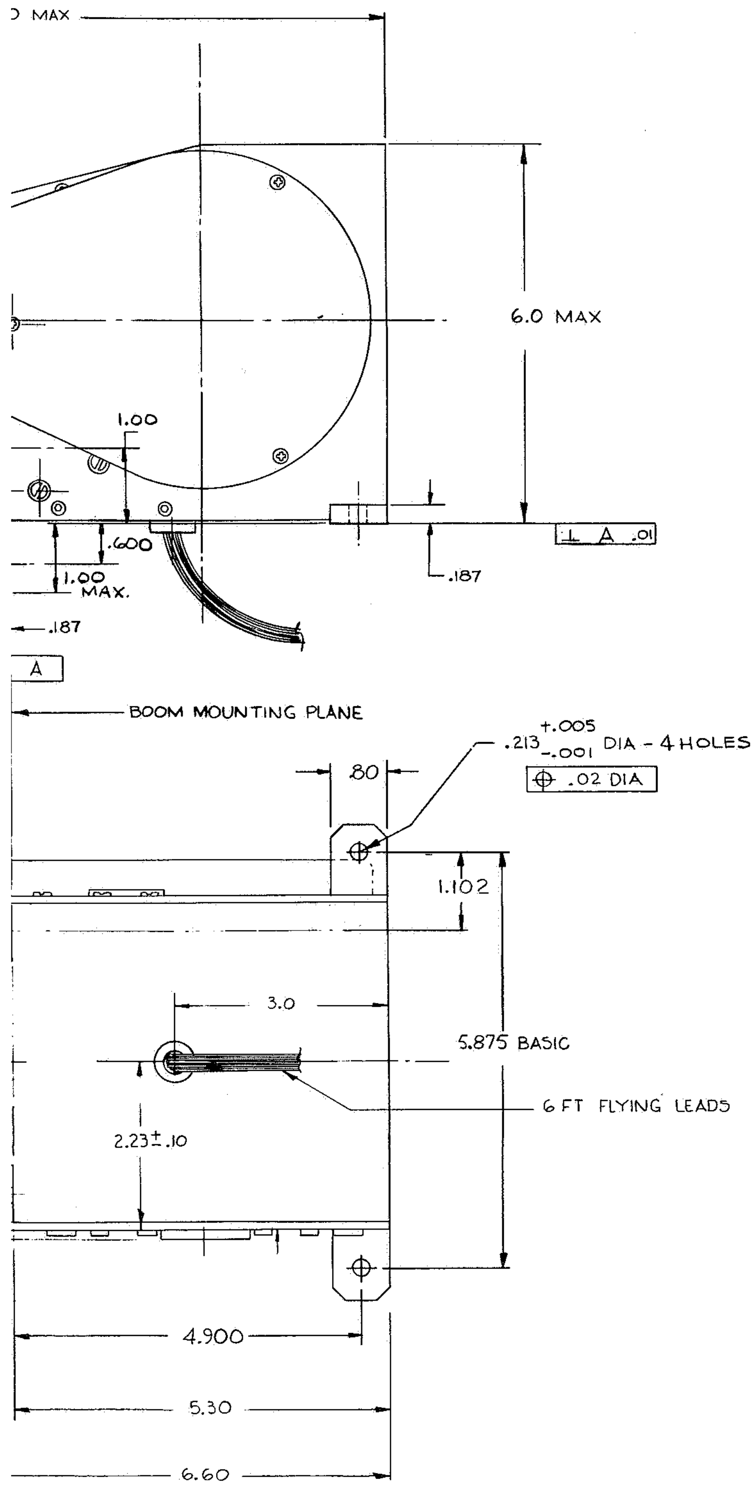

NOTES

1. INTERPRETATION OF DRAWING TERMS AND TOLERANCES PER 118A1664.
2. PART TO BE MARKED WITH MANUFACTURERS IDENT, AND MARK "GE 47E214524P1 PER 118A1526 CLASS 2 ON VENDOR NAMEPLATE APPROVED BY GE.
3. PARTS MUST CONFORM TO REQUIREMENTS OF SVS 7534

Figure 3-5. Outline Drawing of BI-STEM Actuator for Array

3.4 STORAGE DRUM

A LIGHTWEIGHT STORAGE DRUM OF BRAZED BERYLLIUM SHEET HAS BEEN DESIGNED.

The basic drum is made in two identical sections, each cantilevered from a single, center support. Each drum section is 8.0 inches in diameter by 47.1 inches long and is provided with a removable end cap on each end. The inboard end cap acts as a bearing housing and provides the primary load path from the drum skin to the center support. The outboard end cap provides a load path from the drum to the movable outboard end support. Both end caps are attached to the drum by fastening flathead screws through holes in the drum into nut plates in the end cap flanges. The caps are made removable to provide access to the interior of the drum for installing the internal slip rings, the constant torque spring motor, and the preloaded drum bearings.

The drum is essentially a thin-walled cylinder and is fabricated from cross rolled beryllium sheet (see Figure 3-6). The design drawings for the storage drum assembly have been sent to vendors qualified to fabricate with beryllium. Feedback has been received regarding cost and design changes which would improve the producibility of these parts. All beryllium fabricated parts utilize state-of-the-art joining techniques.

The use of beryllium in the drum has resulted in a lighter-weight structure with a slightly more complicated method of fabrication than a conventional aluminum or magnesium unit. A weight increase of 2.4 pounds would result if the drum were fabricated from magnesium. The beryllium drum skin is 0.025 inch thick and is made in four quadrants to simplify the forming tooling. The four circular quadrants can be joined by furnace brazing with silver or aluminum-based braze alloy. Channel-shaped doublers are used inside the tube to back up the longitudinal joints, and a circular, ring doubler is used inside the tube at each end to provide additional material thickness for the countersunk, endcap-mounting holes. One hole is provided in the skin, near the inboard end to permit the electrical connections to be made between the solar array bus bars and the internal drum power takeoff. The hole is reinforced with channel and angle-shaped doublers.

Machining for fastener holes, etc., will be performed on the completed assembly and will be followed by a light etch to remove surface flaws.

The end caps will be machined from a beryllium forging. Each unit consists essentially of a circular, flat sheet, with an outer flange for attachment to the drum, and a center boss for attachment to the support structure. Both caps also contain six equally spaced, radial stiffeners leading from the outer flange to the center boss to strengthen the assembly for bending load.

The inboard end cap has a large center boss, machined to serve as a housing for the two preload bearings. In addition, this end cap also has provision for mounting the output drum of the constant torque spring motor.

Both end caps have nut plates riveted to the inside surface of the circular outer flange. These mate with the countersunk holes in the ends of the drum and provide a means of attaching the drum to the end caps.

The preliminary design drawing of the outboard end cap and inboard end cap are shown as Figures 3-7 and 3-8, respectively.

The slip ring assembly is housed inside the storage drum. This assembly serves the function of transferring the array power from the movable storage drum shell to the stationary support shaft. The drawing for this unit is shown in Figure 3-9 and a detailed design specification is included as Appendix B. In addition to the two power rings, four signal rings are provided on each slip ring assembly. These four signal rings are sufficient for transferring two thermistor signals plus one array voltage tap.

Table 3-4 contains a summary of the key slip ring design parameters.

FOLDOUT FRAME 1

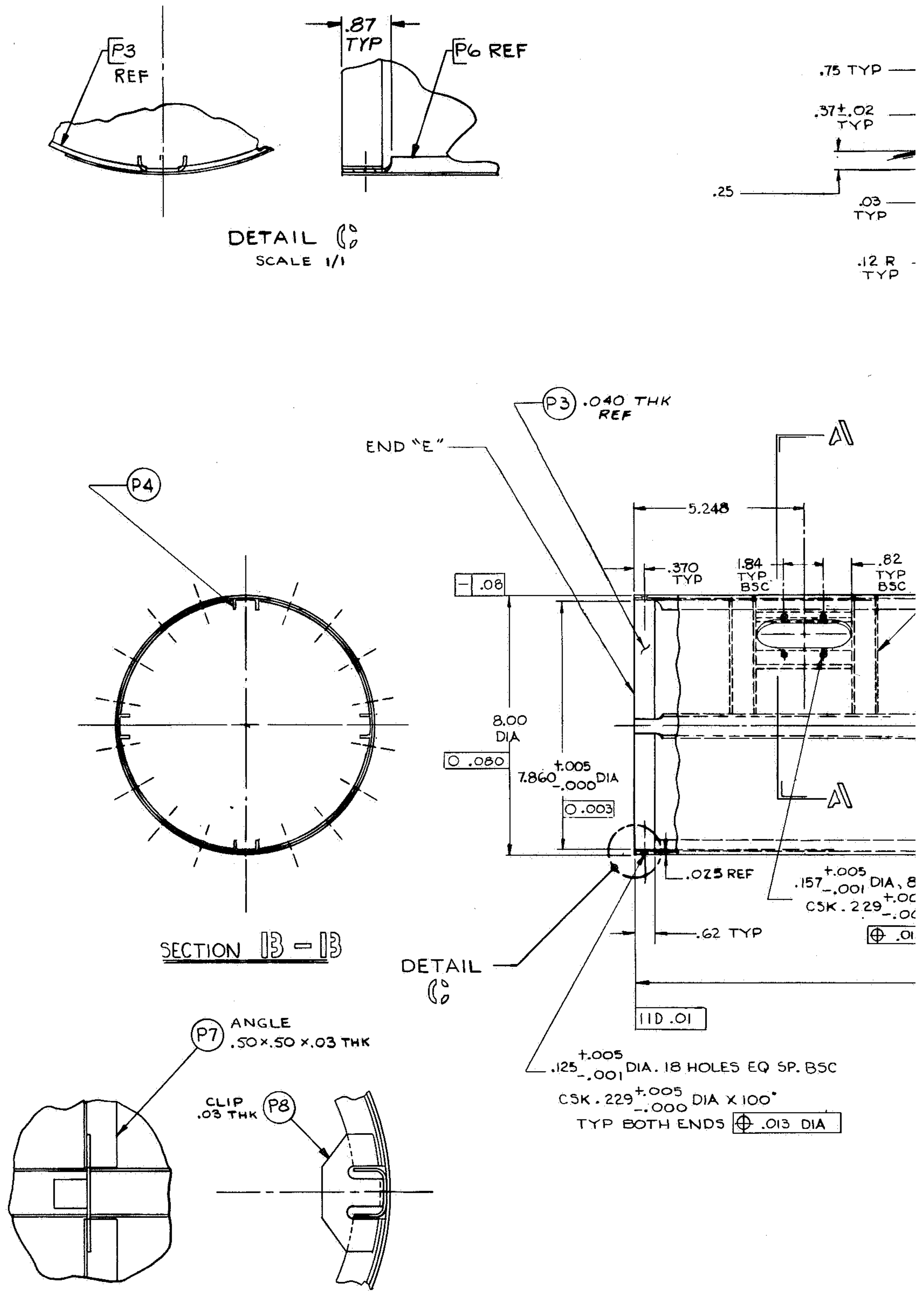

FOLDOUT FRAME 2

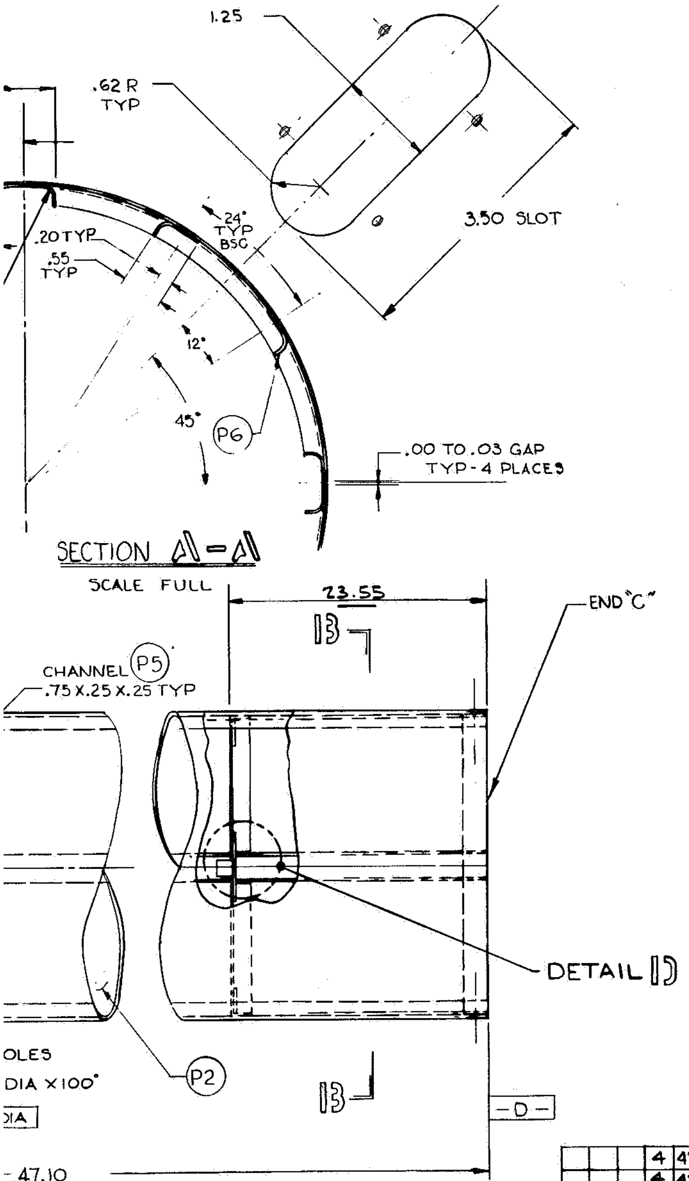

G1

NOTES:

1. INTERPRETATION OF DRAWING TERMS AND TOLERANCES PER 118A1664.
2. END "C" TO MATE WITH 47C214512G1 WITH A CLEARANCE OF .005 MAX.
3. END "E" TO MATE WITH 47E214683G1 WITH A CLEARANCE OF .005 MAX.

G4	G3	G2	G1	IDENTIFICATION NO.	ITEM NO.	DESCRIPTION	STOCK SIZE	MATERIAL	REMARKS
			4	47D214514P8	8	CLIP	.030 THK	BERYLLIUM	CRS S-200-C
			4	47D214514P7	7	ANGLE	.030 THK	BERYLLIUM	CRS S-200-C
			4	47D214514P6	6	ANGLE	.030 THK	BERYLLIUM	CRS S-200-C
			3	47D214514P5	5	CHANNEL	.030 THK	BERYLLIUM	
			4	47D214514P4	4	CHANNEL	.030 THK	BERYLLIUM	
			8	47D214514P3	3	DOUBLER		BERYLLIUM	
			4	47D214514P2	2	DRUM SKIN	.025 THK	BERYLLIUM	CRS S-200-C
			X	47D214514G1	1	DRUM ASSY			

REQUIREMENTS PER ASS'Y — FORM 1-0001 (11-61) — LIST OF MATERIAL

Figure 3-6. Storage Drum Shell

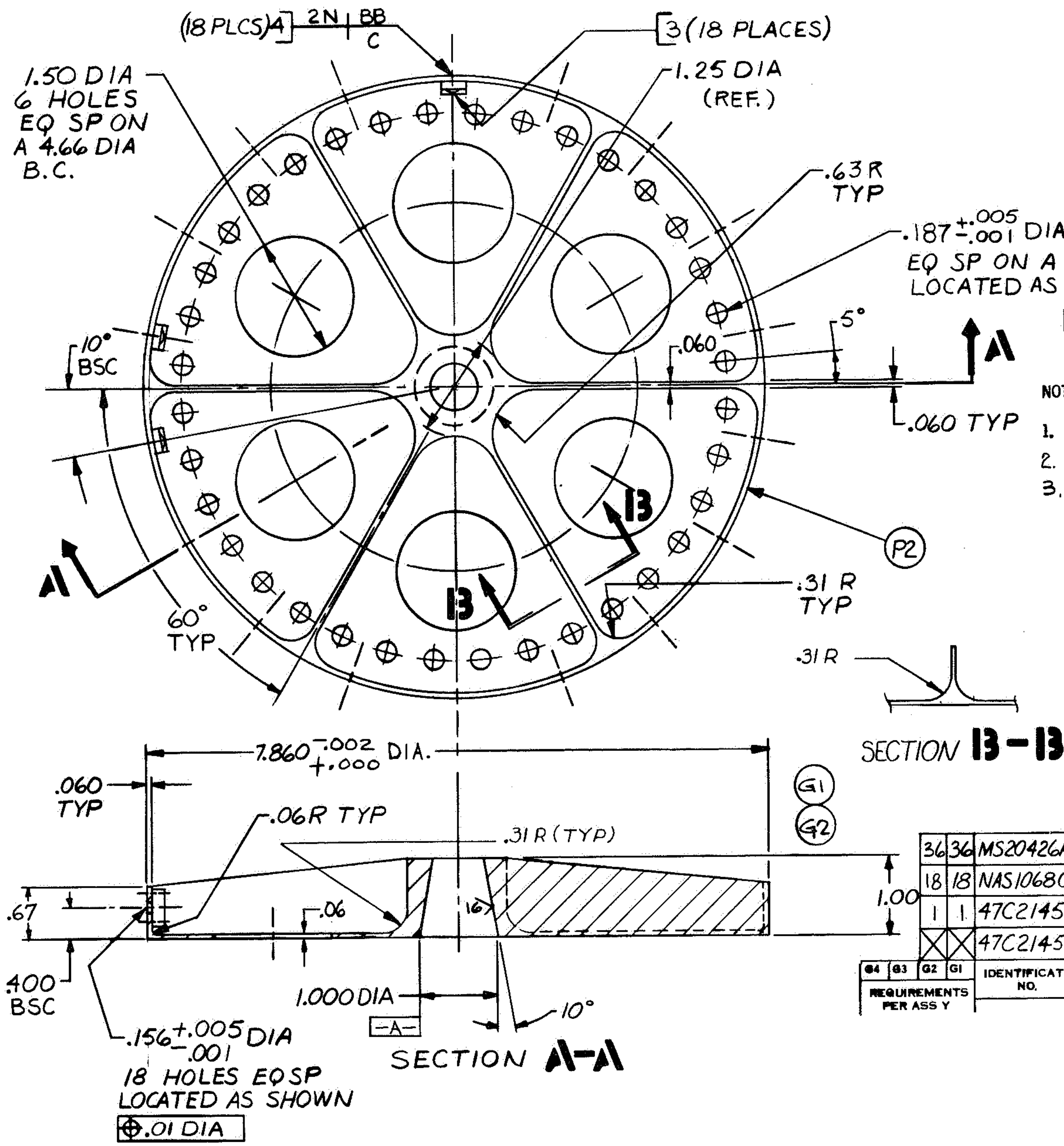

NOTES:

1. INTERPRETATION OF DWG. TERMS AND TOLERANCES PER 118A1664.
2. RIVET PER 171A4287.
3. MATERIAL: —
   G1 ALUMINUM ALLOY 6061-T6
   G2 BERYLLIUM S-200-C FORGING

G4	G3	G2	G1	IDENTIFICATION NO.	ITEM NO.	DESCRIPTION	STOCK SIZE	MATERIAL
		36	36	MS20426AD2	4	RIVET, FLT HD	.062 DIA	
		18	18	NAS1068C04	3	NUT PLATE	#4-40	
		1	1	47C214512P2	2	END, DRUM		
		X	X	47C214512G1	1	ASSY		
REQUIREMENTS PER ASSY								

Figure 3-7. Outboard End Cap

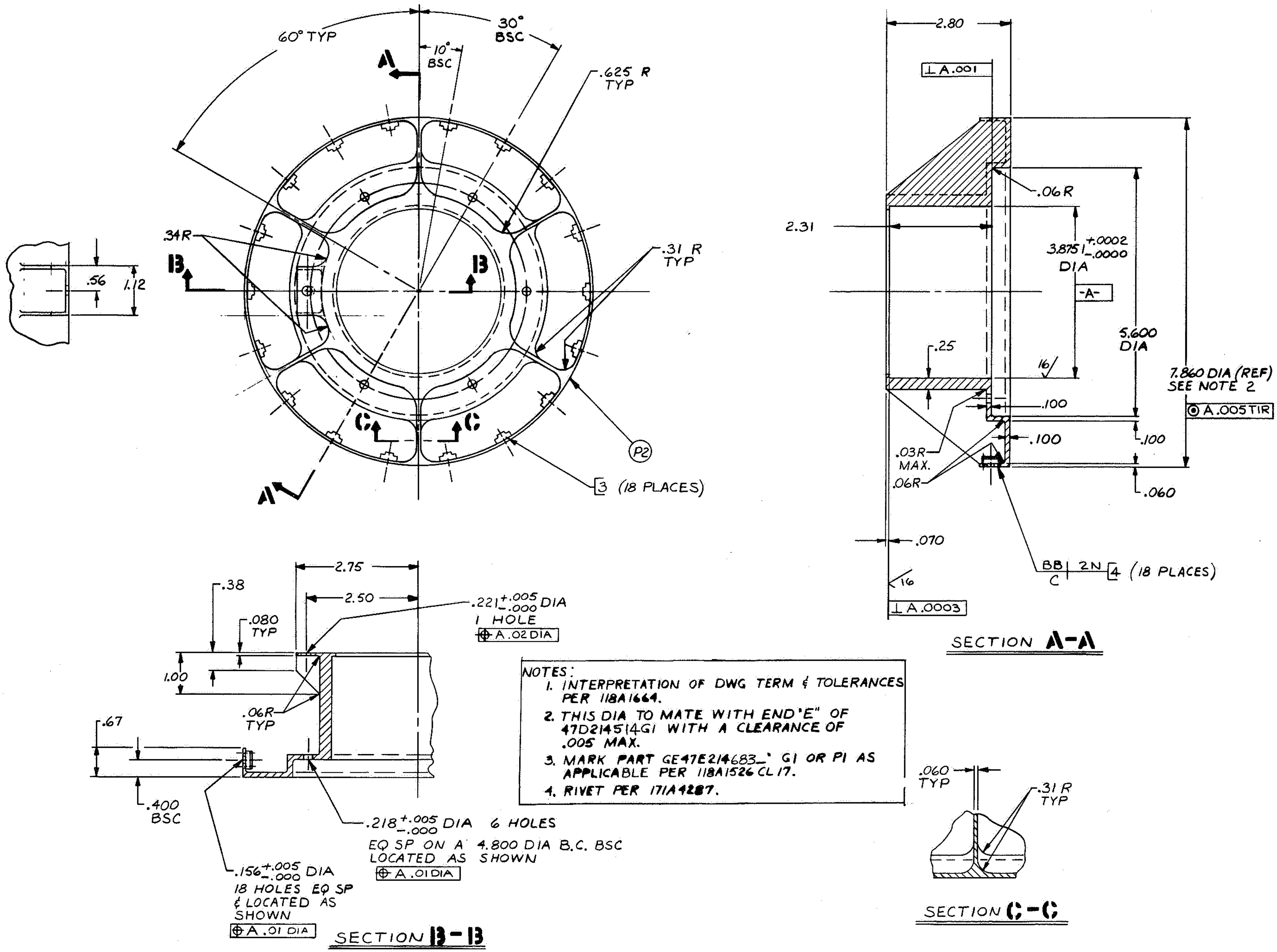

Figure 3-8. Inboard End Cap

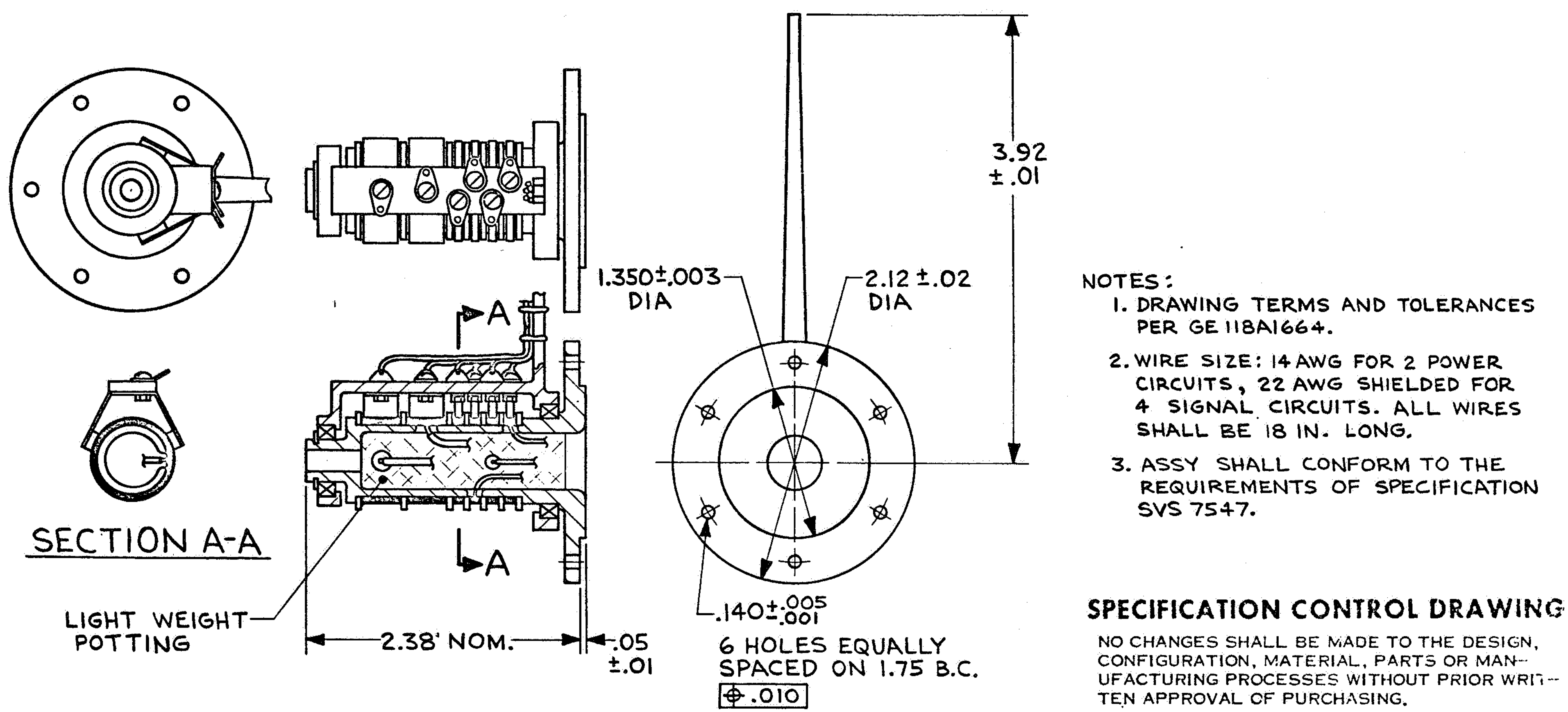

Figure 3-9. Slip Ring Assembly

Table 3-4. Summary of Key Slip Ring Design Parameters

Power Rings per Assembly	2
Signal Rings per Assembly	4
Ring Material	Silver
Ring Diameter	0.75 in.
Brushes per Ring	2
Brush Material	Silver/Copper/ Niobium Diselenide/Graphite
Rated Current per Ring	
Power	15.0 amp dc
Signal	1.0 amp dc
Brush Contact Force	
Power	0.75 lb
Signal	0.10 lb
Starting Torque	
Air	0.7 in-lb
Vacuum	0.4 in-lb
Static Contact Resistance	0.005 ohms
Rated Current Density	
Power	75 $Amp/in.^2$
Signal	55 $Amp/in.^2$
Power Dissipation/Assembly	1.53 watts
Weight/Assembly	0.50 lb

3.5 OUTBOARD END SUPPORT

THIS COMPONENT SUPPORTS THE OUTBOARD END OF THE STORAGE DRUM AND THE LEADING EDGE MEMBER DURING THE LAUNCH PHASE. IT WILL BE FABRICATED FROM ALUMINUM.

The outboard end support is a hinged arm, attached to the vehicle support structure to provide the following functions during ground handling activities and during launch and ascent: (1) support the outboard ends of the drum (2) support the outboard ends of the leading edge member, (3) prevent rotation of the drum about its longitudinal axis (see Figure 3-10). The fixed portion of the hinge is bolted directly to the vehicle mounting structure. The movable support is held in a fixed position relative to the drum and is prevented from rotating about its hinge during launch by a bolt and an electro-explosive separation nut. A tapered plug fixed in the movable support nests into a tapered hole in the drum end cap and provides the means of transferring the launch loads from the drum to the support.

When the separation nut is actuated, the hinged support arm rotates away from the drum and the leading edge member through the action of a torsion spring at the hinge point. A built-in stop limits the travel of the support, and the combined action of the spring and the stop will keep the support a fixed distance from the cantilevered drum. A bolt catcher will retain the released bolt, and there will be no debris or loose parts resulting from the release sequence. Once the support arm pivots out of the way, the drum is free to rotate about its own axis, and the leading edge member is free to move outward when the boom is deployed.

The end support has been designed to take all launch loads imposed on the outboard end of the drum except those loads which are along the longitudinal (or rotation) axis of the drum and the leading edge member. These loads will be in a direction which would tend to pivot the support about its hinge; consequently, the array has been designed to have the drum axial loads imposed only on the center support. The leading edge member longitudinal loads will be imposed upon the leading edge member center support attached to the boom actuator.

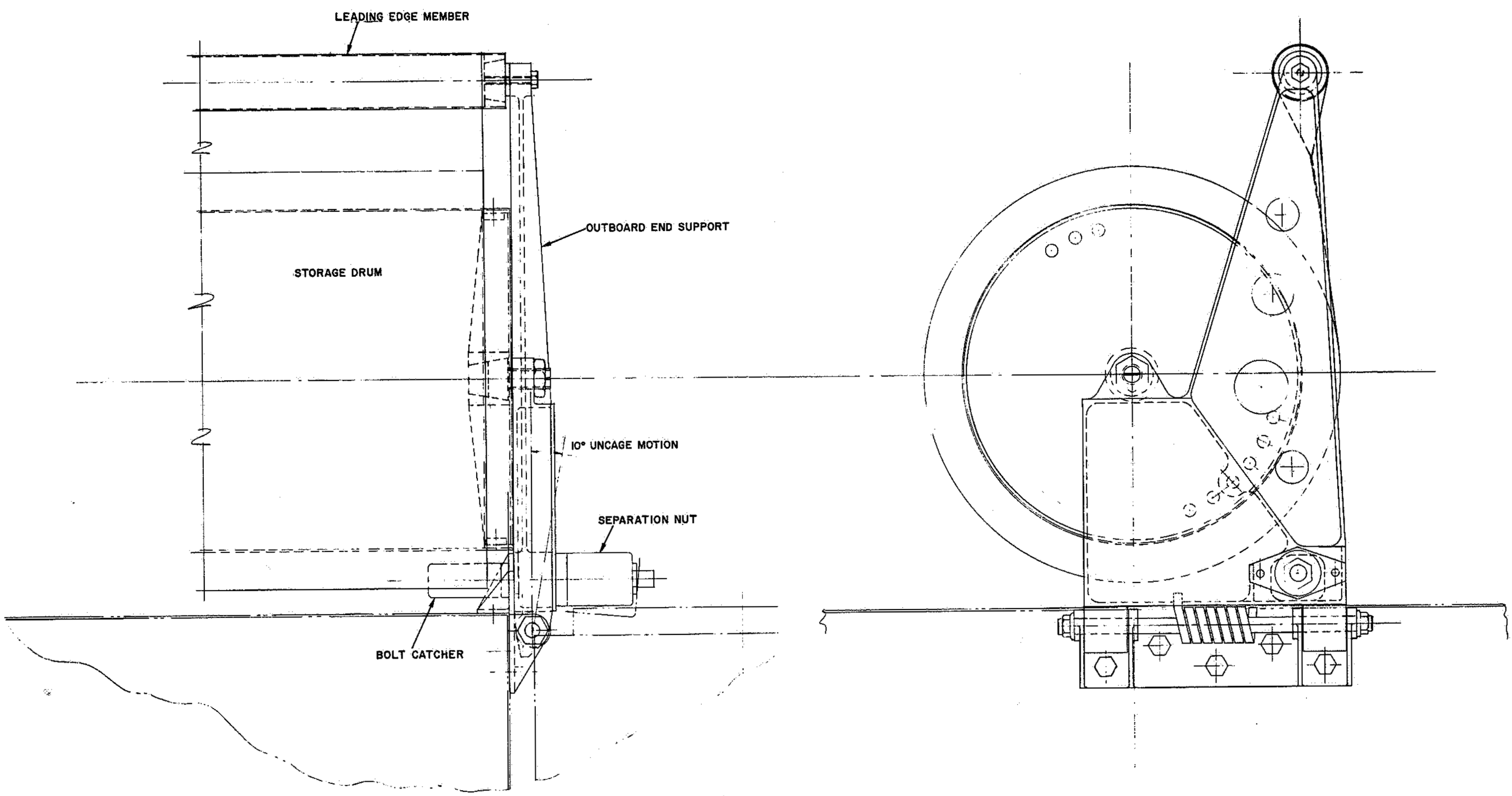

Figure 3-10. Outboard End Support

End Support Details

The basic end support structure is a two-piece hinged assembly. The fixed section is essentially a flat aluminum plate with four raised bosses machined to accept a hinge bolt and to nest into the mating hinge bosses of the movable support. The movable support is a hollow, welded aluminum, box construction, 1 inch thick, and tapering from 6 inches in depth at the hinge end to 5 inches at the drum support end. The support is approximately 6 inches long from the hinge point to the drum support point; however, a 7-inch extension continues beyond the drum support to pick up the support of the leading edge member. The box structure is reinforced at the hinge end, at the drum support point, and at the point of attachment to the separation nut, to provide for the higher local stresses expected in these areas.

The actual support of the outboard drum end is accomplished by a tapered pin in the support, nesting into a mating tapered hole in the outboard end cap of the drum. A 20-degree taper has been used in the design of the pin to ensure that it is self-releasing (industry standard for self-releasing tapers is 16 degrees). In addition, the pin will be coated with a film of teflon to further aid its disengagement from the drum. One end of the pin will be threaded to provide for axial adjustment in the drum.

The drum will be restrained from rotating in the stowed position by a tapered pin in the support which will mate with a series of holes in the drum end cap.

The outboard ends of the leading edge member contain tapered holes which mate with the tapered plugs on the ends of the movable support extensions.

The deployment sequence will be:

a. Signal-to-firing circuit fires separation nut squibs. This disengages the separation nuts (one for each end support of a drum assembly) and ejects the bolts into the bolt catchers. The supports are now free to rotate.

b. The hinge springs act on the movable section of the supports and force the supports to rotate outboard away from the drums.

c. As the supports rotate outboard, the taper pins in the drum and in the leading edge member are removed from their mating holes. The taper ensures that the pins, which describe an arc as they leave their holes, will not bind in the holes.

d. The supports continue to rotate until they are restrained by their built-in stops. The hinge springs will continue to exert a force which will keep the supports fixed against the stops.

e. The end supports are now clear of the drum ends, and the drums are free to rotate about the center support bearings. The leading edge member is now supported only by its center yoke and is free to move when the boom is deployed.

3.6 LEADING EDGE MEMBER

THE LEADING EDGE MEMBER ACTS AS THE TRANSITION PIECE BETWEEN THE OUTER TIP OF THE DEPLOYABLE BOOM AND THE LEADING EDGE OF THE SOLAR ARRAY BLANKETS. IT WILL BE FABRICATED FROM CROSS-ROLLED BERYLLIUM SHEET.

The leading edge member (LEM) is directly attached to the array along its length, and is attached at its midpoint to the boom tip through a bearing which will permit the boom to rotate relative to the LEM.

In the stowed condition, the two movable outboard end supports also support the ends of the LEM through the use of tapered plugs which nest in the open ends of the LEM. When the end supports are released from the drum, they also release the ends of the LEM. The center of the LEM is supported by a yoke attached to the forward part of the boom actuator mechanism.

The LEM length is determined by the width of the solar array. The cross section is designed to provide the stiffness required to maintain the solar array preload.

The LEM is fabricated from two thin-walled tubes, each 1.00 inch in diameter by 49.45-inches long (see Figure 3-11). Each tube is made from a flat sheet, rolled into a circular section and furnace-brazed or adhesive-bonded with a doubler reinforcing the longitudinal joint. These two tubes are joined together at the center fitting to form a single tubular structure which is 100.2 inches long. The center fitting also houses the bearings which permit the deployable boom to rotate relative to the LEM.

FOLDOUT FRAME 1

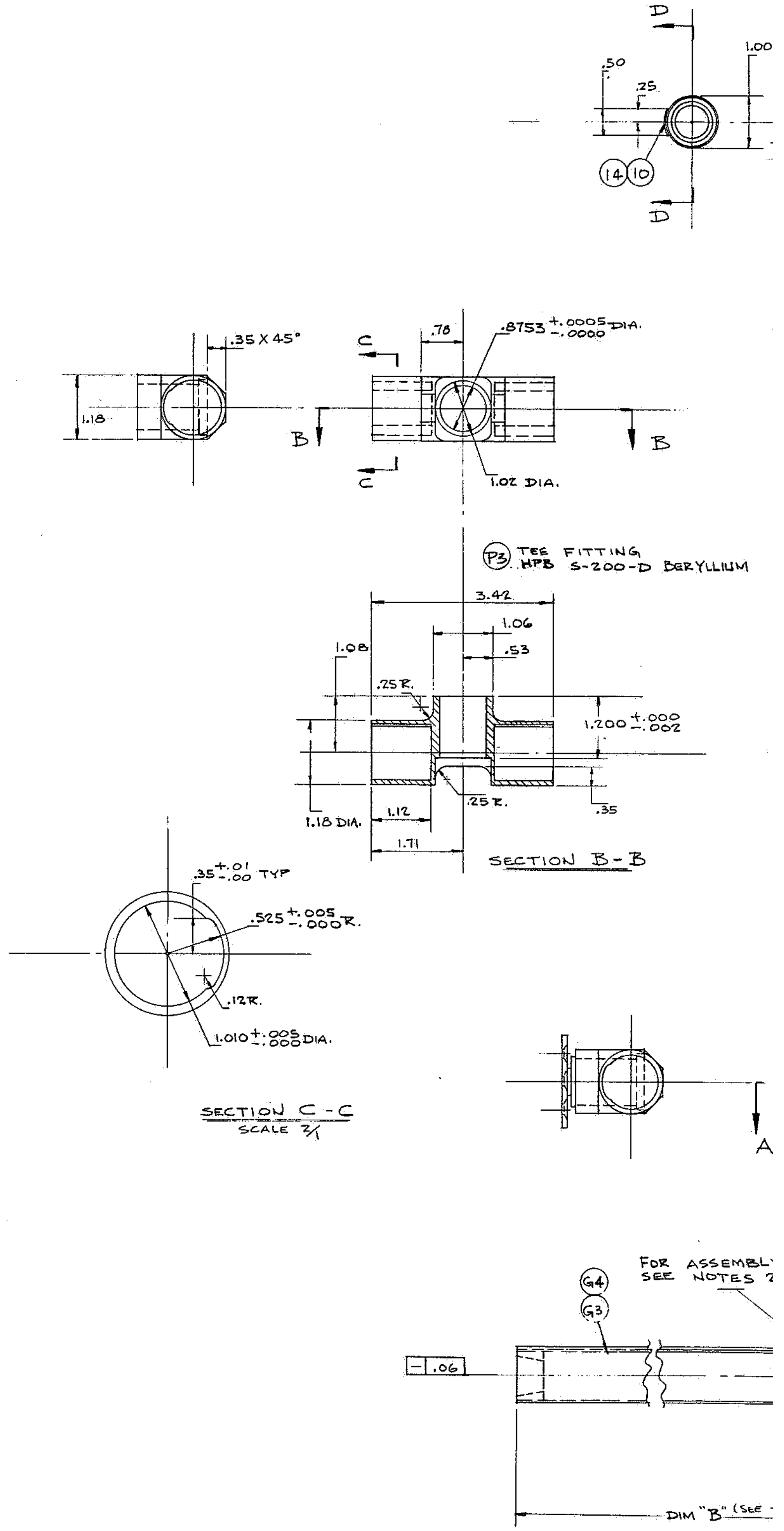

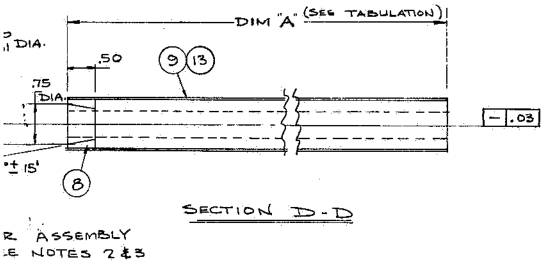

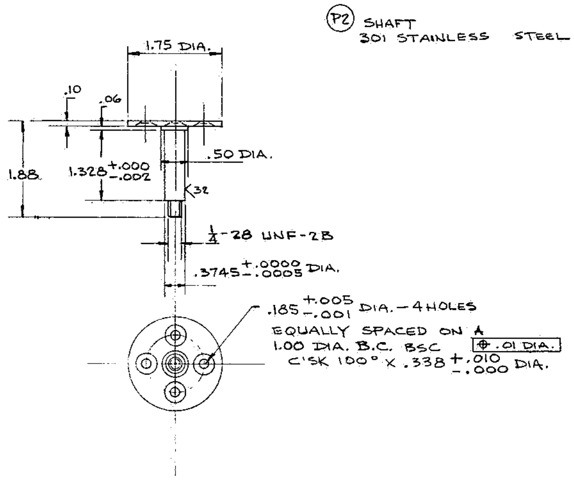

NOTES: —

1. DRAWING TERMS & TOLERANCES PER 118A1664.

2. ALL JOINTS TO BE BONDED USING EPON 934 OR NARMCO 3175C. THE SURFACE PREPARATION SHALL BE AS FOLLOWS
   1. VAPOR DEGREASE
   2. IMMERSE FOR 2 TO 5 MINUTES IN THE FOLLOWING SOLUTION AT 75° F.
      a. 3700 GMS TAP WATER
      b. 250 GMS CONCENTRATED SULPHURIC ACID (SP GR. 1.84)
      c. 2.4 GMS SODIUM DICHROMATE
   3. RINSE, CHECK FOR WATER BREAK AND FORCE DRY.

3. ALTERNATE JOINING METHOD: FURNACE BRAZE WITH A718 ALLOY

	PART NO.	DIM "A" ±.02	DIM "B" ±.02
ENGINEERING DEMONSTRATION MODEL	9 & 10	26.35	27.00
FLIGHT CONFIGURATION	13 & 14	49.45	50.10

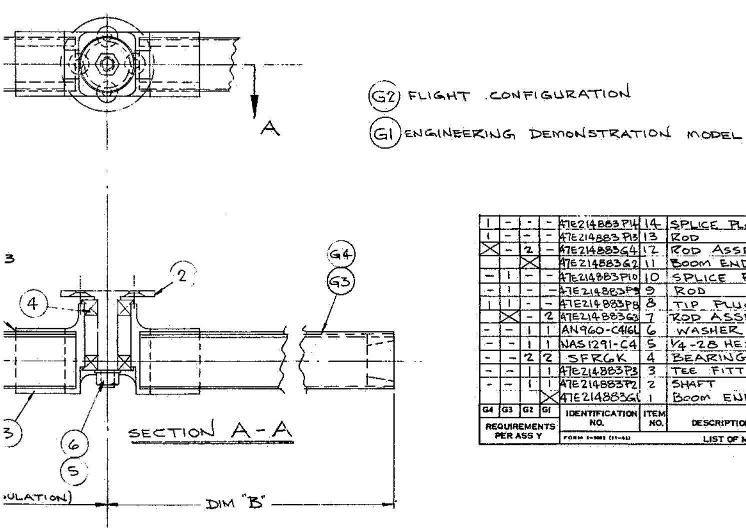

G4	G3	G2	G1	IDENTIFICATION NO.	ITEM NO.	DESCRIPTION	STOCK SIZE	MATERIAL	REMARKS
1	-	-	-	47E214883P14	14	SPLICE PLATE	.02 THK	CRS-200-C BERYLLIUM	
1	-	-	-	47E214883P13	13	ROD	.02 THK	CRS-200-C BERYLLIUM	
X	-	2	-	47E214883G4	12	ROD ASSEMBLY			
		X		47E214883G2	11	BOOM END ASSEMBLY			
-	1	-	-	47E214883P10	10	SPLICE PLATE	.02 THK	CRS-200-C BERYLLIUM	
-	1	-	-	47E214883P9	9	ROD	.02 THK	CRS-200-C BERYLLIUM	
1	1	-	-	47E214883P8	8	TIP PLUG	HPB	S-200-D BERYLLIUM	
	X	-	2	47E214883G3	7	ROD ASSEMBLY			
-	-	1	1	AN960-C416L	6	WASHER			
-	-	1	1	NAS1291-C4	5	1/4-28 HEX. NUT			
-	-	2	2	SFR6K	4	BEARING	BARDON		
-	-	1	1	47E214883P3	3	TEE FITTING	HPB	S-200-D BERYLLIUM	
-	-	1	1	47E214883P2	2	SHAFT	301 STAIN	LESS STEEL	
			X	47E214883G1	1	BOOM END ASSEMBLY			

REQUIREMENTS PER ASS Y — FORM 1-9001 (11-61) — LIST OF MATERIAL

Figure 3-11. Leading Edge Member

3.7 CENTER SUPPORT

THE CENTER SUPPORT, A WELDED ALUMINUM STRUCTURE, IS THE ONLY ATTACHMENT OF THE ARRAY TO THE VEHICLE STRUCTURE IN THE DEPLOYED CONDITION.

The center support is a welded aluminum structure which serves as the primary means of attaching the drums to the vehicle mounting surface. The storage drum is made in two identical halves which are bolted to the right hand and left hand mounting faces of the support. The bottom of the support provides a mounting surface for the boom actuator mechanism which is located between the two drums. The support is attached to the vehicle structure with bolts through holes provided in the support rear mounting surface (See Figure 3-12).

The support structure has been designed to take all the launch loads imposed on the inboard ends of the two drums. Loads on the outboard ends of the drums will be taken by the outboard end supports. In addition, the center support will take all the loads which act along the longitudinal (or rotation) axes of the drums. In orbit, when the outboard end supports have been removed from the drum ends, the drums will be supported as cantilevers from the center support only.

Center Support Details

The support is a welded aluminum structure consisting of a backplate, two flanged vertical side plates, a front horizontal tube, and a central horizontal plate. The complete assembly is 6 inches high by 5.2 inches wide at the back mounting surface. The top surface of the side plates taper from 6 inches at the back to 5.30 inches at the front. The unit is 5.53 inches long from the back mounting surface to the center of the 2.50-inch-diameter tube.

Four mounting holes are provided on the backplate for mounting to the vehicle. Four holes are provided for mounting the boom actuator. Eight holes in a circular pattern are provided in flanges on each side of the horizontal tube for mounting the two drums.

The support has been designed so that the drum mounting flanges are bolted to the tube mounting flanges, thus forming a continuous structure from one drum to the other. The support structure essentially supports this center tube which, in turn, supports the drums.

The power leads from the solar array pass through the drums and terminate on two connectors located on the central horizontal plate of the support.

FOLDOUT FRAME 1

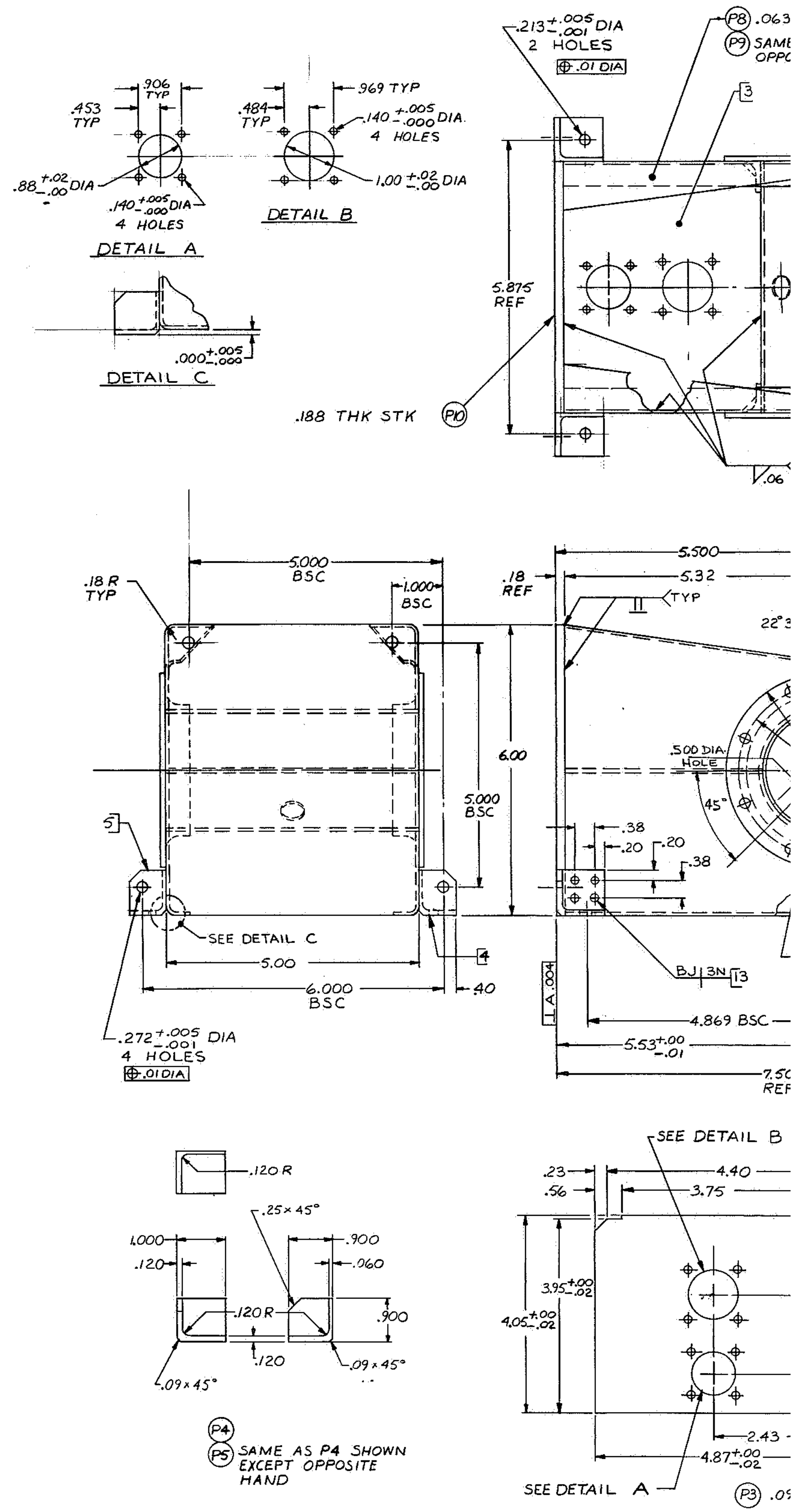

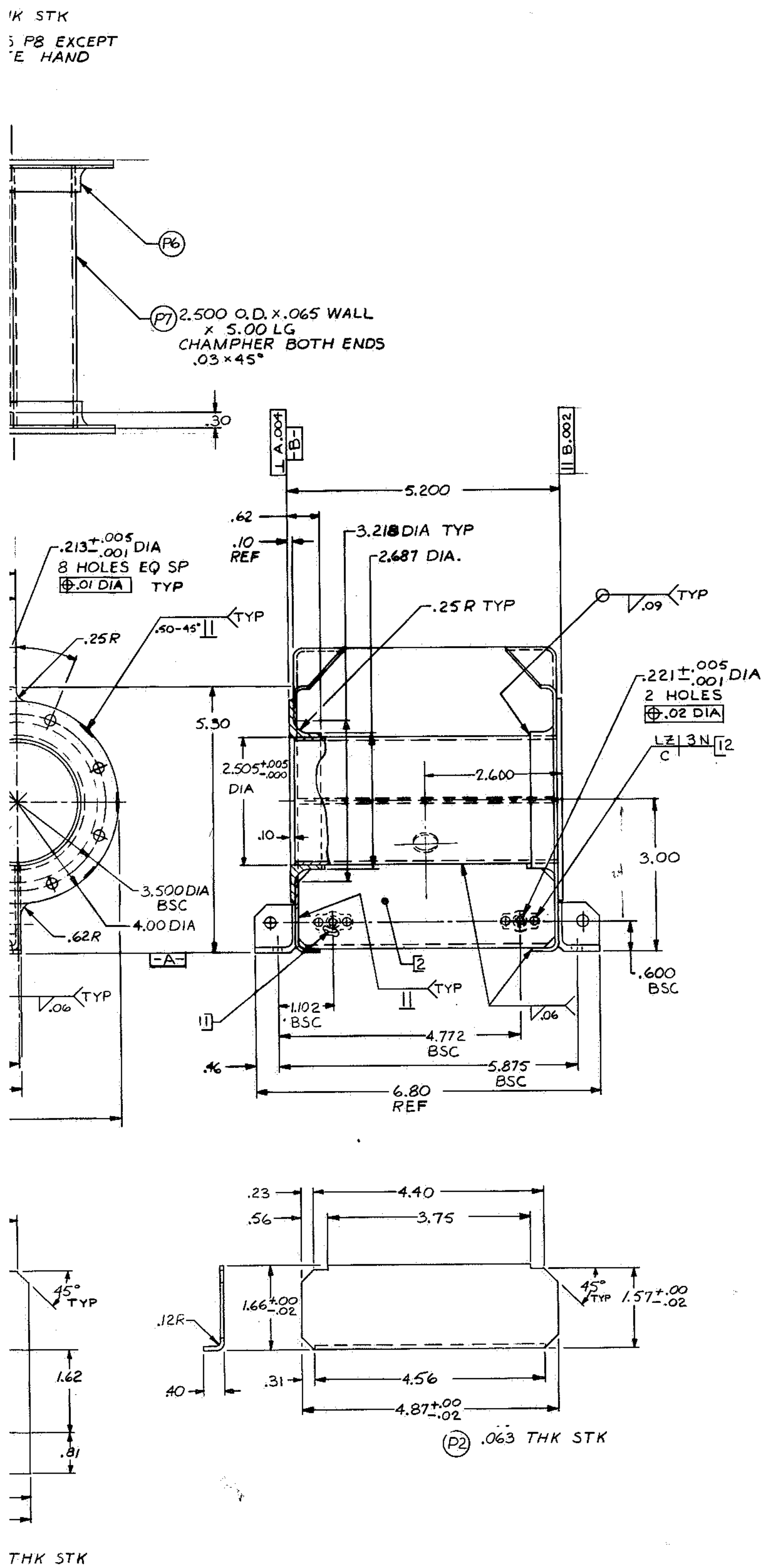

NOTES:

1. INTERPRETATION OF DWG TERMS & TOLERANCES PER 118A1664.
2. INTERPRETATION OF WELD SYMBOLS PER AWS A2.0.
3. RIVET PER 171A4207.
4. ALL BEND RADII TO BE .12 ± .02.
5. FINISH PER 118A1600P13.
6. MARK PART "GE47E214875 " G OR P NUMBER AS APPLICABLE PER 118A1526 CLASS 21.

G4	G3	G2	G1	IDENTIFICATION NO.	ITEM NO.	DESCRIPTION	STOCK SIZE	MATERIAL	REMARKS
			8	MS20470AD3-4	13	RIVET ROUND HD			
			4	NAS1097AD3-5	12	RIVET, FLT HD			
			2	NAS1068C3	11	NUT PLATE	#10-32		
			1	47E214875 P10	10	MOUNTING PL			
			1	P9	9	SIDE COVER			
			1	P8	8	SIDE COVER			
			1	P7	7	SUPPORT TUBE			
			2	P6	6	MOUNTING FLG			
			1	P5	5	MOUNTING FOOT			
			1	P4	4	MOUNTING FOOT			
			1	P3	3	CONNECTOR PL			
			1	P2	2	FACE PLATE			
			X	47E214875G1	1	ASSY			

REQUIREMENTS PER ASS'Y — LIST OF MATERIAL

Figure 3-12. Center Support

SECTION 4
PERFORMANCE ANALYSIS

4.1 DEPLOYED DYNAMICS ANALYSIS

THE LOWEST FIRST-MODE NATURAL FREQUENCY OF THE DEPLOYED ARRAY IS CALCULATED TO BE 0.075 Hz.

The deployed array was analyzed to determine, through a suitable mathematical model, the modes of vibration. A string analysis was performed to approximate the vibration of a rectangular membrane (the array blanket).

String Analysis

A rectangular membrane supported on opposite ends acts as a series of parallel strings in its first mode of vibration. The frequencies of vibration for a string supported at one end and free at the other can be expressed by (Reference 4-1):

$$f_n = \frac{(2n-1)}{4L} \left(\frac{T}{\delta}\right)^{1/2} \tag{4-1}$$

where

n = mode number

L = length of string

P = tension in string (lb)

δ = linear density (slug/ft)

If the area density of the membrane is γ (lb/ft^2), then the linear density of a strip W feet wide is:

$$\delta = \frac{\gamma W}{g} \tag{4-2}$$

For the selected array configuration:

$$L = 34.1 \text{ ft}$$
$$W = 7.68 \text{ ft}$$
$$\gamma = 0.17 \text{ lb/ft}^2$$

Therefore, Equation 4-1 can be expressed as:

$$f_1 = 0.213 \left(\frac{T}{L}\right)^{1/2} \text{ for the first-mode frequency} \qquad (4\text{-}3)$$

Mathematical Model Analysis

The complete deployed array system was analyzed using the mathematical model of Figure 4-1. This model consists of 10 degrees of freedom located at nine mass points. There are nine translational degrees of freedom, eight associated with the blanket out of plane motions (X_1 through X_8), and one associated with the tip of the rod; the single rotation coordinate is located at the center of the leading edge member at the point where it is attached to the deployable rod. The leading edge member is assumed rigid, and the array blankets are considered to act as equivalent strings attached to the leading edge member two-thirds distance from the rod centerline on each side.

The stiffness matrix is written directly and is presented in Figure 4-2. The restoring force caused by the displacement of the string is T/ℓ where T is the tension and ℓ is the length of the string between coordinates. The deployable rod, because of the end bearing, contributes to torsional stiffness to the system.

The mass matrix is a diagonal matrix consisting of the mass associated with each coordinate. Because there are several cases analyzed, the mass matrixes are not presented herein. However, it is noted that the mass associated with coordinate X_9 consists of the following:

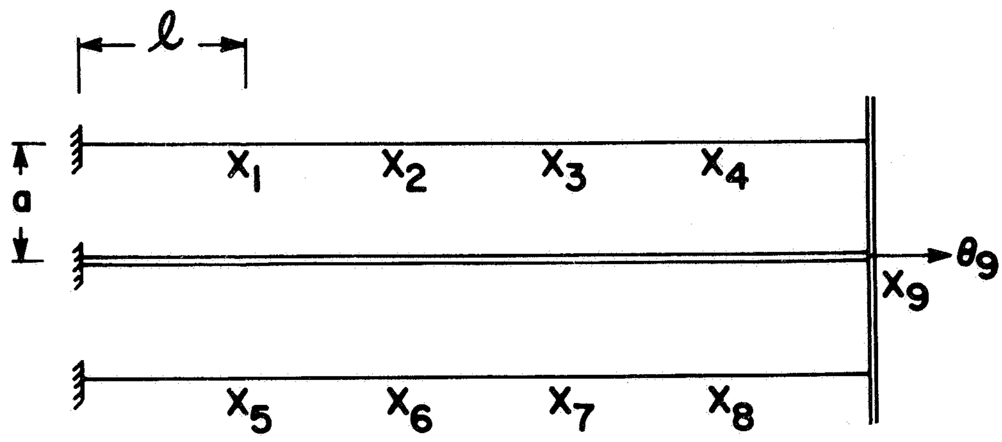

Figure 4-1. Mathematical Model

$$
\left[\begin{array}{cccc|cccc|cc}
2T/\ell & -T/\ell & & & & & & & & \\
-T/\ell & 2T/\ell & -T/\ell & & & & & & & \\
 & -T/\ell & 2T/\ell & -T/\ell & & & & & & \\
 & & -T/\ell & 2T/\ell & & & & & -T/\ell & +Ta/\ell \\
\hline
 & & & & 2T/\ell & -T/\ell & & & & \\
 & & & & -T/\ell & 2T/\ell & -T/\ell & & & \\
 & & & & & -T/\ell & 2T/\ell & -T/\ell & & \\
 & & & & & & -T/\ell & 2T/\ell & -T/\ell & -Ta/\ell \\
\hline
 & & & -T/\ell & & & & -T/\ell & 2T/\ell + K & 0 \\
 & & & -Ta/\ell & & & & -Ta/\ell & 0 & 2T/\ell \; a^2
\end{array}\right]
\bullet
\begin{bmatrix} X_1 \\ X_2 \\ X_3 \\ X_4 \\ X_5 \\ X_6 \\ X_7 \\ X_8 \\ X_9 \\ \theta_9 \end{bmatrix}
=
\begin{bmatrix} F_{X1} \\ F_{X2} \\ F_{X3} \\ F_{X4} \\ F_{X5} \\ F_{X6} \\ F_{X7} \\ F_{X8} \\ F_{X9} \\ M_{\theta 9} \end{bmatrix}
$$

NOTE: K IS THE ROD STIFFNESS IN BENDING.
T IS THE TENSION IN EACH EQUIVALENT STRING.

Figure 4-2. Rod Stiffness Matrix

a. Leading edge member

b. The mass associated with 42 inches of array

c. One-third the rod weight

The moment of inertia associated with coordinate 8 or 9 consists of:

a. Inertia of the leading edge member

b. Effects of point mass under item b above

The dynamic matrices were iterated utilizing the Jacobian technique to determine eigenvalues and eigenvectors.

The results of this analysis are summarized in Table 4-1 for two different blanket preloads. The 4-pound load is the tension selected for the flight design. It yields a first-mode frequency of 0.075 Hz in torsion. The 9-pound preload is possible on the present flight design with a 1.2-pound increase in total system weight (due to the larger Neg'ator springs required). This preload will yield a first-mode frequency of 0.112 Hz.

A pictorial representation of the resulting mode shapes in bending and torsion are shown in Figure 4-3 for the 4-pound preload. The restoring moment about the deployable rod at the tip is shown in Figure 4-4 as a function of leading edge member angular displacement.

Table 4-1. First Mode Natural Frequencies

LENGTH (FT)	PRELOAD (LB)	FREQUENCY (Hz)	TYPE
33.5	4.0	0.099	BENDING
33.5	9.0	0.130	BENDING
33.5	4.0	0.075	TORSION
33.5	9.0	0.112	TORSION

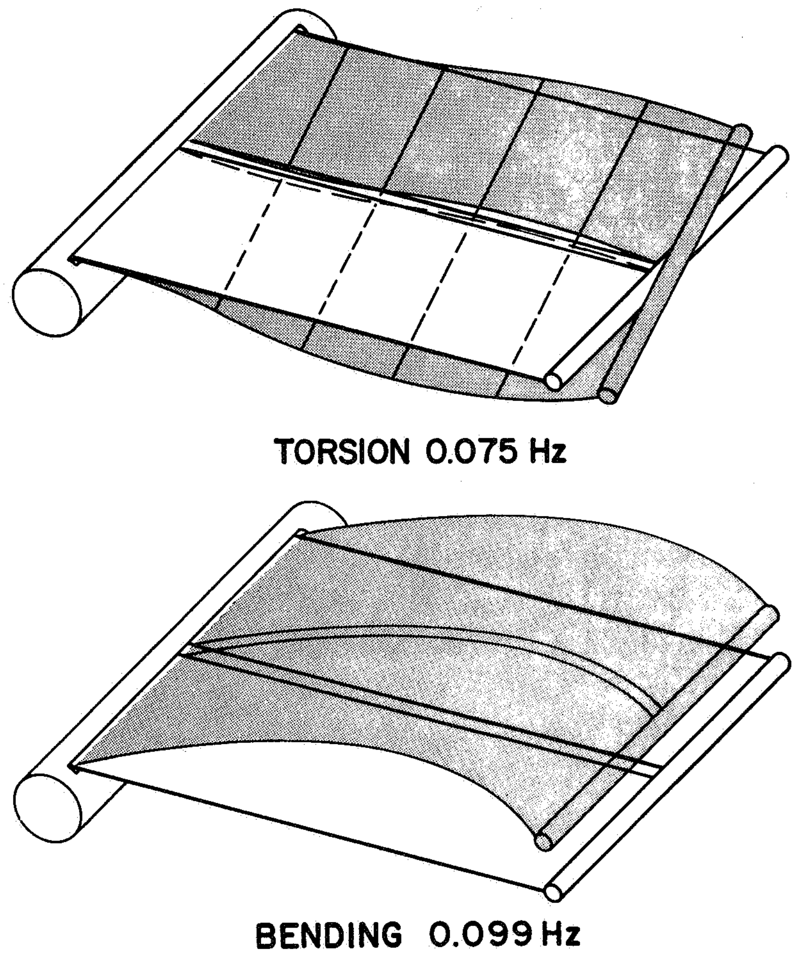

Figure 4-3. Deployed Array Mode Shapes

Equation 4-3 is plotted in Figure 4-5 along with the two points obtained from the mathematical model analysis of the bending mode.

Both of these points fall above the frequency obtained from the string analysis. This is largely due to the effects of rod stiffness which are accounted for in the model.

RESPONSE TO SQUARE WAVE PULSE

The deployed solar array was analyzed to determine its response to the application of a 2×10^{-5} rad/sec^2 square wave pulse about the pitch axis. For the purposes of this analysis a very conservative approach was taken. The following assumptions were made:

a. The pulse is tuned such that a second order resonance occurs (Reference 4-2).

b. No damping is assumed, resulting in an amplification factor of 2.0.

c. The pulses can be applied to the array in the following manner for N cycles.

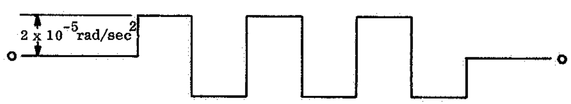

The modal response to an impulse is expressed as:

$$\ddot{\xi} = \frac{\phi^T M a}{M^*} AF \qquad (4\text{-}4)$$

where:

$\ddot{\xi}$ is the modal acceleration

ϕ^T is the transpose of the mode shape

a is the pulse acceleration

AF is the amplification factor

M^* is the generalized mass

M is the mass matrix consistent with ϕ^T

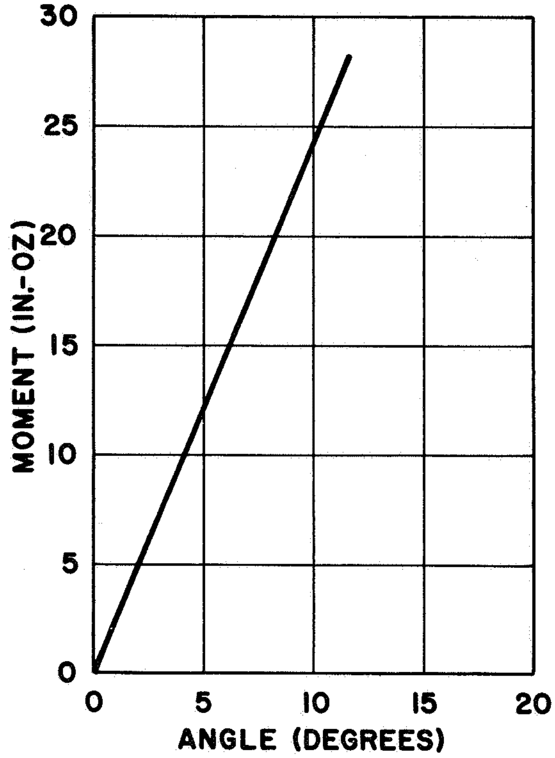

Figure 4-4. Leading Edge Members Restoring Moment as a Function of Angle

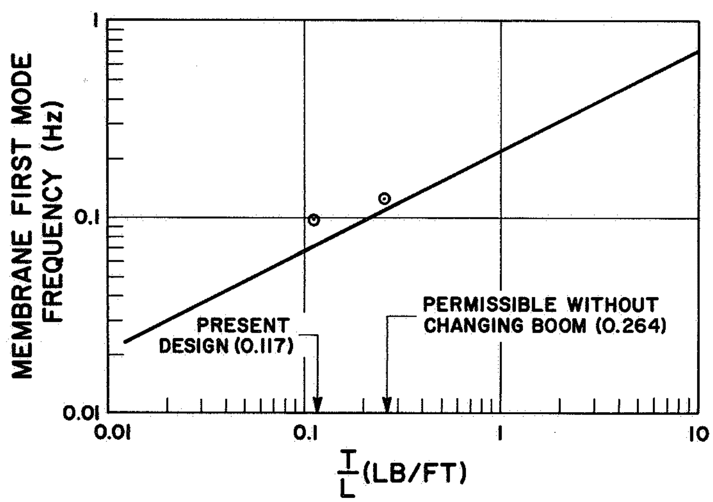

Figure 4-5. Effects of Tension on Membrance Frequency

The physical coordinate response at the array tip is

$$\ddot{\theta} = \phi \ddot{\xi}$$

For the first torsion mode at 0.075 Hz the response is

$$\ddot{\theta} = 5.86 \times 10^{-5} \text{ N rad/sec}^2$$

where N is the number of consecutively applied impulses

The torque generated by this response is

$$T = I\ddot{\theta}$$

$$T = 8.35 \times 10^{-3} \text{ N in-oz}$$

It is seen that the resultant torque is small, and even for numerous applications of the pulse is still quite small.

In a similar manner the response of the array first bending mode to the pulse is obtained. The resultant root bending moment is

$$BM = 0.37N \text{ in.-lb}$$

where N is the number of consecutively applied pulses

The allowable rod bending moment is 734 in.-lb. As can be seen the margin is quite high for any reasonable number of applied pulses.

4.2 STOWED DYNAMICS ANALYSIS

A DYNAMICS ANALYSIS OF THE STOWED CONFIGURATION WAS PERFORMED TO DETERMINE THE LAUNCH LOADS ON THE STORAGE DRUM.

The loads on the storage drum were calculated for the sinusoidal input of 4 g (0-P) specified in Reference 1-1. Although no sinusoidal environment is specified above 200 Hz in the reference, for the purposes of the preliminary analysis it is considered that the 4 g (0-P) environment exists at the first mode frequency of the drum, even if it is in excess of 200 Hz.

Method of Analysis

The determination of the loads consist of analyzing the drum for its natural frequencies and mode shapes and then calculating the response to a 4 g (0-P) sinusoidal input which is considered to act at the frequency of the lowest mode. An amplification factor (Q) of twenty is used for the response calculations.

Mode Shapes and Frequencies

The mathematical models for the selected drum arrangement are shown in Figure 4-6. Because of symmetry only half the drum is modeled. The two models are chosen to represent the symmetric and antisymmetric vibration modes of the drum. There are eleven degrees of freedom for each model. The symmetric model has six translational degrees of freedom and five rotational degrees of freedom while the antisymmetric case has five translational degrees of freedom and six rotational degrees of freedom.

The stiffness matrices for each of the two models is presented in Figure 4-7. The corresponding weight matrices are also presented in Figure 4-7. The weight matrices are presented as rows because the matrix is diagonal. The weight and stiffness matrices are combined to form the dynamic matrix which is then iterated utilizing the Jacobi technique (Reference 4-3) to obtain the mode shapes and frequencies. The mode shapes, normalized to a unit generalized mass, of the first mode for the symmetric and antisymmetric models are presented in Figure 4-8.

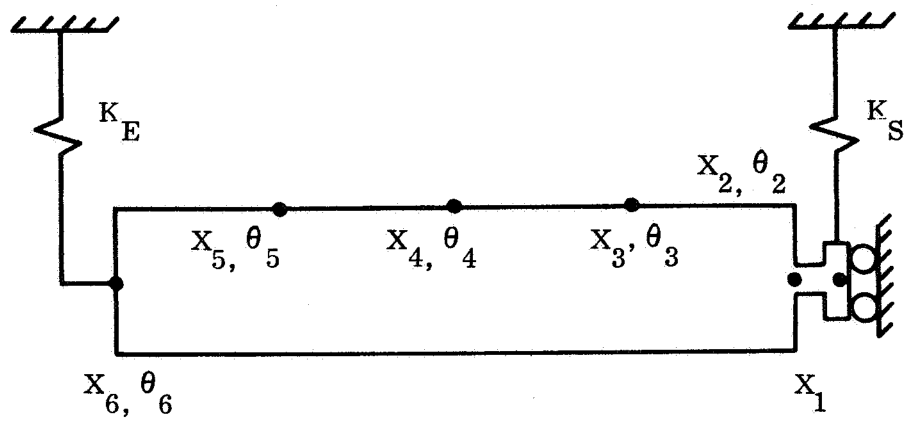

SYMMETRIC MODEL

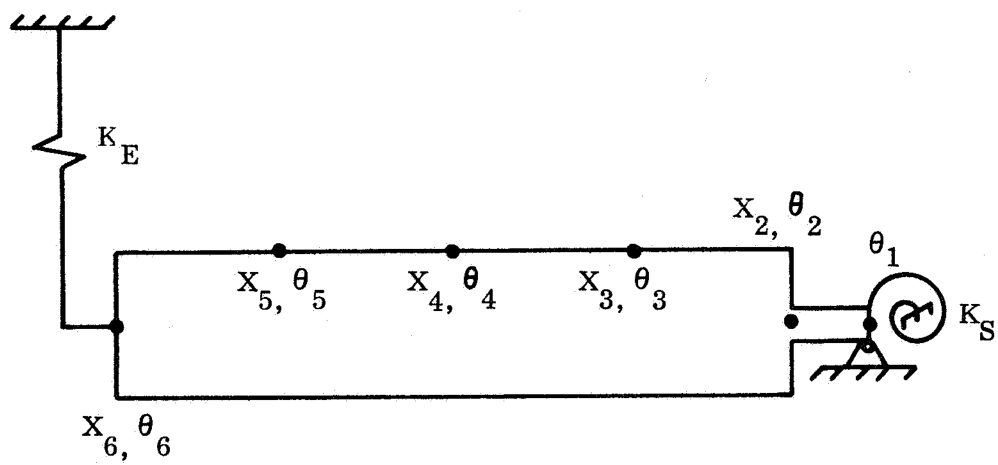

ANTISYMMETRIC MODEL

Figure 4-6. Drum Mathematical Models

Stiffness Matrix - Model 1

0.9152	-.8072	1.8163	0	0	0	0	0	0	0	0	X_1
	2.7256	6.6007	-1.9184	11.2946	0	0	0	0	0	0	X_2
		64.5439	-8.4170	27.3893	0	0	0	0	0	0	θ_2
			3.8368	0	1.9184	11.2946	0	0	0	0	X_3
				177.3248	-11.2946	44.3312	0	0	0	0	θ_3
					3.8368	0	1.9184	11.2946	0	0	X_4
						177.3248	-11.2946	44.3312	0	0	θ_4
							3.8368	0	-1.9184	11.2946	X_5
								177.3248	-11.2946	44.3312	θ_5
									2.1484	-11.2946	X_6
										89.4404	θ_6

= Spring Forces

Mass Matrix - Model 1

6.6											$\ddot{X}_1$
	6.95										$\ddot{X}_2$
		46.6									$\ddot{\theta}_2$
			6.13								$\ddot{X}_3$
				57.0							$\ddot{\theta}_3$
					6.13						$\ddot{X}_4$
						57.0					$\ddot{\theta}_4$
							6.13				$\ddot{X}_5$
								57.0			$\ddot{\theta}_5$
									5.1		$\ddot{X}_6$
										36.3	$\ddot{\theta}_6$

= Inertial Forces

Stiffness Matrix - Model 2

Same as above except
$k_{11} = 6.1489$
$k_{12} = -1.8163$
$k_{13} = 2.72445$

Mass Matrix - Model 2

Same as above except
$m_{11} = 139.0$

Figure 4-7. Mass and Stiffness Matrices

MODE 1 SYMMETRIC - 205 Hz

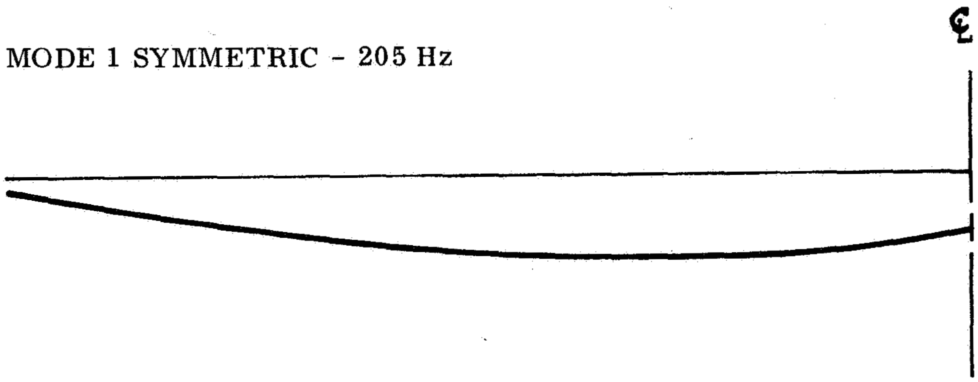

MODE 1 ANTISYMMETRIC - 230 Hz

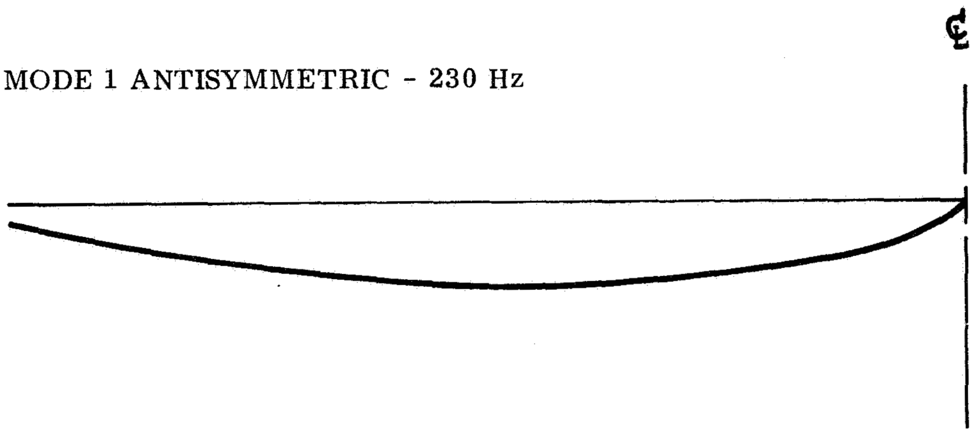

Figure 4-8. Drum Mode Shapes

Response Analysis

The response of the drum to a sinusoidal input is obtained by reducing the system to a series of single degree-of-freedom systems and determining the response of each of the single degree-of-freedom systems to the input. The total response is then obtained by summing these modal responses.

The transformation to model coordinates is accomplished as follows:

$$x = \phi \, \xi \tag{4-5}$$

where:

- x is the physical coordinate
- ϕ is a transformation matrix of mode shapes
- ξ is the modal coordinate

By substituting this transformation into the matrix equation for the system

$$M\ddot{x} + C\dot{x} + Kx = F(t) \tag{4-6}$$

and premultiplying by ϕ^T results in:

$$\phi^T M \phi + \phi^T C \phi + \phi^T K \phi = \phi^T F(t) \tag{4-7}$$

where:

$x, \dot{x}, \ddot{x}$ are the displacement, velocity, and acceleration respectively of each of the mass points

M is a matrix of masses

C is a matrix of damping coefficients

K is the stiffness matrix

$F(t)$ is the forcing function

$\phi^T M \phi = M^* = I$ is the generalized or modal mass

$\phi^T C \phi = C^*$ is the modal damping

$\phi^T K \phi = \lambda$ is a diagonal matrix of system eigenvalues

$F = \phi^T F(t)$ is the modal forcing function

Equation 4-7 is then written as

$$\ddot{\xi} + C^* \dot{\xi} + \lambda \xi = \bar{F} \tag{4-8}$$

Equation 4-8 now represents a series of independent single degree-of-freedom systems which can be solved for ξ.

For the case where $F(t) = F_o \cos \omega t$, the maximum imaginary portion of the response is

$$\xi = \left[(\lambda - \omega^2) + \omega^2 C^{*2} \right]^{-1} \omega^3 C^* M^{*-1} \bar{F} \tag{4-9}$$

which at resonance reduces to

$$\ddot{\xi} = \frac{\omega \bar{F}}{C^* M^*} \tag{4-10}$$

where for an acceleration input

$$\bar{F} = \phi^T F_o = \phi^T M x_{RB} \ddot{x}_S$$

x_{RB} is the rigid body displacement matrix

$\ddot{x}_S$ is the support acceleration

$C^* = 2 \zeta \omega$

$\zeta = C/C_c$

Equation 4-10 can be expressed as

$$\ddot{\xi} = \frac{\phi^T M \, x_{RB} \, \ddot{x}_S}{2 \, \zeta M^*} \tag{4-11}$$

and is the modal response of each mode at its resonant frequency to a sinusoidal forcing function.

To obtain the physical coordinate responses, Equation 4-5 is applied resulting in

$$\ddot{x} = \phi \ddot{\xi} \tag{4-12}$$

The external forces on the system are then expressed as

$$\bar{F} = M \ddot{x} = M \phi \ddot{\xi} \tag{4-13}$$

For the drum load calculations only the first mode was used in the response calculations: the resultant external forces are presented in Table 4-2 for both the symmetric and antisymmetric models.

Table 4-2. External Drum Forces

	Symmetric Model (f_1 = 205 Hz)			Antisymmetric Model (f_1 = 230 Hz)		
Coordinate	Shear (lb)	Moment (in.-lb)	Acceleration (g's)	Shear (lb)	Moment (in.-lb)	Acceleration (g's)
1	468	0	71.0	0	1736	0
2	569	+80	81.9	298	180	42.9
3	579	+30	94.5	455	101	74.2
4	545	-90	88.9	512	-38	83.6
5	356	-200	58.0	369	-179	60.2
6	58	-150	11.4	100	-144	16.3

4.3 DEPLOYABLE BOOM ANALYSIS

THE 1.34 IN. DIAMETER "OFF-THE-SHELF" BI-STEM IS MORE THAN ADEQUATE FOR THE ORBITAL LOADING CONDITIONS.

Introduction

This section contains the structural analysis for the storable extendible boom element of the roll-up solar array. The member is subjected to deployed condition environment as sited in Reference 1-1 and must deploy in a 1g field to demonstrate the operating function of the arrays release, deployment, and locking mechanisms, with suitable test equipment. The 1g demonstration will be accomplished by an Engineering Demonstration Model as described in Section 6.

The deployed condition environment is schematically represented in Figure 4-9. The blanket preload, required to keep the array surface plane and to provide a minimum natural frequency of 0.04 Hz, is the primary structural load. This loading is coupled with the thermal bending of the rod due to the temperature gradients associated with a solar illumination at 260 mw/cm^2 intensity. A pitch angle acceleration of 2×10^{-5} $radians/sec^2$ may also be applied to the array in combination with the above loading conditions; however, the magnitude of the resultant force is so small as to render this condition negligible. (See Section 4.1).

The structural requirements associated with the aforementioned deployed condition are:

a. The boom element shall have a positive margin of safety for both ultimate and limit design loads as defined in Reference 1-1.

b. Under the above loading, with the exception of dynamic load inputs, the solar array surface shall maintain a plane normal to the sun within $\pm 10^\circ$. Thus the angle α, shown in Figure 4-9 shall be such as to limit the resultant tip deflection of the rod end to be less than $\ell \sin 10^\circ$.

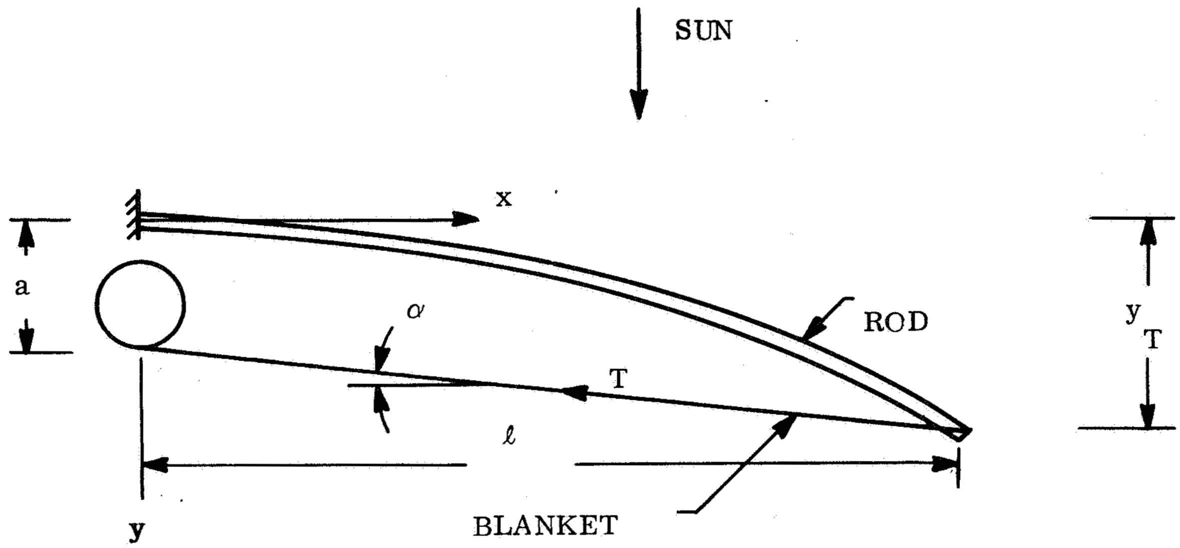

a. SYSTEM SKETCH

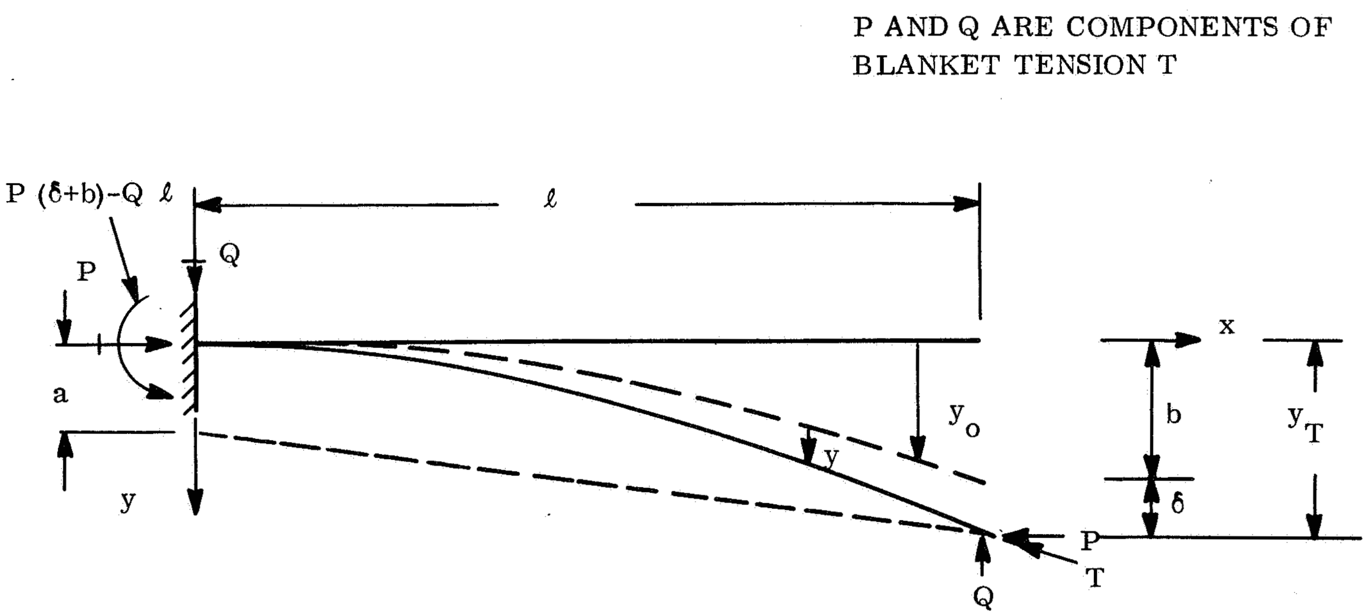

b. FREE-BODY DIAGRAM OF DEPLOYMENT ROD

Figure 4-9. Deployment Rod Orbital Thermostructural Loading

The extension rod for the 1g demonstration model will be loaded as shown in Figure 4-10. In addition to the blanket preload, a vertically deployed array will apply forces to the rod at its end directed parallel to the local vertical. The forces applied at the rod tip will be the gravity forces associated with blanket and end rod weights. The weight of the boom element will also be significant. For this loading condition, the boom element must maintain structural integrity or else deployments aids are needed.

Analysis - Deployed Condition

The details of the analysis of the extension rod for the deployed condition are shown in Appendix C. As mentioned, the rod is subjected to a temperature gradient and the solar panel blanket tension. The analysis contained herein is for the geometry of Figure 4-9, which shows an offset or eccentricity between the extension rod and the blanket at the drum end (i.e., distance a in Figure 4-9), as was the case in the early stages of this study. In the selected configuration, there is no such offset. However, to obtain results for the present configuration, it is only necessary to set a = 0 in the solution obtained. Thus, the effect of such an offset can be assessed and the solution of the problem is more general.

In order to facilitate the integration of the beam-column equation the unloaded rod deflection curve under a linear temperature gradient across the rod section has been assumed to be parabolic that is (see Figure 4-9)

$$y_o = k x^2 = \frac{b}{\ell^2} x^2 \tag{4-12}$$

where b is the tip deflection of a rod of length ℓ for a given temperature gradient ΔT. Although the actual rod curvature due to such a gradient would be constant, it is felt that this assumption will give sufficiently accurate results. For a perfectly straight rod to which is applied a gradient ΔT, the tip deflection will be:

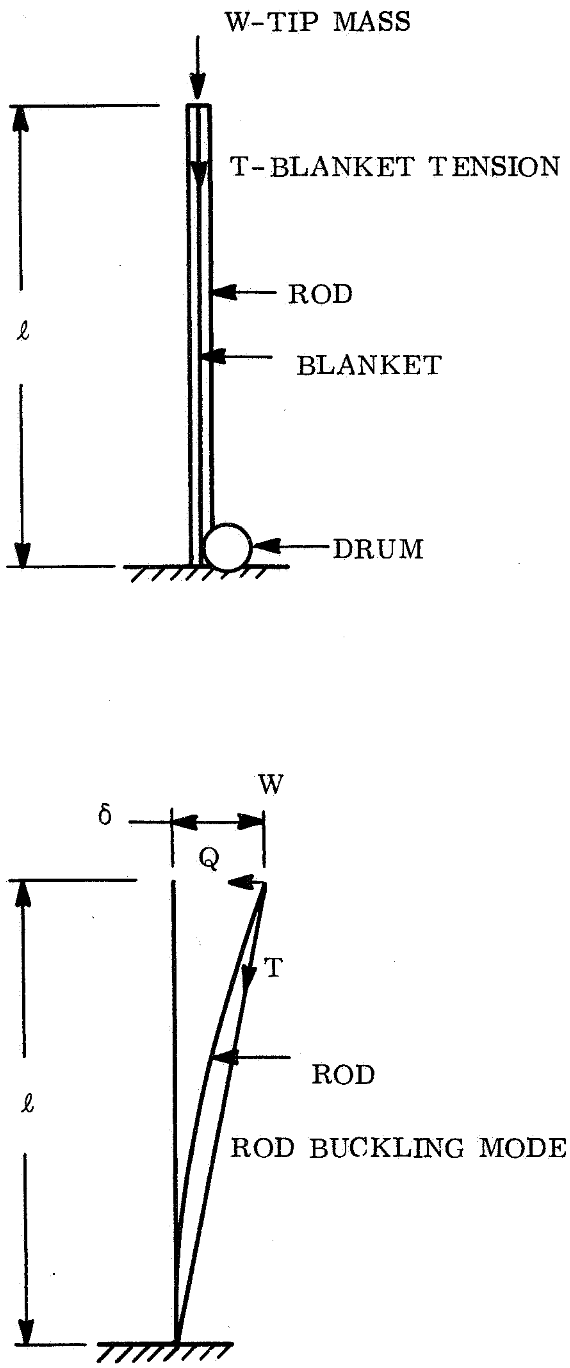

Figure 4-10. Rod Loading - 1g Demonstration Model

$$b = \frac{\alpha \, \Delta T \, \ell^2}{4 \, r} \qquad (4\text{-}13)$$

where α - coefficient of thermal expansion

r - rod radius

At this point, the differential equation of the elastic curve can be solved. We have

$$EI \frac{d^2y}{dx^2} = -M = - \left\{ P\,(y+y_o) + Q\ell - P\,(\delta + b) - Qx \right\} \qquad (4\text{-}14)$$

where P and Q are the components of the blanket preload T and y and δ are as shown in Figure 4-9. The solution of the above for the resultant deflection curve for the boundary conditions of a cantilever beam is:

$$y = -\frac{Q}{kP} \sin kx + \left\{ \frac{Q\ell}{P} - \delta - b - \frac{2b}{k^2 \ell^2} \right\} \cos kx$$

$$- \frac{b}{\ell^2} x^2 + \frac{Q}{P} x + \delta + b + \frac{2b}{k^2 \ell^2} - \frac{Q\ell}{P} \qquad (4\text{-}15)$$

where

$$k = \sqrt{\frac{P}{EI}}$$

E - Modulus of elasticity

I - Rod Moment of inertia

At this point δ must be determined. At $x = \ell$, $y = \delta$ and using $\frac{Q}{P} = \frac{b+\delta-a}{\ell}$,

$$\delta = b \left\{ \frac{2\,(1-\cos k\ell) - k\ell \sin k\ell}{k\ell \sin k\ell} \right\} + a \left\{ \frac{\tan k\ell - k\ell}{\tan k\ell} \right\} \qquad (4\text{-}16)$$

or

$$\delta = \delta_1 + \delta_2 \qquad (4\text{-}16a)$$

$$\delta = \frac{b\left\{2\,(1-\cos k\ell) - k\ell \sin k\ell\right\} + a\left\{k\ell \cos k\ell\,(\tan k\ell - k\ell)\right\}}{k\ell \sin k\ell} \tag{4-16b}$$

Equation 4-16 is arranged such that the contribution of the deflection δ due the thermal gradient (δ_1) and the blanket offset (δ_2) can be obtained separately. We can see from Equation 4-16b that at $\sin k\ell = 0$, δ is infinite, and the critical load corresponds to $k\ell = \pi$ and

$$P_{CR} = \frac{\pi^2 EI}{\ell^2} \tag{4-17}$$

Thus the critical load is the same as a pin-ended column. Also, by making "a" negative, we can decrease the deflection when ΔT is applied as shown in Figure 4-9.

To obtain the bending moments on the rod substitute Equations 4-15 and 4-16 into 4-14. To obtain the location of the maximum bending moment we have:

$$\frac{dM}{dx} = 0 \tag{4-18}$$

Solution of Equation 4-18 for x yields:

$$x = \frac{1}{k} \tan^{-1} \left\{ \frac{2b\,(1-\cos k\ell) - a k^2 \ell^2 \cos k\ell}{\left[a k^2 \ell^2 + 2b\right] \sin k\ell} \right\} \tag{4-19}$$

Substituting Equations 4-19, 4-15, and 4-16 into 4-14 gives the magnitude of the maximum bending moment. At $x = 0$ we can obtain the root bending mount which is:

$$M_R = T\,a \tag{4-20}$$

The total deflection of the rod tip is:

$$y_T = b + \delta \tag{4-21}$$

In order to satisfy the requirements of Reference 1-1 it is necessary that:

$$y_T < \ell \sin 10^{o} \tag{4-22}$$

and that the stresses induced in the rod in this condition are of such a magnitude as to insure a positive margin of safety.

The solutions for Equations 4-13 and 4-16a have been programmed on the GE deskside time-shared computer system. The program also gives the permissible deflection, the maximum bending moment on the rod and its location and the root-bending moment.

Stress-free rod curvature developed during fabrication can be included in the above analysis, if it is again assumed that the associated rod deflection is parabolic, merely by modifying b such that

$$b = b' + b'' \tag{4-23}$$

where

b' - rod tip deflection due to a temperature gradient

b'' - rod tip deflection due to initial rod curvature.

The deployed analysis was performed using the following rod characteristics:

Rod	-	Bi-STEM
Diameter	-	1.34 in.
Thickness	-	0.007 in.
Weight	-	6.37 lb
Material	-	Silver Coated Stainless Steel
Length	-	33.5 ft.
Youngs Modulus	-	29×10^6 Psi
Minimum Moment of Inertia	-	0.01185 in.^4
Coefficient of Thermal Expansion	-	9.3×10^{-6} in./in./^{o}F
Solar Absorbtance	-	0.12
Emittance	-	0.04

For a temperature gradient at 53.9°F based on the analysis of Reference 4-4 and a blanket tension of 4.0 pounds, the following results were obtained:

Rod Tip Deflection	- 35.68 in.
Permissible Deflection	- 69.81 in.
Maximum Bending Moment (at rod mid-length)	- 46.44 in.-lb (ultimate)

Ultimate Bending Strength = 984 in.-lb (Reference 4-5)
M.S. = high

Analysis - 1 g Demonstration Model

The forces applied to the extendible boom in the 1 g field are as shown in Figure 4-10. In addition to the blanket tension (T), there will be additional forces (W) consisting of rod end fittings, edge member, and Kapton strips, and solar cells (see Section 6), which, unlike the force T, are directed along the local vertical. It has been shown in the previous paragraphs that such a member loaded at its tip by a force directed through a fixed point at or near its base (i.e., such as the rod in the deployed condition) has a critical buckling load equal to the Euler buckling load for a pin-ended column. However, it is well known that a column loaded by a force, such as W in Figure 4-10 directed as shown is a fixed-free Euler column and fails at a value of load equal to $(\pi^2 EI)/4\ell^2$ which is one-quarter of the pin-end critical load. The column shown in Figure 4-10 has a critical load which is within a range bounded by the fixed free and the pined-pined Euler buckling loads.

The analysis for the extension rod loaded by tip forces Q and P is shown in Appendix A. It should be noted that the deflection is opposed by the lateral force, Q, which is a component of the blanket tension force T. The result obtained solving for a tip deflection δ is:

$$\delta = -\frac{Q}{Pk}(\tan k\ell - k\ell) \qquad (4\text{-}24)$$

For the demonstration model of Figure 4-10 we have:

$$a = 0$$

$$Q = T \frac{\delta}{\ell}$$

$$P = T + W$$

If the above relations are substituted into Equation 4-24, we have:

$$\delta \left[1 + \frac{T}{P\,k\ell} \left(\tan k\ell - k\ell \right) \right] = 0$$

For δ other than zero, the quantity in brackets must be zero, which is satisfied by:

$$\tan k\ell = - \frac{W}{T}\, k\ell \qquad (4\text{-}25)$$

The preceding solution does not account for the distributed loading associated with the members weight which is significant in a 1g field. This effect would be more complicated to deal with in this manner; so an approximate critical load was assumed for this study by applying a percentage (i.e., 30 percent in this case) of the total rod weight to the tip. Thus W will include, in addition to the weight of the other items mentioned, three-tenths of the weight of the rod.

For the Engineering Demonstration Model loading:

$$T = 4.00 \text{ lb}$$

$$W = w_1 + w_2 + 0.30\, w_3$$

where

w_1 = weight of leading edge member
= 1.13 lb

w_2 = weight of array strips (with cells)
= 1.20 lb

w_3 = weight of deployable rod
= 6.37 lb

$W = 4.24$ lb

For $\frac{W}{T} = 1.06$. Figure 4-11 shows the graphical solution of Equation 4-25 ($m = 2.04$).

$$(T + W)_{CR} = \frac{m^2 EI}{\ell^2} = \frac{(2.04)^2 \ (29 \times 10^6) \ (0.01185)}{(402)^2}$$

$$(T + W)_{CR} = 8.85 \text{ lb}$$

$$T + W = 4.00 + 4.24 = 8.24 \text{ lb (limit)}$$

$$MS = \frac{8.85}{1.25\ (8.24)} - 1 = -0.14$$

<u>Discussion</u>

The preceding analysis indicates that the structural safety margin for the off-the-shelf BI-STEM rod is high when subjected to the deployed condition environment, but is negative if extended vertically to its full length in 1 g for the demonstration model. Therefore, it can be concluded that:

a. A smaller BI-STEM unit could be considered for use in a flight system.

b. The present demonstration model can not be extended to its full length without experimental determination of the load carrying capability for the 1g vertical deployment. Such an experimental determination has been made and is described in Section 6.3.

The deflection calculated for the BI-STEM rod is within that allowed to satisfy the requirements in Reference 1-1. However, uncoated BeCu would deflect considerably less in the same environment and would do so with a positive margin of safety for the deployed condition. Of course, in a 1 g field, a BeCu rod would fail at a column load some 50 percent lower than a stainless steel member.

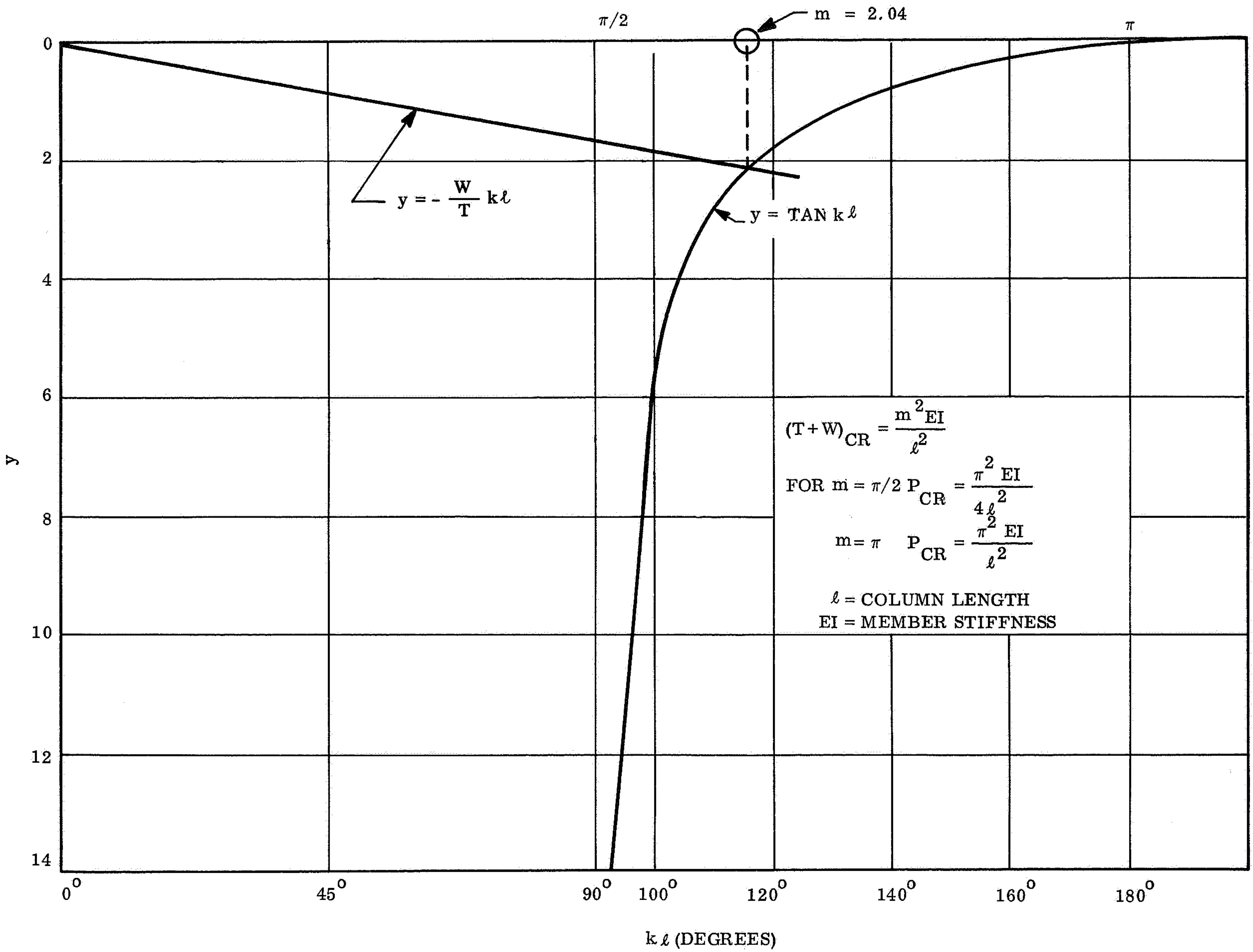

Figure 4-11. Critical Buckling Loads for 1g Modal Rod

4.4 STOWED CONFIGURATION STRUCTURAL ANALYSIS

A STRUCTURAL ANALYSIS OF THE STOWED CONFIGURATION HAS BEEN PERFORMED IN SUFFICIENT DETAIL TO SUBSTANTIATE THE INTEGRITY OF THE MAIN STRUCTURAL MEMBERS AND TO ISOLATE POSSIBLE TROUBLE AREAS IN THE DESIGN.

The structural analysis of the roll-up array stowed configuration has been based on the state-of-the-art preliminary design analytical methods and will serve as a basis for further optimization studies during Phase II of the program. Consideration has been given to both dynamic and thermal environments in applying the most severe design conditions to the structural elements and, in addition, adequate margins of safety were maintained in joints and other places of stress concentrations to minimize the effects of fatigue during random and acoustic excitations.

The primary consideration in sizing the support structure was to minimize weight wherever possible; however, it was also necessary to provide sufficient stiffness in the inner and outer supports to dynamically isolate them from the storage drum. This is necessary to attenuate the drum response during vibration. The maximum loads on the drum are a result of the sinusoidal environment and were derived from the mathematical model described in the dynamic analysis section. The results of the dynamic analysis are shown in the loading diagram on Page D-1 of Appendix D.

The storage drum is the main structural member in the support, so a major portion of the analytical effort has been spent to ensure its feasibility and the integrity of the design. The drum reacts the loads from the solar array and transfers them through shear and bending to the inner and outer end supports. From the outer support, the loads are diffused directly into the vehicle structure. The torsion in the outer support, which is caused by the partial end fixity on the drum, is reacted by the torque box located on the lower portion of the end support. The load path to the center support goes through a set of bearings and a support tube which reacts the fixed end moments from the drum. Longitudinal loads (along the centerline of the drum) are reacted as thrust loads on the bearings, transferred through the support tube and sheared directly into the vehicle structure through the plate on which the connectors mount. The outer supports are not intended to be part of the load path for this loading condition.

The drum consists of a cylindrical shell and inner and outer end caps all of which are beryllium. This is an ideal material for this application, because it provides a stiffness-to-weight ratio and possesses excellent thermal properties thereby reducing the effects of thermal loadings. The shell is made in four pieces and fabrication consists of bonding the quadrants to channels that run longitudinally to the end caps. The bonding should not present any structural problem as far as loads are concerned since the shear stresses in the bond are low.

The detailed work sheets for this structural analysis are included as Appendix D. A summary of the significant results of this analysis is contained in Table 4-3.

Table 4-3. Stress Analysis Summary

Member	Material	Critical Condition *	M.S.
• Storage Drum Shell	Be	• Buckling of shell	+0.25
		• Bearing load due to blanket	High
		• Shear stress in longitudinal joints	High
• Outboard End Cap	Be	• Crippling of radial webs	+0.49
		• Bearing in tapered hole	+0.84
• Inboard End Cap	Be	• Crippling of radial webs	High
		• Bearing radial load	+0.15
		• Bearing thrust load	High
• Leading Edge Member	Be	• Bending of rod	High
		• Shear stress in longitudinal bond	High
• Outboard End Support	Al	• Shear load at hinge	+0.58
		• Bearing load at hinge	+0.53
• Center Support	Al	• Crippling of tube	High
		• Bending of flange	+0.11
		• Shear in weld	+0.63

* Using ultimate factor of safety of 1.25 applied to limit loads obtained from 4.0 g (O-P) sine vibration input.

4.5 ELECTRICAL PERFORMANCE ANALYSIS

THE ELECTRICAL PERFORMANCE OF THE ARRAY WAS CALCULATED USING THE GE-MSD SOLAR ARRAY I-V CURVE COMPUTER PROGRAM.

A set of coefficients for use in the GE-MSD Solar Array I-V Curve Computer Program was generated for two cell types: (a) 8-mil thick, 2-ohm-cm, and (b) 8-mil thick, 10-ohm-cm. This computer program calculates the current/voltage characteristics of the whole array, taking into account the following performance parameters:

a. Solar intensity

b. Temperature

c. Solar incidence angle

d. Series cells in a string

e. Parallel cells in a string

f. Number of strings

g. Basic cell characteristics (temperature-dependent, I-V characteristics based on measured cell data)

h. Losses and uncertainties

The output of the program is a listing, for each different operating condition, of voltage versus total current and power. It calculates the array output based on the I-V characteristics of a single cell, adjusting the voltage and current scale factors to account for the numbers of cells in series and parallel. The single-cell, I-V curve is obtained from

$$I = I_{sc} - \frac{V}{R_p} - I_o \left[e^{K(V+R_s I)} - 1 \right] \qquad (4\text{-}25)$$

where

I = cell current output

V = voltage on cell.

The coefficients are:

I_{sc} = Illumination current (virtually equal to the short circuit current)

R_p = Shunt resistance of the cell

I_o = Reverse saturation current of the ideal diode characteristic

K = Coefficient of the exponent, $(V + R_s I)$

R_s = Series resistance of the cell.

The coefficients are treated as functions of temperature, using sixth-degree polynomial approximations to more accurately reflect changes in cell characteristics with temperature.

The correction for angle of incidence includes the cosine and an allowance for increased reflection from the cell and filter at large incidence angles, and is applied to I_{sc} as a multiplier. Other loss factors are also applied to I_{sc}, and the voltage component of radiation damage is applied as a downward voltage shift to the basic I-V curve.

I-V calculations were made using this program with 8-mil, 2 ohm-cm cell characteristics and with 8-mil, 10-ohm-cm cell characteristics. These results were checked against the empirical data contained in Reference 4-6 for various temperatures ranging from +120 to -120^{o}C. Figure 4-12 shows some of these data plotted on Figure 4 of Reference 4-6 for 2-ohm-cm cells. Figure 4-13 shows some of these data plotted on Figure 8 of Reference 4-6 for 10 ohm-cm cells. There is very good agreement between these curves and the calculated points obtained from the I-V Curve Computer Program.

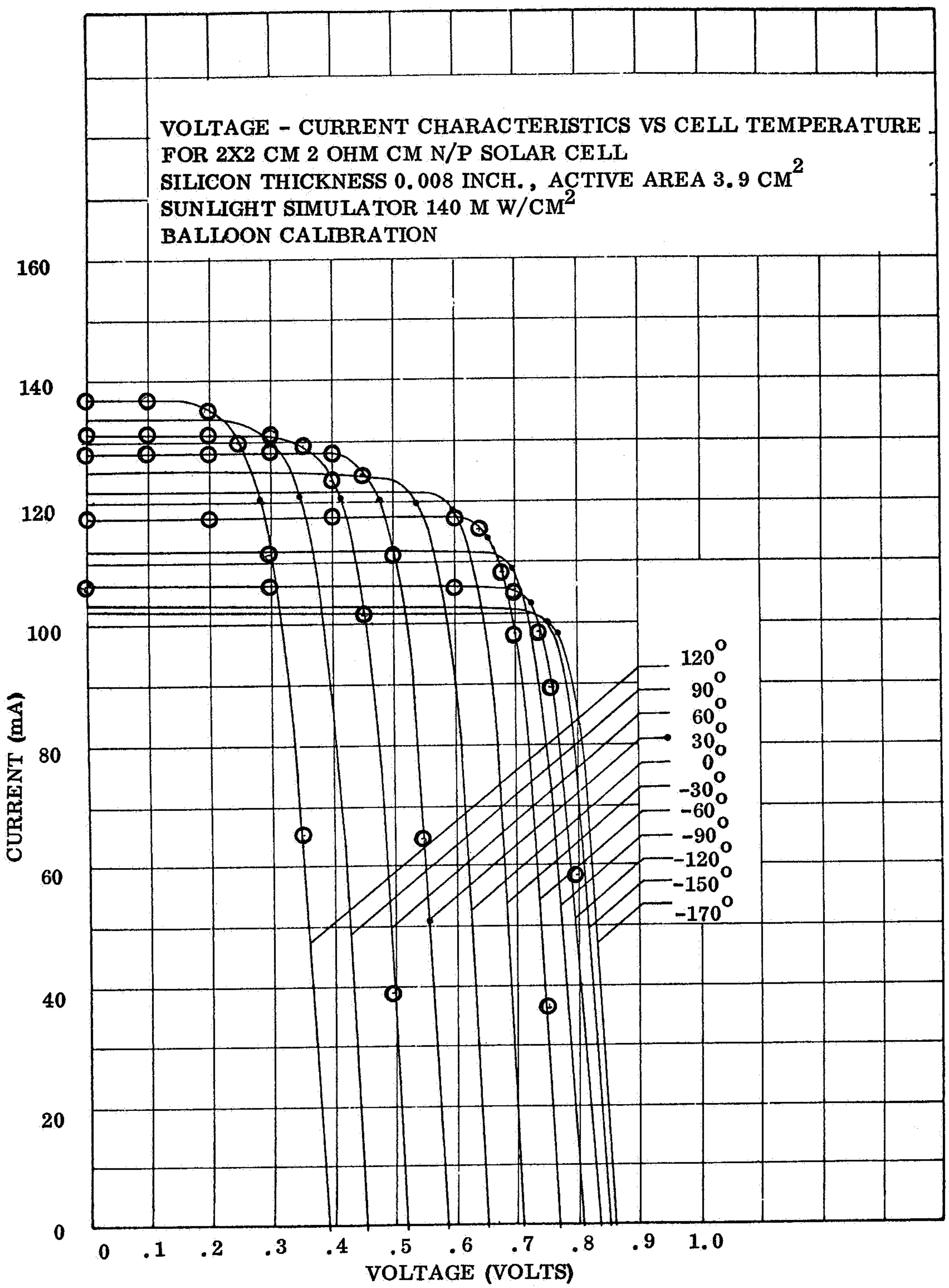

Figure 4-12. Solar Cell Characteristics, 2-Ohm Cm, 8-Mil

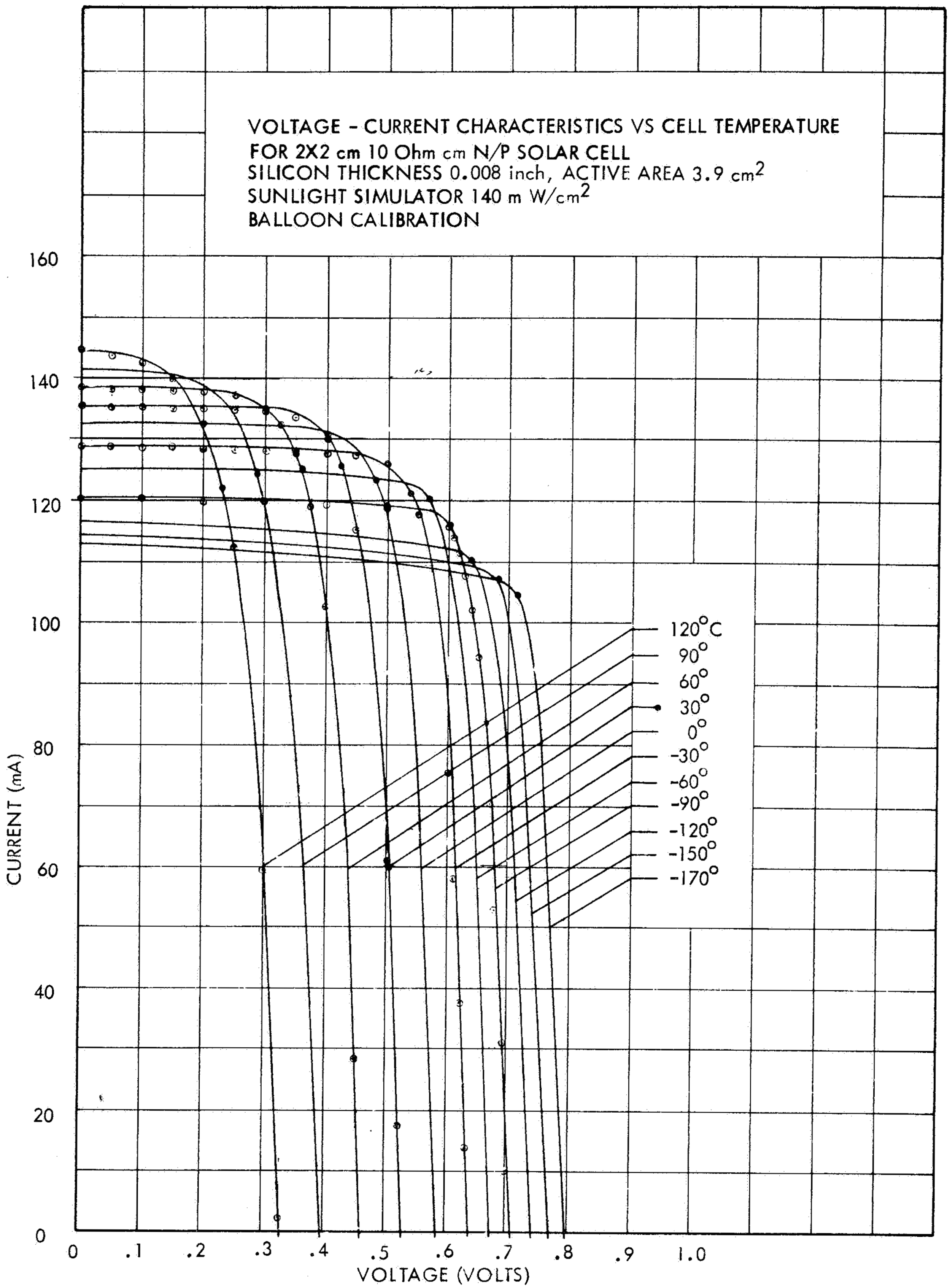

Figure 4-13. Solar Cell Characteristics, 10-Ohm-Cm, 8-Mil

This program with the appropriate set of cell coefficients was used to obtain the array I-V curves shown in Figures 4-14 and 4-15 for 2-ohm-cm and 10 ohm-cm cell, respectively.

The utilization of 2 ohm-cm cells results in a calculated maximum power (at $55^{o}C$) of 2523 watts at 102 volts. This is based on 3.8 cm^2 of active area per cell (bar contact) and includes an estimated short-circuit current loss of six percent (1.5 percent for cover glass transmission and 4.5 percent for manufacturing and assembly) and the loss associated with a 10-degree solar angle of incidence.

The similar curve utilizing 10-ohm-cm cells results in a calculated maximum power of 2294 watts at 90 volts.

Thus, cells with a 2-ohm-cm base resistivity are required to meet the requirements of 10 $watts/ft^2$ of module area.

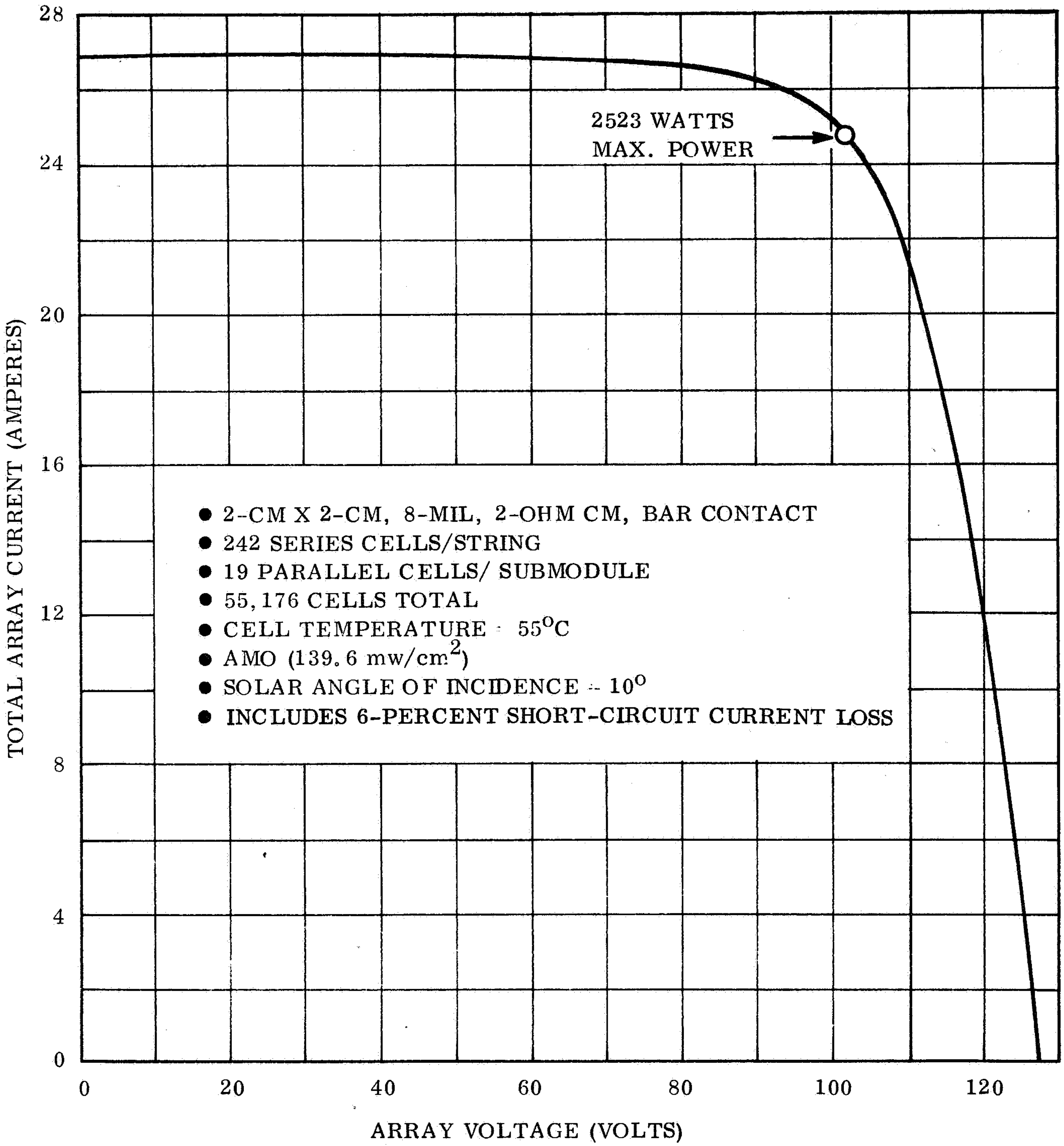

Figure 4-14. Array I-V Curve, 2-Ohm-Cm, 8-Mil

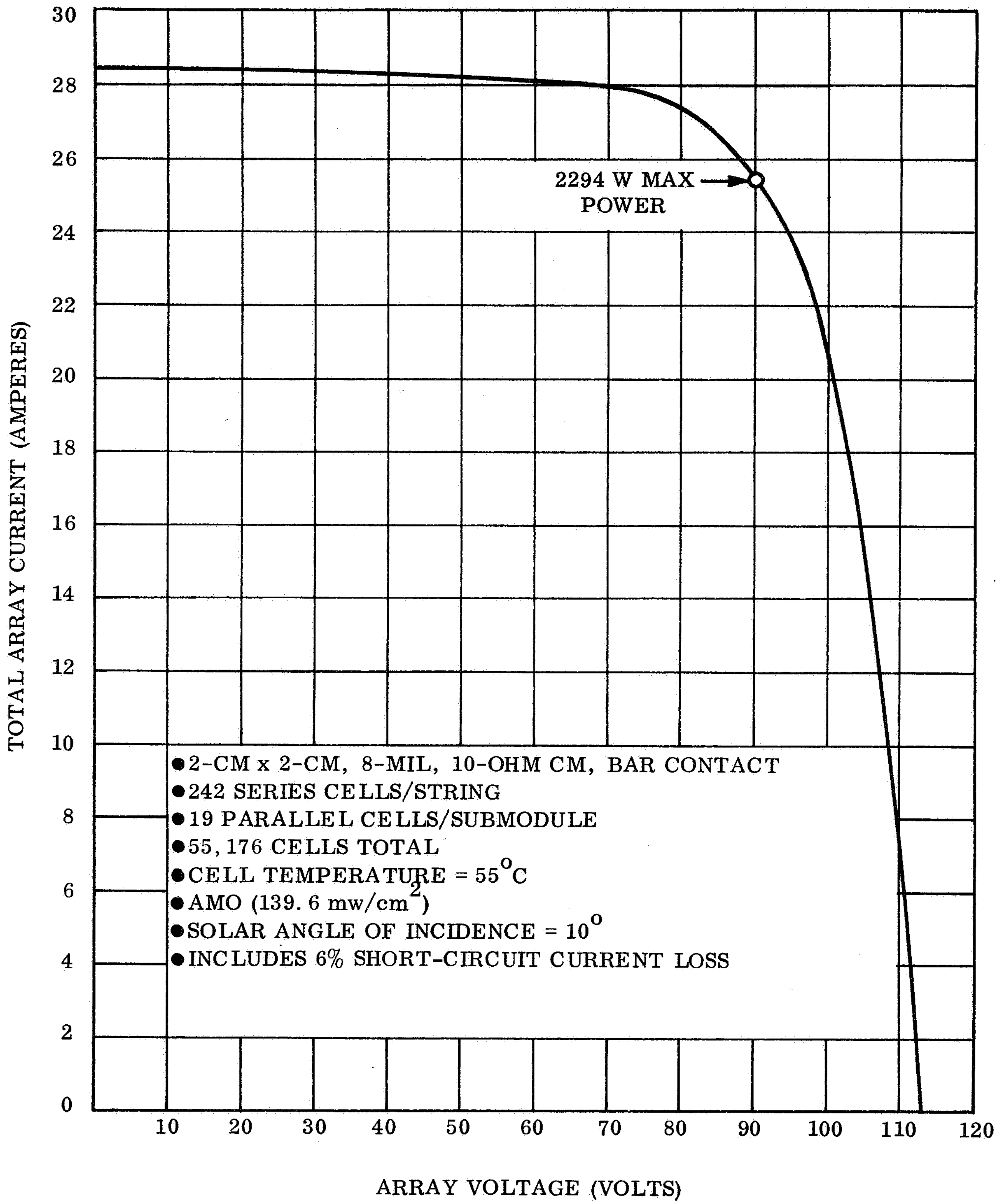

Figure 4-15. Array I-V Curve, 10-Ohm-Cm, 8-Mil

4.6 THERMAL ANALYSIS

4.6.1 ARRAY TEMPERATURE ANALYSIS

THE AVERAGE ARRAY TEMPERATURE AT 1.000 AU IS 123°F (50.5°C). THIS TEMPERATURE CAN BE MAINTAINED WITHOUT RESORTING TO OPTICAL COATINGS ON THE ARRAY BACK SURFACE.

A thermal analyses of the deployed roll-up solar array has been conducted to determine the equilibrium temperatures at 1.000 AU and at 0.733 AU. The geometric relationship of the array and vehicle is shown in Figure 4-16. The cell side of the array is assumed to have an unobstructed view of space. The conversion of solar to electrical energy is taken as 10 watt/ft^2 of array, and the cell packing factor is 0.90. The vehicle wall was assumed to have an emittance of 0.8 and behave as an adiabatic body. The optical properties of the array constituents are summarized in Table 4-4.

Table 4-4. Optical Properties of Array Components

	α_s	ϵ[1]
Solar cell/filter/glass composite	0.71[3]	0.8
2 mil Kapton backed by solar cells	--	0.67[2]
Inactive array surface	0.70	0.65

Notes:

1. α_s = solar absorptance, ϵ = infrared emittance
2. Estimated value based on previous measurements by the General Electric Company on bare Kapton H film
3. Measurements made by the General Electric Company show lower α_s values for N/P than for P/N cells, due to higher reflectance in the near-infrared at the back of the cell. Filter is the blue type, with a cut-on at 0.41 μ.

In order to more accurately assess the vehicle effects upon the array temperature, a radiation network was constructed which considered five bodies rather than simply the vehicle and the array each as a lump. The array was divided into three sections, each 133 inches in length; the vehicle itself was broken up into two halves, each 96 inches in length. The drum was not included because of its generally small influence on the array. The temperature differential across the entire array is estimated to be 0.75° C under a solar illumination of 260 mw/cm^2 in a space environment. A large part of this drop develops through the adjacent layers of adhesive and Kapton (each 2 mils thick) at the back face of the array.

A typical equation of the network is shown below, and represents the heat balance per unit area of an array section.

$$S \alpha_s - P = (F_{F-S} \bar{\epsilon}_F + F_{B-S} \bar{\epsilon}_B) B_A + (F_e F)_{B-V_1} (B_A - B_{V_1}) \qquad (4\text{-}26)$$

$$+ (F_e F)_{B-V_2} (B_A - B_{V_2})$$

where:

S = incident solar flux at 1.000 AU (or 0.733 AU)

α_s = solar absorptance of the array front surface

P = solar energy converted

F = geometric view factor

F_e = emittance factor

B = black body emission

$\bar{\epsilon}$ = average surface infrared emittance

Subscripts

F = front array surface

B = array back surface

V_1 = vehicle section nearest array

V_2 = vehicle section furthest from array

A = array

S = black space

A solution of the five equations of the network resulted in the following temperatures

	1.000 AU	0.733 AU
Array Section Furthest from Vehicle	121^{o}F (49.4^{o}C)	224^{o}F (106.7^{o}C)
Array Section Nearest to Vehicle	125 (51.7)	226 (107.8)
Array Section Located Between the Above	122 (50.0)	225 (107.2)
Vehicle Section Nearest the Array	-82 (-63.3)	-16 (-26.7)
Vehicle Section Furthest from Array	-168 (-111.1)	-116 (-82.2)

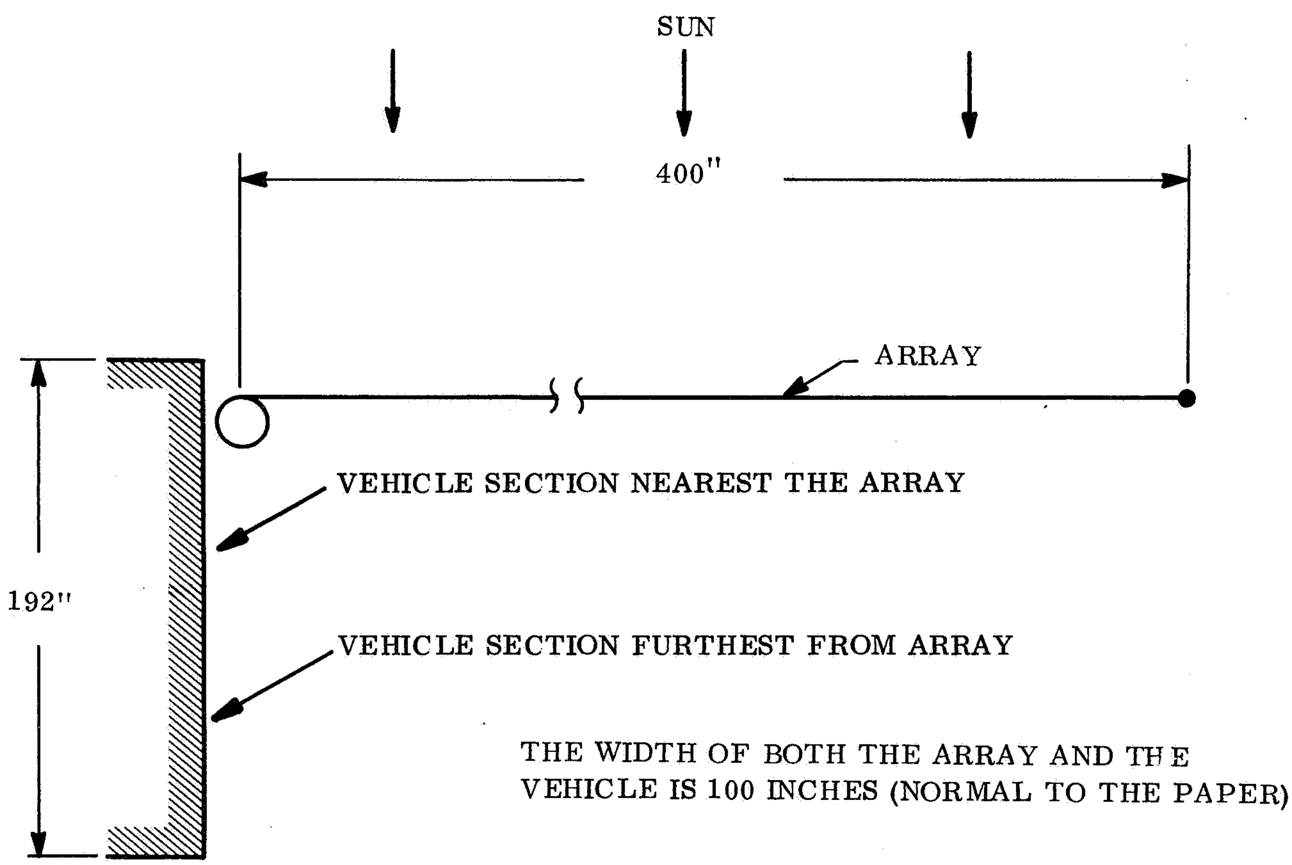

Figure 4-16. Array/Vehicle Geometric Relation

The temperature history of the array after emergence from a planetary shadow is shown in Figure 4-17.

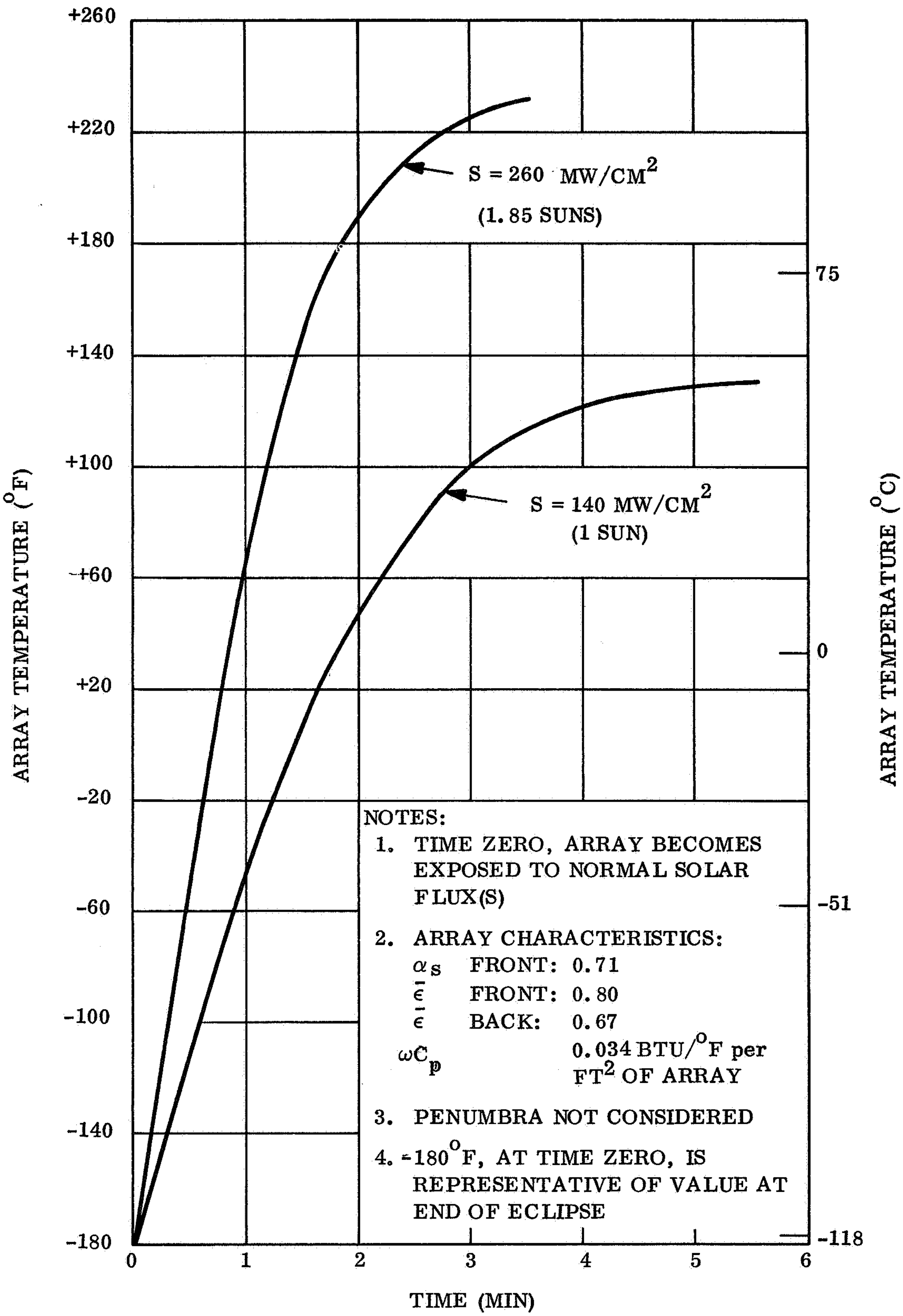

Figure 4-17. Temperature History of Array After Emergence From Planetary Shadow Into Sunlight (Array Deployed)

4.7 ARRAY BLANKET EDGE CURLING ANALYSIS

OBSERVABLE ARRAY BLANKET EDGE CURLING SHOULD NOT OCCUR ON THE FLIGHT CONFIGURATION ROLL-UP SOLAR ARRAY DESIGN.

Figure 4-18 illustrates the edge curling phenomenon observed on the full-size demonstration model which was displayed at the mid-term contract review presentation. This type of edge curling can readily be observed on an ordinary household roll-type window shade. Some possible explanations for the edge curl phenomenon considered here are as follows:

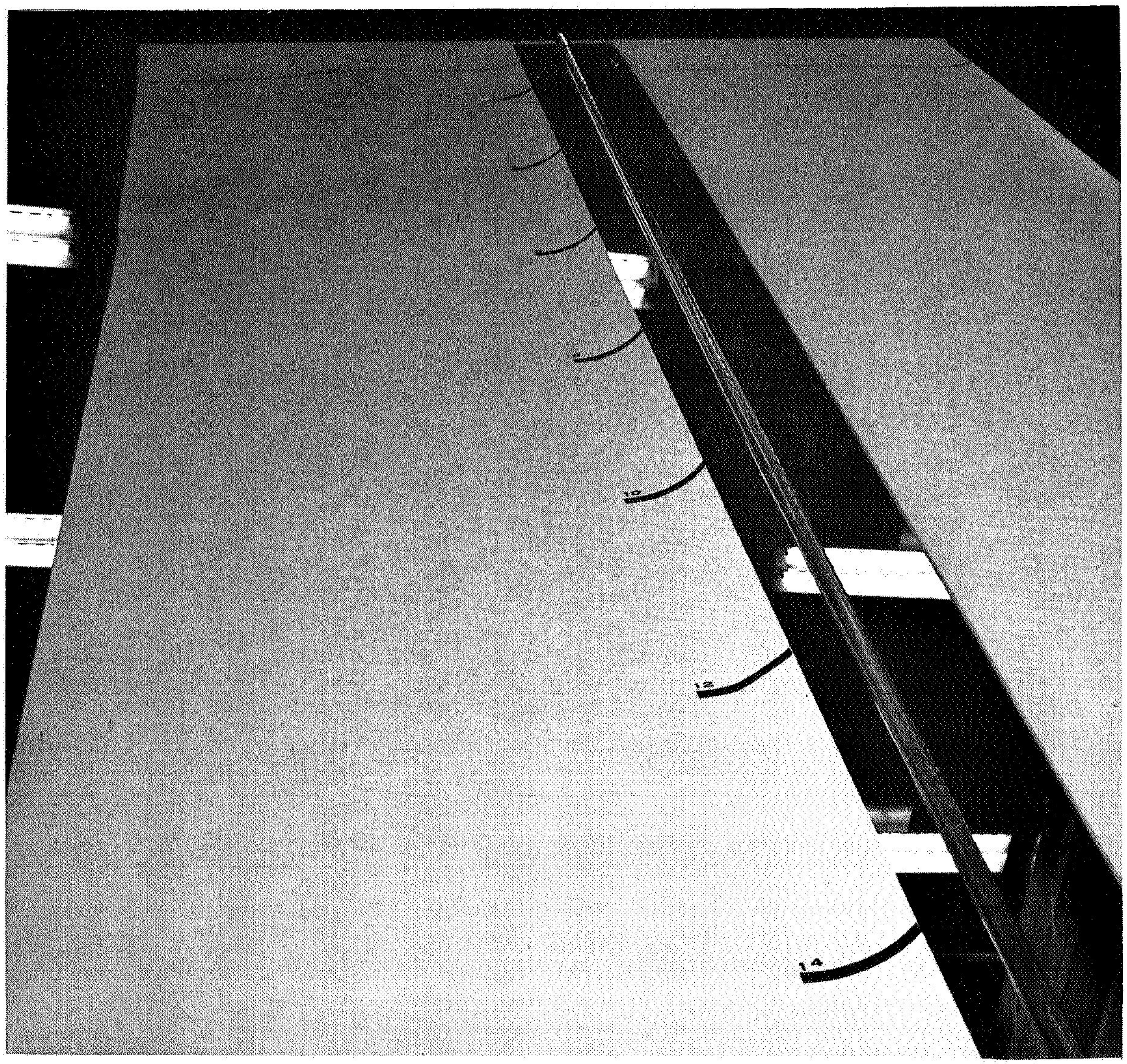

Figure 4-18. Blanket Edge Curl on a Solar Array Demonstration Model Using a Paper Blanket

a. It is induced by the stresses produced in the blanket by the effects of the end loads applied to the blanket.

b. It is induced by the stresses resulting from the unrolling of the blanket from the drum. Stresses are created because of the normal residual curvature formed in a sheet when it is wrapped around a drum.

c. It is induced by the edges being of greater length than the center section, due to previous high edge loadings or environmental effects.

It was concluded from consideration of these explanations that the stress patterns in the blanket due to the normal deployed loading conditions do not produce edge curl (explanation a) and that, although the phenomena of explanations b and c can explain observed edge curls for some materials and conditions, they do not apply to the material and loading conditions for the array blanket. Therefore, the overall conclusion is that the edges will not curl on the proposed array blanket.

EFFECTS OF END LOADS

Unrestrained Sheet

First, the possibility that edge curl can result from the tension loads developed in the blanket by the deployment rod was explored using simple analytical models. A thin flat sheet of material (not subjected to end restraints) with tensile forces p uniformly distributed along the ends, was considered as shown in the following sketch:

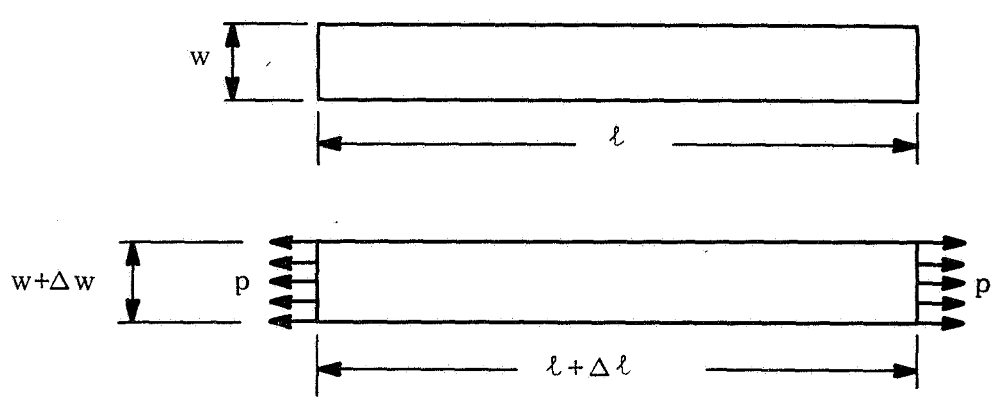

Under these conditions, the length, ℓ, will change due to a uniform unit strain resulting from the direct tensile stresses. The unit strain, $\Delta\ell/\ell$, is given by $\frac{\Delta\ell}{\ell} = \frac{S}{E}$, where S is the stress and E is the modulus of elasticity. In addition, the tensile stresses will produce a uniform lateral contraction of the sheet proportional to Poisson's ratio (μ), $\frac{\Delta w}{w} = -\mu\frac{S}{E}$.

The conclusion drawn is that these uniformly distributed stresses and strains could not produce out-of-plane deflections; and therefore no explantion of the edge curl phenomenon is provided.

Sheet With End Restraints

The next approach was to consider the effects of the ends of the sheet being laterally restrained as they are on the drum and leading edge member of roll-up array. The lateral strain and associated edge displacement, Δw, are then fully suppressed at the ends; while lateral contraction midway between the ends and away from the end effects will be practically unsuppressed, as in the sheet without end restraints. A nonuniform stress and strain distribution, therefore, results between the restrained edges of the sheet and the unaffected midsection, with the possibility of the sheet assuming the shape shown in the following sketch (exaggerated for explanatory reasons):

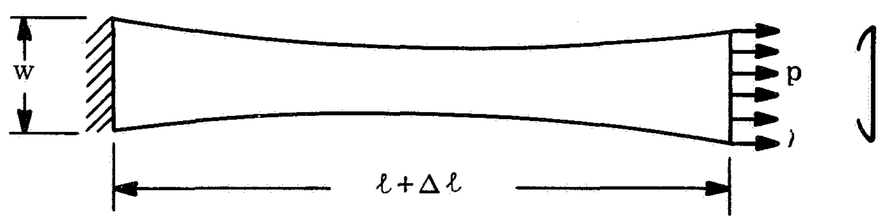

To establish bounds on the differences in length between end and center fibers, a uniform stress distribution along the length, ℓ, is assumed, though variations across the sheet will be allowed.* The lengthwise strain of the center fibers near the ends of the sheet will be slightly less than before. This is due to the suppression of lateral strain and is given by the relationship, $\epsilon_{\ell} = (1 - \mu^2) \frac{S}{E}$, where ϵ_{ℓ} is the unit strain in the direction of ℓ. However, the strain at the edge of the sheet, where the lateral restraint is zero, is still given by the previously developed relationship, $\epsilon_{\ell} = \frac{S}{E}$.

These equations (for two locations in the sheet near an end) illustrate the varying effects of the end restraint on the equations governing the fiber stresses. A complete analysis of the stress and strain distribution throughout the sheet is complex and not readily amenable to hand calculations. However, General Electric's Missile and Space Division has a computer program (SAFE) which allows a detailed solution of this problem and could be used if deemed necessary. This program is described at the end of this Section. However, before this program can be used, consideration must be given to the fact than analyses of nonuniform local end-load problems show that the effects of stress and strain become negligible at a distance from the end of the sheet that is approximately equal to the width.

The fact that the length/width ratio of the proposed array blankets is approximately 9:1 led to the conclusion that nonuniform stresses due to end effects would not explain the edge curl observed at the midsection of the blanket away from the ends. There is also no obvious stress or strain pattern that causes out-of-plane displacements. Therefore, a computer program stress analysis was not carried out, and other explanations of the edge phenomenon were sought.

To verify this conclusion, a simple test was conducted to confirm that end loads will not produce the stresses required to produce the edge curl. This test is described in the next section.

---

* This stress distribution cannot be the actual stress distribution in the blanket, but it provides results which give greater insight into the problem.

Test Sheet

An initially flat sheet of 1-mil Kapton-H film of approximately the same length/width ratio as the proposed array blanket was looped around a pencil at each end (the loop was closed with mylar tape) and pulled by hand to provide end tension loads. In this simple experiment, no tendency for edge curling was observed under either low or high end loads. This confirms the above analytical conclusion that blanket end tensile loads do not induce edge curling.

EFFECTS OF WRAPPING BLANKET ON DRUM

Consideration of the effects of wrapping the blanket on the drum led to the following explanation of the edge curling phenomenom observed in the demonstration model and in household window shades. However, experience with the Kapton-H film indicates that an occurrence would not exist in an array blanket using this material.

If it is hypothesized that wrapping the blanket material onto the drum will stress the material so highly as to produce a permanently curved deformation, then when the sheet is pulled flat by the end loads, the tension load distribution through the thickness of the sheet would become unequal by an amount equal to the magnitude of the additional tension loads in the top fibers required to bend the sheet flat. At a distance from the ends of the sheet, where end effects may be ignored, the otherwise uniform tensile stress distribution through the thickness would be modified by the addition of tension and compression (stresses probably nonlinear in distribution) such as the following:

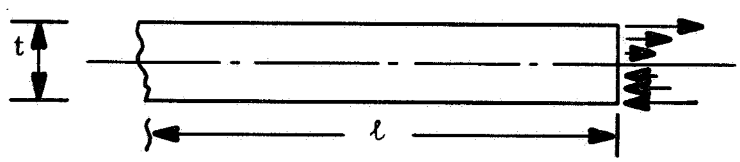

The tensile stresses in the top fibers will tend to produce lateral contraction of the top fibers across the width of the plate, and correspondingly, the compression stresses in the bottom fibers will tend to produce lateral expansion across the width of the plate. It is apparent that these combined contraction and expansion tendencies through the thickness of the sheet will tend to produce a curvature across the width of the sheet. With the sheet restrained flat at the ends, the net result would be an edge curl. Thus, it may be concluded that if the blanket material properties are such that it takes on the curved shape of the drum after wrapping, the above analysis could explain its edge curvature. Experience with paper and window shades, which do tend to take a curved shape after wrapping, would indicate the analysis is applicable to these materials. However, experience with Kapton-H film, which does not assume any residual curvature even after being wrapped on a lead pencil, would indicate the analysis does not apply to the proposed array blanket material.

EFFECTS OF BLANKET EDGE STRETCHING

The following analysis shows that the flatness of a sheet is highly dependent upon all elements being of equal length. Therefore, if the edges of the sheet should become permanently stretched relative to the center section, this could explain the out-of-plane edge curvature. Again, experience with paper material, where stresses and/or mositure absorption due to edge exposure or handling could cause edge lengthening, indicates the applicability of this explanation to the paper blanket of the demonstration model. Similarly, recognizing that window shades are often pulled down at the edges might explain a stretched edge condition there. However, with controlled handling of a material like Kapton-H film, this edge stretching would not be expected. The following example illustrates the sensitivity of the out-of-plane deflections to a difference in element lengths.

Assume a blanket length of 409 inches. If the outer edges were 0.0019 inch longer than the midsection, then, maintaining compatibility at parallel ends and assuming the edges take a circular arc shape, the corresponding out-of-plane displacement, h, is 0.53 inch, as subsequently illustrated. The angle formed by the normals at the ends of the arc is less than 0.10 degrees.

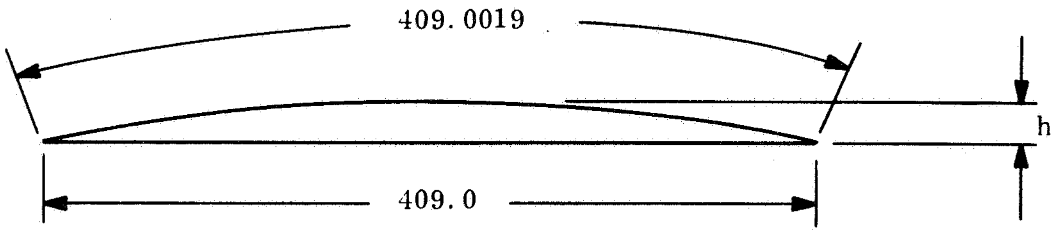

STRESS ANALYSIS FINITE ELEMENT PROGRAM (SAFE)

SAFE is a general computer program developed by General Electric for the structural analysis of isotropic and/or orthotropic bodies using finite element techniques. In general, SAFE has the capability of computing stresses, strains, and displacements throughout the cross section of an axisymmetric or in the plane of a planar body. The loading must be axisymmetric (or in-plane) but otherwise may vary arbitrarily. In addition to arbitrary thermal gradients, loading functions may include pressures, shears, arbitrary loads, or displacements, and body forces or accelerations which may be specified within any point of the model. The model may have as many as six distinct materials, all of which may be temperature dependent.

It is possible to have individual properties in every element. This allows great flexibility in solving complex thermostructural problems, evaluating edge stress problems, and computing the effects of geometric and material discontinuities on the stress distribution. The program also provides optional graphic output, on the SC-4020 printer-plotter, of all computer data from the main computational link. The plot program can be run separately with saved tapes at any time in order to obtain additional output not requested at the time of the initial run. Graphic output options include a deformed grid and plots of any of the stress or strain components, either as contour plots or as distribution plots at any given station.

ANALYTICAL TECHNIQUES

The analytical techniques described in References 4-7 and 4-8 are also applicable to this problem. However, they have not been programmed for a digital computer and therefore would be less convenient than the SAFE Computer Program.

4.8 WEIGHT AND POWER SUMMARY

THE SELECTED ROLL-UP SOLAR ARRAY DESIGN PROVIDES 2469 WATTS OF NET POWER AT THE SPACECRAFT INTERFACE. THE CALCULATED WEIGHT OF THE SYSTEM IS 76.4 POUNDS WITH A RESULTING POWER-TO-WEIGHT RATIO OF 32.3 WATTS PER POUND.

A detailed weight breakdown for the proposed rollup solar array is shown in Table 4-5. Some component weights reflect the actual weights of the components as fabricated for the Engineering Demonstration Model. For example, the outboard end caps for the model were fabricated using the flight design drawing, except that the material was changed from beryllium to aluminum. Therefore, the actual weight of this part, when corrected for the material density difference, was used in the weight summary table. The array blanket weight has been substantiated, in part, by actual weight measurements on modules which were fabricated for thermal cycling tests.

The power output summary for the proposed array is shown in Table 4-6. The array raw output of 2523 watts is the maximum power calculated with an array temperature of 55^{o}C, 10 degrees solar angle of incidence and a total short-circuit current loss of 6 percent. The array bus strip losses and the slip ring and harness losses were subtracted from this raw array power to yield the net power available at the spacecraft interface.

The resulting power-to-weight ratio for the array is $\frac{2469}{76.4} = 32.3$ watt/lb.

Table 4-5. Weight Summary

Component		Weight (lb)
Array Blanket		42.0**
Storage Drum		14.6
Shell	5.6	
Outboard End Cap	0.8*	
Inboard End Cap	2.2*	
Bearings	1.0	
Neg'ator & Mounting Hardware	1.3	
Slip Rings	1.0	
Support Shaft	2.5	
Power Feedthroughs	0.2	
Outboard End Support		5.0
Stationary Part	0.6*	
Movable Part	2.9*	
Spring	0.3*	
Bolt & Hardware	0.3	
Separation System	0.9	
Center Support		1.7*
Leading Edge Member		1.0
Tube	0.8	
Center Fitting	0.2	
Solar Panel Actuator		11.5
Thermal Control Coatings		0.1
Wiring and Connectors		0.5
	Total	76.4

* Based on measured weights of parts fabricated for the Engineering Demonstration Model
** Verified by modules constructed for thermal cycling tests

Table 4-6. Power Output Summary

• Array Raw Output	2523 Watts
(Includes Losses Associated with:	
(1) 55°C Array Temperature	
(2) 10° Angle of Incidence	
(3) 6% Short-Circuit current loss	
• Array Bus Strip Losses at 55°C	50
• Slip Ring and Harness Losses	4
Net Power Available at Spacecraft Interface	2469 Watts

SECTION 5

TRADEOFF STUDIES

5.1 SINGLE BOOM VERSUS DOUBLE BOOM

THE SINGLE-BOOM CONCEPT HAS BEEN CHOSEN AS THE PREFERRED SYSTEM BECAUSE IT RESULTS IN THE LOWEST SYSTEM WEIGHT AND IS THE LEAST COMPLEX SYSTEM. IN ADDITION, THE SHORTER DRUM ASSOCIATED WITH THE SINGLE BOOM PERMITS MORE OPTIONS IN DRUM DESIGN AND ATTACHMENT TO THE VEHICLE.

The purpose of this task was to define the deployment concept and select the optimum configuration for the roll-up solar array. Various array concepts or arrangements were evaluated, and the configuration selected consisted of a single assembly in each spacecraft quadrant, mounted in a fixed position with the drum axis normal to the spacecraft vertical axis. This study was continued to determine the optimum configuration of the drum-boom system, and the results are presented in this section. No attempt was made to select a boom and deployment system or to fix a drum design.

Early system sizing work utilizing parametric representations of the Hunter STACER rods and aluminum drum weights were performed yielding the results shown in Table 5-1.

It is seen that the optimums are not sharp for either the single or double rod configuration. Subsequent analyses and configuration design studies were based on a double rod system 156 inches wide and a single rod system 102 inches wide (see Figure 5-1). Subsequent system weight studies with other types of rods (reported in Reference 1-2) resulted in smaller weight differences between the single and double rod configuration than shown in Table 5-1.

The two candidates are compared in Table 2-2. The single rod system is clearly the preferred system and consists of a fixed (nondeployable) drum, mounted close to the vehicle support structure, with a single boom attached to the midpoint of the solar array panel leading edge.

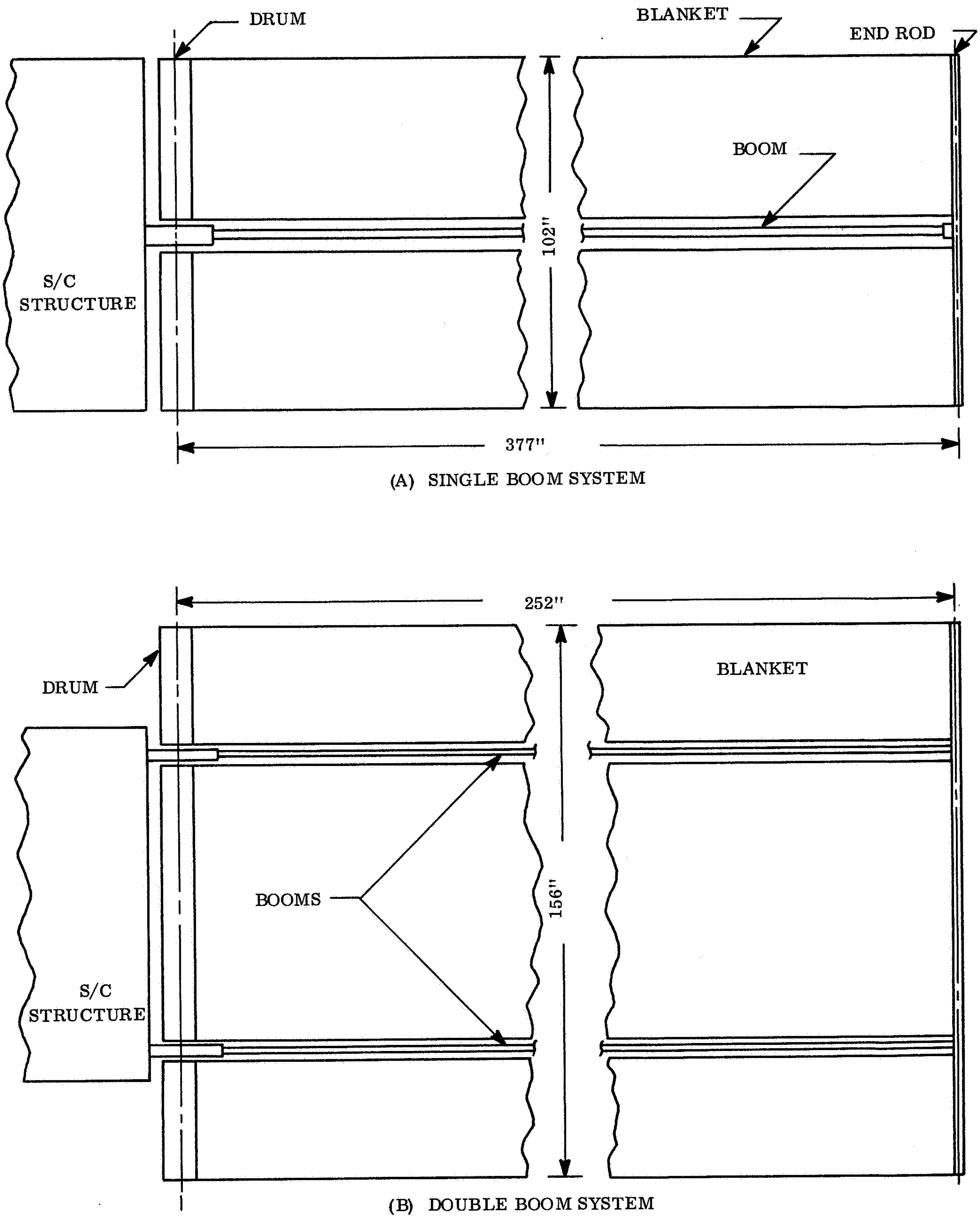

(B) DOUBLE BOOM SYSTEM

Figure 5-1. Typical Single and Double Boom Configurations

Table 5-1. System Weight Variations as a Function of Aspect Ratio

Drum Width (ft)	Array Length (ft, Rod Length)	Rod Tape Weight (lb)	Drum Weight (lb)	Total Weight (lb)	Specific Power (watts/lb)
Double Rod System Variations as Function of Drum Width					
13.0	19.228	7.737	16.384	90.439	27.643
12.0	20.830	8.744	15.430	90.246	27.702
11.0	22.723	10.007	14.476	90.307	27.683
Single Rod System Variation as Function of Drum Width					
12.0	20.833	4.372	15.430	77.279	32.351
11.0	22.723	5.003	14.476	76.709	32.591
10.0	24.996	5.812	13.522	76.316	32.758
9.0	27.773	6.877	12.567	76.180	32.817
8.0	31.245	8.327	11.613	76.428	32.710

Table 5-2. Comparison of Single and Double Rod Systems

Feature	Description
System Weight	Single boom system is lighter than double boom for all types of rods studied. Weight differences ranged from 5 pounds for Moly 180^{o} overlap stem rods to 0.8 pound for BeCu BI-STEM rods.
Drum	Single rod system has shorter drum and is not wider than vehicle. The shorter drum provides more design options: a single drum, two drums cantilevered from a center support, two drums simply supported at ends, etc.
Complexity	The single rod system is preferable, since no rod deployment synchronization is required.
Flexibility and Stability	Single boom is at a disadvantage because of credibility of torsional stiffness and stability. Dynamics analysis in Section 4-1 established the feasibility of utilizing substrate tension to provide structural stiffness for both torsion and bending.
Vehicle Mounting	The single rod system allows simple single-point vehicle mounting while the double rod system requires multipoint mounting.

5.2 SELECTION OF A BOOM TYPE

THE BI-STEM WAS SELECTED BECAUSE OF ITS LIGHTWEIGHT (11.5 LB), COMPACT SIZE (11 INCHES HIGH), DEMONSTRATED CAPABILITY, AND OFF-THE-SHELF AVAILABILITY (15-WEEK DELIVERY).

There are several suitable deployable boom types which are available to meet the requirements of this design. A study of these alternative approaches was made to determine the best candidate for this application. The types considered in the study are summarized in Figure 5-2. Three of these types were analyzed to determine the component size and weight necessary to meet the structural requirements of this design. A summary of these results is shown in Table 5-3. No design data were received on the welded edge rod and the STACER rod. Therefore, no evaluation could be made of these candidates.

The BI-STEM manufactured by SPAR Aerospace Products is the lowest weight and also has the lowest component length. Note that in addition to affecting component weight, the component length also affects the weight of brackets which are required to support the array storage drum.

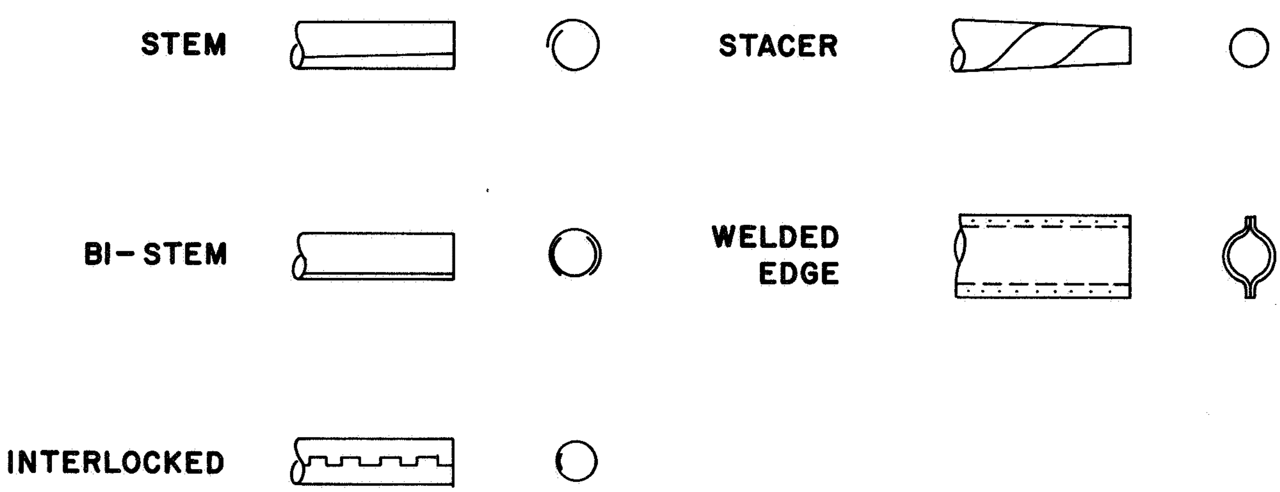

Figure 5-2. Types of Deployable Booms Considered

Table 5-3. Deployable Boom Design Parameters - 33.5-ft Extension

BOOM TYPE	CONFIG-URATION	DEPLOYER WEIGHT (LB.)	BOOM WEIGHT (LB.)	TOTAL WEIGHT (LB.)	COMPONENT LENGTH (IN.)
STEM	1.5 x .006 Be Cu OR S/S	8.1	5.1	13.2	18
INTERLOCKED	1.5 x .006 Be Cu OR S/S	9.4	3.8	13.2	30
BI-STEM	1.34 x .007 Be Cu OR S/S	5.1	6.4	11.5	11
WELDED EDGE	NO DATA RECEIVED				
STACER	NO DATA RECEIVED				

5.3 POWER TAKEOFF CONSIDERATIONS

INTERNAL SLIP RINGS WERE SELECTED FOR THE POWER TAKEOFFS. THIS SELECTION WAS MADE BASED ON MINIMIZING THE TOTAL SYSTEM WEIGHT.

Tradeoff studies have been conducted to determine the optimum method for transferring the array power from the moving drum to the stationary support structure and for providing the necessary array blanket preload force. Four basic configurations have been considered:

a. Two Neg'ator constant torque spring motors to provide the blanket preload force and four separate spiral wrapped copper (OFHC102) bus strips which have an insignificant effect on the blanket preload.

b. Four separate beryllium copper (BERYLCO 10) spiral wound clock springs. These springs function as both the power takeoff leads and the blanket preload force springs.

c. Two sprial-wound clock springs. These springs act as both the power takeoff leads and the blanket preload force springs. Both power leads are carried on the same strip by laminating two BeCu (BERYLCO 10) conductor strips between polyimide film.

d. Two Neg'ator constant torque spring motors to provide the blanket preload force and two internal slip ring assemblies for the power transfer.

Analysis of Spiral Wound Configurations

For the analysis of the first three configurations, all power takeoff leads were assumed to be wound as spiral power springs. Figures 5-3 and 5-4 show the wound and unwound configurations, respectively. The number of turns on the arbor (n_2) in the wound conditions is given by (Reference 5-1):

$$n_2 = \frac{\sqrt{\left(\frac{4}{\pi}\right) \ell h + d_1^2} - d_1}{2h}$$

where:

h = thickness of the strip

ℓ = active length of the spring strip

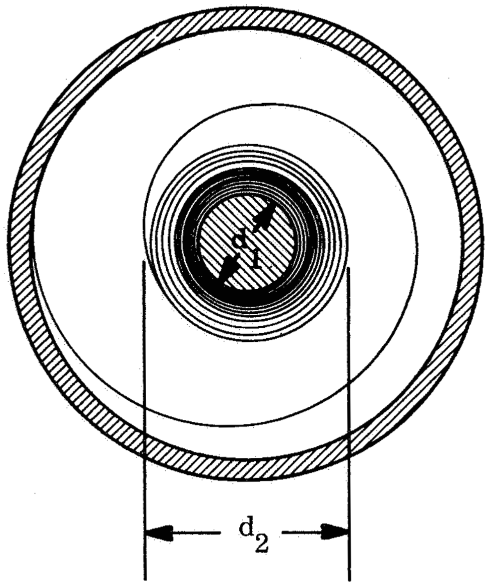

Figure 5-3. Power Spring Wound on Arbor

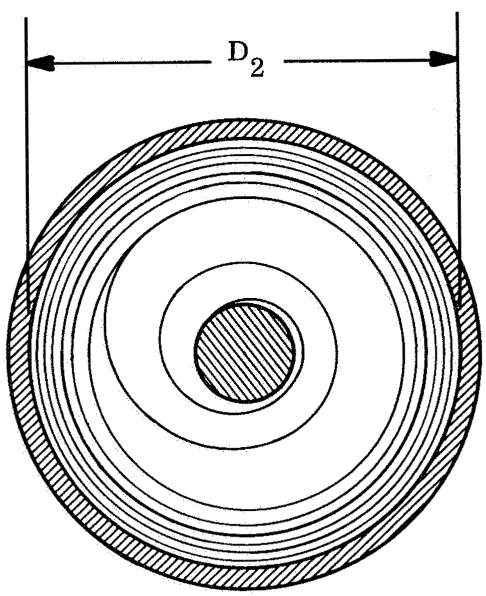

Figure 5-4. Power Spring Unwound and Resting Inside Case

The number of turns on the inside of the case in the unwound condition (n_1) is given by (Reference 5-1):

$$n_1 = \frac{D_2^{\,2} - \sqrt{D_2^{\,2} - \left(\frac{4}{\pi}\right) h \ell}}{2h}$$

The total number of turns (N) delivered by the spring is:

$$N = n_2 - n_1$$

The moment in the fully wound condition (M) is given by (Reference 5-2):

$$M = \frac{2\pi I E N'}{\ell + \pi (d_1 + h)}$$

where

$$N' = n_2 - n_o$$

$$n_o = \frac{\sqrt{\left(\frac{4}{\pi}\right) h \ell + d_1^{\,2}} \; (n_2)}{2 (D_2 - h)}$$

I = moment of inertia of strip

E = modulus of elasticity of strip

The bending stress in the strip is:

$$S = \frac{Me}{I}$$

where e = distance from neutral axis to outer most fiber

The first three basic configurations were analysed for the condition that 8 in.-lb is required per drum in the fully deployed state to provide the required array blanket preload. The measure of performance used to compare the various approaches was effective weight. Effective weight is defined as follows:

$$\text{Effective Weight} = \text{Total Spiral (or slip ring) Weight} + \text{Total Neg'ator Weight (if any)} + \frac{\text{Total Power Loss in Spiral}}{30}$$

The last term has been included to account for the fact that a power loss in the array subsystem must be, from the systems viewpoint, compensated for by an increase in array power (and weight). The specific array power as a goal in this contract is 30 watts/lb.

Figure 5-5 is a plot of effective weight versus strip width for Configuration 1. The copper strip thickness has been varied to show the effect of this parameter. A thickness of 1 mil has been allowed on each side of the copper for a high emittance coating. For each strip thickness there is an optimum strip width. Strip thicknesses greater than 0.002 inch result in increased stress in the copper and strip thickness less than 0.002 inch result in increased spiral weight. The torque developed by the 2.00-inch-wide strip when fully wound is 0.02 in.-lb per spiral.

Figure 5-6 is a plot of effective weight and stress versus strip thickness for configuration 2. The minimum effective weight occurs for a thickness of 0.02 inch. The stress at this thickness is 126,000 psi. A design of this configuration would have to utilize a strip thickness which is less than the optimum to reduce the stress in the spiral.

Figure 5-7 is a plot of effective weight and stress versus strip thickness for Configuration 3. Note in this case there is only one spiral per drum and it must develop 8 in.-lb when fully wound. The thickness of the center polyimide film is 0.010 inch in this plot. Center film thicknesses greater than 0.010 inch result in excessive stress and thicknesses less than 0.010 inch result in higher effective weights. A BeCu thickness of 0.008 inch results in the minimum effective weight, but this thickness would have to be reduced to reduce the stress in the strip.

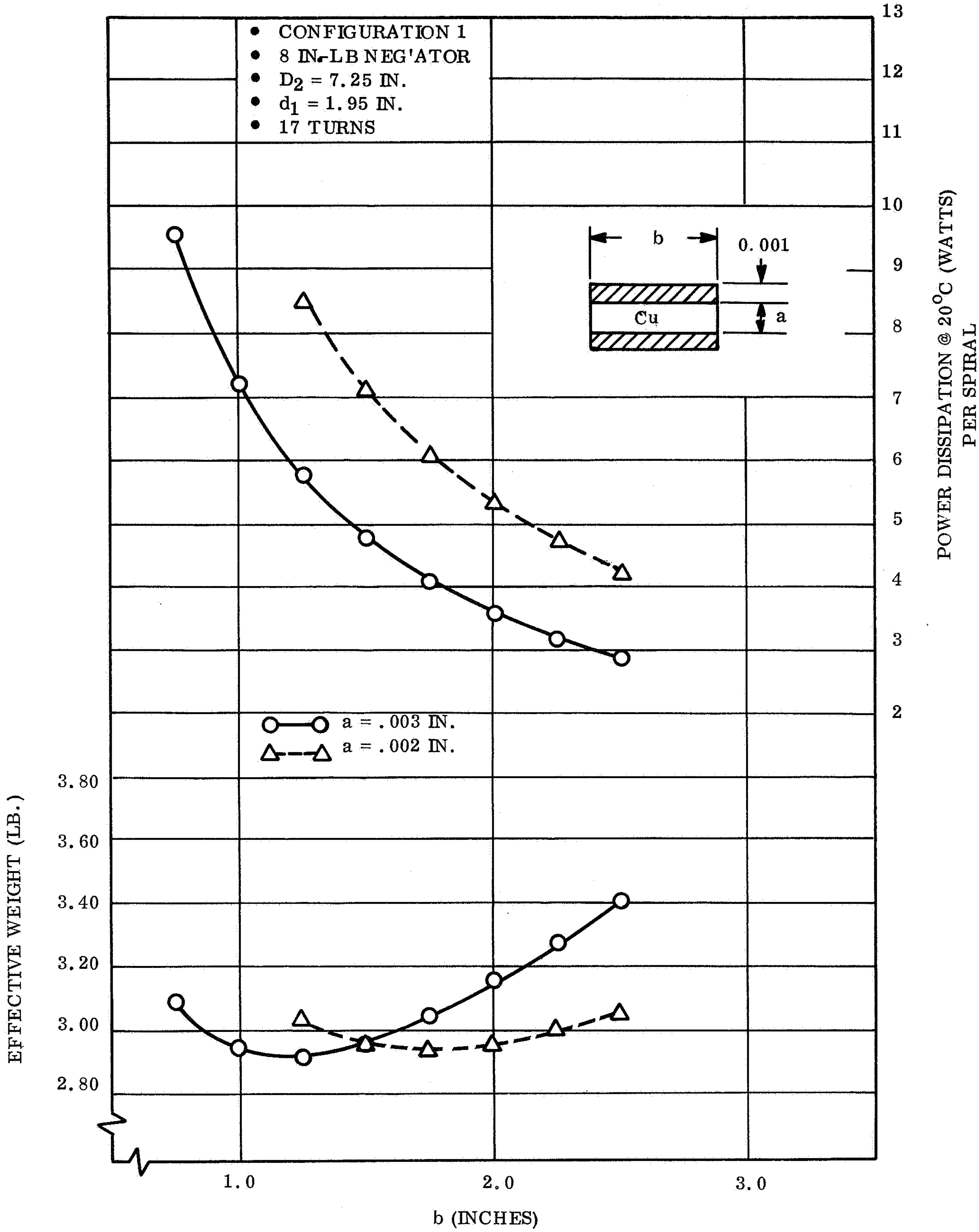

Figure 5-5. Effective Weight of Configuration 1

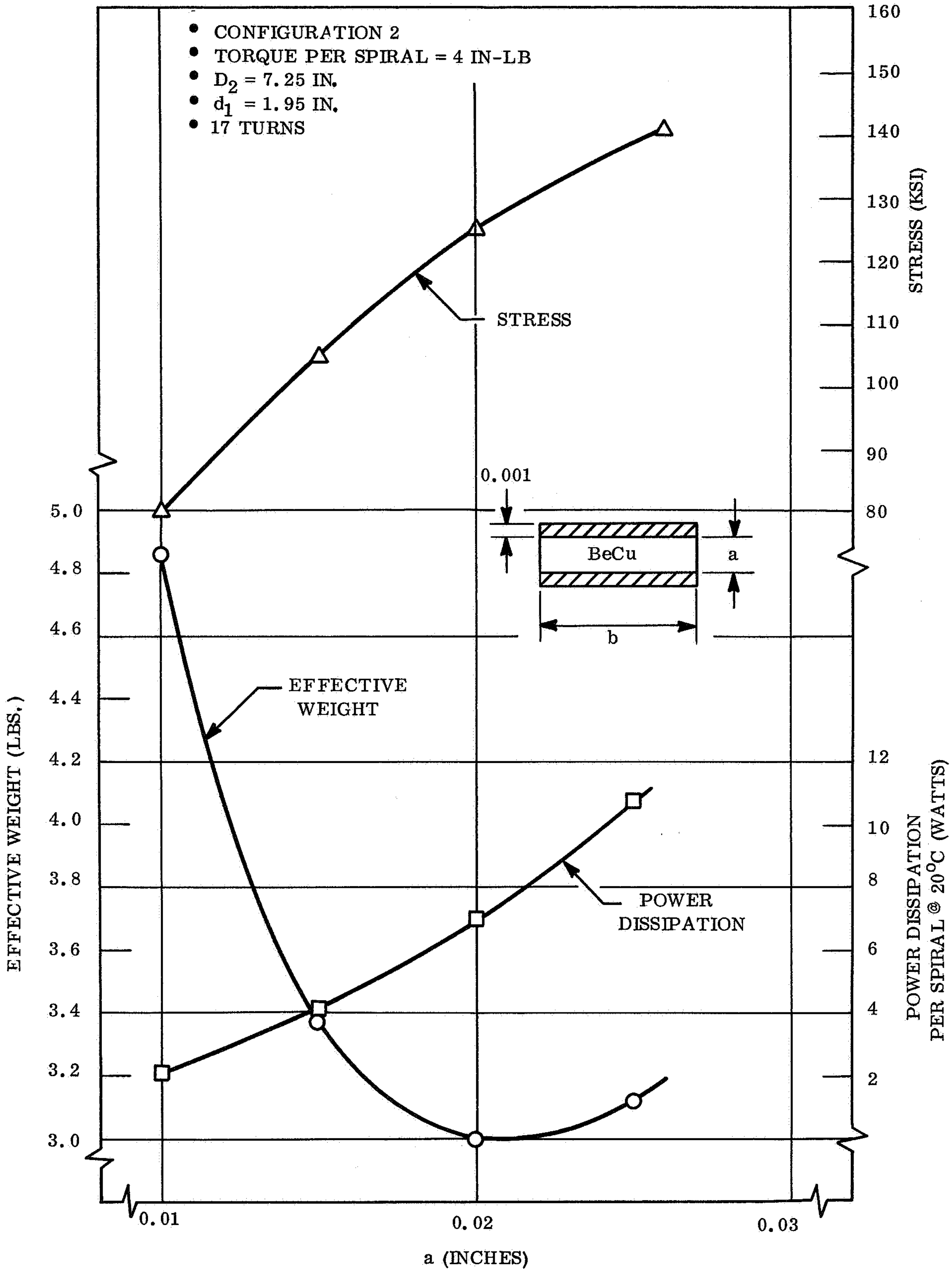

Figure 5-6. Effective Weight of Configuration 2

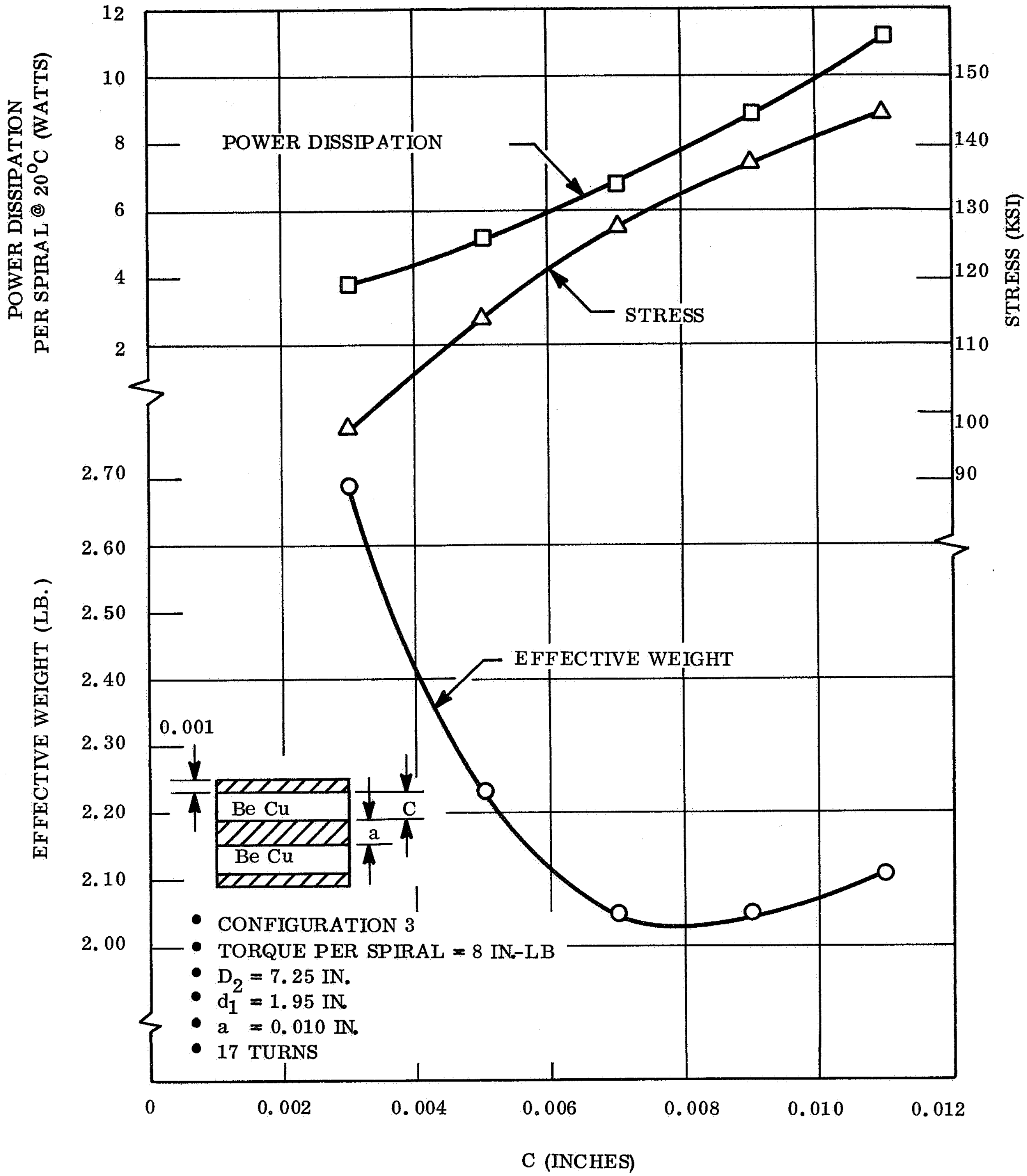

Figure 5-7. Effective Weight of Configuration 3

Analysis of Slip Ring Configuration

A design analysis of a slip ring assembly to accomplish the power transfer from the movable drum to the stationary support structure was performed for comparison with the spiral wound flat strip configurations. The design parameters of this assembly are described in Section 3.4. From these data, the effective weight of the slip ring configuration is given by:

$$\text{Effective Weight} = 1.0 + 1.3 + \frac{3.0}{30}$$

$$= 2.4 \text{ lb}$$

Conclusions

The parameter used for this evaluation is the effective weight of the system. If the effective weight of each configuration is compared, the slip ring approach is superior in performance and was therefore selected as the method of power transfer from the movable drum to the stationary support structure. It is expected that the development cost of the slip ring assembly will be more than a spiral wound copper strip.

5.4 BUS STRIP OPTIMIZATION

THE ARRAY MAXIMUM POWER VOLTAGE WAS SELECTED BASED ON TRADEOFF STUDIES WHICH CONSIDERED THE BUS STRIP WEIGHT PLUS THE SYSTEM WEIGHT PENALTY ASSOCIATED WITH POWER LOSS IN THE BUS STRIP.

Schjel-Clad L-5550* material was selected as the array bus strip conductors. This material is 1/2 oz/ft^2 copper laminated with 1/2 mil mylar. It has been evaluated electrically and under flexure for another similar application. A desk-side computer program was written to size the bus strip conductors as a function of power loss and array electrical interconnection arrangement. Figure 5-8 shows the bus strip weight required to obtain three specified power losses (i.e., 1, 2, and 3 percent) for a range of array maximum power voltages. As can be seen from these curves, the bus strip weight becomes an important factor for voltages below about 80 volts. It is also evident that weight continually decreases with increasing voltage so that other considerations will provide the restraints that will limit the voltage level.

Figure 5-9 is a plot of effective weight versus voltage drop for a number of different maximum power voltage. The voltages considered are the ones that result from integral numbers of series strings of solar cells fitted within the established length of the array blanket. The effective weight is defined as the weight of the bus strip plus the system weight penalty associated with the bus strip power loss (i.e., 30 watts per pound). As can be seen from the curves of Figure 5-9, for a given voltage, there is an optimum bus strip loss. Based on this consideration, an array maximum power voltage of 102 volts (at 55°C, 1.00 AU) was selected as the design point. Higher voltages were not considered as practical because of the problems associated with power conditioning at these voltages.

*Trade name of G.T. Schjeldahl Company

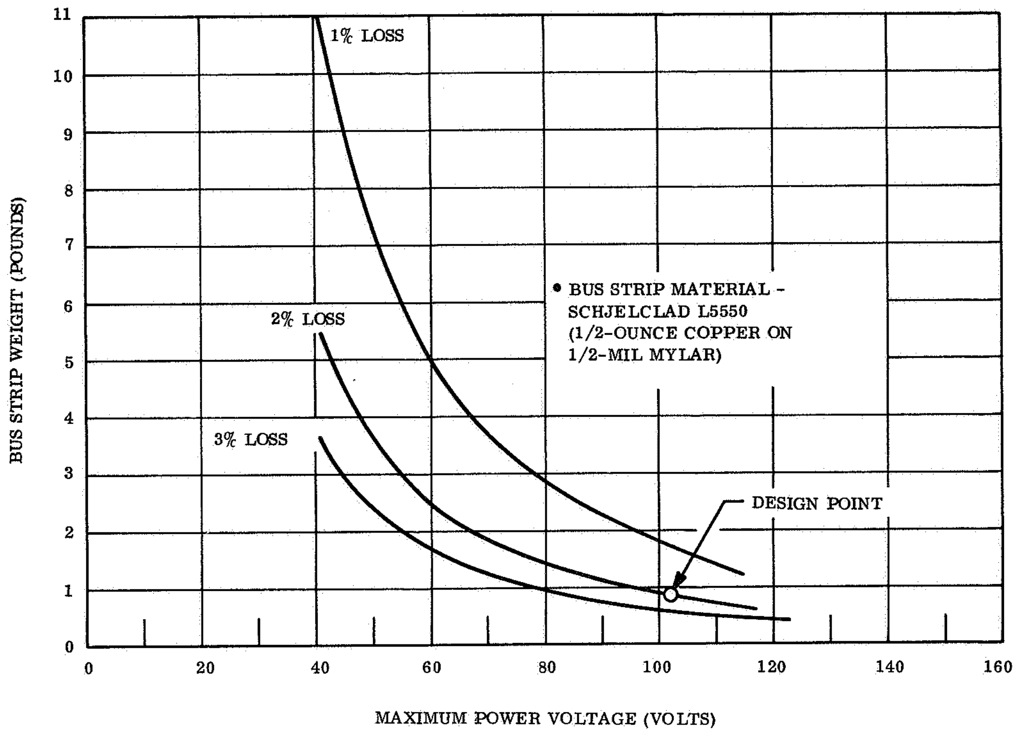

Figure 5-8. Bus Strip Weight versus System Voltage

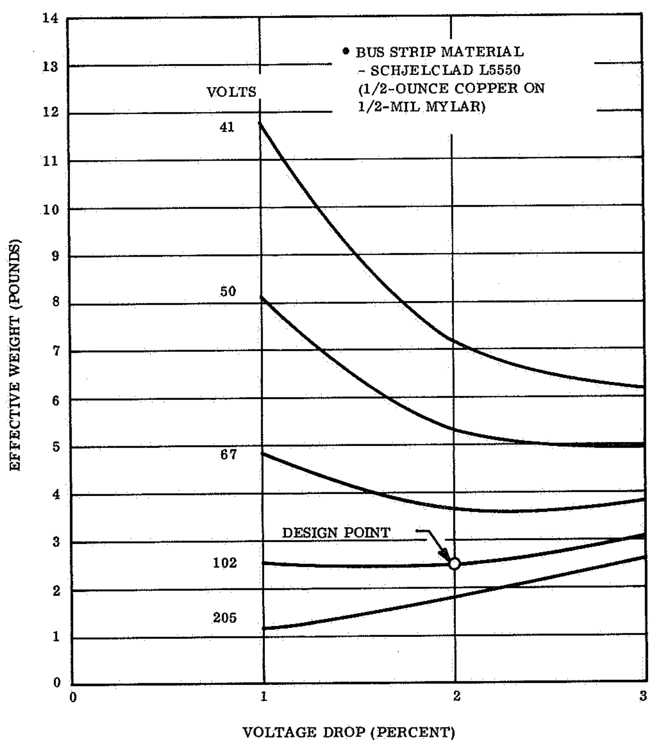

Figure 5-9. Effective Weight (Bus Strip Plus System Weight Penalty) versus Voltage Drop

5.5 DRUM SUPPORT CONSIDERATIONS

A TWO-DRUM-PER-PANEL SYSTEM WAS SELECTED. EACH DRUM IS SUPPORTED AT THE INBOARD END BY A PAIR OF PRELOAD BEARINGS AND AT THE OUTBOARD END, DURING LAUNCH, WITH A TIE-DOWN SYSTEM. THE DEPENDENCE OF DRUM BEARING ALIGNMENT ON STRUCTURAL INTERACTIONS WITH THE VEHICLE WAS THE MAJOR DESIGN CONSIDERATION AFFECTING THIS SELECTION.

Table 5-4 shows the four basic bearing and support arrangements which were considered as candidate methods for mounting the storage drum.

Approach I - Two 4-foot cantilevered drums with the free ends snubbed during launch. The load paths consist of taking the launch loads out through the bearings at the center support and through the end snub. Drum axial loads are taken out through the center support only.

Approach II - Two 4-foot simply supported drums. The launch loads are taken out through the bearings and supports provided at the center and at both ends of the drum.

Approach III - One 8-foot simply supported drum. The launch loads are taken out through the bearings and support at both ends of the drum.

Approach IV - Two fully cantilevered 4-foot drums. The launch loads are taken out through the bearings at the center support of the drums.

The weight of the drum and associated supporting brackets was calculated based on the dynamic analysis of Section 4.2 and preliminary stress analysis. Magnesium was used as the drum material in this analysis. The maximum shear load and maximum bending moment for each approach is included in the table.

Two major design considerations emerged from this tradeoff study:

a. The dependence of drum bearing alignment and preload on structural interactions with the vehicle.

b. Weight of drum and supports.

Table 5-4. Drum Support Tradeoff Factors

APPROACH I (RELEASABLE END SUPPORTS)	APPROACH II (PERMANENT END SUPPORTS)	APPROACH III (SINGLE, SIMPLY SUPPORTED DRUM)	APPROACH IV (CANTILEVERED DRUMS)
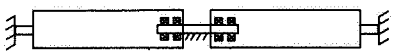	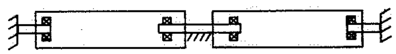	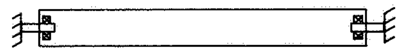	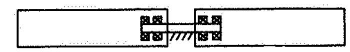
• Dual drum • Inboard bearings are preloaded pair • Outboard end of each drum is simply supported during launch phase; supports are released prior to array deployment • Drum and support weight = 18.6 lb • Maximum bending moment = 15,500 in-lb • Maximum shear load = 825 lb	• Dual drum • Single bearing inboard and outboard end of each drum • Drum and support weight = 17.4 lb • Maximum bending moment = 15,500 in-lb • Maximum shear load = 805 lb	• Single drum • Single bearing inboard and outboard end • Drum and support weight = 20.9 lb • Maximum bending moment = 58,000 in-lb • Maximum shear load = 1,860 lb	• Dual drum • Inboard bearings are preloaded pair • Outboard ends are not supported • Drum and support weight = 22.6 lb • Maximum bending moment = 70,800 in-lb • Maximum shear load = 2,850 lb
PROS	PROS	PROS	PROS
• Bearing preload and starting torque is independent of vehicle structural interactions • Boom actuator can be mounted on center support • Shorter drums are easier to fabricate • Array wiring can be brought out of the center • Shorter width array panels are easier to assemble and wire • The outboard end of each drum can be open to allow access to the drum interior	• Boom actuator can be mounted on center support • Shorter drums are easier to fabricate • Array wiring can be brought out of the center • Shorter width array panels are easier to assemble and wire • Lightest weight drum and supports	• Shorter boom length	• Bearing, preload and starting torque is independent of vehicle structural interactions • Boom actuator can be mounted on center support • Shorter drums are easier to fabricate • Array wiring can be brought out of the center • Shorter width array panels are easier to assemble and wire • The outboard end of each drum can be open to allow access to the drum interior
CONS	CONS	CONS	CONS
• Slightly heavier than Approach II	• Bearing alignment and preload is dependent on vehicle structural interactions	• Bearing alignment and preload is dependent on vehicle structural interactions • Boom actuator must be mounted separately • Wiring from the array must exit through the ends of the drum • Long drum is more difficult to fabricate • Heavier than Approach II	• Much heavier than Approach III

Approach II yields the minimum weight drum and supports, but the bearing alignment and preload is a function of the uncontrollable structural interactions with the vehicle. Approach I is slightly heavier than Approach II, but the bearing alignment is virtually independent of the vehicle structure.

Based on these considerations Approach I was selected as the method of bearing arrangement and support.

SECTION 6

ENGINEERING DEMONSTRATION MODEL

6.1 DESCRIPTION OF DESIGN

THE ENGINEERING DEMONSTRATION MODEL PRESENTS A CREDITABLE DEMONSTRATION OF THE DEPLOYABILITY OF THE PROPOSED FLIGHT ARRAY CONCEPT.

The Engineering Demonstration Model (EDM) is a deliverable end item under the contract. The stated purpose of this model is to demonstrate the deployability of the design concept for the 30 Watts Per Pound Roll-up Solar Array. The contract allowed a range of requirements that were bounded by the resources available for the model. The force of gravity complicated the design of the model as it is desirable that deployment be accomplished without extensive support equipment. The model is used for demonstration purposes and provides an engineering tool for the development of the detailed system design.

Based upon the above considerations the primary requirements for the model are to:

a. Present a creditable demonstration of the deployability of the array design in a 1g field.

b. Be composed of flight type design components wherever possible within the constraint of the deployability in a 1g field.

c. Demonstrate the producibility of the flight solar panel design concept.

d. Demonstrate that the analytical model for the deployed first mode natural frequencies in bending and torsion is accurate.

e. Demonstrate the construction and interconnection of a series string of solar cells which produce the full system voltage.

f. Provide an engineering design tool that feedbacks information into the design of the flight unit.

g. Provide a system that can be used for demonstration purposes that requires a minimum of deployment aids.

Figure 6-1 shows photographs of the EDM in the stowed configuration. This model is essentially the flight solar panel design with the following exceptions:

a. The model has been scaled down in width. The inside width of each drum has been reduced from 47.1 inches to 24.0 inches.

b. The array blankets have been replaced with 4.0-inch wide, 1-mil Kapton strips. One series string of solar cells (240 cells in series by 2 cells in parallel) is installed on one of these strips to demonstrate the construction and interconnection.

c. Flight design materials are replaced with more conventional materials where it does not compromise the requirements for the model. For example, the boom is not silver plated, the bearings contain conventional oil lubrication, and aluminum is substituted for beryllium.

The two drums are mounted on a test stand which simulates the vehicle interface. This stand is equipped with a level and leveling screws to establish the nominal rod center line along the local vertical. The drums and leading edge member are caged as in the flight design, except that the separation nuts are released pneumatically. The power supply and controls for the BI-STEM are contained in a control box on the test stand.

Pneumatics System

The separation nuts (Hi-Shear Part No. SN7311-2) are designed for actuation with pyrotechnic cartridges. This is a one-shot operation because the nuts are not reusable due to contamination from the explosive. To ensure reuse of the separation nuts on the model, they are actuated pneumatically. A schematic diagram of the self-contained, high-pressure pneumatics system is shown in Figure 6-2. A high pressure reservoir (2100 psig, 57 in.^{3}) is strapped to the test stand of the model. This pressure is applied to the separation nuts through a flexible hose connected to a 2-way, 2-position solenoid actuated value. A push button switch on the control panel applies power to the solenoid to initiate release of the outboard end supports. A relief valve, pressure gage, cylinder valve, and charge/vent valve are also provided in the system as shown in the schematic. The cylinder can be recharged with nitrogen or air through the charge/vent valve, as required, or the system may be supplied from an external reservoir through this same valve.

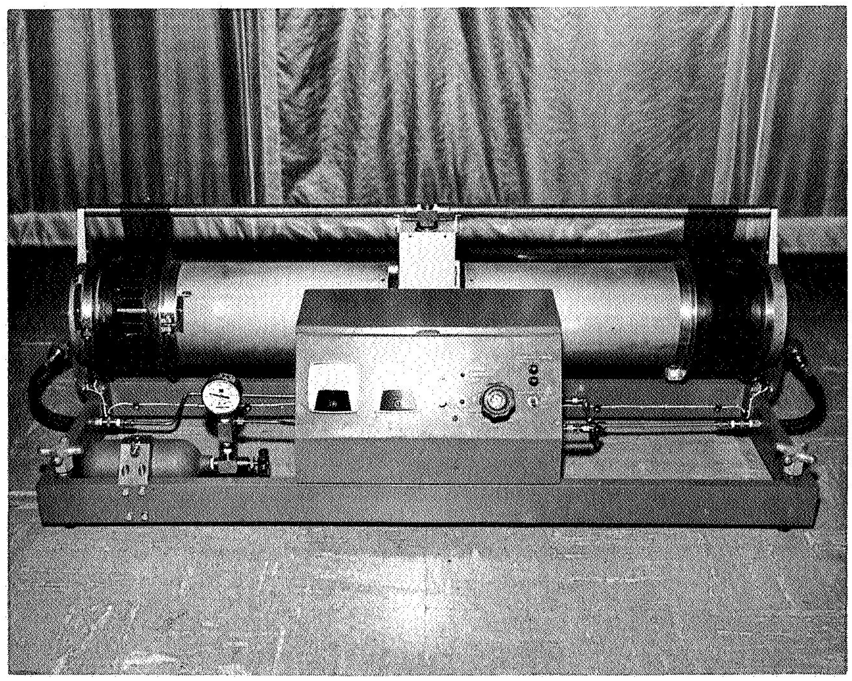

(a) View from Control Panel Side

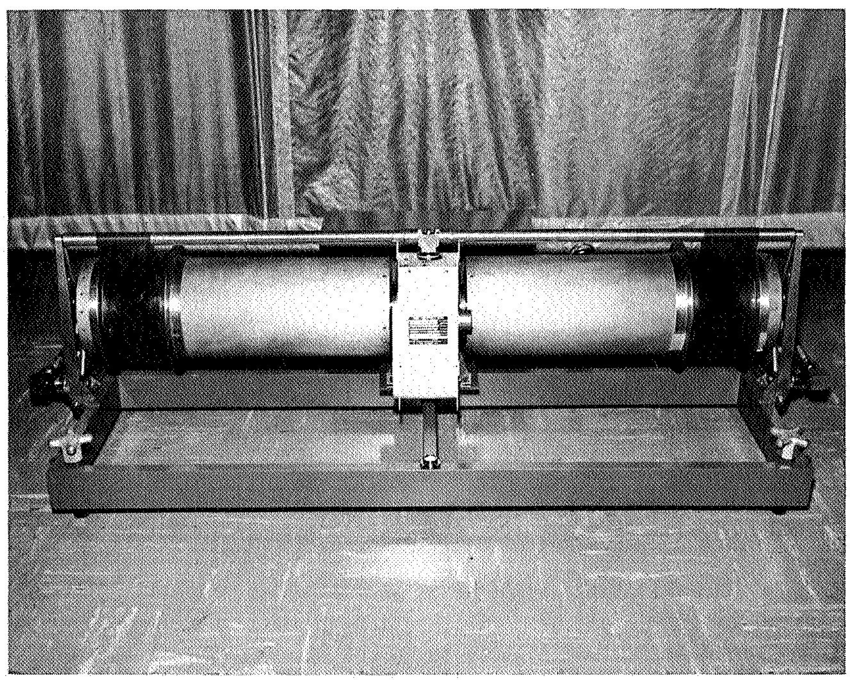

(b) View from BI-STEM Side

Figure 6-1. Engineering Demonstration Model - Stowed Configuration

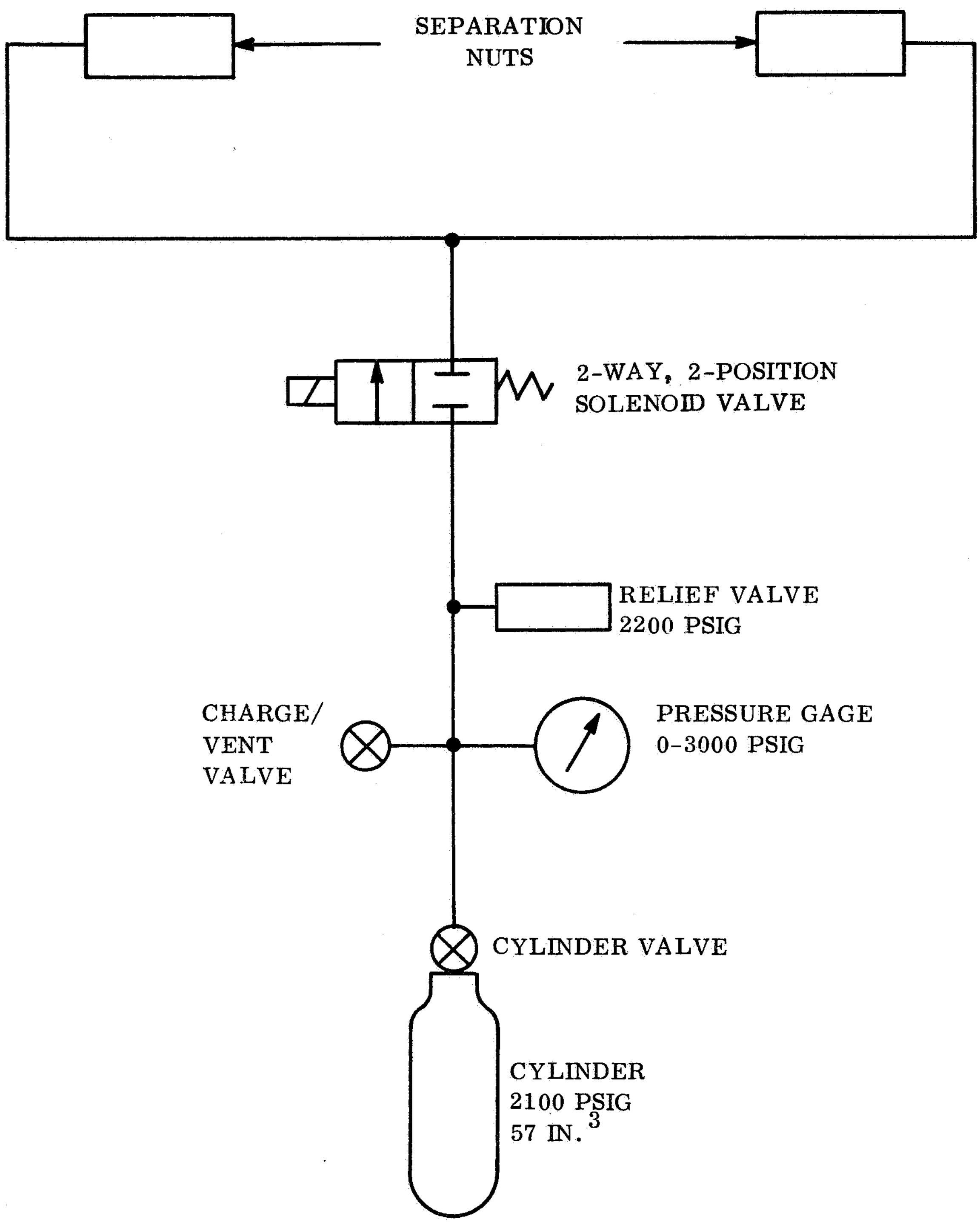

Figure 6-2. Schematic Diagram of the Separation Nut Actuation System

Electrical System

Electrical power (18 to 30 vdc) is required for the BI-STEM motor and the solenoid valve. Figure 6-3 is a schematic of the proposed electrical system that controls the power for these functions. This electrical system is self-contained in that it includes a 4-ampere hour, rechargeable alkaline battery. A DPST toggle switch (SW6) turns the battery power on or off. External power jacks (Figure 6-4) are located on the control panel in order for a laboratory dc power supply to furnish the power for motor operation or for recharging the battery. A DPDT toggle switch (SW5) controls the power to the BI-STEM motor. This switch has three positions: EXTEND, NEUTRAL, and RETRACT. In the EXTEND position, power is applied to the BI-STEM motor in the extend direction through switches SW1, SW3, and SW4. SW1 is the BI-STEM extension limit switch which changes

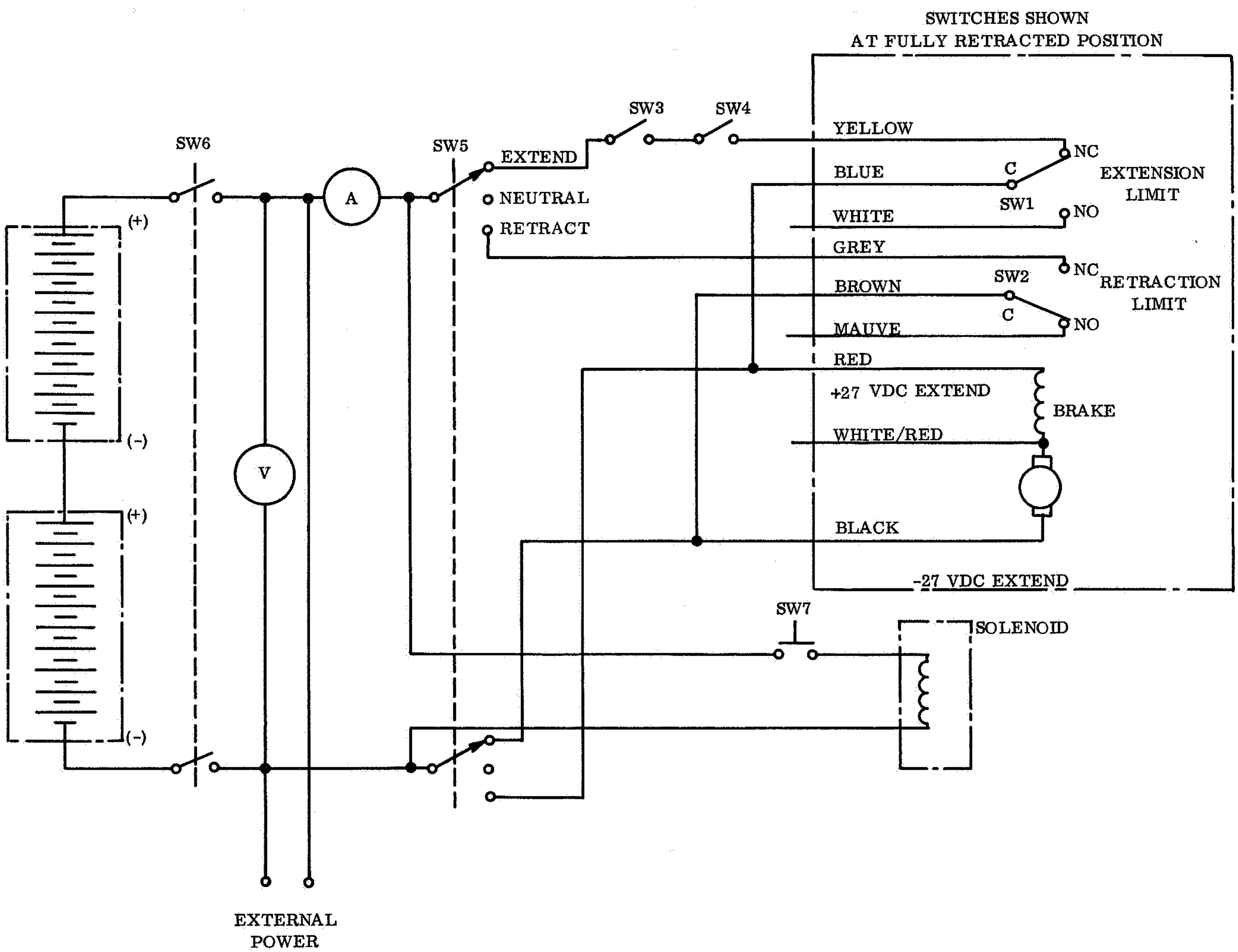

Figure 6-3. Electrical Schematic Diagram of the Engineering Demonstration Model

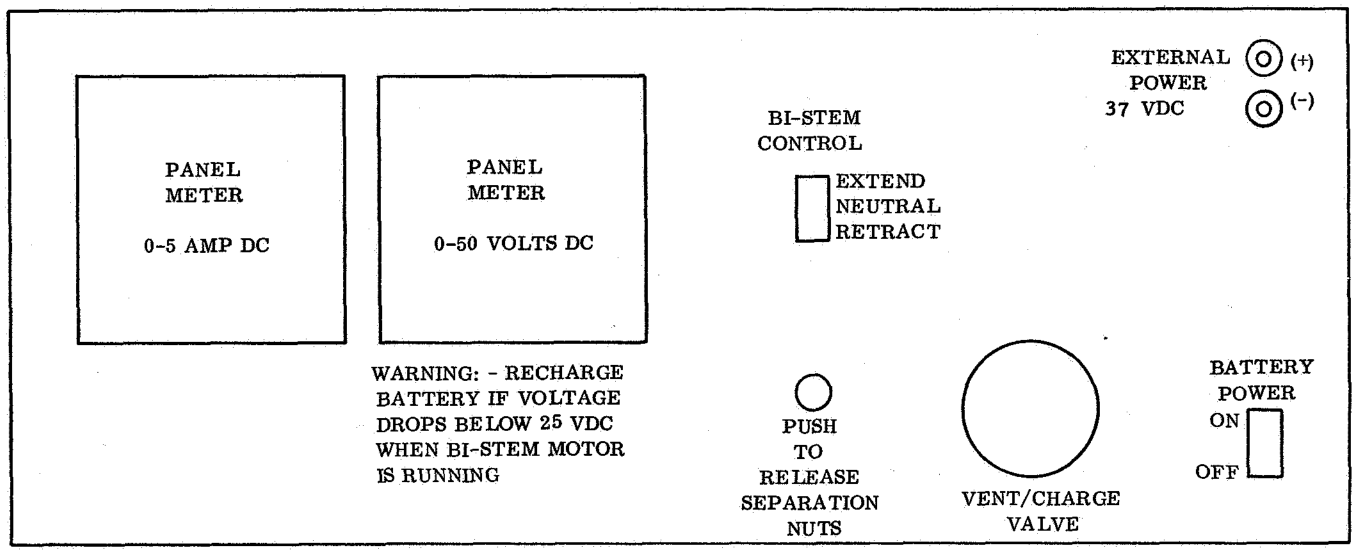

Figure 6-4. Control Panel Layout

position when the full extension of 33.5 feet is reached. Microswitches SW3 and SW4 are located on the outboard end supports. These switches (one on each support) are held open, as shown, when the outboard end supports are in the closed, or stowed, position. Thus, power can not be applied to extend the rod until the end supports have been released.

With SW5 in the RETRACT position, power is applied to the BI-STEM motor in the retract direction through the retraction limit switch, SW2. This switch changes position as soon as the rod is extended beyond its fully retracted position. A push button switch (SW7) applies power to the solenoid valve in order to actuate the separation nuts.

6.2 FABRICATION OF THE MODEL

THE FABRICATION OF THE EDM UTILIZED PROCESSES WHICH WERE, IN MOST CASES, TYPICAL OF THOSE TO BE USED FOR THE PROPOSED FLIGHT DESIGN ARRAY.

The full-size array blankets are replaced with 4.0-inch wide strips on the EDM. These strips were constructed using processes which are representative of those proposed for the full-size array blanket.

Bonding Conductors to the Blanket Substrate

Figure 6-5 shows the semiautomated bonding equipment used to bond materials to Kapton with Schjeldahl GT-100 adhesive. This unit was developed for the fabrication of thin film solar cell modules (NASA-Lewis Contract NAS3-10605) and was modified and used to bond the Schjel-Clad L5550 conductors to the Kapton strip for the EDM. The use of this equipment provides accurate and repeatable control of heat, pressure, and dwell time during bonding; such control would normally be operator-dependent using conventional hand methods.

Foam Button Application

Figure 6-6 shows a step-by-step pictorial presentation of the application of RTV 560 foam buttons to the Kapton substrate. This process was developed and used for the array strips on the EDM. When compared to the spray application of buttons, it has the advantages of being very controllable and requiring less equipment, facility and labor expenditures. Photograph (a) of Figure 6-6 shows the button locating template positioned on the substrate. This template is 0.020 inch thick. The holes are 0.188 inch in diameter spaced on a 0.818-inch pitch. The RTV 560 foam formulation is applied to fill all the holes in the template (see Figure 6-6 b) and scraped off to obtain the uniform height (a function of the template thickness). Figure 6-6 (c) shows the template removal following the application of the RTV compound. Three hours are required for the buttons to cure before that section can be rolled up. The resulting buttons are 0.25 inch in diameter and 0.03 to 0.04 inch high with a weight per unit substrate area of 0.0055 lb/ft^2.

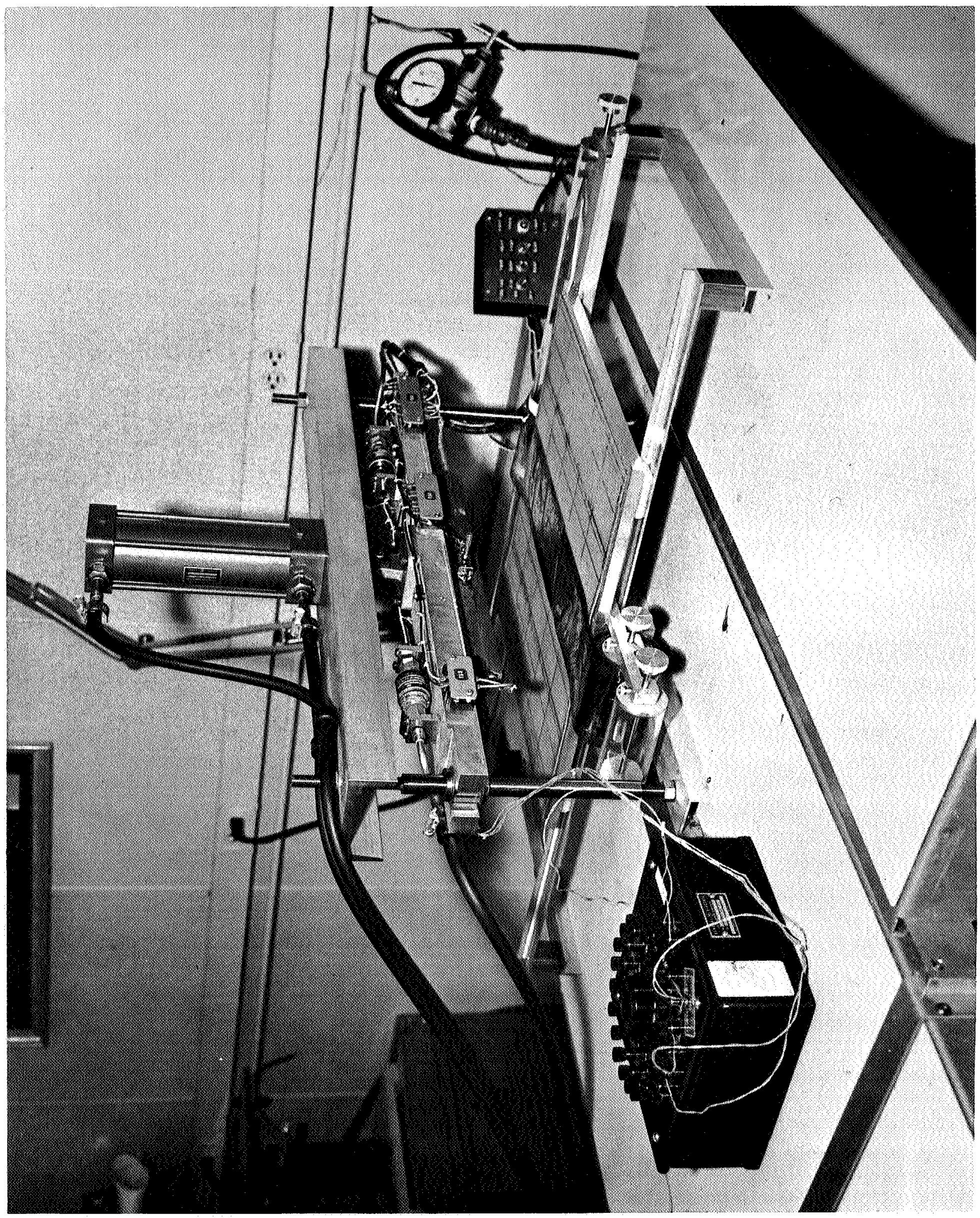

Figure 6-5. Kapton Bonding Equipment and Set-up

FOAM BUTTON APPLICATION PROCESS

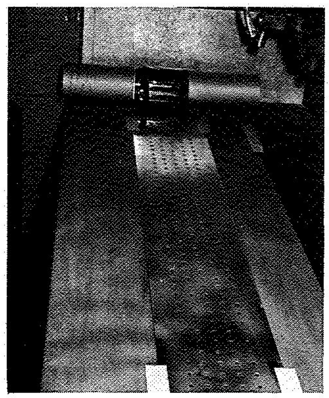

a. BUTTON LOCATING TEMPLATE POSITIONED ON SUBSTRATE

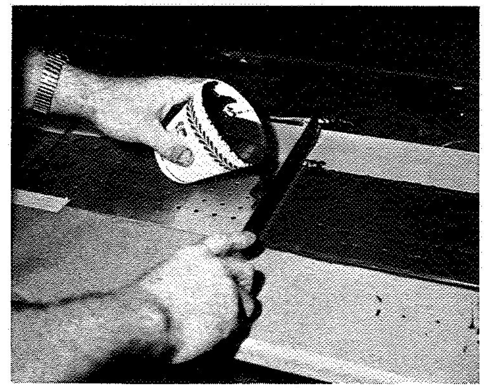

b. APPLICATION OF 560 FOAM FORMULATION

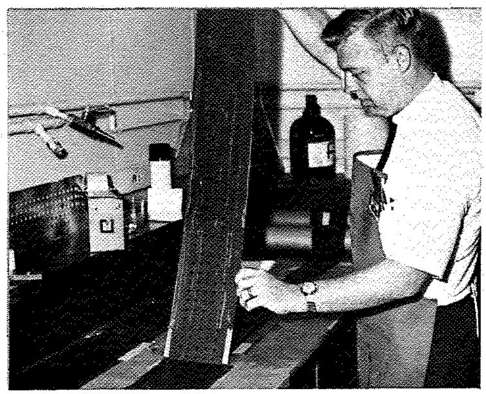

c. TEMPLATE REMOVAL

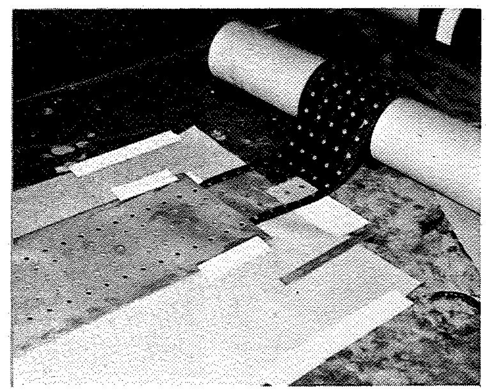

d. COMPLETE SECTION ROLLED UP & NEXT SECTION READIED FOR APPLICATION

Figure 6-6. Foam Button Application Process Steps

Bonding Modules to the Flexible Substrate

Figure 6-7 shows the bonding process and tooling used to bond the solar cell modules to the Kapton substrate strips. The solar cell modules (each module 20 cells in series by 2 cells in parallel) are placed face down on a Teflon-lined surface in the bonding fixture (see Figure 6-7a). The fixture is provided with guides that position the modules accurately with respect to the Kapton substrate. The surfaces to be bonded are then cleaned by wiping with reagent grade methanol. The adhesive is weighed, and mixed in accordance with GE Specification 171A4435 and is applied in controlled amounts to the back of the cells. The Kapton is then placed over the cells. A foam pad is placed on the top of the assembly to act as a cushion for the cells and to provide constant positive pressure during the cure cycle. The resilience of the foam also compensates for the raised foam buttons to achieve uniform distribution of pressure. A plate is then placed on top of the foam and clamps are used to apply bonding pressure. (See Figure 6-7b).

SOLAR CELL BONDING

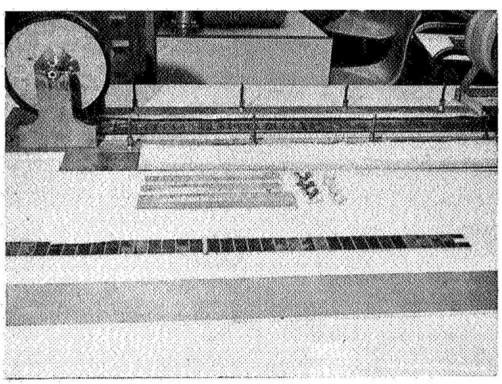

a. SET UP & TOOLING FOR BONDING SOLAR CELL MODULES TO "KAPTON" BLANKET SUBSTRATES

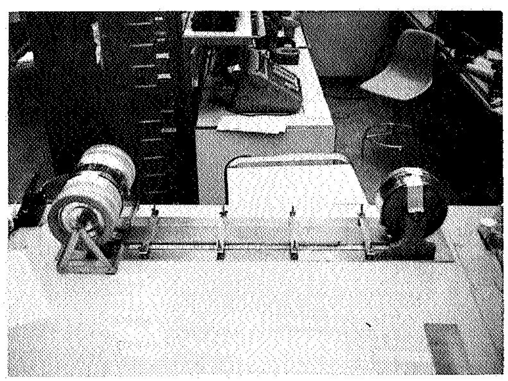

b. MODULES BONDED & FIXTURED FOR OVEN CURING OF ADHESIVES

Figure 6-7. Bonding of Solar Cells to "Kapton" Substrate Roll-up Array

After bonding, the cover glass surfaces are cleaned by wiping with methylene chloride to remove any excess SMRD 745.

The feed- and take-up drums on the fixture make it possible to use existing oven facilities to bond the modules in easily bondable increments.

Cover Glass Bonding

Bonding of the 0.003-inch glass cover slide to the 0.008-inch solar cell is performed in the fixture shown in Figure 6-8. Control of the Sylgard 182 bond thickness to less than 0.001 inch is attained by the spring load on the glass. This load is between 60 and 100 grams because of the individual spring variation and produces uniform squeeze-out as determined from measurements of the total unit thickness, which ranges between 0.0102 and 0.0126 inch. These values were measured on a randomly selected sample of 24 assemblies. The thickness of each assembly was measured in five places, and the average thickness was recorded. The average thickness among the 24 samples was 0.0111 inch.

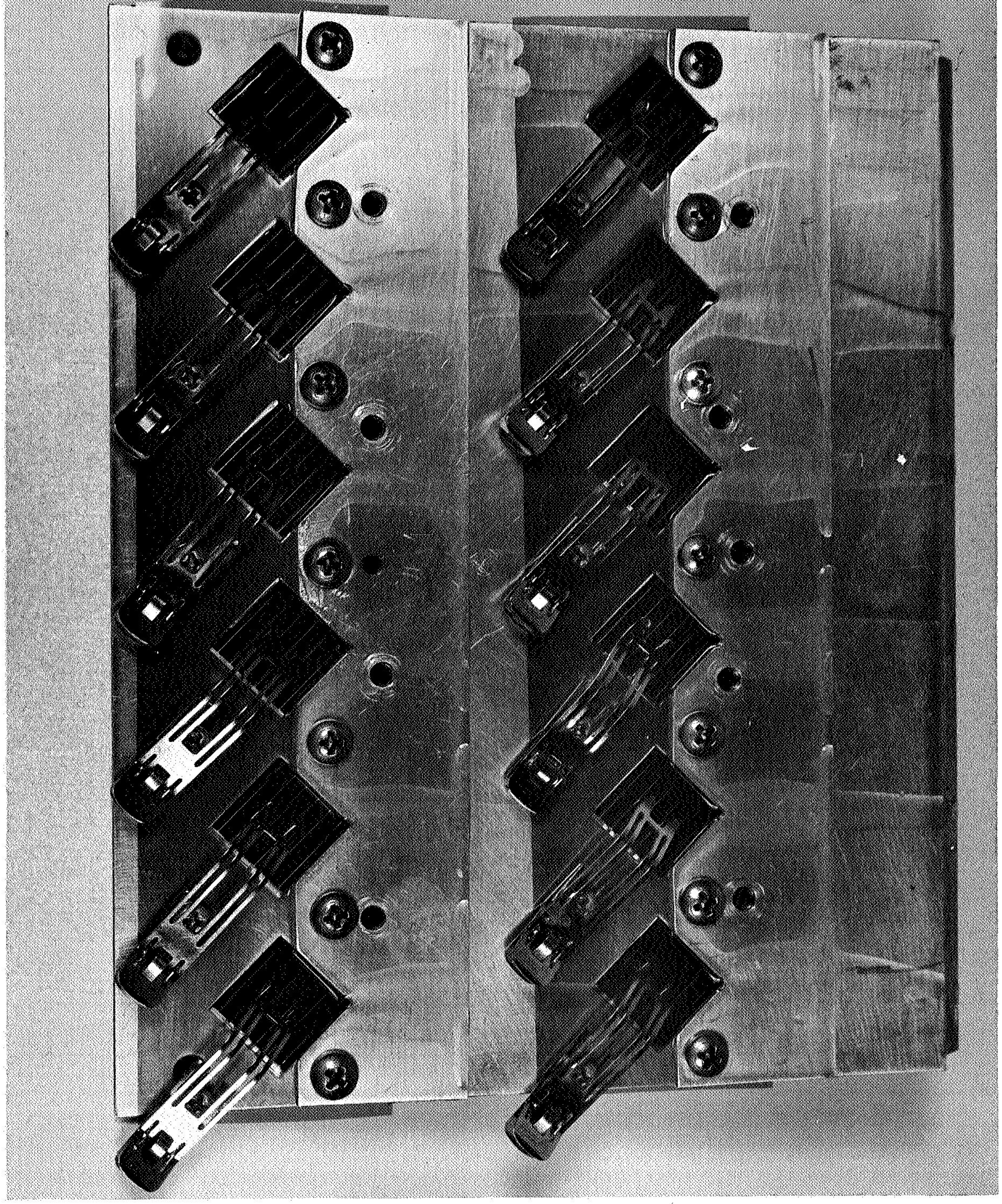

Figure 6-8. Cover Glass Installation Fixture

6.3 DEPLOYMENT

THE ENGINEERING DEMONSTRATION HAS BEEN DEPLOYED VERTICALLY UPWARD TO A FULLY EXTENDED LENGTH OF 33.5 FEET UNDER THE ARRAY TENSION LOAD.

On May 16, 1968, the partially completed EDM was deployed vertically upward, unaided, to the fully extended length of 33.5 feet. Four-inch-wide, 1-mil Kapton strips were used to simulate the full array blankets. Motion picture coverage of this deployment was provided.

On June 6, 1968, the completed EDM was again deployed vertically upward. In this case, one 4-inch-wide Kapton strip was mounted with 480 cells and the other strip was mounted with 480 glass blanks to simulate the cells. This configuration adds approximately 1.4 lb to the boom tip load at full extension when compared to the configuration which was deployed on May 16, 1968. An attempt was made to deploy this completed EDM to the fully extended length of 33.5 feet. BI-STEM stall was experienced at approximately 31 feet, and it was apparent that the boom would fail as a beam-column if the safety line were released. Subsequent disassemble and inspection of the BI-STEM revealed a back-wound tape. This condition was caused by the excessive column load as the boom approached full extension. The damaged tape was replaced.

Based on these experiences with the completed model the following deployment restrictions must be observed:

a. It is important to level the test stand, using the bubble level provided, before deployment.

b. Vertical upward deployment of the complete model should be restricted to 25 feet with no deployment aids.

c. For deployments to the fully extended length it is necessary to observe either of the following conditions:

   1. Replace the cell-covered-strips with plain Kapton strips.

   2. Provide a counterbalancing deployment aid at the top of the boom.

Figure 6-9 shows three photographs of the deployment sequence. The pneumatically actuated separation nut system was used to release the outboard end supports before BI-STEM deployment. Figure 6-10 shows this outboard end support in the launch position and in the released position.

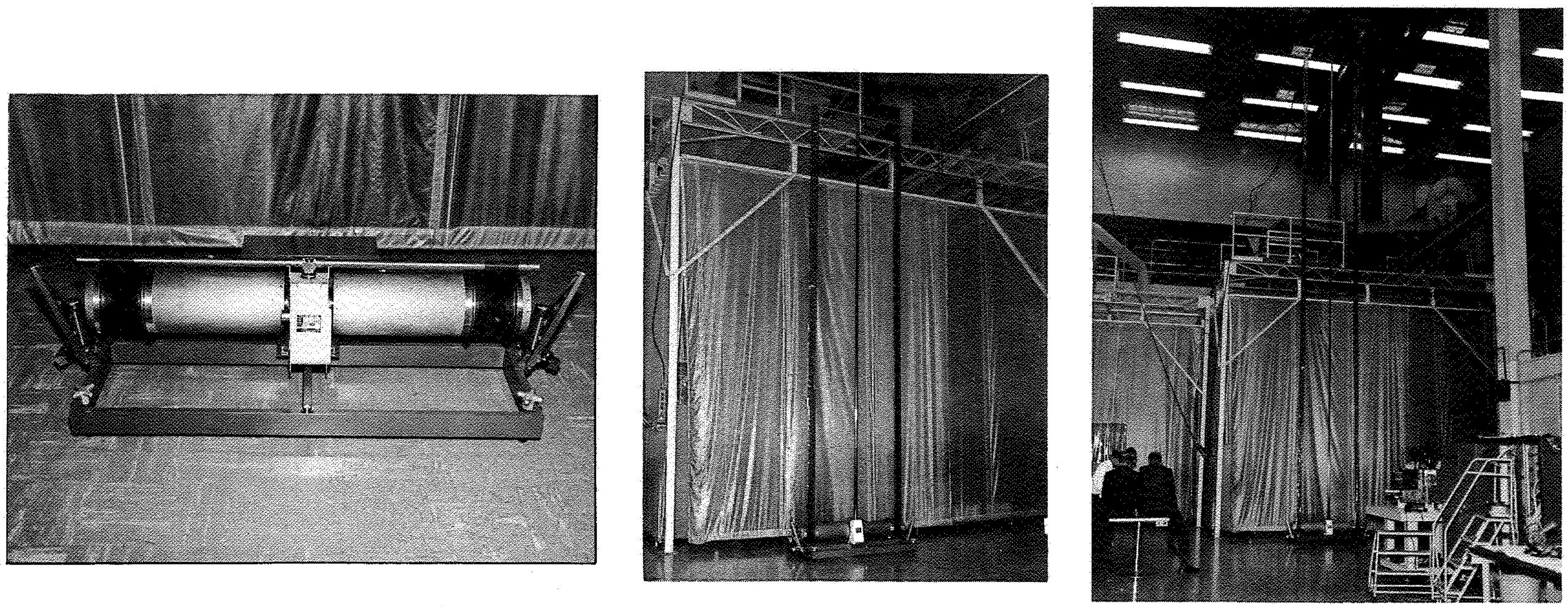

(a) Uncage (b) Mid-travel (c) Fully Extended 33.5 Feet

Figure 6-9. EDM Deployment Sequence

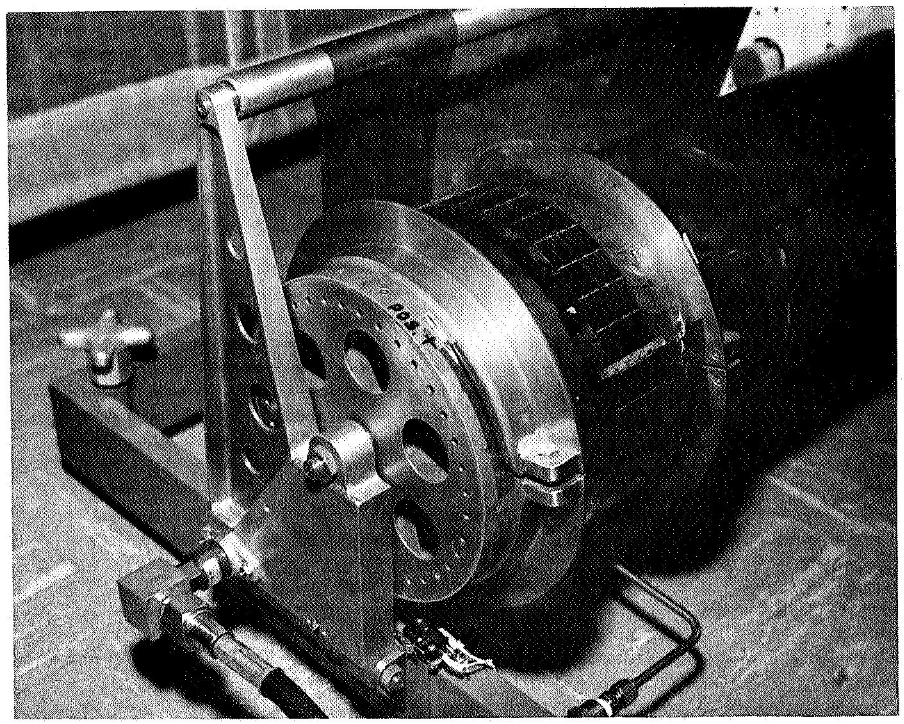

(a) Launch Stowed Position

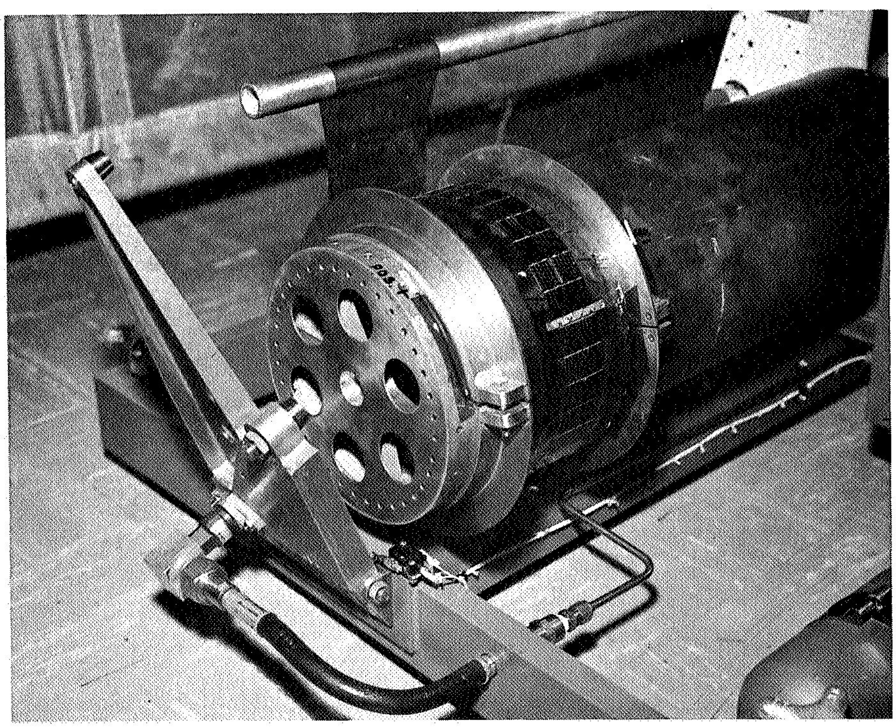

(b) After Actuation

Figure 6-10. Outboard End Support Actuation

6.4 ELECTRICAL PERFORMANCE OF THE ARRAY STRIP

A SUNLIGHT ILLUMINATION TEST OF THE ARRAY STRIP WAS CONDUCTED TO VERIFY THE ELECTRICAL PERFORMANCE.

On June 6, 1968, at the array strip on the EDM (240 series cells by 2 parallel cells) was deployed vertically upward (16.5 ft) in sunlight to verify the electrical performance of this typical example of the proposed flight array construction. Figure 6-11 shows photographs of the test set-up for this performance check. The I-V curve shown in Figure 6-12 was obtained on the array strip.

A few words on the safety hazards associated with solar arrays which have maximum power voltages of approximately 100 volts may be appropriate at this time. The small array strip which is mounted on the EDM is capable of causing death by ventricular fibrillation when illuminated with normal room lighting. The resistance measured between two electrodes placed on the skin can vary from 500 ohms to 5 kΩ, depending upon moisture, oils in the skin and the amount of dead skin under the electrodes. Currents in the $< 100\,\mu$a range may cause fibrillation under certain conditions. The danger is most serious in those situations where currents may pass directly through the heart. For these reasons, it is important that solar arrays of this type be treated with the same respect as a normal 110 VAC power line.

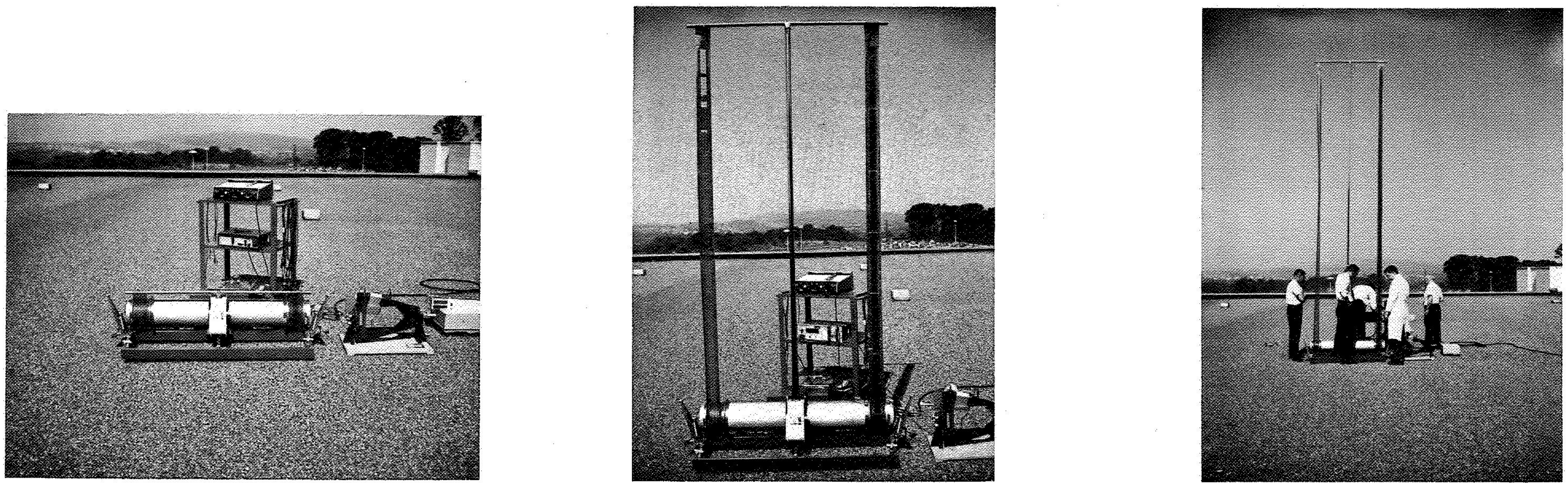

(a) Prior to Deployment

(b) Deployed 8.5 ft

(c) Deployed 16.5 ft

Figure 6-11. Photographs of Array Strip Electrical Performance Test

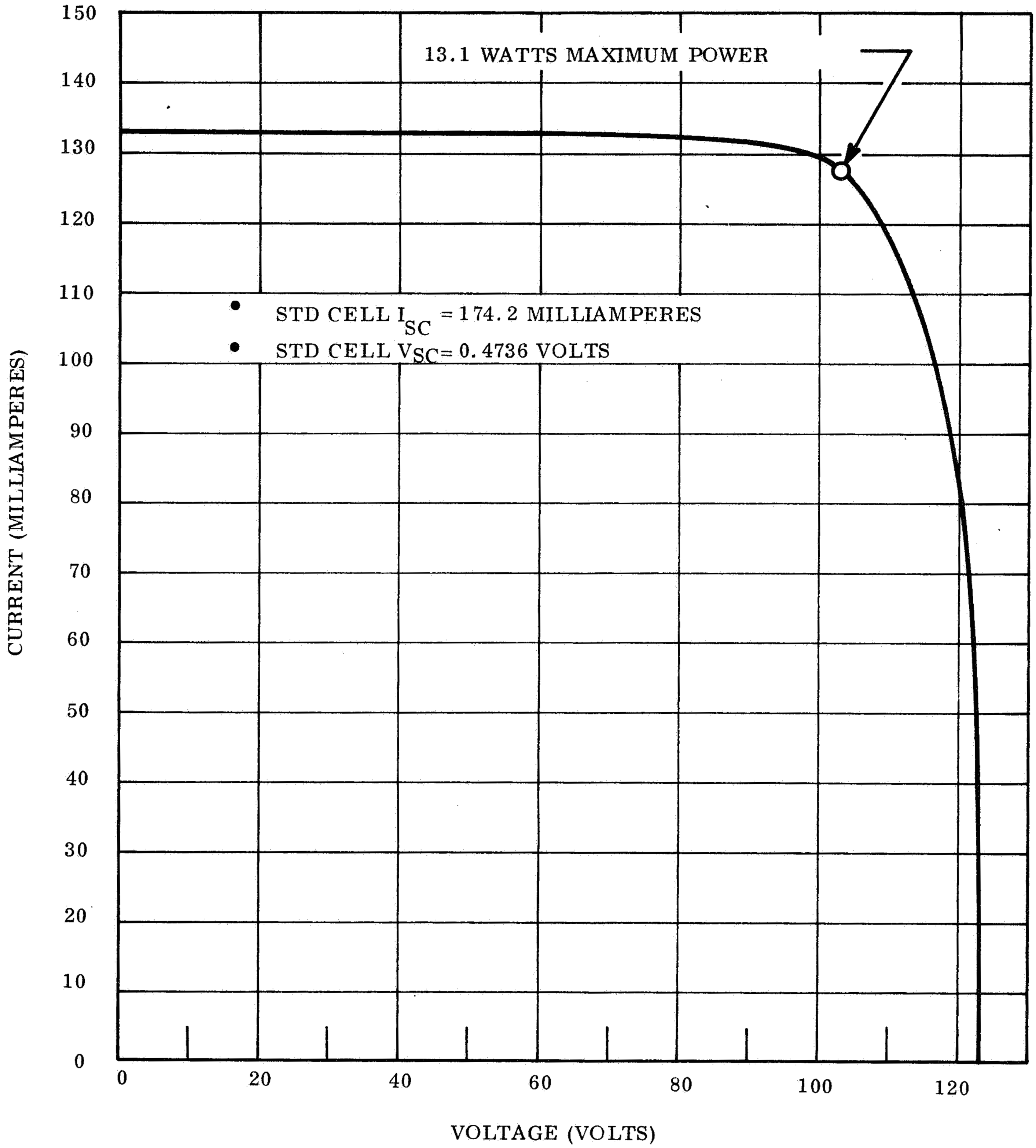

Figure 6-12. I-V Curve-Sunlight Illumination

SECTION 7

RELATED STUDIES AND ACTIVITIES

7.1 THERMAL CYCLING TEST RESULTS

> THE SILVER EXPANDED METAL INTERCONNECTION HAS SUCCESSFULLY SURVIVED 117 THERMAL CYCLES BETWEEN -200°F (-129°C) AND +200°F (93°C). PROBLEMS WERE EXPERIENCED WHEN THE TEMPERATURE RANGE WAS EXTENDED FROM -250°F (-157°C) TO +200°F (93°C).

A thermal cycling test program was initiated to verify the structural integrity of various types of interconnections when used in the roll-up array application. Thus far, two types of interconnections have been investigated. The first type is the photoetched configuration shown in Figure 7-1. This interconnection is fabricated from 3-mil thick BeCu (BERYLCO 10). The second type is fabricated from silver expanded metal (Exmet Corp. 2Ag7-2/0E) as shown in Figure 7-2.

Three 5-cell by 5-cell modules were fabricated utilizing the photoetched interconnection. Modules No. 1 and 2 were of identical construction and were bonded by the same process (solar cells face-up during bonding operation). Figures 7-3 and 7-4 show the front and rear sides of Module No. 1, respectively. Module No. 3 was fabricated using tabs modified with shorter feet to reduce the length of the region subjected to thermal expansion differential strains and was bonded with the face-down process planned for use with the large area modules. This bonding process resulted in the SMRD 745 material spreading into the inner loop of the tabs to a much larger extent than was experienced with the face-up bonding, with the corresponding loss of flexibility.

Each of these three modules was mounted on the heat sink of the thermal cycling chamber as shown in Figure 7-5. The open-cell foam is used to apply light pressure to hold the module in contact with the heat sink. The open-cell nature of this foamed sheet allows the cells to be illuminated through a window in the chamber. The module short-circuit current is continuously monitored during the test. These tests were run between -200 and +200°F and for durations of 114, 105, and 100 cycles, respectively for Modules No. 1, 2, and 3.

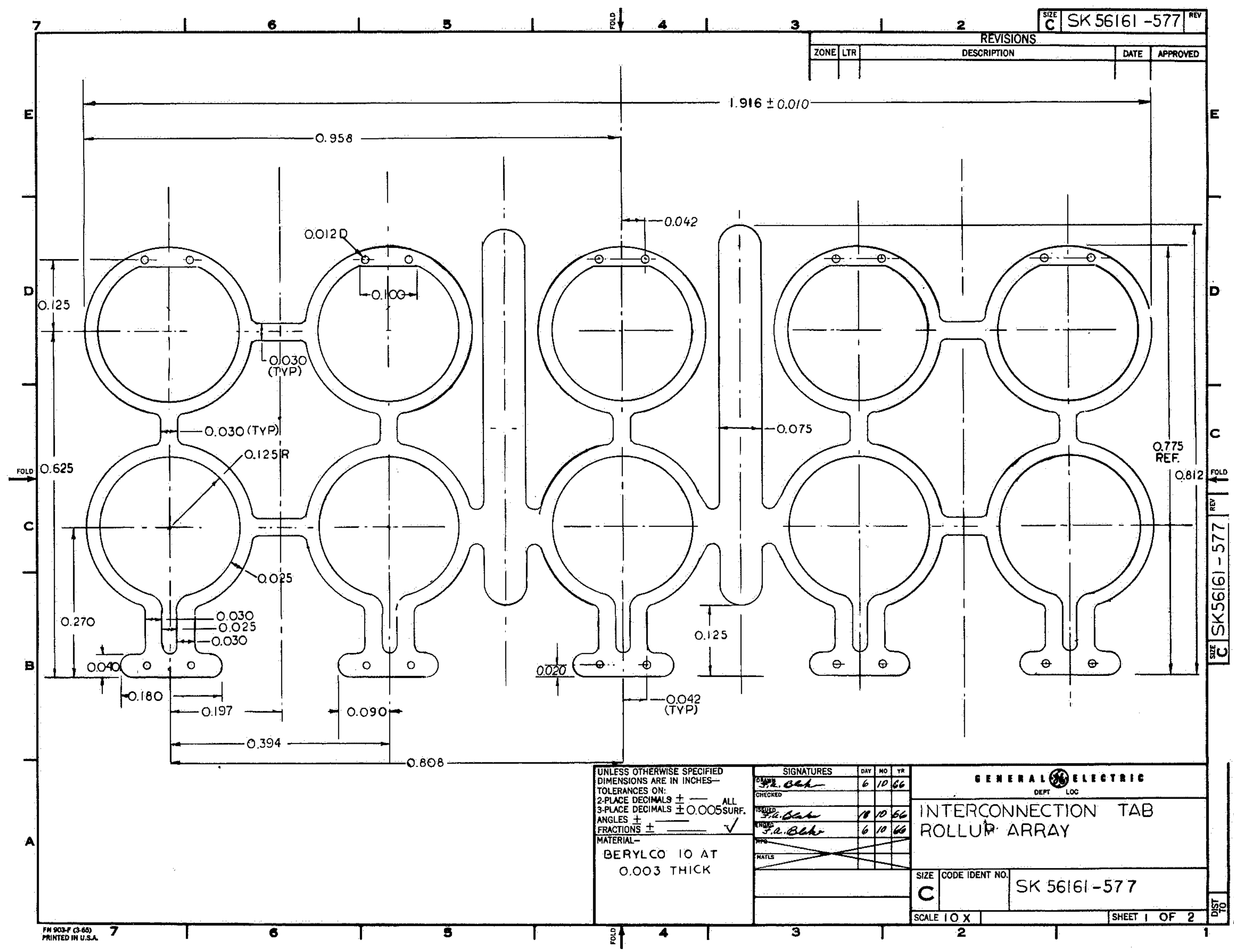

Figure 7-1. Drawing of Photoetched Interconnection

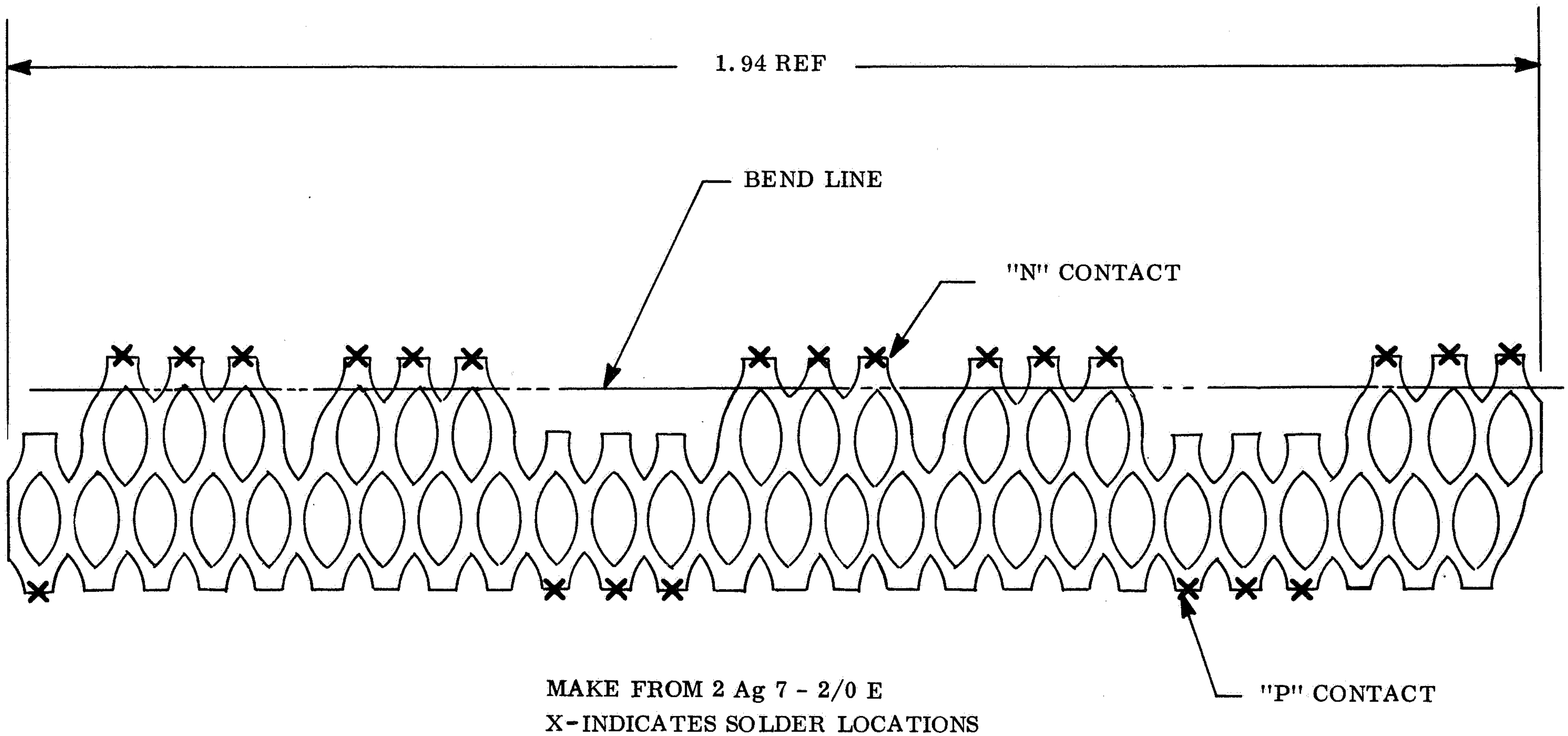

Figure 7-2. Interconnection for 5 by 5 Module

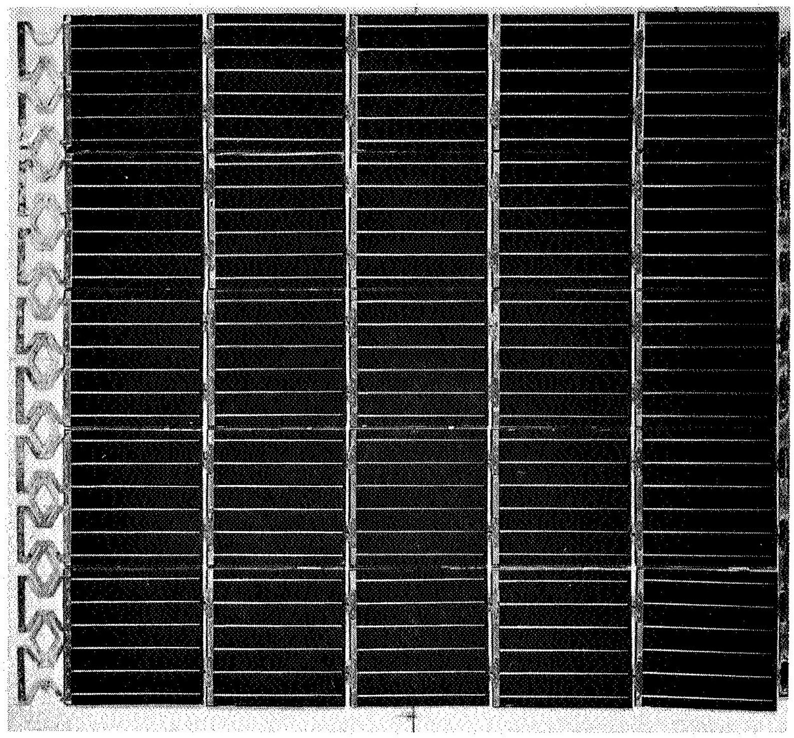

Figure 7-3. 5 by 5 Cell Module - Front Side

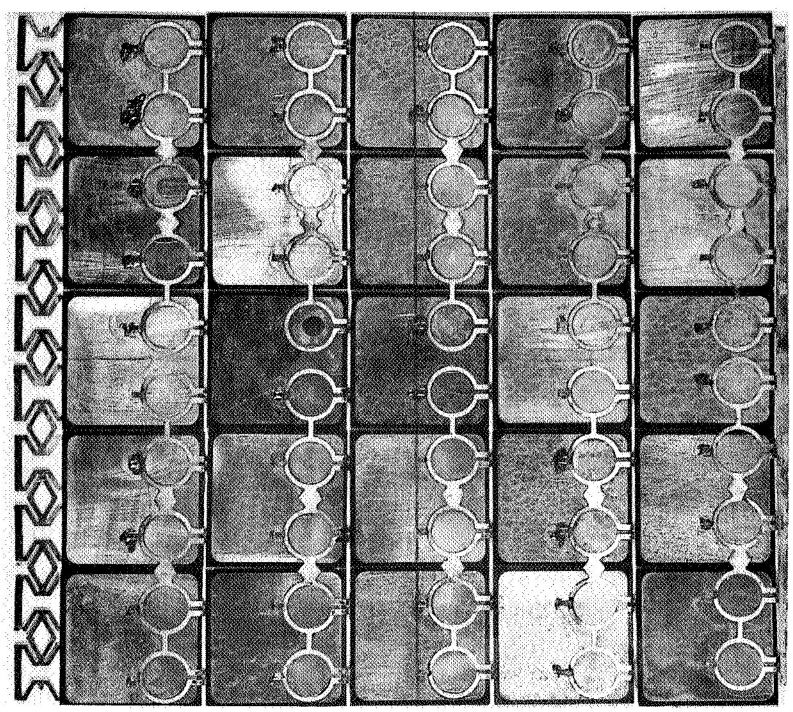

Figure 7-4. 5 by 5 Cell Module - Back Side

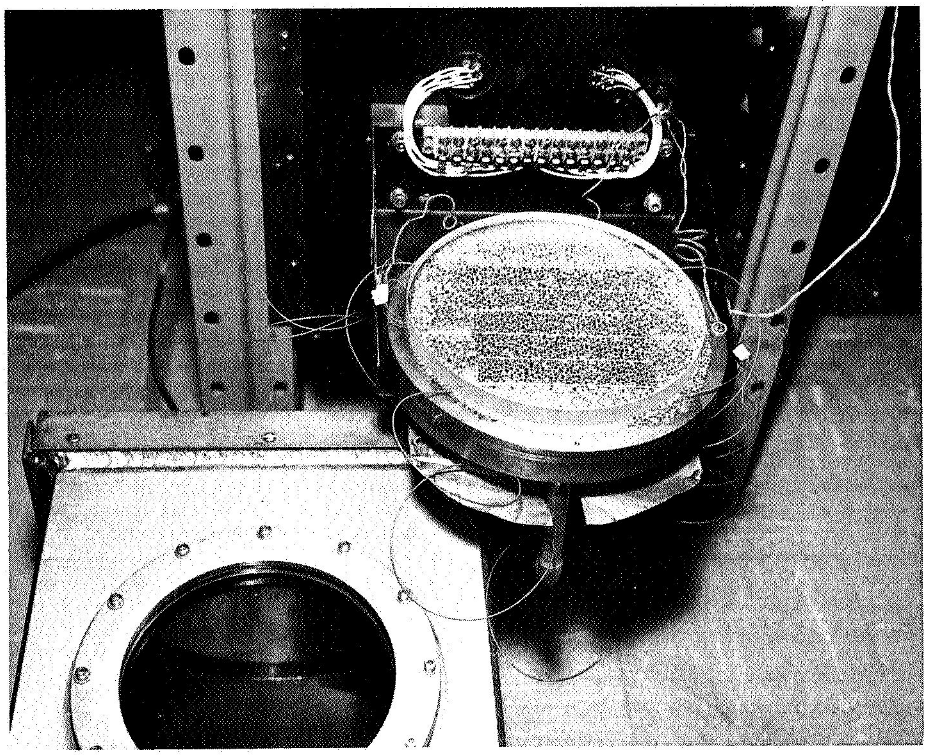

Figure 7-5. Thermal Cycling Test Set-Up

Tests 1 and 2 showed stable electrical output during the cycling operation, as shown in Table 7-1. Both specimens were damaged during the removal from the chamber with the result that inspection damage origins were not clearly definable. However, the occurrence of two crystal flake failures at the interconnection feet on Module 1 (see Figure 7-6) and three similar failures on Module 2 were likely results of thermal cycling forces rather than handling damage.

Degradation of the electrical performance of Module No. 3 initiated at cycle 28 and steadily progressed throughout the remainder of the test, as shown in Table 7-2. Microscopic examination of the module after the test revealed that three cells had completely loosened negative interconnection feet (see Figure 7-7), and the six other negative tab feet had flaking cracks started.

Table 7-1. Electrical Performance of Thermal Cycling Modules 1 and 2 During ±200°F Tests

Cycle No.	Module 1 Performance Short Circuit Current (ma)		Module 2 Performance Short Circuit Current (ma)	
	+200°F	-200°F	+200°F	-200°F
1	331	210	341	214
10	335	214	340	212
20	338	215	338	216
30	337	214	338	216
40	335	213	338	211
50	332	210	337	210
60	334	213	336	209
70	334	212	336	208
80	332	211	335	208
90	332	210	335	207
100	331	209	334	207
105			335	207
110	329	209		
114	329	208		

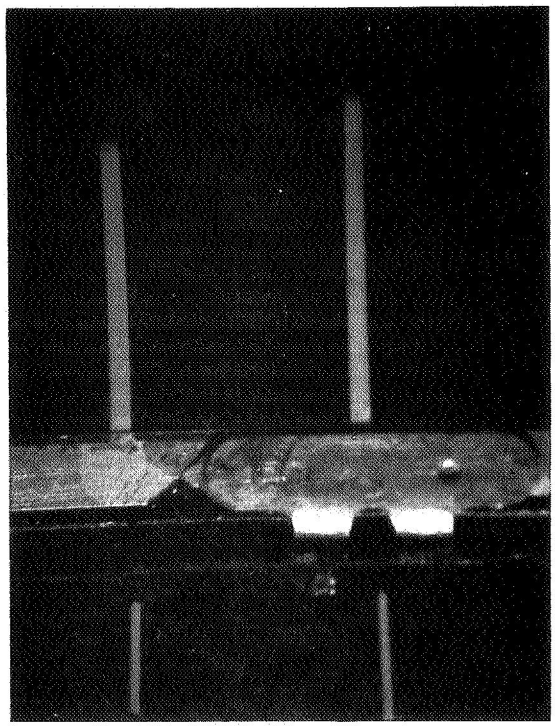

Figure 7-6. Photograph Showing Crystal Flake Failure at Foot-Module No. 1

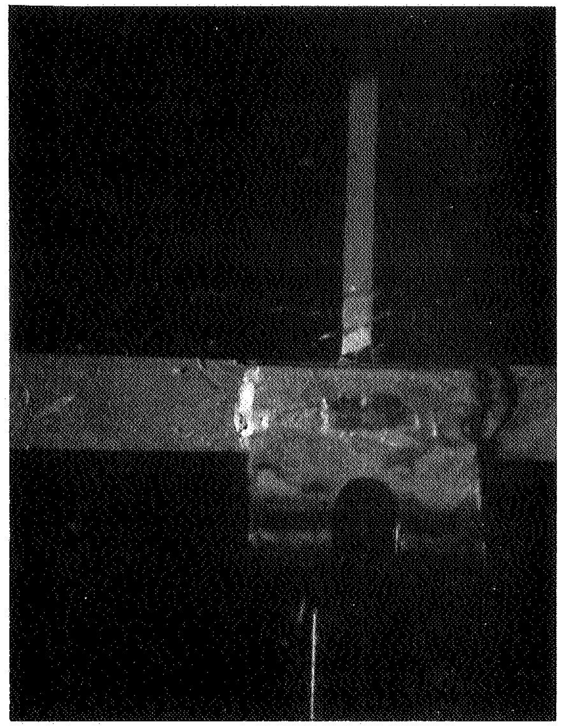

Figure 7-7. Photograph Showing Crystal Flake Failure at Foot-Module No. 3

While the results of test three were overly severe due to the reduction in flexibility from the bonding process, the similarity to the isolated failures in Modules No. 1 and 2 substantiated that the photoetched interconnection is poorly mated when used with the thin 0.008-inch cells.

In view of the failures which were experienced with the photoetched interconnection, a fourth module was constructed using the silver expanded metal interconnection. Photographs of this module, before the bonding of the substrate, are shown in Figure 7-8. Tape was used to isolate the adhesive from the interconnection during the bonding of the cells to the Kapton substrate. This module was mounted in the thermal cycling chamber and subjected to 117 cycles between -200 and +200°F. Visual inspection following this test revealed only one area of damage, as shown in the photograph of Figure 7-9. This photograph shows that two feet have cracked out. This damage was believed to be caused by the blob of adhesive (SMRD 745) which is covering the two feet.

Table 7-2. Electrical Performance of Thermal Cycling Module 3 During $\pm 200^{\circ}$ F Test

Cycle No.	Module 3 Performance Short Circuit Current (ma) +200°F	-200°F	Comments
1	327	202	
10	328	202	
20	326	201	
28	310	198	Indication of partial cell open during cycle
30	310	198	
34	308	198	Indication of full open cell during portion of cycle
40	310	198	Intermittent steps 1-5 times/cycle
50	310	178	Intermittent steps 1-5 times/cycle
60	309	198	Intermittent steps 1-5 times/cycle
70	309	178	Intermittent steps 1-5 times/cycle
80	308	170	Intermittent steps 1-5 times/cycle
90	308	160	Intermittent steps 5-10 times/cycle
100	308	160	Intermittent steps 5-10 times/cycle

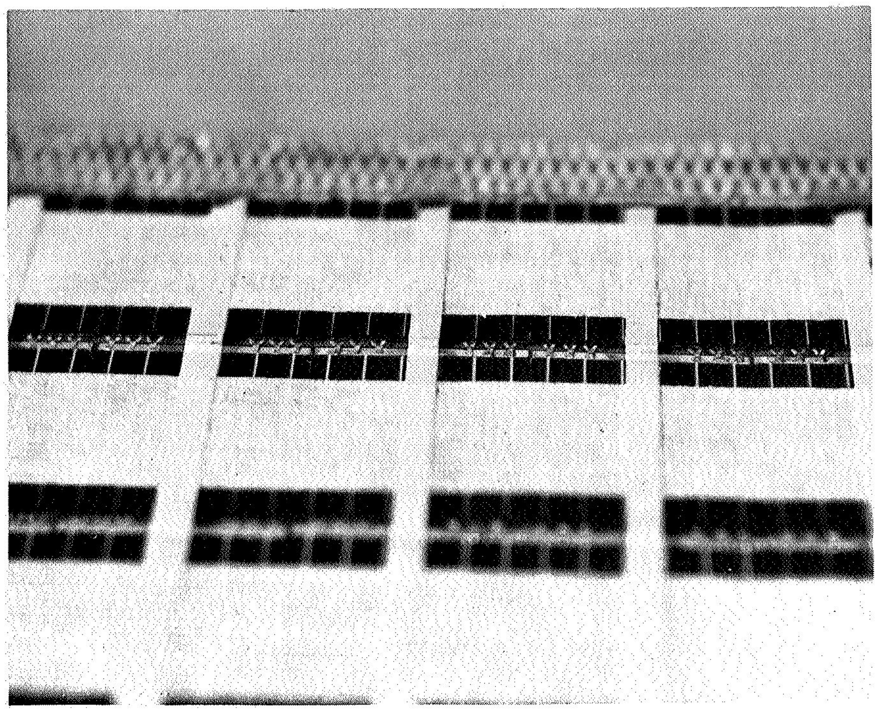

(a) Front

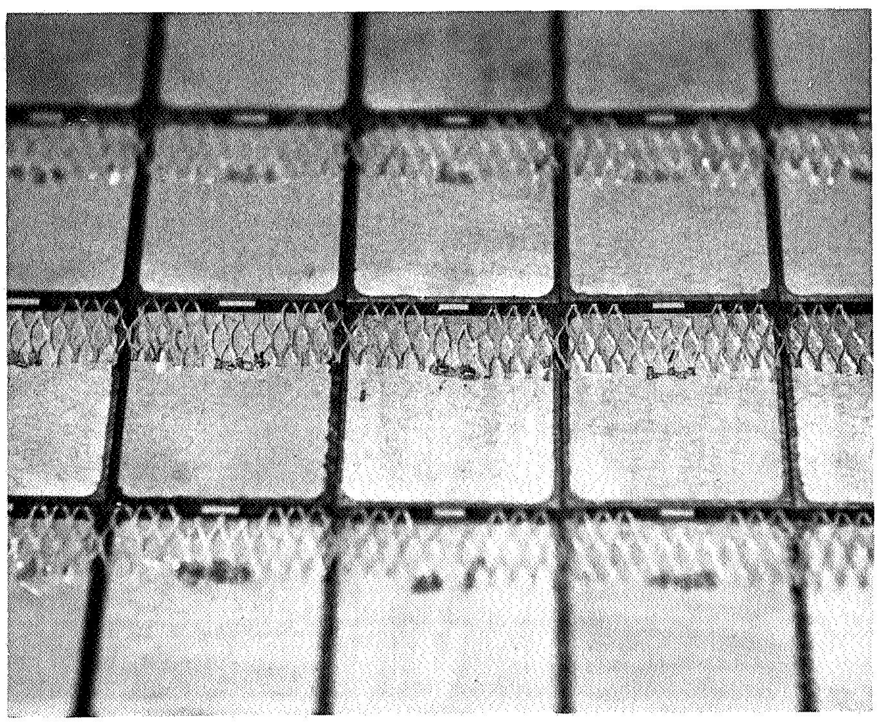

(b) Rear

Figure 7-8. Module Constructed Using Expanded Metal Interconnection

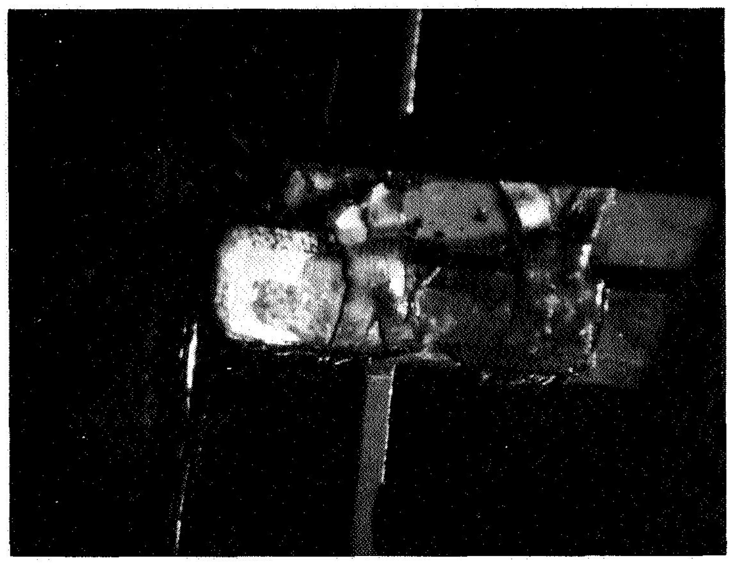

Figure 7-9. Thermal Cycling Damage After 117 Cycles Between -200 and +200°F

No other damage was detected within the module; and it was generally concluded that the module had successfully passed this phase of the test. The testing of this module was continued over a wider temperature range, from -250°F to +200°F. Eighty-eight additional cycles were completed between these temperature extremes. Visual inspection following this test revealed extensive damage. Only two cells within the module were undamaged. Photographs of several typical damage areas are shown in Figure 7-10. This damage is generally of two types: (1) cracked-out feet (Figure 7-10 a and b) and (2) fractured interconnection strands (Figure 7-10 c).

Several observations can be made based on these test results:

a. The 3-mil BeCu photoetched interconnection appears too stiff for use with these 8-mil solar cells.

b. The silver expanded metal interconnection functioned successfully between -200 and +200°F, but experienced extensive damage when the temperature range was expanded from -250 to +200°F.

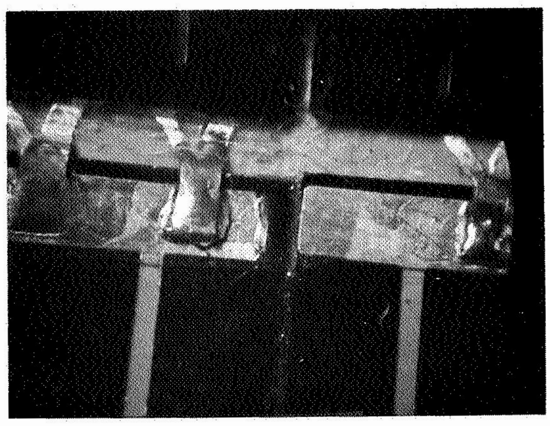

(a)

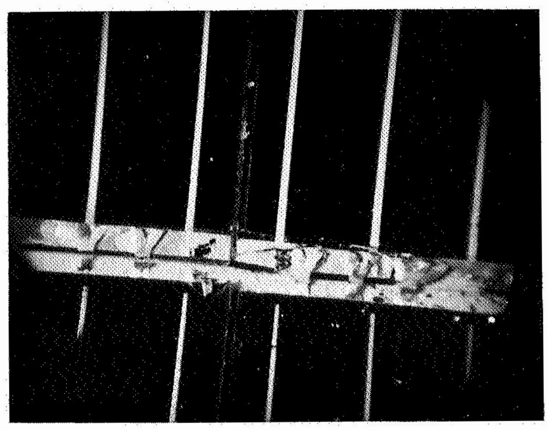

(b)

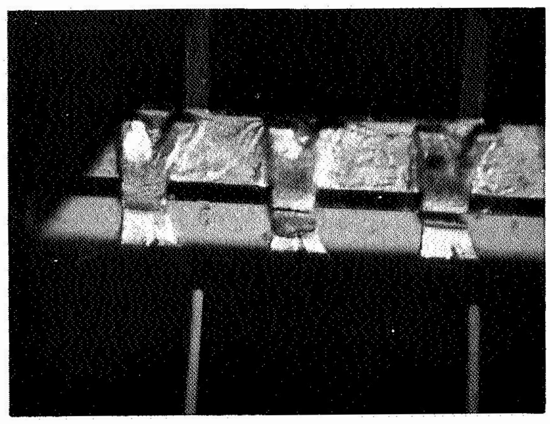

(c)

Figure 7-10. Thermal Cycling Damage (117 Cycles Between -200 and +200°F and 88 Cycles Between -250 and +200°F)

c. It is questionable whether either BeCu or Ag interconnections can be made compatible with these solar cells over the temperature range from -250 to +200°F due to the large difference in the coefficient of thermal expansion of these two metals when compared to silicon.

7.2 BEARING AND LUBRICATION CONSIDERATIONS

THE SELECTED BEARING FOR THE STORAGE DRUM IS A THIN SECTION, ANGULAR CONTACT, INSTRUMENT BEARING, SIMILAR TO THE TAR SERIES MANUFACTURED BY THE SPLIT BALLBEARING DIVISION OF MPB. THE LUBRICANT SYSTEM RECOMMENDED FOR CONSIDERATION ON THIS PROGRAM IS LUBECO 905, DRY FILM LUBRICANT.

The selected bearing was chosen because of its high load capacity and light weight and because of the successful past use of similar bearings in the Nimbus II satellite solar array drive mechanism. This unit continues to operate perfectly in space after 24 months of flight.

Because the rotating drum, in its operating configuration, will be supported on one end and free on the other end, two preloaded bearings will be used per drum.

Bearing races and balls will be made from 440C stainless steel. It is anticipated that the array may be in its extended position for weeks (or months) at a time, during which time there will be small amplitude oscillations of the bearings. When the array is retracted, the retracting force will be 4 pounds from the spring motors. Thus, it is important to have bearings with the following characteristics:

a. Capability of withstanding the static (nonrotating) radial and thrust loads of launch

b. Retention of lubricating properties in space environment

c. Low starting torque after prolonged idle periods in space

Item a will be accomplished by the selection of the right size bearings for the anticipated loads. Items b and c are related to the lubrication and design of the retaining ring.

Discussion

The present design requirement is for operation at $-150^{\circ}F$. The bearing is exposed to the high vacuum of the space environment. This eliminates the possibility of using oil or grease lubricants. There are few oils which will perform satisfactorily at this low temperature and those that will are too volatile for use in vacuum. This limits the choice to dry lubricants. These are usually categorized into one of two groups:

a. Transfer films: The bearing retainer is made from or coated with a plastic which transfers to the balls and then to the raceways. This provides a readily sheared film between the balls and the races which is then the lubricant. Reinforced Teflon is the most commonly used material.

b. Dry films: This system consists of a solid material which has one readily cleaved plane along which sliding can take place. Molybdenum disulfide is most commonly used. This material is attached to the surface to be lubricated usually with a binder such as sodium silicate or epoxy although systems employing electroplating and *in-situ* formation of the lubricating material are also being employed.

Materials Recommendation

Two materials have been evaluated in laboratory testing and on flight hardware, and should be considered as possible lubrication systems for the roll-up solar array.

Lubeco 905

This material is a molybdenum disulfide dry film applied by a proprietary electrophoretic process. It is from Lubeco, Incorporated, Compton, California. It has been tested under simulated space conditions by Hughes Aircraft and is rated by them as one of the best dry films. It is the dry film lubricant used on the Surveyor and Lunar Orbiter spacecraft. It has also been tested in the Voyager program discussed below.

The normal thickness of the material is 0.0003 inch, so that allowance should be made for this in specifying bearing internal clearances.

It should be applied to the inner and outer races and to the retainer, but not to the balls. A fully machined bronze retainer should be used.

The bearings should be procured in the unassembled condition and the coating applied. The coated parts should be inspected with a low power microscope up to 40X magnification. After assembly by the manufacturer the bearings should be again inspected.

After assembly, the bearings should be run in to burnish the coating. This should be done first by hand and any debris blown out with clean, dry gas, i.e., not shop air but gas from a dry cylinder or dry system. A millipore or other suitable filter should be employed. This should be done in the controlled environment of a clean room of class 100,000 or better per Federal Standard 209.

After running in by hand, the bearings should be run at 100 rpm for 1 hour and again blown out. This should be repeated if necessary until no dusting occurs.

Reinforced Teflon

Teflon which is reinforced with glass fibers has been tested for use on ball bearings. It is available in two forms. One contains molybdenum disulfide and is sold under the tradenames "Bar Temp" by Barden, Incorporated, a bearing manufacturer, and "Duroid" by Rodgers Corporation, a plastics processor.

In tests at Lockheed Missiles and Space Company, R-3 size bearings (3/16-inch bore, 1/2-inch O.D.) employing Rulon C retainers operated for over 10,000 hours in vacuum at 8000 rpm (References 7-1 and 7-2). Thrust loads were 1/4 to 1 pound per bearing; radial loads were 135 grams per bearing. Pressures were 10^{-7} to 10^{-8} torr. The data is summarized in Table 7-3.

Bearings employing Duroid 5813 retainers and no other lubricant have been successfully tested in vacuum at NASA Goddard (Reference 7-3). Radial loads were from 0.8 ounces to 7.5 pounds; bearing sizes were from R-2 to R-9. In tests at Lockheed under the same conditions as for Rulon C above, Duroid 5813 gave a lifetime of over 5000 hours in one test, but increasing the thrust load reduced the lifetime to less than 100 hours. This data is also included in Table 7-4. Duroid 5813 has also been used in tape recorders installed on spacecraft (Reference 7-4).

Rulon A and Duroid 5813 are both being tested in the Voyager test program. They have been among the best materials tested.

Table 7-3. Bearings with Self-Lubricating Retainers

Bearing Type	Instrument size ball bearings
Race and Ball Material	440C Stainless steel
Retainer Material	Rulon C
Notes	For low-speed applications, bearing should first be run in at 500 to 1000 RPM at light load (approximately 1/4 lb) for 1 hour to assure transfer of film from retainer. Bearing must be supplied <u>without</u> oil lubrication.

Speed	Load per bearing: Radial	Load per bearing: Thrust	Temp (°F)	Pressure (torr)	Lifetime	Comments
8000 RPM	137 grams	1/4 lb	125 to 210	4×10^{-7} to 2×10^{-8}	12,600 hr	Reference 7-1. Angular contact bearings R-3 size, two bearings tested. Test discontinued, bearings still operating.
8000 RPM 53 minutes in one direction 7 minutes power off, 53 minutes in opposite direction; repeat.	137 grams	1/4 lb	125 to 180	5×10^{-7} to 6×10^{-8}	8600 hr	Reference 7-2. Angular contact bearing, R-3 size, two bearings tested.
8000 RPM	137 grams	1 lb	145 to 170	4×10^{-6} to 6×10^{-8}	3100 hr	Reference 7-2. Angular contact R-3 bearing, short life is attributed to no thrust load for first 500 hr of testing, two bearings tested.
8000 RPM	136 grams	1/4 lb	90 to 140	760	30,000 hr	Reference 7-2. Still running at end of test, angular contact bearing, R-3 size, two bearings tested.
8000 RPM	136 grams	1/2 lb	130 to 145	1×10^{-7} to 3×10^{-8}	10,770 hr	Reference 7-2. Angular contact bearing R-3 size, two bearings tested.
8000 RPM	138 grams	1 lb	125 to 140	1×10^{-7} to 3×10^{-8}	10,700 hr	Reference 7-2. Test still running when discontinued. Angular contact bearing R-3 size, two bearings tested.
						Material also used in the following flight applications (Reference 7-4) Pegasus 1 & 2 Output shaft bearings

Table 7-4. Bearings with Self-Lubricating Retainers

Bearing Type	Instrument size ball bearings
Race and Ball Material	440C stainless steel
Retainer material	Duroid 5813, 60% Teflon - 40% glass fibers with molybdenum disulfide, from Rodgers Corporation; Bar Temp from Barden Corporation is the same material
Notes	When used at low speed bearings should be first run in at 500-1000 RPM at light load (approximately 1/4 lb) for 1 hour to assure transfer of film from retainer. Purchase without oil lubricant.

	Load per bearing					
Speed	Radial	Thrust	Temp (°F)	Pressure (torr)	Lifetime	Comments
1800 RPM	2.1 oz	Light, not reported	Not reported	5×10^{-8}	1700 hr +	Reference 7-3. Test still running when discontinued; R-2 size-bearing. Two bearings per test.
1800 RPM	10.7 oz	Light, not reported	Not reported	5×10^{-8}	2500 hr +	Reference 7-3. Bearing still running when discontinued; R-3 size bearing. Two bearings per test.
100 RPM	4.5 lb	Light, not reported	Not reported	5×10^{-8}	8200 hr +	Reference 7-3. Test still running; R-4 size bearing. Two bearings per test.
10 RPM	1.5 lb	Light, not reported	Not reported	5×10^{-7}	10,515 hr	Reference 7-3. R-4 size bearing. Two bearings per test.
100 RPM	1.5 lb	Light, not reported	Not reported	5×10^{-8}	8200 hrs +	Reference 7-3. Test still running; B542 tube type bearing. Two bearings per test.
8000 RPM	0.8 oz	Light, not reported	Not reported	5×10^{-7}	4380 hr	Reference 7-3. R-4 size bearing. Two bearings per test.
1 RPM	1.3 lb	1 1/4 lb	Not reported	9×10^{-9}	5800 hr +	Reference 7-3. Test still running. R-6 size bearing. Two bearings per test.
Oscillating 0 - 50° in. 30 sec	7.5 lb	Not reported	Not reported	9×10^{-9}	5800 hr +	Reference 7-3. Test still running; R-9 size bearing. Two bearings per test.
Oscillating 0 - 50° in. 30 sec	1.5 lb	1 1/4 lb	Not reported	9×10^{-9}	5800 hr +	Reference 7-3. Test still running. R-6 size bearing. Two bearings per test.
8000 RPM	137 grams	1 lb	Not reported	10^{-7} to 10^{-8}	28 hr	Reference 7-1. R-3 angular contact bearings; two bearings tested.
8000 RPM	137 grams	1/2 lb	Not reported	10^{-7} to 10^{-8}	62 hr	Reference 7-1. R-3 angular contact bearings; two bearings tested.
8000 RPM	137	1/4 lb	Not reported	10^{-7} to 10^{-8}	5100 hr	Reference 7-1. R-3 angular contact bearings; two bearings tested.
8000 RPM	137	1/4 lb	Not reported	10^{-7} to 10^{-8}	67 hr	Reference 7-1. R-3 angular contact bearings; two bearings tested.
8000 RPM 53 minutes in one direction, 7 minutes power off, 53 minutes in opposite direction, and repeat	137	1/4 lb	Not reported	10^{-7} to 10^{-8}	90 hr	Reference 7-1. R-3 angular contact bearings; two bearings tested.
8000 RPM	137	1/4 lb	Not reported	760	18,800	Reference 7-1. R-3 angular contact bearings; two bearings tested. Reference 7-4. Material also used in the following flight applicative Nimbus Tape recorder bearings.

Although the above bearings were with solid retainers of reinforced Teflon, there should be no problem in using inserts of this material in metal retainers. For the size bearing involved in this application this type is more desirable, since a retainer solely of Teflon this large is difficult to machine and hence is not commonly available and also would be too flexible.

Since these bearings depend on a transfer film, they need to be run in to establish such a film. The tentatively recommended run-in is at 100 rpm with a 2-pound radial load and a 1-pound thrust load for 1 hour, followed by 1 hour at 100 rpm with a 4-pound radial load and a 2-pound thrust load. This is subject to revision based on final decision on determination of preload.

Appropriate GE Experience

As part of the Voyager work, a program testing instrument-size bearings in vacuum is being conducted. The test fixture consists of six shafts mounted on a single rack. Each shaft is driven by its own motor. On the shaft are two pairs of test bearings. One pair supports a 1-1/2 pound weight; the other pair, a 3 pound weight. These provide radial loads which are evenly distributed between the two bearings a pair. Calibrated springs provide a thrust load of 1 pound to the more heavily loaded pair of bearings and 3/4 pound to the more lightly loaded. The shaft is supported on the rack by two bearings. A photograph of this equipment is shown in Figure 7-11.

The bearings are all R-4 size, 1/4-inch bore, 5/8-inch O.D. On each shaft, the same lubricant was used for the four test bearings, and, in so far as possible, for the support. (Due to the insufficient numbers of acceptable test bearings, bearings with Bar Temp/ Duroid 5813 were used for support bearings in some cases.)

A strain gauge system is used for determining torques of each pair of test bearings. Thermocouples in the support bearing housings measure the temperature there.

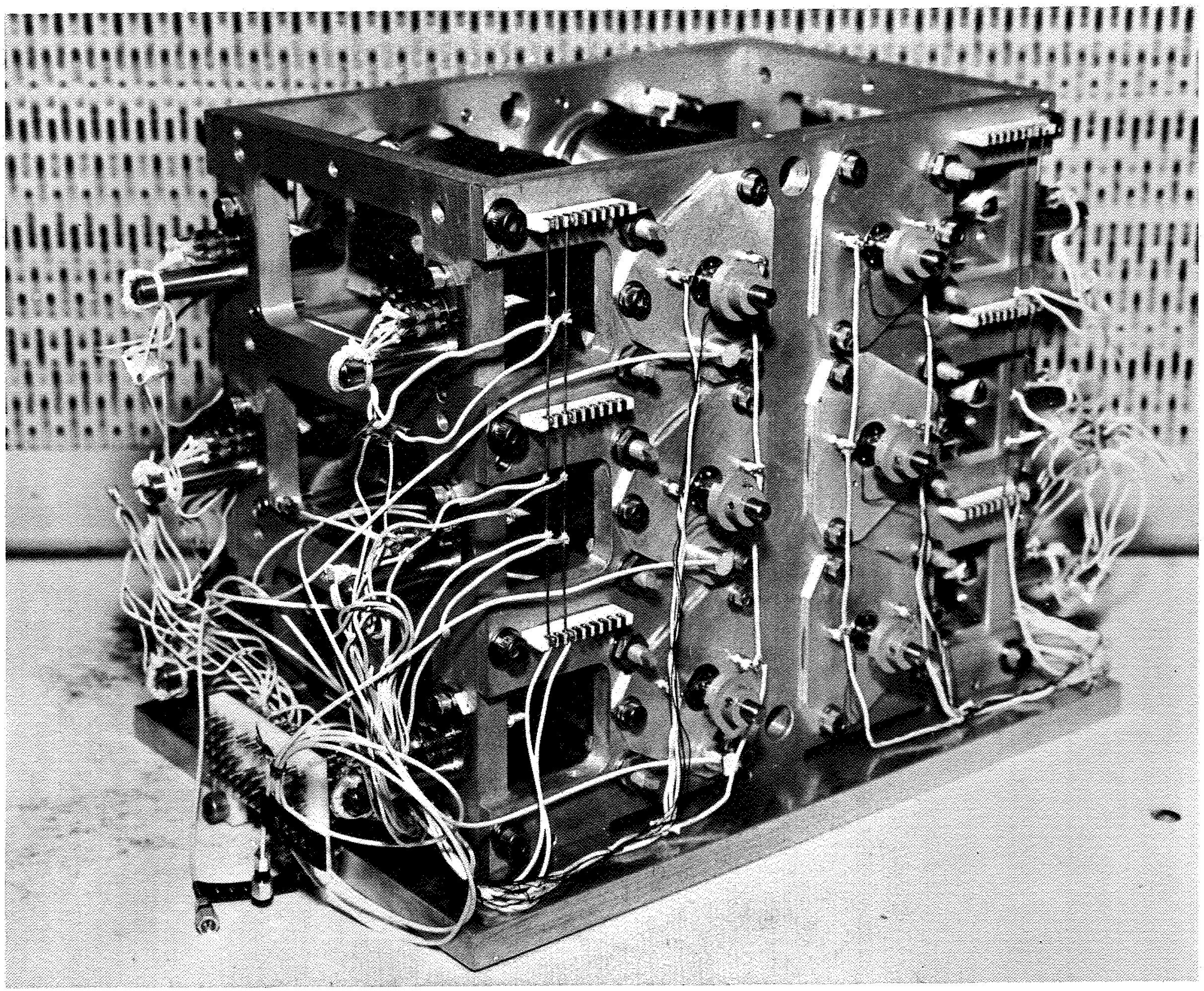

Figure 7-11. Bearing Test Fixture

Two of the above fixtures were fabricated. Each was installed in a separate, new vacuum system.

Test pressures have been 10^{-9} to 10^{-10} torr predominantly with some periods at 10^{-8}.

Test speed has been 480 rpm.

The work has been divided into the following phases:

Phase A 48 hours in vacuum run with reversal every 2 hours.

Phase B The following repeated ten times on each shaft:

a. 4 minutes clockwise operation

b. 2 minutes dwell

c. 4 minutes counterclockwise

d. 2 minutes dwell

e. Repeat

Phase C

a. Dwell 72 hours

b. Operate motors individually until change of torque is less than 10% of average torque

c. Repeat for a total of three times

d. Perform a through c with 48 hour dwells, 24 hour dwells, 6-hour dwells, and 1-hour dwells

Phase D Operate continuously for 100 hours each week with a reversal after 50 hours. Leave idle on the weekends.

In addition to the above, a brief operation in air was also conducted to verify instrumentation and motor operation.

Of particular interest to this application are the long idle periods. In addition to the ones programmed, the tests were stopped at the end of 1967 for 288 hours. There were no anomalies in restarting.

The tests are presently stopped for the evaluation of results. The first fixture has completed 140×10^6 revolutions and the second has completed 70×10^6 revolutions.

7.3 MATERIALS SELECTION

ALL POLYMERIC MATERIALS WHICH ARE UTILIZED IN THE PROPOSED DESIGN HAVE BEEN REVIEWED IN REGARDS TO SUITABILITY FOR USE IN A SPACE ENVIRONMENT.

The polymeric materials which are proposed for the 30 Watts per Pound Roll-Up Solar Array have been reviewed with respect to the experimental data contained in Reference 7-5. This report presents data on the behavior of polymeric materials in a thermal-vacuum environment. Loss of weight and the amount of released material which may condense on cool surfaces adjacent to the warmed polymer are important criteria in the determination of a material's suitability for use in a space environment. The criteria proposed in Reference 7-5 is stated as follows:

> "Thus, a polymeric material should not be considered suitable for use in spacecrafts or be subjected to further evaluation, unless it exhibits a 1-percent or less weight loss and a 0.1-percent or less maximum volatile condensable materials (VCM) content on exposure to the thermal-vacuum environment of 125°C and 10^{-6} torr."

Table 7-5 is a summary of the organic materials proposed for use in the roll-up solar array, along with the corresponding values for percent weight loss and percent by weight of VCM. An examination of this table shows that the foamed RTV 560, which is used for the cushioning buttons on the rear side of the array substrate, does not meet the established criteria for an acceptable material. However, it is still desirable to consider the use of foamed RTV 560 for the following reasons: (1) it has experimentally demonstrated the ability to protect the cell/glass combination, (2) it provides high frictional damping which limits the axial motions of the wraps on the storage drum, and (3) processes for aerospace applications are already developed. In order to reduce the weight loss and VCM values, it is proposed to "post-cure" the array substrate with the foamed buttons under the vacuum and at an elevated temperature for a minimum of 48 hours. Note that the buttons are a nominal 0.040-inch thick, and the total weight of the foamed material on the 250-ft^2 array is 1.50 pounds.

The SMRD 745 is a proprietary General Electric adhesive formulated especially for space applications. It has no plasticizers, but derives its flexibility from the backbone polymer chain itself. Therefore, it is intrinsically a low outgasser. Our tests have shown that it falls in the same outgassing range as typical rigid epoxy compounds.

Table 7-5. Roll-up Array Polymeric Materials VCM Data
(24 Hours at 125°C and 10^{-6} Torr, VCM Collectors at 25°C)

Material	How Used	Treatment	Total Weight Loss (%)	VCM Wt. (%)	Reference
Epon 934	Bonding beryllium	1 hour @ 82°C	0.10	0.08	7-5
Kapton-H Film	Array substrate	As received	0.14	0.09	7-5
Delrin	Neg'ator take-up spool	As received	0.58	0.06	7-5
Sylgard - 182	Cell-to-cover glass bond	As received	1.5 @ 100°C 0.5 @ 50°C	*	7-6
RTV -560	Cushioning buttons	24 hrs @ 150°C	1.03	0.68	7-5
SMRD 745	Cell-to-substrate bond	*	*	*	*
Epiall 1914	Drum power feed-thru slip ring dielectric	24 hrs @ 150°C	0.55	0.03	7-5
GT-100	Bus strip-to-substrate bond	*	*	*	*

*No data available at the time of this writing.

7.4 GSE PRELIMINARY DESIGNS

THE CONCEPTUAL DESIGN OF THE GROUND EQUIPMENT REQUIRED TO SUPPORT THE HANDLING AND TESTING OF A FLIGHT CONFIGURATION ARRAY HAS BEEN COMPLETED.

All equipment which is not a part of the solar array design, but is required to complete the program, is classified as support equipment and divided into two categories: (1) handling equipment and (2) test equipment.

Handling Equipment

Table 7-6 summarizes the proposed items of handling equipment and lists the intended uses.

1. Holding Fixture - A holding fixture is required from the earliest steps in the manufacturing process through the final testing phases. The holding fixture is a tubular framework which has provisions for the attachment of the center support and the two outboard end supports of the array (see Figure 7-12). Provisions will also be made for attaching the handling sling and other fixtures or stands required during systems testing. The holding fixture will simulate the spacecraft structure to which the array will eventually be attached and will provide the means for keeping the three hardpoints in the proper relative position.

2. Dolly - The dolly will consist of a four-wheel cart which will be primarily utilized for in-plant transportation and temporary storage (see Figure 7-13). The roll-up solar array will be positioned on the dolly at work bench height so that any required assembly, repair, and inspection functions can also be performed on the entire assembly or the individual blanket assemblies.

   The holding fixture attached to the array will interface with and be attached to the dolly on a built-up box section. Attachment in this fashion will preclude the possibility of the bracketry impeding the operation of the array and provide complete accessibility.

3. Shipping Container - The shipping container will provide the necessary environmental protection required during shipment of the array to off-site testing facilities and to other locations as specified by the customer (see Figure 7-14). The shipping container will also be utilized during acceleration testing to provide a wind shroud. The design will consist of a long rectangular box with provisions for lifting with the handling sling or forklift. Two trunnions will protrude from each side for interfacing with the acceleration fixture. Provisions will be made for an instrumentation penetration of the shipping container to be utilized during the acceleration tests. The array will be attached

Table 7-6. Handling Equipment Summary

Item	Use
1. Holding fixture	a. Assembly fixture b. Testing base c. General handling
2. Dolly	a. Assembly and repair workstand b. In-plant transportation c. Storage - short term d. Inspection stand
3. Shipping container	a. Transportation protection b. Acceleration test shroud c. Storage - long term
4. Handling sling	a. General handling of the solar array assembly and/or shipping container
5. Dust cover	a. Storage - short term

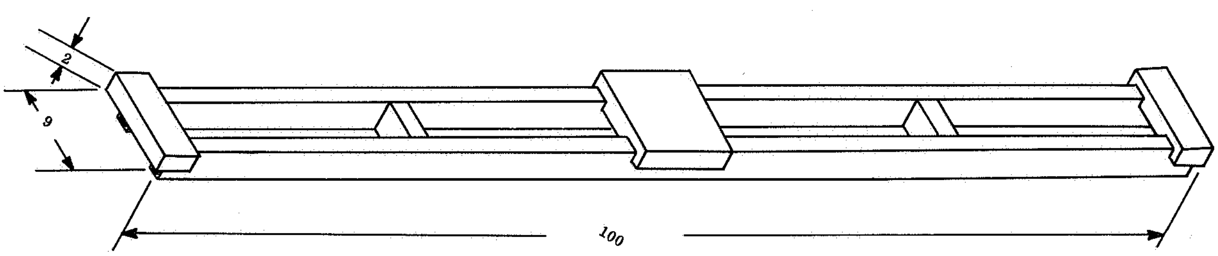

Figure 7-12. Holding Fixture

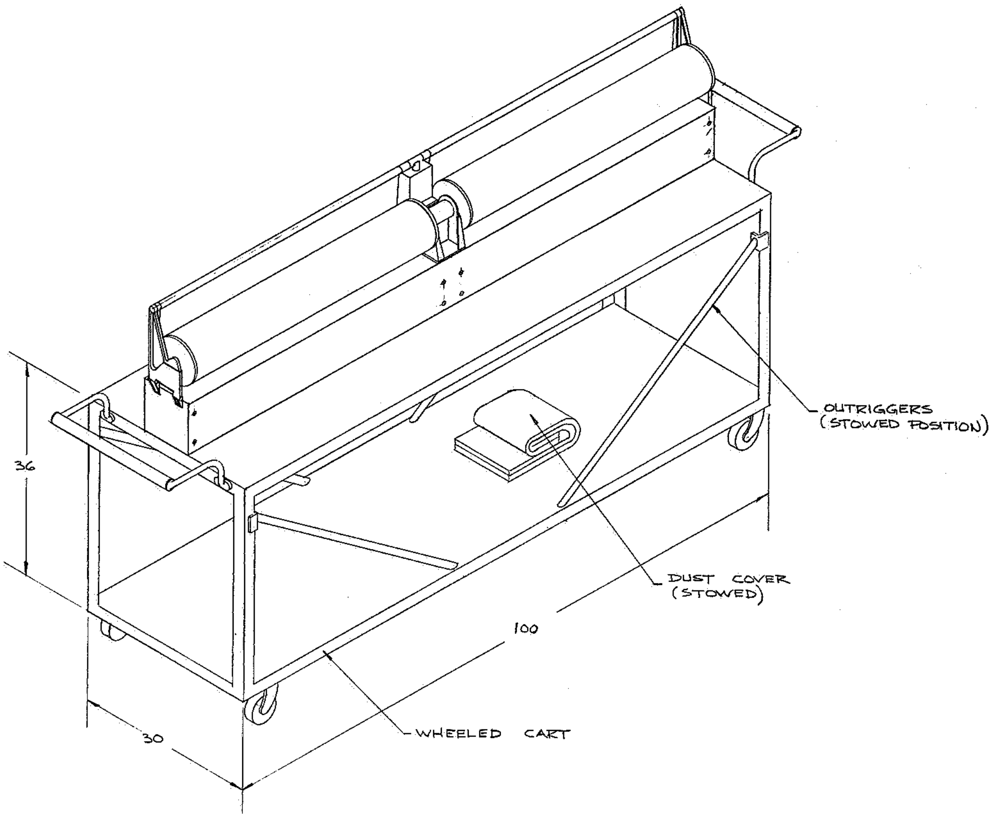

Figure 7-13. Dolly

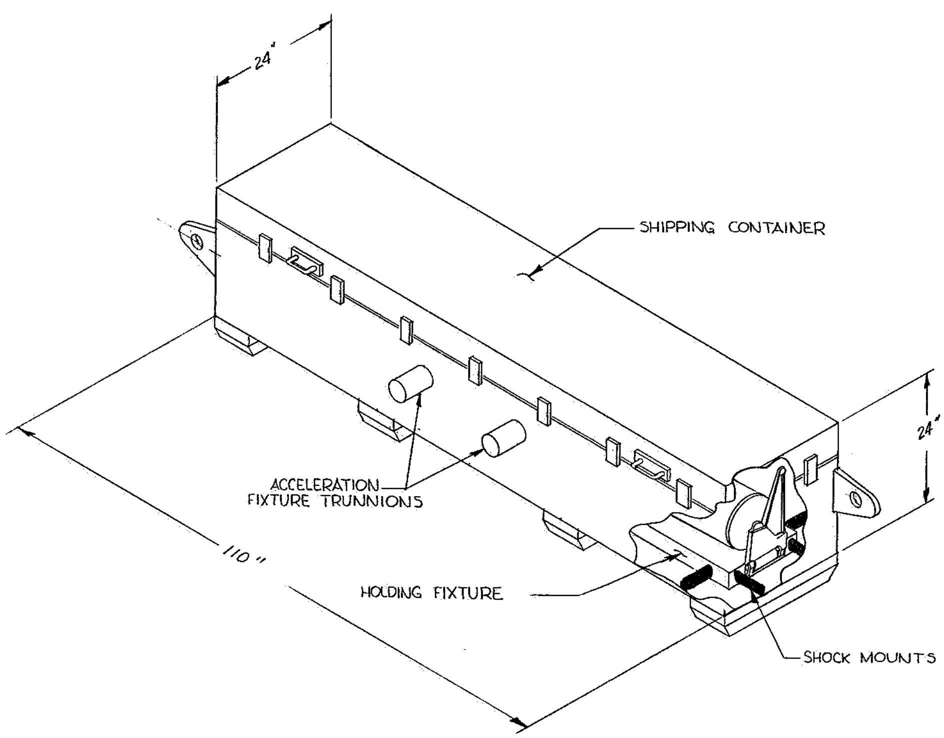

Figure 7-14. Shipping Container

to the holding fixture within the container. The holding fixture will be shock-mounted to the interior of the shipping container to provide the necessary isolation.

4. Handling Sling - The handling sling is required to provide a positive means of lifting and positioning the array assembly and holding fixture during the development testing and the lifting of the shipping container (see Figure 7-15). The handling sling will consist of a spreader bar with wire rope legs at each end. A ring will be positioned at the spreader bar midpoint for interfacing with the crane hook.

5. Dust Cover - The dust cover consists of plastic sheeting for covering the array during periods of temporary storage and transportation between buildings.

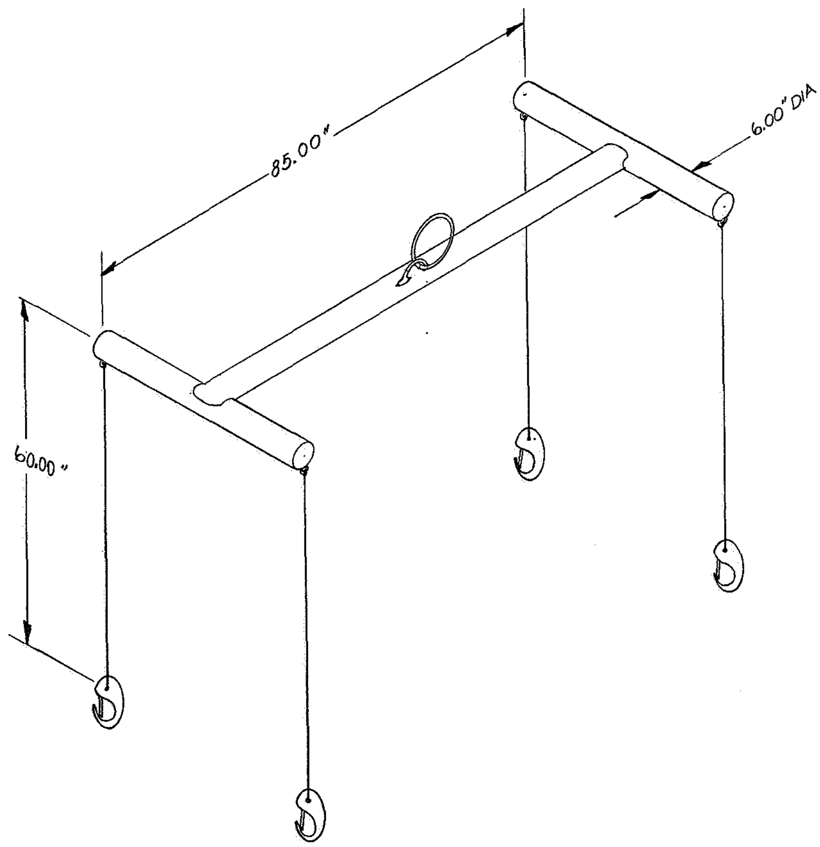

Figure 7-15. Handling Sling

Test Equipment

Table 7-7 summarizes the proposed items of test equipment and lists the intended uses.

Table 7-7. Test Equipment Summary

Item	Use
1. Vertically upward deployment aid	a. Demonstration of deployment in lg environment b. Inspection and illumination
2. Vertically downward deployment aid	a. T/V testing b. Modal survey - deployed
3. Vibration fixture	a. Sine and random test b. Modal survey - stowed
4. Shock fixture	a. Shock test
5. Acceleration fixture	a. Acceleration test
6. Inertial properties measurement equipment	a. Moments of inertia b. Products of inertia
7. IR lamp array	a. Thermal testing
8. Electro-optical readout equipment for T/V and modal testing	a. Modal testing
9. Performance test set	a. Array performance tests b. Deployment tests

1. Vertically Upward Deployment Aid

The key feature of the "vertically upward deployment" test which enables it to meet the criteria of attaining realistic rod loading while at the same time allowing sufficient freedom for torsional and bending motions is the variable counterweight assembly shown in Figure 7-16.

This unit (mounted approximately 4 feet above the limit of the deployed array travel) consists of two drums on a common axis which are mounted on overhead tracks, and upon which are coiled lightweight and heavyweight steel cables. The two sets of tracks at right angles to each other provide capability of two-axis positioning such that the lightweight attachment cable can be kept in the position of the local vertical with

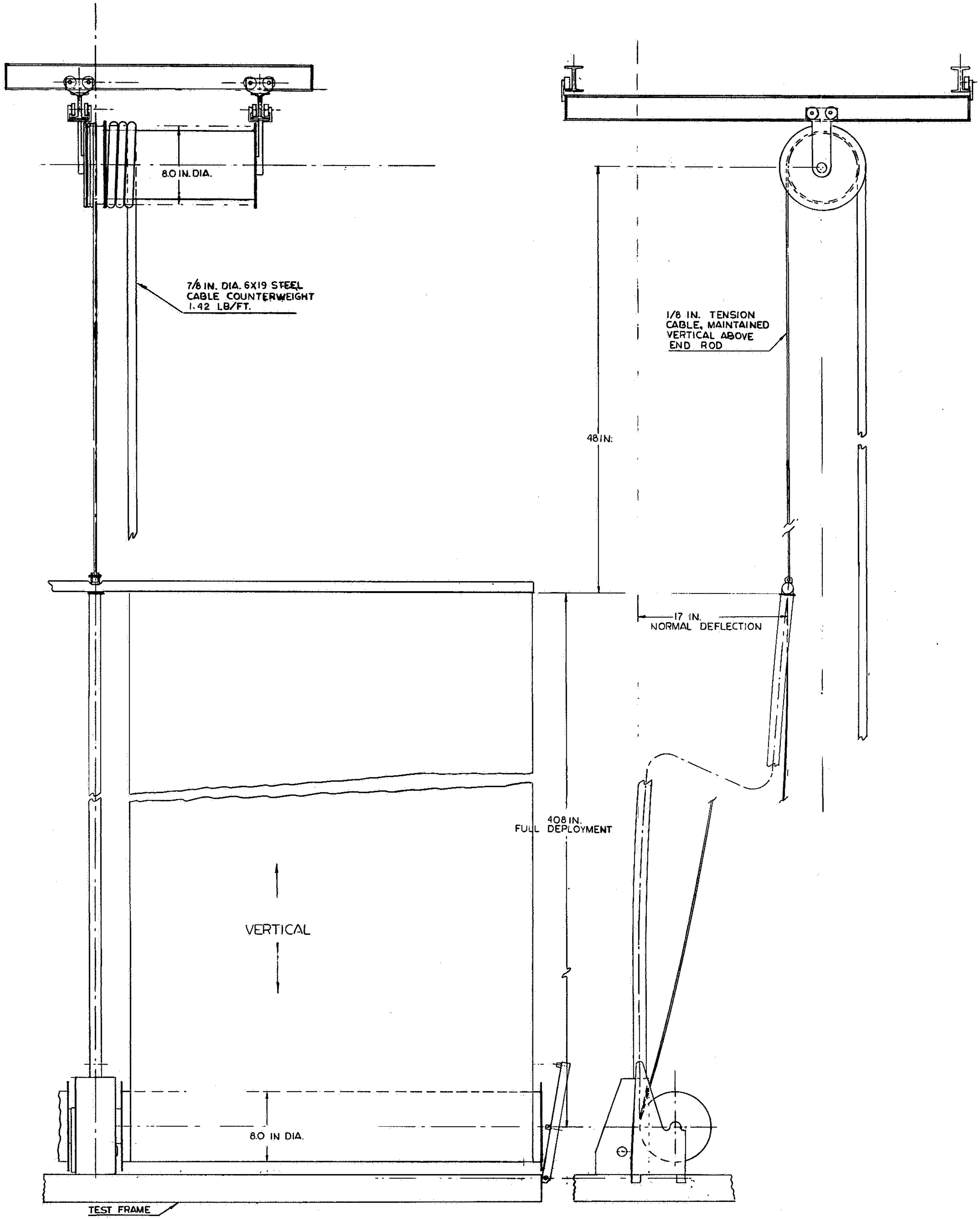

Figure 7-16. Vertically Upward Deployment Aid

respect to the tip of the erection rod and thereby not induce lateral loadings to either aid or penalize the rod performance. The heavyweight cable is a 7/8-inch steel cable selected because its 1.42 pounds per foot weight closely matches the 1.46 pounds per foot of the array and rod, which must be counterbalanced to eliminate the gravity effect on the deployment rod.

Rotation of the counterweight drum is under positive control in both the deployment and retraction operations, without the addition of any rotary drive. The initial unbalance from the length of cable used to simulate the leading edge member provides the constant driving torque unbalance throughout the deployment operation. During retraction, the erection rod load is reduced by the amount of the unbalance, with both the remaining rod load and the unbalance neutralization force being supplied by the NEG'ATOR springs inside the drum.

Positioning of the attachment cable in the local vertical will be monitored by optical means and controlled by servo type drive motors on the overhead dollies.

By compensating for the gravitational loads of the rod and array blanket as the deployment operation is performed, the counterweight also assures that the blanket tension conditions at the point of tangency between the blanket and the drum simulate the orbital case. The only tension present at this section is that provided by the blanket tension NEG'ATOR springs. This condition permits realistic evaluation of the wrapping performance with regard to mechanical integrity and also permits realistic evaluation of the tracking performance of the re-wrapped blanket as it is wound onto the drum. This tracking performance will enable selection of the simplest and most effective tracking control to be made with confidence, since the effects of blanket stiffness, blanket friction, and edge guidance forces can be observed.

2. Vertically Downward Deployment Aid

Evaluation of the requirements of the deployed modal testing and of the thermal vacuum testing resulted in the selection of the vertically downward deployment approach rather than the vertically upward approach used in the bulk of the deployment testing. For the modal test the main reason for the selection was that while the attachment of the compensation cable to the end rod provided a static simulation of the orbital loading, it provided an unwanted lateral compensation to dynamic motions induced by vibration. The problems associated with positioning the variable counter-weight to eliminate the lateral loadings while in the vacuum chamber with limited visual access caused the downward deployment to also be selected for the thermal vacuum test.

Two lightweight attachment cables are mounted at the inboard ends of the drums and wrap up on the drums as the array blanket unwraps. This wrapping-up of the attachment cables picks up compensation weights in the form of steel cables coiled on the test floor, thus preventing unloading of the deployment rod. Caution will be maintained in the retraction operation in this installation since the loads in the blanket at the point of tangency with the drum are nearly an order of magnitude greater than the orbital loads, and thereby present an invalid tracking characteristic.

3. Vibration Fixture

The vibration fixture is essentially a box beam structure which will have provisions for directly mounting the array on either of two adjacent faces (without the holding fixture). A sketch of the vibration set-up showing the fixturing is shown in Figure 7-17. The exciters (either 3 or 4) will be attached directly to the box beam structure. Team bearings will be used to provide the necessary support, lateral stiffness and constraint.

4. Shock Fixture

Shock test fixture is not the same as the vibration fixture. It consists of the holding fixture modified to include additional stiffness at the exciters and at the Team bearing locations.

5. Acceleration Fixture

The acceleration fixture is a steel framework used to mount the array/shipping container on the centrifuge arm in the six required positions (see Figure 7-18).

6. Inertial Properties Measurement Equipment

The inertia properties measurement equipment consists of a Pelton interface fixture and a bifilar pendulum fixture. The Pelton interface fixture will be used to mount the array, on the holding fixture, to the Pelton machine for the determination of the array products of inertia (Ixy, Ixz, and Iyz). The bifilar pendulum fixture will be used to suspend the array as a pendulum for the determination of the moments of inertia (Ixx, Iyy, Izz).

7. IR Lamp Array

The IR lamp array will be similar to that used in testing the Apollo radiator at General Electric. The thermal fixture, or infrared energy array, will be suspended in a vertical position facing the solar array, as shown in Figure 7-19. It will be 12 feet wide by 39 feet high and will consist of a series of nine vertical, hollow aluminum pipes which are connected at either end to a horizontal aluminum header. The entire structure will be of welded construction, butt joint, and suitably leak-checked for vacuum test use. Overall structure leak rate will be kept below 1×10^{-6} standard cm^3/sec of helium, as determined by using a helium mass spectrometer. Longitudinal fins will be welded to the vertical pipe risers, to fit into the mounting block slot at the rear of the reflectors, and provide a conductive cooling path. Water will be circulated through the entire structure to provide cooling directly to the reflectors, which combined with the radiative cooling of the

FOLDOUT FRAME 1

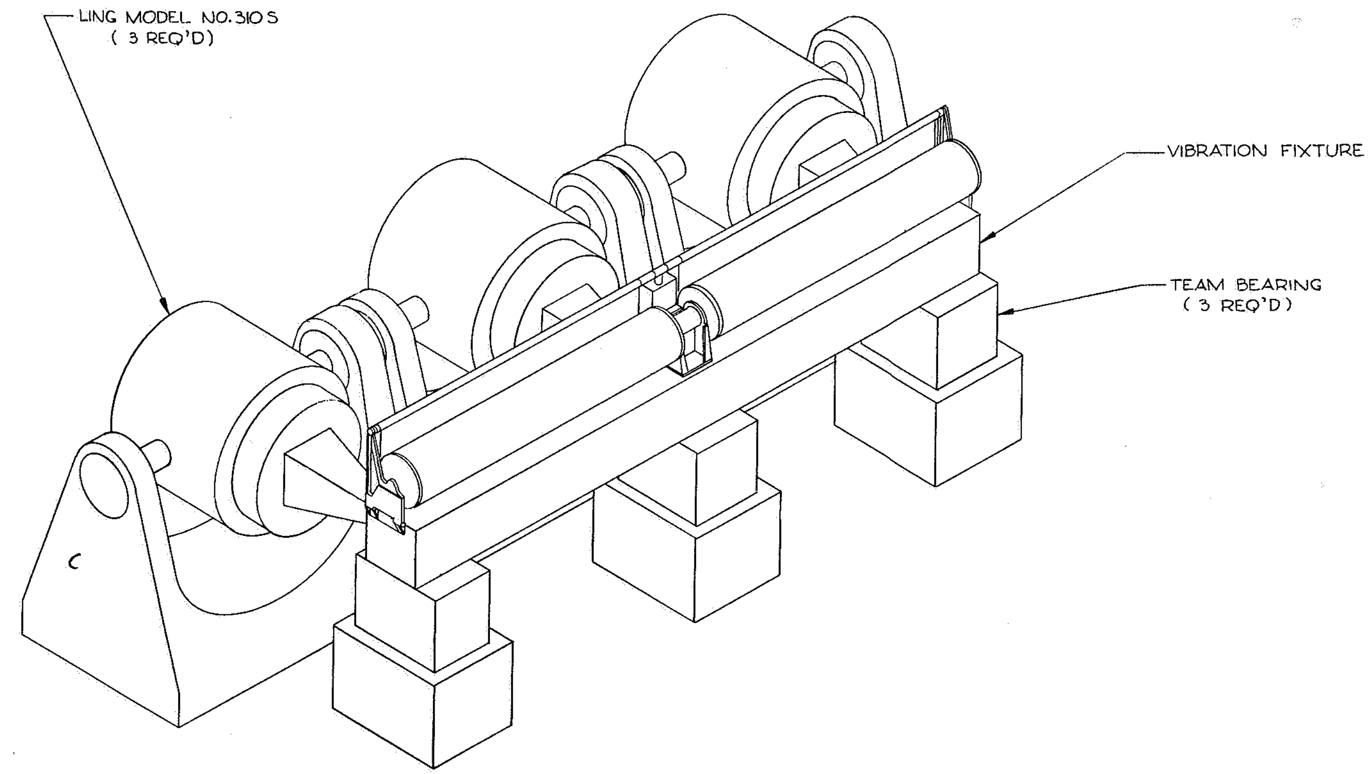

FOLDOUT FRAME 2

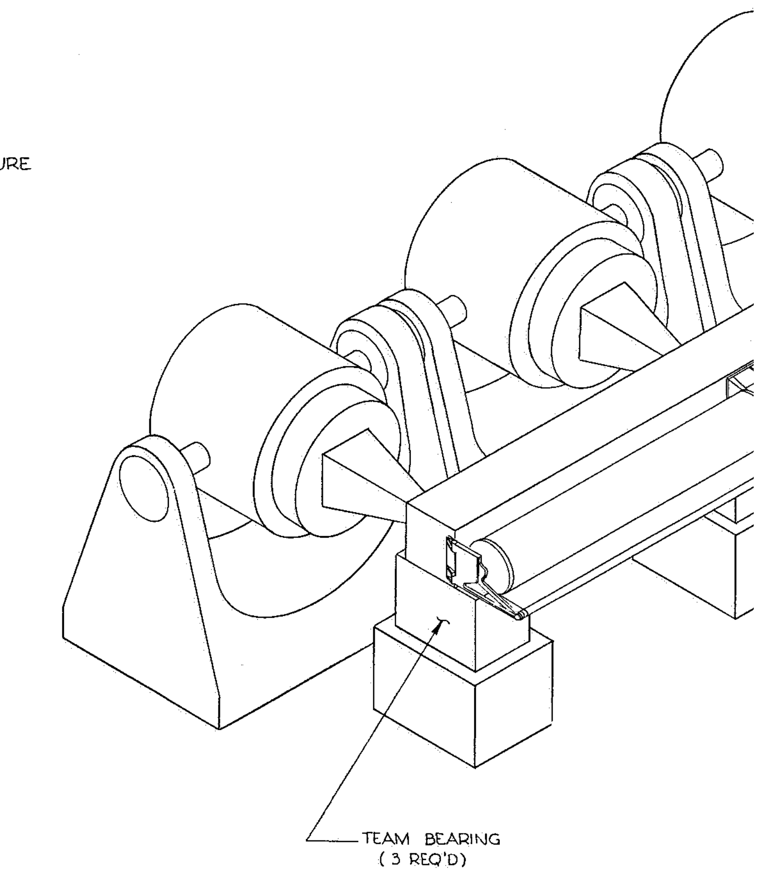

FOLDOUT FRAME 3

FOLDOUT FRAME 4

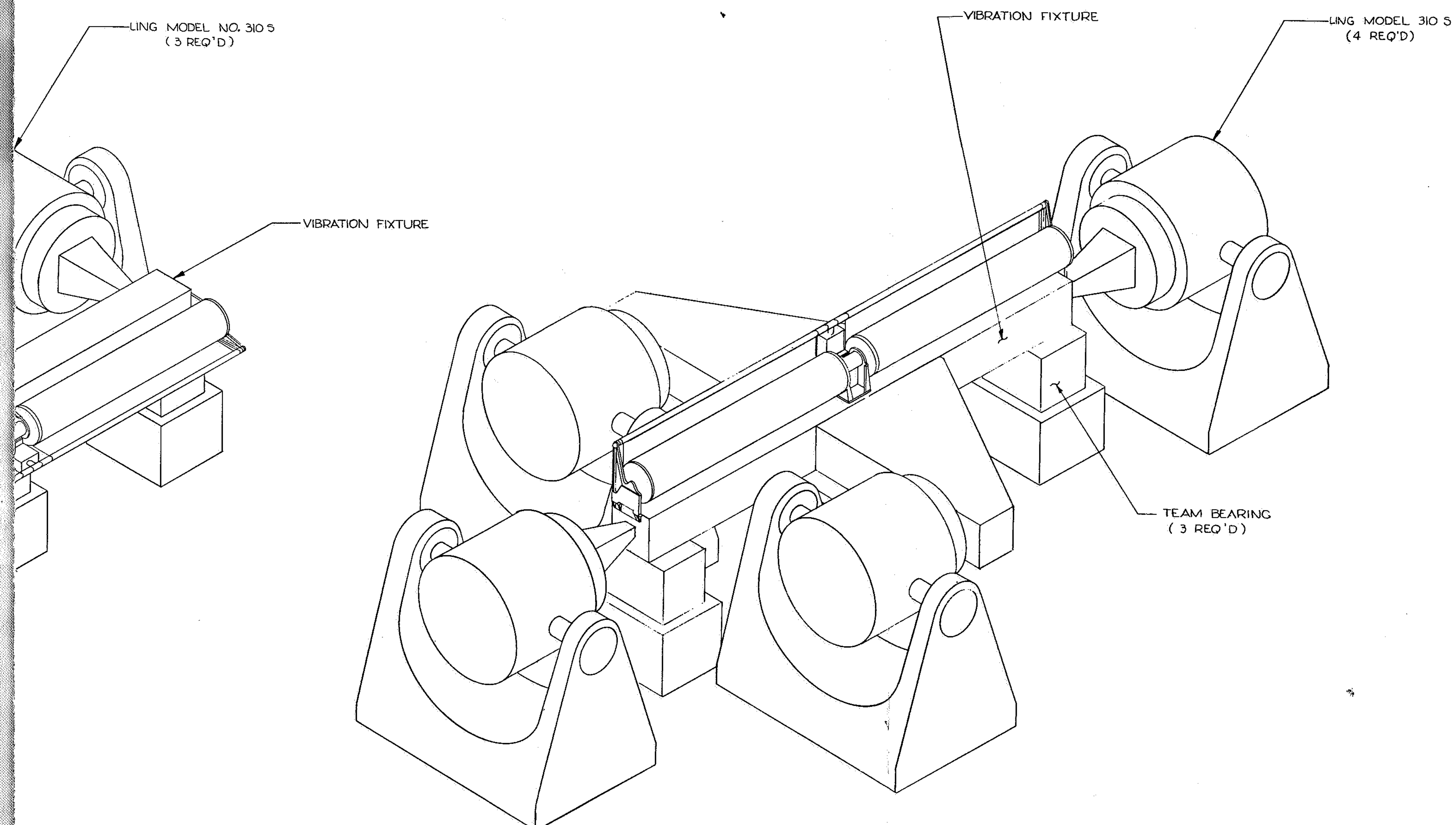

Figure 7-17. Vibration Test Setup

FOLDOUT FRAME 2

FOLDOUT FRAME 3

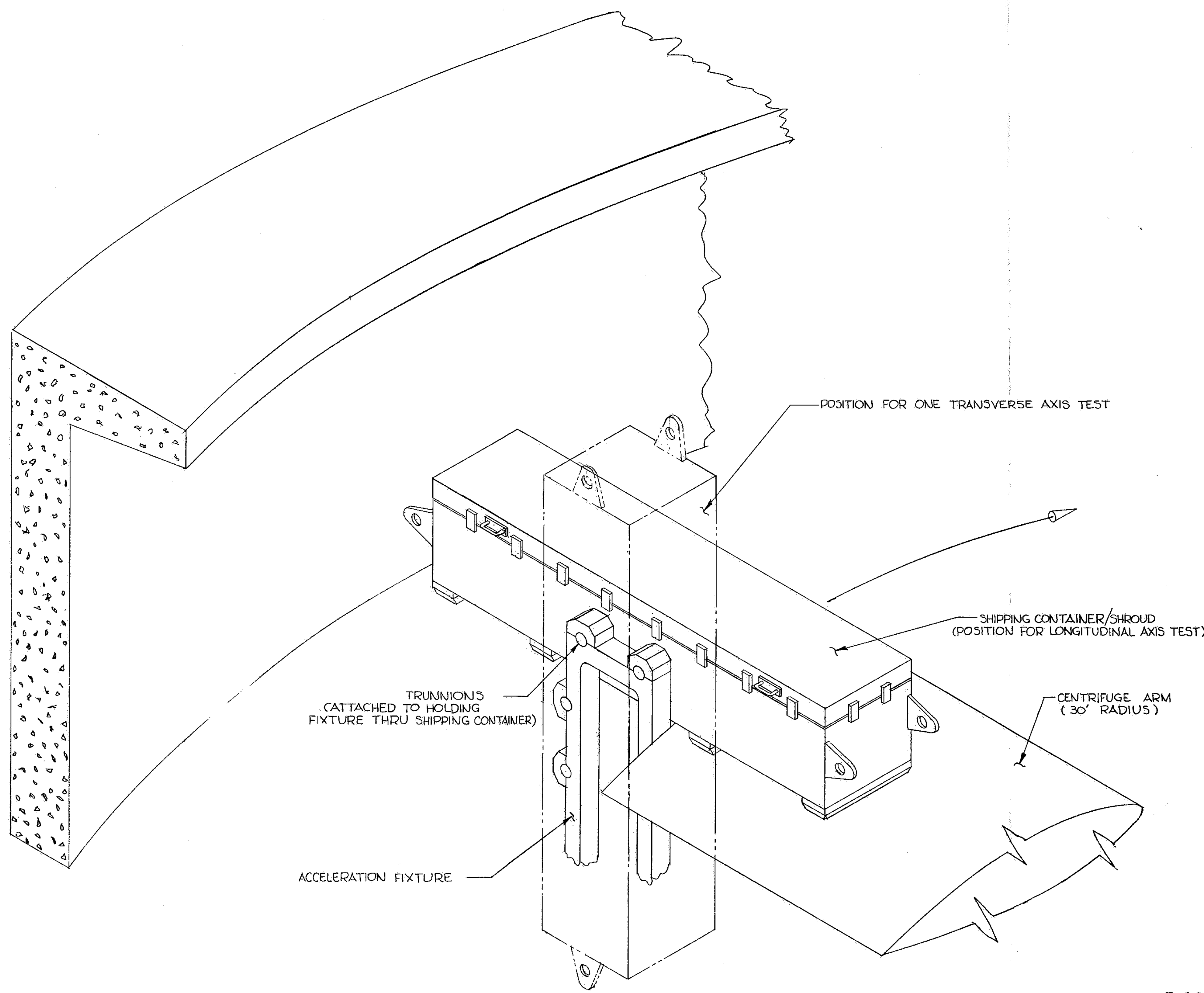

Figure 7-18. Acceleration Test Setup

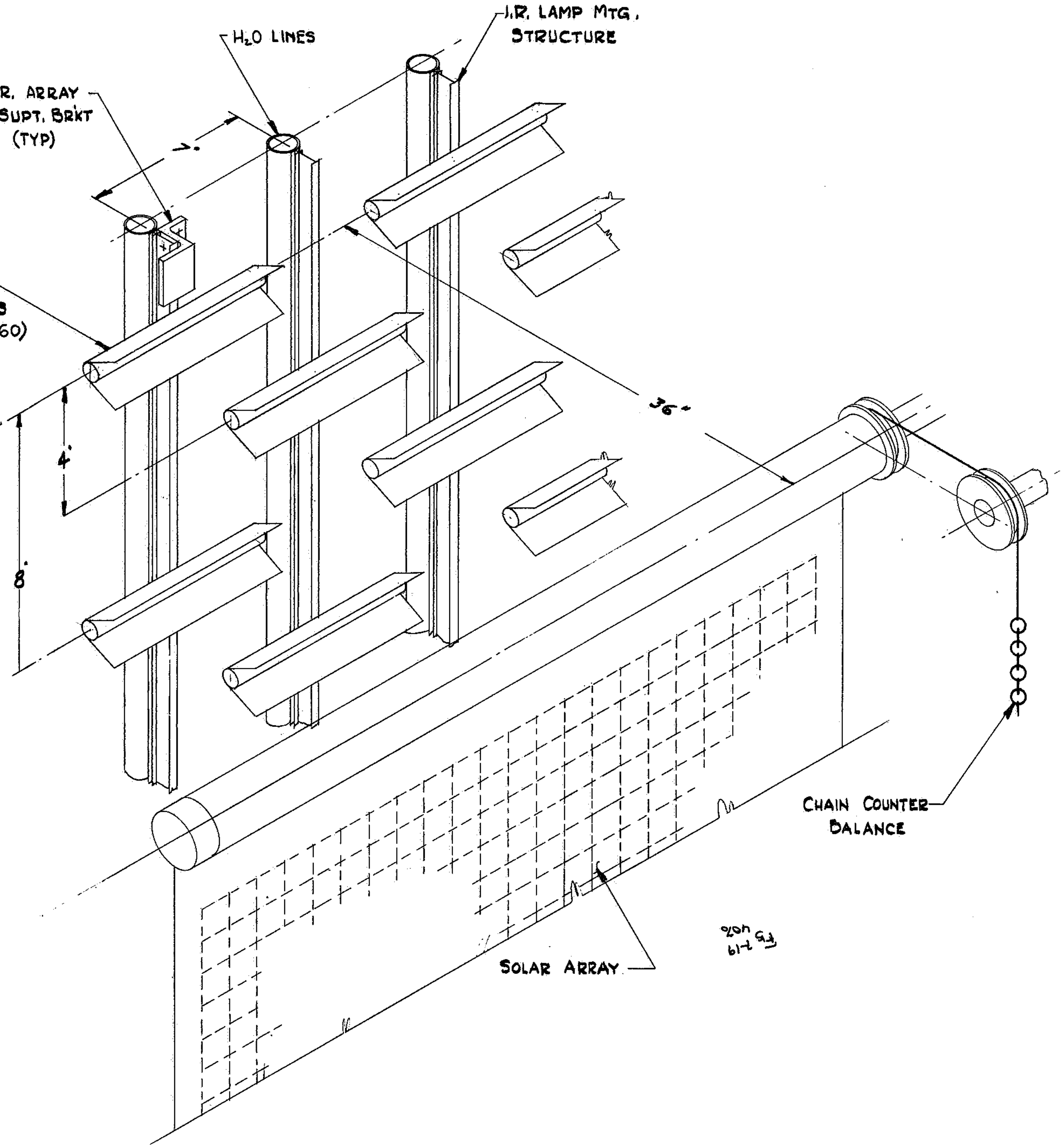

Figure 7-19. IR Lamp Array

chamber shroud (at a nominal temperature of -300°F) will maintain the reflectors at the proper operating temperature, and keep them from overheating. A 50-gpm flow of water will be needed to dissipate the expected 88,000 Btu/hr of heat energy with a 4 degree F temperature rise.

This lamp array will have approximately 250 modular radiant heating units mounted to it, facing the solar array. Each modular unit will be tightly strapped to a vertical riser by a stainless steel clamp. A 500-watt General Electric iodine cycle quartz-line lamp of the 500 T3 series will be mounted in each unit. The entire array will be run with 100 volt power, which General Electric has found to be the best voltage for IR system vacuum operation to avoid arc-over. Arc lamps will be wired with Teflon-coated wire. This will eliminate contamination due to vacuum outgassing and sublimation often prevalent to other insulation materials. The entire fixture will be constructed using only aluminum or stainless steel. It will be supported by hanging from the upper support framework, and will be a tension structure that is self-supporting; it will expand or contract without restraint from the top hanger point when under temperature change.

Power control to each of the five control zones will be accomplished by thermocouple temperature sensing to a Research Inc., Thermac controller.

Six channels of an available Research, Inc. multichannel system will be utilized for controlling the input power to the IR lamps. Each channel consists of a Thermac temperature controller, a power controller, and a 480/115 volt transformer.

The Thermac controlleressentially compares the set-point signal to the control sensor signal. It is this unit which allows closed loop operation of the time varying temperature function within the limits of the power, cooling, and thermal inertia of the rollup array and fixture. The thermal controller also provides manual control for open loop operation. A limiter control is also included which allows the load voltage to be limited to some desired value. In addition, proportional band, rate, and reset action are provided. These features aid control accuracy, prevention of overshoot, and improvement of proportional band control. The comparison of control signal to set-point results in a dc error signal. This is fed to the power controller.

The power controller consists of a pair of ignition tubes, a magnetic amplifier, and two thyratron tubes. The error signal from the Thermac controller is fed to the magnetic amplifier, which conditions the signal to the grids of the thyratrons. These tubes produce the pulse used to fire the ignitions. The load is supplied by the output of the ignitions through a step-down transformer to reduce the voltage inside the vacuum chamber to 115 volts or less.

8. Electro-optical Readout Equipment for T/V and Modal Testing

Electro-optical tracking devices (PhysiTech Model 39A or equivalent) are required to measure the deflections occurring during the modal testing. These devices cannot operate in a hard vacuum, so they must be enclosed in a pressure-tight container with two optical quality portholes for sighting and viewing. High intensity lighting of the targets is required for discrimination of the targets against background. The canned devices must be able to traverse the length of the blanket assemblies to observe each of the targets. The canned devices will be guided by a rack and lifted by a chain drive (see Figure 7-20). Remote positioning of the devices for each target will be accomplished by a series of pre-positioned limit switches.

Stationary brackets will be required for canned electro-optical devices which will be constantly viewing the base and leading edge member of the downward deployed rollup solar array.

9. Performance Test Set

An array test cabinet will be utilized to assure efficiency of performance testing. The unit will control and monitor the array performance tests throughout the program. Items which will be included are:

a. DC power supply to provide the deployment and retraction power to the BI-STEM motor
b. Control switching to enable operation of the BI-STEM
c. Variable resistance load panel capable of absorbing and dissipating the array generated power
d. Switching to enable loading of individual module or the entire array (This is only a two position setup; the leads to an individual module are external and not part of the system harness.)
e. Two digital voltmeters for monitoring of solar cell standards and the load voltage or current signals
f. Thermocouple recorder to monitor selected temperatures
g. X-Y plotter to enable attainment of continuous voltage-current characteristic curves
h. Pyrotechnic control panel which controls separation nut timing and bridge wire current

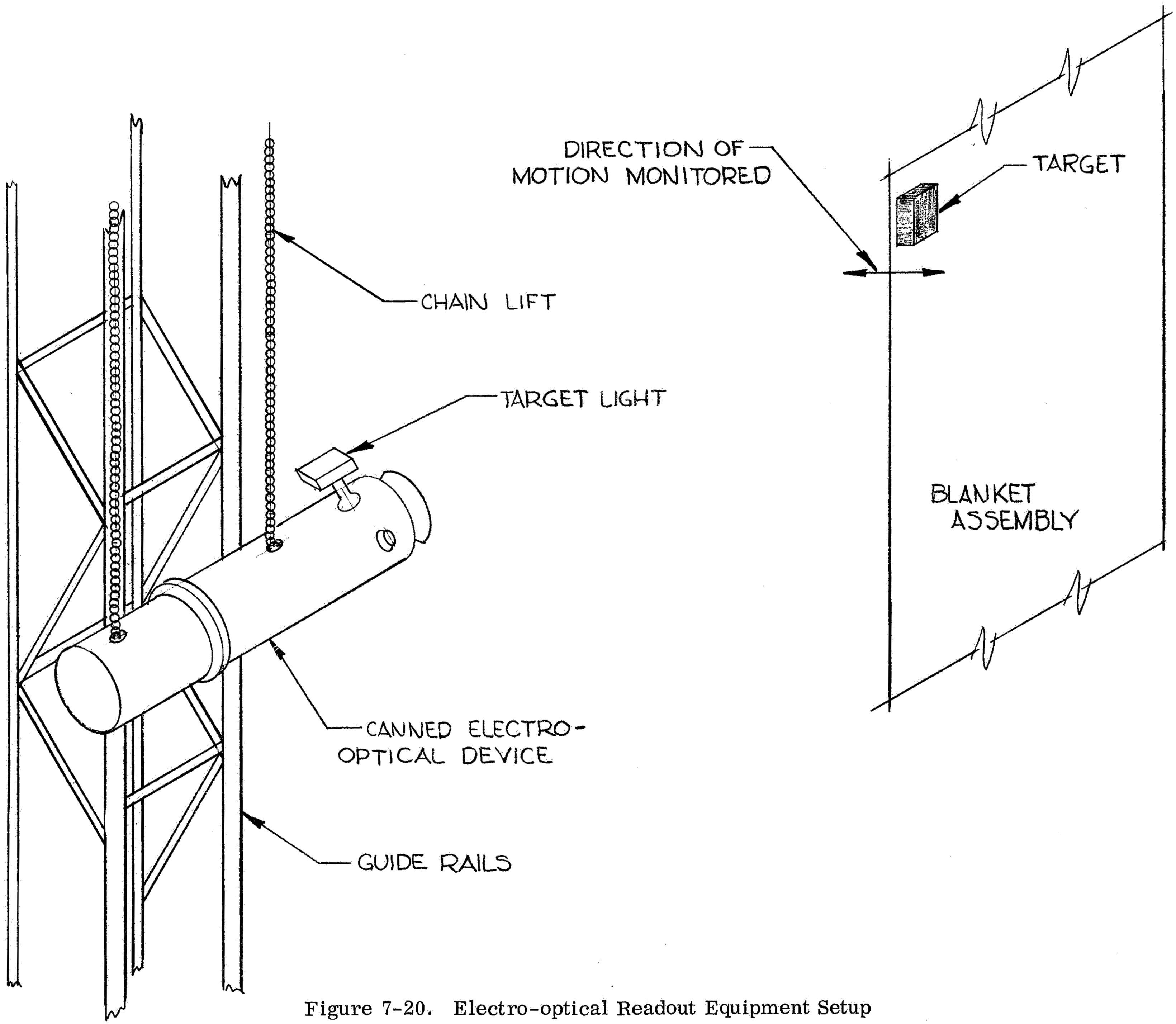

Figure 7-20. Electro-optical Readout Equipment Setup

7.5 ARRAY BLANKET REPAIRABILITY

SOLAR CELLS CAN BE REMOVED AND REPLACED ON THE ARRAY BLANKET WITHOUT DAMAGE TO ADJACENT CELLS.

Evidence that the module construction fulfills the repairability requirement that defective cells can be replaced in a fabrication repair area without damage to adjacent cells, electrical insulation, or mounting substrate resulted when such a repair was required on the blanket of the Engineering Demonstration Model. Upon removal from the curing oven fixture, one cell was broken at the corner. A repair procedure was planned and performed successfully. The narrowness of the model string of cells made the repair easier than it would have been on a full size module, and it was decided to check the procedure further by reworking cells in one of the thermal cycling modules. The following procedure would be employed for repair of the full-size module or panel and is based on the successful removal of a cell from the thermal cycling module.

Solar Cell Replacement Repair Procedure - Rollup Array Panel

Step 1. Unsolder the negative contact of the cell from the interconnection tab (Figure 7-21a).

Step 2. Cut 1/8-inch round holes in Kapton substrate above the positive contact solder joint (Figure 7-21b).

Step 3. Insert cell width shim under loose end of cell until it puts lifting off pressure on the positive tab (Figure 7-21c).

Step 4. Unsolder positive contact (Figure 7-21d).

Step 5. Continue insertion of cell width shim under cell until cell to substrate bond is released. Under this condition of forced separation, the bond separates at the back of the cell (Figure 7-21e).

Step 6. Remove damaged cell from module (Figure 7-21f).

Step 7. Clean bond residue off Kapton substrate by using methylene chloride.

Step 8. Clean and re-tin interconnection tabs.

Step 9. Insert new cell into position and secure with tape.

Step 10. Solder positive and negative contacts to interconnection tabs. (The reasons for the hole in the substrate over the positive tab is primarily to ensure the quality of the new electrical joint.)

Step 11. Insert the SMRD 745 substrate bonding material between the cell and substrate and cure bond for 16 hours in an oven at 150°F. At this time, a small Kapton patch is bonded over the positive contact access hole.

Step 12. Remove from the oven, remove the positioning tape, and clean cell surface.

SOLAR CELL REPLACEMENT PROCEDURE

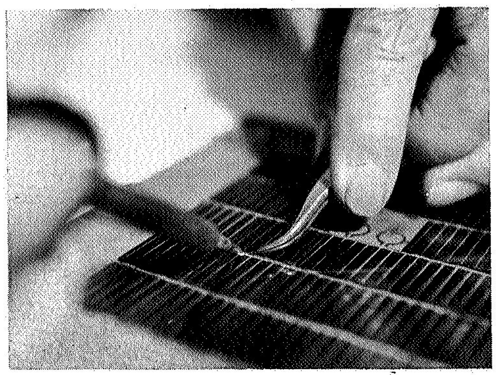

a. UNSOLDERING THE NEGATIVE CONTACT DURING CELL REPLACEMENT OPERATION

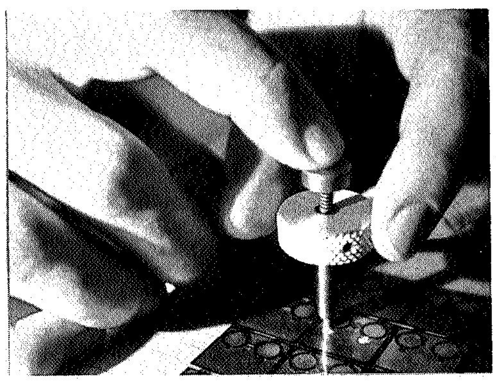

b. CUTTING OF POSITIVE TAB ACCESS HOLE IN SUBSTRATE

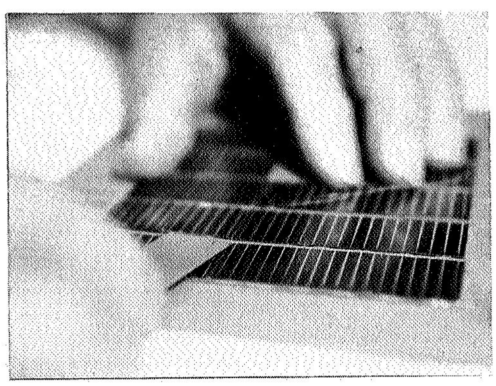

c. INSERTION OF SHIM UNDER CELL AT POSITIVE TAB END

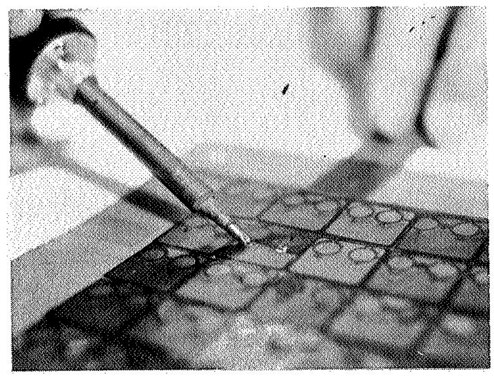

d. UNSOLDERING POSITIVE TABS

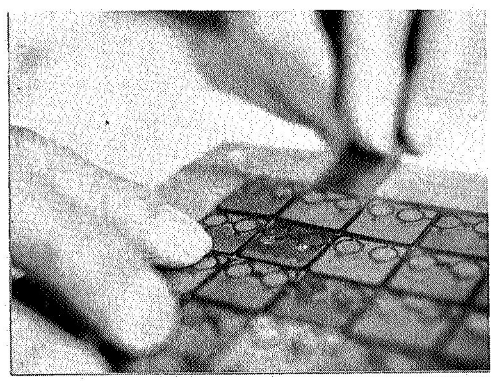

e. SEPARATION OF CELL TO SUBSTRATE BOND BY SHIM INSERTION

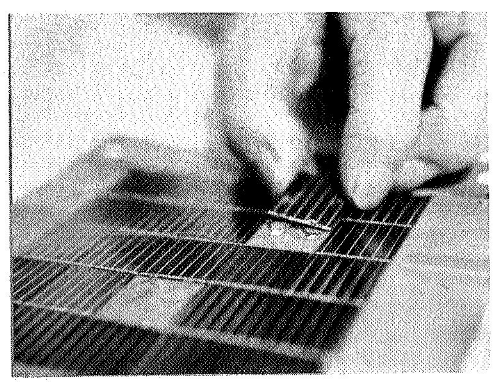

f. REMOVAL OF CELL

Figure 7-21. Solar Cell Replacement Repair Procedure

SECTION 8

REFERENCES

1-1 JPL Specification SS501407 Revision A, "Roll-up Solar Cell Array, 30 Watts Per Pound, Detail Requirements For."

1-2 "Feasibility Study - 30 Watts Per Pound Roll-up Solar Array," Quarterly Technical Report No. 1, GE Document No. 67SD4403, October 15, 1967.

4-1 Kinsler, L.E., and Frey, A.R., Fundamentals of Acoustics, 2nd edition.

4-2 Jacobsen, L.E., and Ayre, R.S., Engineering Vibrations, McGraw Hill, 1958.

4-3 Harris and Crede, Shock and Vibration Handbook, Volume 2, McGraw-Hill, 1961.

4-4 Florio, F.A. and Jasper, P.E., An Analytical Representation of Temperature Distribution in Gravity Gradient Rods, TIS No. 65SD294, August 6, 1965.

4-5 MacNaughton, J.D., Weyman, H.N., and Groskopfs, E., "The BI-STEM - A New Technique in Unfurlable Structures," presented at the 2nd Aerospace Mechanisms Symposium, May 4-5, 1967.

4-6 Ralph, E.L., "Performance of Very Thin Silicon Solar Cells," presented at the 6th Photovoltaic Specialists Conference.

4-7 Horvay, G. "The End Problem of Rectangular Strips," Journal of Applied Mechanics, March, 1953.

4-8 Horvay, G., and Born, J.S., "Tables of Self-Equilibrating Functions," Journal of Mathematics and Physics, Vol. XXXIII, No. 4, January, 1955.

5-1 Wahl, A.M., Mechanical Springs, McGraw-Hill Book Co., New York, pp. 146-152, 1963.

5-2 Gross, Seigfried, Calculation and Design of Metal Springs, Chapman and Hall Ltd., London, pp. 112-123, 1966.

7-1 Clauss, F.J., Lubrication Evaluation, Lockheed Missile and Space Company, April 1966.

7-2 Young, W.C. Lubrication Evaluation, Lockheed Missile and Space Company, Report A707712, October 1964.

7-3 Evans, Vest and Ward, "Evaluation of Dry Film Lubricating Materials for Spacecraft Applications," Presented at AIAA Sixth Structures and Materials Conference, Palm Springs, California, April 1965.

7-4 Rittenhouse and Singletary, Space Materials Handbook, Supplement I to the Second Edition, NASA SP-3025, pp. S-36-38, 1966.

7-5 Muraca, R.F. and Whittick, J.S., Polymers for Spacecraft Applications, Final Report, JPL Contract No. 950745, September 15, 1967.

7-6 Whipple, C.L., "Progress Report - Thermal-Vacuum Performance of Silicones," Aerospace Applications Laboratories, Dow Corning Corporation, Midland, Michigan, September 20, 1963.

APPENDIX A
SOLAR ARRAY ACTUATOR SPECIFICATION

General Electric Company
Missile and Space Division
Space Systems Organization
P.O. Box 8555
Philadelphia, Pennsylvania 19101

SOLAR PANEL ACTUATOR

Prepared By: D. N. Matteo Date: ____________
D. N. Matteo, Engineer
Reaction & Actuation Equip. Eng.

Approved By: ________________________ Date: ____________

Approved By: ________________________ Date: ____________
K. L. Hanson, Manager
Roll-Up Solar Array Program

General Electric Company
Missile and Space Division
Space Systems Organization
P.O. Box 8555
Philadelphia, Pennsylvania 19101

SOLAR PANEL ACTUATOR

1.0 Scope

This specification covers design, fabrication and test requirements for a solar panel actuator to be used by the General Electric Company as part of an Engineering Prototype model of a deployable solar array system. The design and assembly of this Engineering Prototype model is a task in the second phase of a program to develop a solar array system to provide an extendible and retractable solar power collection and conversion system for use on earth orbiting, interplanetary, and planet orbiting spacecraft.

The solar panel actuator covered by this document will herein after be referred to as the component.

2.0 Applicable Documents

2.1 Drawings

GE Source Control Drawing 47E214524.

2.2 Specifications

GE Specification 146A9560, preparation for delivery of commercial shipments.

3.0 Requirements

3.1 General Requirements

The component is intended for use as an actuation device for a roll-up type solar cell array. It shall consist of two main subdivisions, an extendible and retractable boom and a deployer mechanism. In the launch mode, the entire boom shall be stowed within the deployer mechanism (except as specified elsewhere, herein). Upon command, the deployer mechanism shall extend the boom to the fully extend length or any fraction thereof, while sustaining the loads imposed by the solar array blanket assembly which will be attached to the boom tip. Upon command, the deployer mechanism shall retract the boom to any desired fraction of fully extended length, while sustaining the blanket loads.

3.2 Detail Design Requirements

The requirements delineated herein apply to all components produced in compliance with this specification.

3.2.1 Actuation Capability

With the loads specified in paragraph 3.2.8 applied to the boom tip the component shall be capable of extending to any fraction (including 100%) of the fully extended boom length (paragraph 3.2.2).

The component shall be capable of retracting to any fraction of fully extended boom length (including fully retracted position) under the same loading conditions as described above for extension.

The component shall be capable of extending and retracting under load while being subjected to the solar flux conditions outlined in paragraph 3.2.8.2, but while in a zero acceleration field.

3.2.2 Fully Extended Length

Fully extended boom length is defined as 33.5 feet $\pm$ 2.0 inches, measured from the exit of the deployer mechanism to the end of an attachment plug mounted at the tip of the boom. The component shall function as defined in paragraph 3.2.1 up to 100% of this length, except that the loads of paragraph 3.2.8 are limited as specified therein.

3.2.3 Total Boom Element Length

The component shall be manufactured with a minimum of 40 feet of boom length. The component shall function as defined in paragraph 3.2.1 when equipped with this length boom. Prior to deliver GE will specify the length ($\leq$ 40 feet) at which the boom is to be delivered.

3.2.4 Extension and Retraction Rates

The boom extension and retraction rate shall be 1.5 in/sec $\pm$ 1 in/sec.

3.2.5 Component Weight

The maximum total component weight shall be 11.0 pounds including the weight of the boom element.

For the purpose of this weight requirement, the boom element length shall be that required to extend the boom to the fully extended length (paragraph 3.2.2).

However, the deployer unit capability, motor size, etc. shall be those required to reliably function with the total boom element length (paragraph 3.2.3).

NOTE: Minimal component weight is of extreme importance in this application. Accordingly, every effort should be made to reduce the weight as far below the specification weight as possible.

3.2.6 Component Size

With the component in the stowed condition the component shall fit entirely within the following envelope:

A right, rectangular prism of the dimensions:

5.5 in. x 6.0 in. x 11.0 in., as delineated on GE Drawing 47E214524.

See GE Drawing 47E214524 for relationship of this envelope with boom deployment axis and other portions of the component.

3.2.7 Component Mounting

The component mounting provisions shall be per GE Drawing 47E214524.

3.2.8 Loading Conditions

The component (including its extended boom) shall endure each of the following loading conditions without failure, malfunction, or violation of the constraint specified. The loading conditions, lengths, and constraints of this paragraph apply regardless of the actual boom length delivered.

3.2.8.1 <u>Blanket Tension/Gravity</u> - (All loads specified herein are cumulative)

(a) Blanket Tension - 4.0# applied at attachment at the boom tip and directed at a fixed point regardless of boom tip motion (extension, retraction or deflection). This fixed point is defined as the boom exit point on the deployer mechanism. This load will act at any time the boom is extended from its stowed condition and is independent of the length of boom extended, up to 100% of fully extended length (paragraph 3.2.2).

(b) Tip Weight - A mass mounted at the boom tip equal to 1.2 pounds in the 32.2 ft/sec^2 gravity acceleration field. With the boom deployment axis vertically upward this weight will act along the local vertical regardless of the amount of boom extension or deflection.

(c) Boom Weight - The weight of the boom element when deployed vertically upward in the 32.2 ft/sec^2 gravity acceleration field, regardless of deflection and anywhere from zero to 100% of fully extended length (paragraph 3.2.2).

(d) Constraints - With the above loads cumulatively applied, the following constraints apply:

The boom shall sustain the above loads without failure and without

the use of any deployment aids. This constraint applied from stowed position up to 100% of fully extended length (paragraph 3.2.2).

3.2.8.2 Thermal/Blanket Tension - (In Orbit Condition) (All loads specified herein are cumulative.)

(a) Blanket Tension - Same as paragraph 3.2.8.1 (a).

(b) Solar Flux - All portions of the extended boom will be exposed to solar flux of 260 mw/cm^2 incident on one-half of the boom periphery while the other half is exposed to black space, under hard-vacuum conditions.

(c) Constraints - Under the combined thermal and structural loading conditions of 3.2.8.2 (a) and (b) above and while in a zero "g" acceleration field:

- o The boom shall not deflect laterally farther than 50 inches at the tip, at fully extended length (paragraph 3.2.2).
- o The boom shall sustain the above loads without failure.

3.2.9 Straightness and Alignment

3.2.9.1 Boom Deployment Axis - The boom deployment axis will be generally understood to mean the line along which the centroid of the boom tip travels as it is deployed. For the purpose of this specification this axis will be defined as a straight line perpendicular to the boom mounting plane and passing through the boom centroid at the deployer exit point.

3.2.9.2 Boom Mounting Plane - The boom mounting plane will be defined as a plane generally perpendicular to the 11.0 inch dimension of the component envelope (paragraph 3.2.6) which plane determines the alignment of the component with its support structure about the two axes mutually perpendicular to the boom deployment axis and each other. The boom mounting plane is delineated on GE Drawing 47E214524.

3.2.9.3 Boom Alignment and Straightness - When deployed to fully extended length and with the boom deployment axis vertically upward, the boom profile shall be such that its tip falls within a 1½ foot diameter circle centered on the boom deployment axis when deployed vertically upward and when it is entirely unloaded (except for its own weight). These deflections to be measured relative to the boom deployment axis.

3.2.10 Deployment Motor

The component shall extend and retract the boom by the action of an integrally mounted motor (within the envelope defined in paragraph 3.2.6).

3.2.10.1 Motor Voltage and Power - The type of motor selected by the supplier for this application shall be a result of consideration of the life requirement delineated in Section 3.2.16. Accordingly, both +27 VDC and 400 cycle, 115 VDC shall be considered as potentially available power. The supplier's quotation shall include a definition of the type and amount of power required.

3.2.10.2 Motor Reversal - Motor wiring shall be such that external switching can effect reversal of the direction of boom deployment.

3.2.10.3 Limit Switches - The component shall be equipped with three limit switches, one which is mechanically actuated at fully extended length, one which is mechanically actuated when the boom is totally stowed within the component, and one which is mechanically actuated when the boom is within 6 inches of full retraction.

The wiring of all switches is to be brought out of the component separate from the motor wiring.

3.2.10.4 Connectors - No connectors are required. Six foot long, #22 A.W.G., Teflon coated wire flying leads will be provided on all wires requiring external connection.

3.2.11 Caging

All tip mounted masses will be externally caged by other components in the system. The boom tip will be restrained against extension or retraction motions during the launch phases by this external caging. Accordingly, no tip-mass caging requirements apply to the component.

3.2.12 Tip Attachment

In order to facilitate the attachment of solar array hardware to the boom tip, a tip plug will be required. This tip plug shall be equipped with internally threaded holes per GE Drawing 47E214524. This tip plug and its attachment to the boom element shall be capable of transmitting all loads specified in paragraph 3.2.8 to the boom without failure.

3.2.13 Bearings and Lubricants

Bearings and lubricants shall be selected with particular attention to the life (Section 3.2.16) and service condition (Section 3.3) requirements. All bearings and lubricants selected shall have the prior approval of the cognizant GE engineer.

3.2.14 Telemetry

Other than the limit switches specified in paragraph 3.2.10.4 (which may be used for both telemetry and power cut-off), no telemetry will be required.

3.2.15 Attachment to Forward End of Deployer

The component shall be equipped with six internally threaded holes at the boom exit end of the deployer as defined on GE Drawing 47E214524. GE will attach rigid brackets to each of the two patterns of three holes. The component shall be capable of sustaining without failure or subsequent malfunction a 25 pound static load applied in any direction to each of these rigid brackets at the point defined as the "load application point" on GE Drawing 47E214524.

3.2.16 Life

The component shall be capable of 150 cycles of full and/or partial extensions and retractions without malfunction. The component shall be capable of flawless operation after a 1 year soak at the operating conditions of Section 3.3.1.

3.2.17 Duty Cycle

The worst case component duty cycle will be 25% on 75% off, where the 25% on time shall consist of a minimum of one full cycle of extension and retraction under load (paragraph 3.2.8.1).

3.3 <u>Service Conditions</u>

The component shall operate under any natural exposure to any natural combination of the environments of Section 3.3.2.

3.3.1 Operating Conditions

3.3.1.1 Radiation - Total accumulative radiation dosage shall be 10^7 rads.

3.3.1.2 Temperature (Steady State) - -50°C to +60°C

3.3.1.3 Pressure - 760 mm Hg to 10^{-10} mm Hg

3.3.1.4 Thermal Shock - Transient thermal shock from -100°C to +75°C at rates not less than 30°C per minute, acting only on extended boom.

3.3.2 Non-Operating Conditions (Stowed Configuration)

3.3.2.1 Temperature (Steady State) - -50°C to +60°C.

3.3.2.2 Humidity - 93% ± 3% at +30°C ± 2°C.

3.3.2.3 Pressure - 760 mm Hg to 10^{-10} mm Hg.

3.3.2.4 Vibration - In the stowed condition, with the boom tip externally restrained against extend or retract motion and attached to a rigid fixture at the mounting points delineated in GE Drawing 47E214524, the applicable vibration environment is:

SINUSOIDAL
(ALONG 3 MUTUALLY PERPENDICULAR AXES)

Frequency (C.P.S.)	Acceleration (g's, 0 to peak)	Sweep Rate
5-13	limited to 0.5 inch double amplitude	1 octave per minute
13-50	4.0 g	
50-150	8.0 g	
150-485	12.0 g	
485-730	Limited to .001 inch double amplitude	
730-2000	27.0 g	

RANDOM GAUSSIAN
(ALONG 3 MUTUALLY PERPENDICULAR AXES)

Frequency (C.P.S.)	Duration	PSD Level (g^2/cps)	Wide Band (20-2000) g rms level
20 to 90	1 minute (each axis)	Increasing at 6 db/ octave	33.0
90-700		1.0	
700-2000		Decrease at 6 db/ octave	

3.3.2.5 Acceleration - ± 9.0 g ± .5 g at C.G. along 3 mutually perpendicular axis and varying across the component by not more than 1.0 g from the specified 9.0 g, when mounted per GE Drawing 47E214524.

3.3.2.6 Acoustics (Stowed Configuration) - The acoustic environment is represented by a random incidence, reverberant sound field. Duration shall be 60 seconds. Table I defines the one-third octave sound pressure test levels and the allowable tolerances. Below 80 cps, the spectrum shall be rolled off at a rate of 24 db/octave or greater. Above 10,000 cps, any one-third sound pressure level (SPL) shall not exceed 99 db/octave.

NOTE: The overall SPL will be approximately 150 db ref to 2×10^{-4} dynes/cm^2; however, the spectral levels within each one-third octave band shall be controlled.

3.3.2.7 Shock (Stowed Configuration) - The shock environment in the three orthogonal axes, is illustrated in Figure 1.

Table I. Acoustic Test Levels

1/3 Octave Band Center Frequency (cps)	Sound Pressure Level in 1/3 Octave Bands (db ref 2×10^{-4} dynes/cm^2)	Tolerance Band (db)	
80	132.5	+4	-4
100	138.0	+3	-3
125	138.0	+3	-3
160	138.0	+3	-3
200	138.0	+3	-3
250	143.0	+3	-3
315	143.0	+3	-3
400	143.0	+3	-3
500	140.0	+3	-3
630	137.0	+3	-3
800	133.5	+3	-4
1000	130.5	+3	-4
1250	127.5	+3	-4
1600	124.0	+3	-4
2000	121.0	+4	-4
2500	118.0	+4	-5
3150	115.0	+4	-5
4000	111.5	+4	-5
5000	108.5	+4	-5
6300	105.0	+4	-5
8000	102.0	+4	-6
10000	99.0	+4	-6

4.0 Quality Assurance Provisions

In order to assure conformance to the requirements to this specification the following tests shall be performed on the units specified.

4.1 Engineering Development Unit*

The engineering development shall be subjected to design certification testing as defined in Section 4.3.

4.2 Engineering Prototype Unit(s)*

All engineering prototype units shall be subjected to acceptance testing as defined in Section 4.4.

* The engineering prototype and engineering units may be, as defined by the Purchase Order (or subcontract), combined into a single unit.

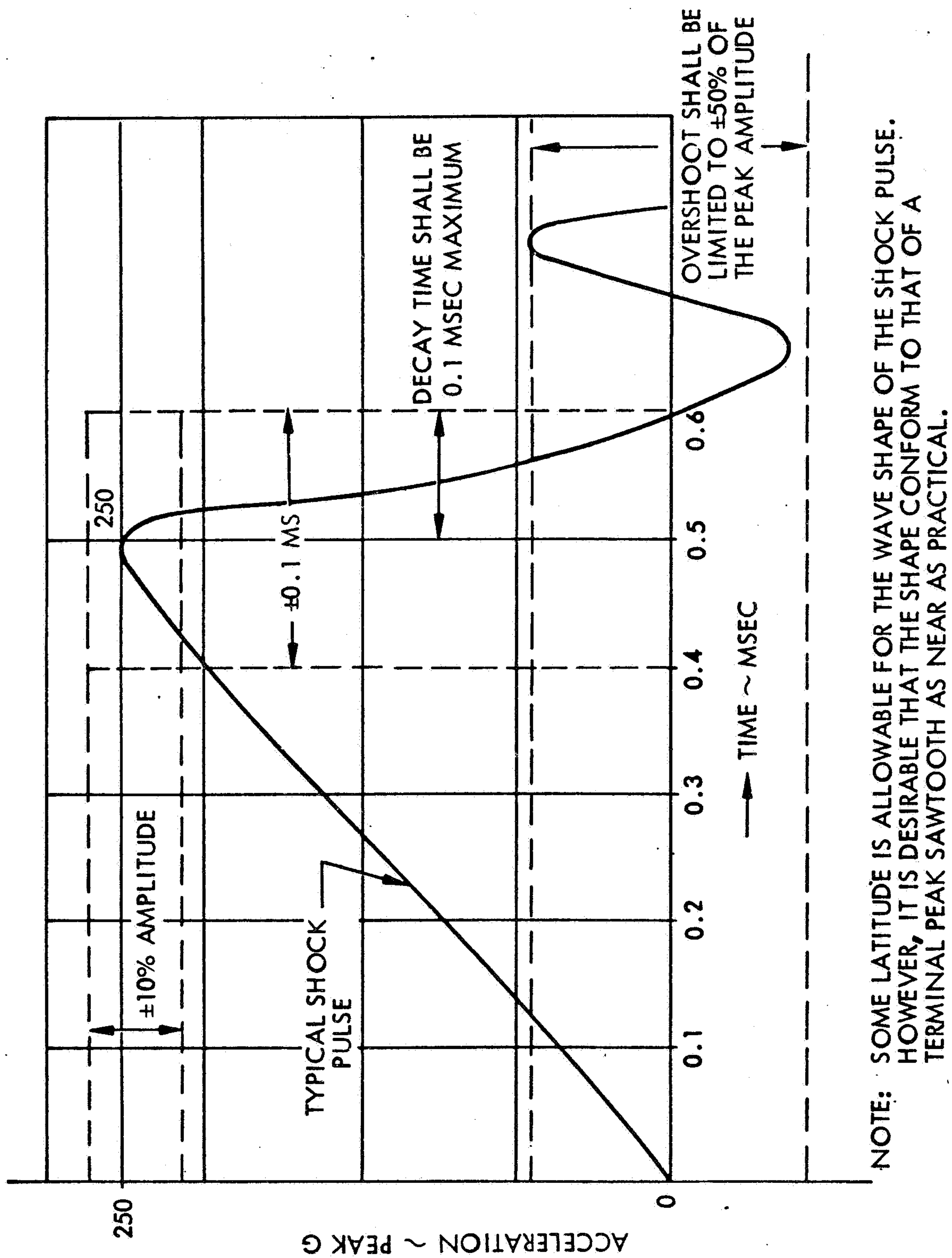

Figure 1. Shock Pulse

4.3 Design Certification

4.3.1 Examination of Product

4.3.1.1 Visual and Mechanical Inspection - The component shall be visually and mechanically inspected to determine that materials, finishes, design, workmanship, construction, weight, dimensions, and markings conform to the applicable drawings and to the requirements of this specification.

4.3.1.2 Circuit Isolation, Continuity and DC Resistance - The component shall be checked for conformity with the electrical requirements of the applicable drawing and this specification when measured with a voltmeter and/or ohmmeter.

4.3.2 Straightness and Alignment

The component shall be checked for conformity with the requirements of paragraph 3.2.9.3 by vertical deployment in a one "g" field as specified in that paragraph.

4.3.3 Functional and Static Load Test

The component shall be tested to demonstrate all the requirements of paragraph 3.2 except that the requirements of paragraph 3.2.8.2 will be demonstrated by analysis in lieu of test as defined in Note 10.1. The test required by this section shall be performed before and after those of 4.3.4.

4.3.4 Environmental Tests

4.3.4.1 The component shall be tested to demonstrate its ability to withstand the environment defined in Section 3.3.2.4, without structural failure or subsequent malfunction.

4.4 Acceptance Tests

The component shall be tested per Sections 4.3.1, 4.3.2, and 4.3.3 except that tests per Section 4.3.4 shall be replaced by a workmanship vibration test, consisting of:

Frequency (cps)	g's 0-Peak	Sweep Rate
10-50	2 g	4 octaves per minute
50-500	4 g	
500-2000	2 g	

5.0 Preparation for Delivery

The component shall be prepared for delivery in accordance with GE Specification 146A9560.

6.0 Drawings

The supplier shall deliver with the component a complete set of production drawings defining the component in its most up-to-date configuration. In addition, the supplier shall supply such drawings as will be from time-to-time (prior to delivery) required by GE to define the design and interface details of that component.

7.0 Design Review

GE reserves the right to review the design details from time-to-time as the design progresses. These reviews will take the form of informal sessions wherein GE engineers are acquainted with the manner in which the requirements of this specification are being met. These sessions will also be used to identify areas where mutual benefit can be derived by analytical support being applied by GE.

8.0 Access to Analysis

GE shall have access to all analysis performed in configuring the component to meet this specification.

9.0 Definitions

NOT APPLICABLE

10.0 Notes

10.1 GE assumes responsibility for showing analytical proof of meeting the constraints of Section 3.2.8.2 provided that:

- o The component satisfied the requirement of Sections 3.2.8.1 and 3.2.9.3, and
- o The configuration of boom is such that its most pessimistic thermal bending performance can be approximately by a 1.4 inch diameter, .007 inch wall, seamless, stainless steel tube coated on its O.D. with a thermal control coating with a solar absorptivity of 0.12 or less.

APPENDIX B

SLIP RING ASSEMBLY SPECIFICATION

General Electric Company
Missile and Space Division
Valley Forge Space Technology Center
Box 8555
Philadelphia, Pennsylvania 19101

Specification No. SVS 7547

PRELIMINARY

SLIP RING ASSEMBLY

ROLL UP SOLAR ARRAY

Prepared By: R. W. Stanhouse Date: 5-3-68
R. W. Stanhouse
Reaction & Actuation Equip. Eng.

Approved By: C. C. Rich / R. Stanhouse Date: 5-6-68
C. C. Rich, Manager
Reaction & Actuation Equip. Eng.

Approved By: K. L. Hanson Date: 5/6/68
K. Hanson, Manager
Space Power Equipment

Slip Ring Assembly
Roll Up Solar Array

1.0 Scope

1.1 This specification covers the design, fabrication and test requirements for a slip ring assembly to be used on a roll up solar cell array in a space application.

2.0 Applicable Documents

2.1 The following documents of exact issue shown form a part of this specification to the extent defined herein.

Specifications

MIL

MS 33586A	Metal, Definition of Dissimilar
MIL Q 9858	Quality Control Systems Requirements

Standards

MIL-STD-447

MIL-D-70327

MIL-STD-202

2.2 The following documents form a part of this specification to the extent defined herein:

Specification

Drawings (General Electric)

47B214689	Slip Ring Assembly Roll Up Solar Array
118A1600	Finishes and Coatings
118A1526	Identification Marking

3.0 Requirements

3.1 The slip ring assembly shall consist of two power rings, four signal rings, their associated brush holder, brushes and electrical connections.

3.2 Level of Tests

The level of tests shall be as specified in the Work Statement or purchase order and shall conform to one of the following:
(1) Engineering Tests
(2) Qualification Tests
(3) Acceptance Tests

3.3 Design and Construction

The assembly shall be designed and constructed in accordance with Drawing 47B214689 and to the requirements specified herein.

3.3.1 Interchangeability

All parts having the same manufacturers part number shall be interchangeable as defined in 3.1 of Standard MIL-STD-447. Changes in the vendor's part number shall be in conformance with 3.5.4 of Specification MIL-D-70327.

3.3.2 Mounting

Mounting holes shall be provided as shown on Drawing 47B214689. The assembly shall be capable of meeting all the performance requirements of this specification, when mounted at any attitude.

3.3.3 Screw Thread Locking Devices

All threaded parts shall be positively locked by self locking devices, locking component or other approved methods.

3.3.4 Wiring

All internal wiring and leads shall be electrically insulated from the case. Leads shall be restrained to minimize the effects of vibration.

3.3.5 Slip Rings

Each slip ring shall be electrically insulated from all other parts of the assembly. The insulation shall be designed to prevent wear products from forming electrical conducting paths between adjacent slip rings and between slip rings and other parts of the assembly.

3.3.6 Electrical Leads

Each slip ring shall be equipped with an integral electrical lead as shown on Drawing 47B214689.

3.3.7 Brush Assembly

The brush holders shall be designed to maintain electrical contact between slip rings and brushes when exposed to any combination of environments defined in the specification.

3.3.8 Weight

The weight of the assembly is critical and shall not exceed 0.50 lbs exclusive of leads.

3.3.9 Material

3.3.9.1 Slip Ring Material - The slip ring material shall be silver or coin silver.

3.3.9.2 Brush Material - The brush material shall consist of a silver, copper, Niobium Diseleaide and graphite alloy.

3.3.10 Bearings

The bearing shall be of the thin race type for minimum weight and size.

3.3.11 Lubrication

Lubrication shall be dry lubrication to avoid unwanted outgassing products. Because of the relatively low duty cycle requirement, "burnished on" molydisulfide is considered to be adequate. However, final selection of the lubricant must be approved by the cognizant General Electric Engineer.

3.3.12 Finishes

Unless otherwise specified herein, all finishes shall be in accordance with Standard 118A1600.

3.3.12.1 Metals - Metal parts shall be inherently corrosion resistant or shall be protected against corrosion by means of chemical or electrolytic finishes and treatments, or a combination of both.

3.3.12.2 Dissimilar Metals - Contact between dissimilar metals as defined by Standard MS 33586 should be avoided. Where it is necessary that dissimilar metals be assembled in intimate contact with each other, an interposing insulating or mutually compatible material shall be used.

3.4 Performance and Product Characteristics

3.4.1 Insulation Resistance

The insulation resistance of the assembly shall be not less than 1000 megohms between mutually insulated points when measured in accordance with Method 30, Test Condition B of Standard MIL-STD-202.

3.4.2 Dielectric Strength

The assembly shall withstand a potential of 1000 volts, root mean square (rms) 60 cycles per second (cps) between all mutually insulated points for a period of one minute, in accordance with Method 301 of Standard MIL-STD-202. There shall be no evidence of electrical or mechanical failure.

3.4.3 Brush Contact Force

The radial contact force between any slip ring and its associated brush contact shall be approximately as shown below but shall be governed by the other performance and service requirements.

Power ring	.75 lbs
Signal ring	.10 lbs

3.4.4 Contact Resistance

The static resistance between any slip rings and its associated brush contact (exclusing the leads) shall not exceed .005 ohms. While carrying rated current and operating at a speed of 5 revolutions per minute (rpm) the peak/peak resistance shall not exceed .02 ohms.

3.4.5 Torque

The running & starting torque of the assembly shall not exceed 0.7 in-lbs in air and 0.4 in-lbs in vacuum.

3.4.6 Current Carrying Capacity

The slip rings and associated brush assembly shall be capable of continuously carrying the following loads:

Power rings	15.0 amperes DC Max.
Signal rings	1.0 amperes DC Max.

3.5 <u>Service Conditions</u>

The assembly shall be capable of meeting the requirements of 3.3 under any natural combination of the conditions specified in 3.5.1 and after exposure to any natural combination of the conditions specified in 3.5.2.

3.5.1 Operating

3.5.1.1 Vacuum - Air pressure 5×10^{-10} millimeters of Mercury (mmHg).

3.5.1.2 Temperature - Ambient temperature range from -100°C to +55°C.

3.5.2 Non Operating

3.5.2.1 Vibration - Random and sinusoidal vibration as shown in Tables I and II.

Table I. Random Vibration

Frequency Range (Hz)	Power Spectral Density (g^2/Hz)	Wide Band rms (g level)
90-700	1.0	33.0
20-90	Increasing at 6 db/oct	
700-2000	Decreasing at 6 db/oct	

Table II. Sinusoidal Vibration

Frequency Range (Hz)	Input g pk	Sweep Rate (Oct/Min)
5-170	4.0 g pk	1.0
170-700	Straight Line on Log Log Plot	
700-2000	27.0 g pk	

3.5.2.2 Acoustics - The acoustic environment is represented by a random incidence, reverberant sound field. Duration shall be 60 seconds. Table III defines the one-third octave sound pressure test levels and the allowable tolerances. Below 80 cps, the spectrum shall be rolled off at a rate of 24 db/octave or greater. Above 10,000 cps, any one-third sound pressure level (SPL) shall not exceed 99 db/octave.

NOTE: The overall SPL will be approximately 150 db ref to 2×10^{-4} dynes/cm^2; however, the spectral levels within each one-third octave band shall be controlled.

3.5.2.3 Shock - The shock environment in three orthogonal axes is illustrated on Figure 1.

3.5.2.4 Static Acceleration - The steady acceleration environment is 9 gps at the approximate center of mass of the array, in both directions along an axis which is parallel to the launch vehicle axis of thrust, and in two other orthogonal directions which are also perpendicular to the axis of thrust. The acceleration gradient across the assembly shall be less than 10 percent of the acceleration of the mass center. There shall be a total of six tests (one in each of the six directions) and the acceleration load shall be applied for five minutes during each test.

3.5.2.5 Thermal Environment - Transient thermal shock from -100 to +75°C affecting structure as well as solar cells at a rate not less than 30°C per minute.

Table III. Acoustic Test Levels

1/3 Octave Band Center Frequency (cps)	Sound Pressure Level in 1/2 Octave Bands (db ref 2 x 10^{-4} dynes/cm^2)	Tolerance Band (db)	
80	132.5	+4	-4
100	138.0	+3	-3
125	138.0	+3	-3
160	138.0	+3	-3
200	138.0	+3	-3
250	143.0	+3	-3
315	143.0	+3	-3
400	143.0	+3	-3
500	140.0	+3	-3
630	137.0	+3	-3
800	133.5	+3	-4
1000	130.5	+3	-4
1250	127.5	+3	-4
1600	124.0	+3	-4
2000	121.0	+4	-4
2500	118.0	+4	-5
3150	115.0	+4	-5
4000	111.5	+4	-5
5000	108.5	+4	-5
6300	105.0	+4	-5
8000	102.0	+4	-6
10000	99.0	+4	-6

3.6 Life

The assembly shall be designed to meet the life requirements of 3.6.1 and 3.6.2.

3.6.1 Operating

The assembly shall be capable of operating for a period of one year in space at rated power transfer with up to 100 rotational cycles occurring during this period. A rotational cycle consists of 15 revolutions in one direction followed by 15 revolutions in the opposite direction. In space the assembly shall cycle through a small angular range (± 2 degrees) at low orbital frequency for extended periods at the mid point of a cycle. A design goal of three years shall be applied.

3.6.2 Storage

The assembly shall be capable of meeting the requirements of 3.4 after a one year storage period (assuming some "run in" prior to test and usage).

3.6.3 Reliability

Reliability shall be defined as the probability that the component shall operate for a one year period under any natural combination of requirements defined in this specification. The assembly shall be designed with an ultimate goal of obtaining .999 reliability with a 95% confidence level. The vendor shall be aware of the parts that are most susceptible to failure and concentrate on providing the best possible material to achieve trouble-free operation.

3.7 Nameplates and Marking

The assembly shall be marked in accordance with Standard 118A1526.

3.8 Drawings and Drawing Changes

The vendor shall prepare a set of drawings in accordance with Specification MIL-D-70327, Class 2, showing the assembly and all details. After the vendors drawings are approved, no changes shall be made without the prior written approval of GE/MSD. This requirement shall also apply to sub-vendors. Approval of changes shall not relieve the vendor of full responsibility for the results of such changes.

3.9 Serial Number(s)

Each assembly shall be marked with a GE/MSD assigned serial number.

3.10 Workmanship

The assembly shall be constructed in a thoroughly workmanlike manner. Particular attention shall be paid to the finish of the slip rings and brushes, impregnation of leads, curing of the epoxy, freedom of parts from burrs and sharp edges. In general, the workmanship shall conform to the applicable portions of Specification MIL-Q-9858.

4.0 Quality Assurance Provisions

4.1 To insure satisfactory quality, compliance with the requirements of Section 3.0 of this specification shall be demonstrated by subjecting each assembly to the tests and procedures defined herein. (See 3.2 for test levels to be used.)

Classification of Tests

The inspection and testing of the assembly shall be classified as follows:

(a) Qualification Tests (see 4.2)
(b) Acceptance Tests (see 4.3)

4.2 Qualification Tests

One assembly shall be subjected to the tests in the order shown as specified in Table 1 and described under 4.6 of this specification.

4.3 Acceptance Tests

Each flight assembly shall be subjected to the acceptance tests in the order shown as specified in Table 1 and described under 4.6 of this specification.

TABLE 1 - TESTS		Qualifica.	Acceptance
Test	Test Paragraph		
Visual and mechanical inspection	4.6.1	X	X
Insulation resistance	4.6.2	X	X
Dielectric strength	4.6.3	X	X
Brush contact force	4.6.4	X	X
Contact resistance	4.6.5	X	X
Torque	4.6.6	X	X
Vibration	LATER		
Vibration			
Acceleration			
Thermal Vacuum			
Thermal Vacuum			

4.4 Procedure In Case Of Failure

If a failure, malfunction or out of tolerance performance occurs, testing shall immediately cease. A detailed analysis will be made to determine the reason for the failure, and the necessary corrective action to be taken. If the corrective action affects the validity of previous test results, such tests shall be repeated. A Failure Analysis and Failure Report shall be made for each test failure.

4.5 Test Facilities, Measurements and Tolerances

Test facilities, measurements and tolerances shall conform to standard requirements for high reliability equipment. The vendor shall have available a set of master gages, standards, and appropriate instruments for the conduct of regularly scheduled calibrations of his inspection equipment. Records of such calibration shall be maintained, dated and signed by the vendor and made available for GE inspections.

4.6 Test Methods

4.6.1 Visual and mechanical inspection

Each assembly shall be subjected to a visual and mechanical inspection to determine that the materials, finish, design, construction weight, dimensions, markings, and workmanship conform to the applicable drawings and to the requirements of this specification.

4.6.2 Insulation Resistance

Each assembly shall conform to the insulation resistance requirements of 3.4.1.

4.6.3 Dielectric Strength

Each assembly shall withstand the dielectric requirements of 3.4.2. This test shall be conducted one time only.

4.6.4 Brush Contact Force

The contact force between each brush and its associated slip ring of each assembly shall be within the limits of 3.4.3.

4.6.5 Contact Resistance

4.6.5.1 Dynamic Noise - The contact resistance between each slip ring and its associated brush contact shall not exceed the requirements of 3.4.4. The speed at which the test is performed shall be 5 ± 1 revolutions per minute.

4.6.5.2 Static Resistance - The resistance from the end of the rotor lead wire to the terminal lug on the brush block shall not exceed .031 ohms for the signal ring and .010 ohms for the power rings.

4.6.6 Torque

Each assembly shall conform to the torque requirements of 3.4.5. At the end of the torque test the slip rings and brushes shall be examined for evidence of any wear and wear products. Affirmative results shall be noted.

4.6.7 Qualification

One assembly shall be subjected to all of the non operating environmental levels defined in Section 3.5.2. At the completion of each type of environmental exposure, the assembly shall be checked for conformance with the requirements of 4.6.4, 4.6.5 and 4.6.6.

4.6.8 Acceptance

Each flight unit shall be subjected to environments to be specified by General Electric Company. At the completion of each environmental exposure, the assembly shall be checked for conformance with the requirements of 4.6.4, 4.6.5, and 4.6.6.

5.0 Preparation for Delivery

5.1 Marking

Interior packages shall be marked for identification with the name, drawing number and serial number.

5.2 Packing

The assembly shall be sealed in a moisture proof bag and packaged in a container which shall provide safe efficient domestic shipment.

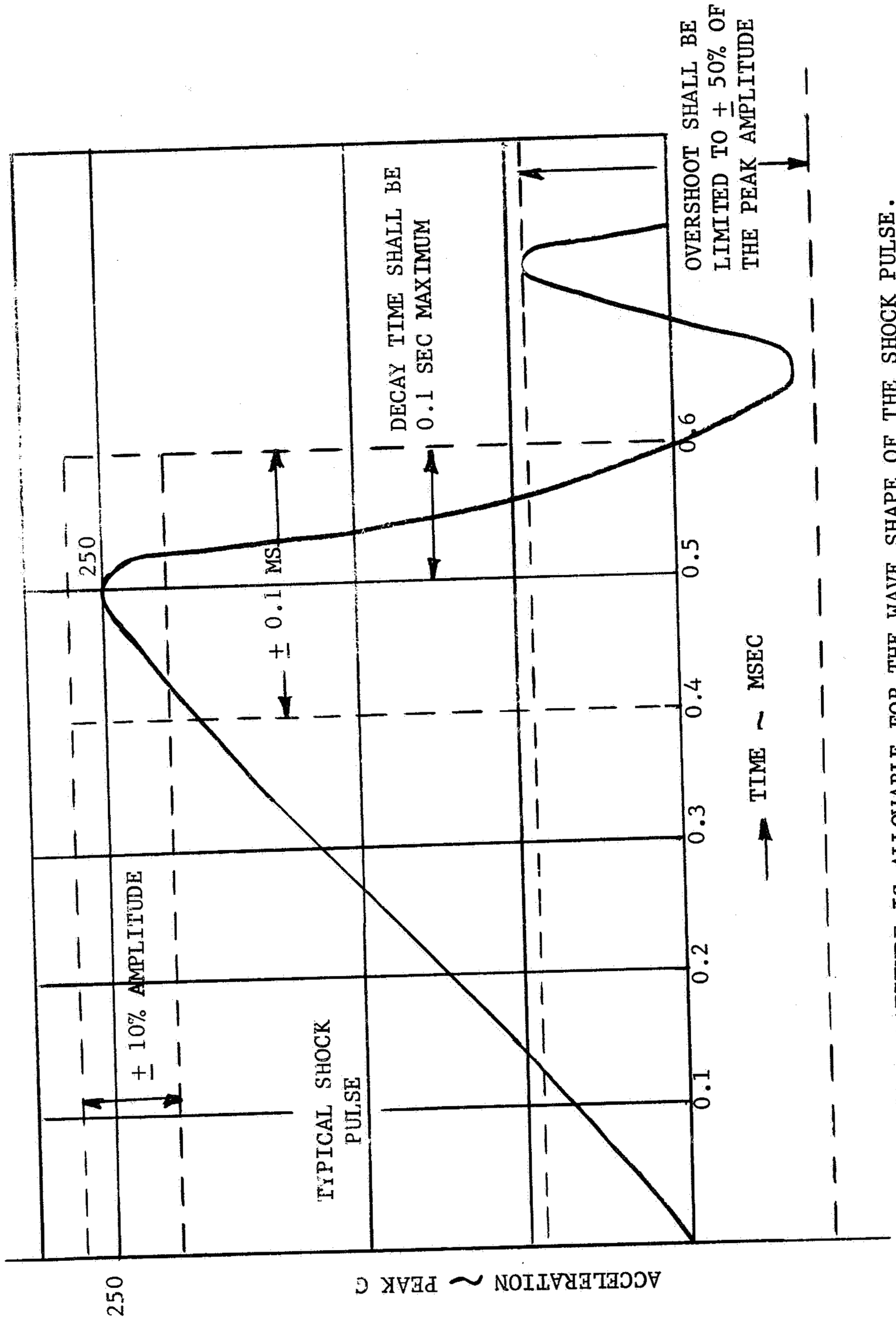

NOTE: SOME LATITUDE IS ALLOWABLE FOR THE WAVE SHAPE OF THE SHOCK PULSE. HOWEVER, IT IS DESIRABLE THAT THE SHAPE CONFORM TO THAT OF A TERMINAL PEAK SAWTOOTH AS NEAR AS PRACTICAL.

FIGURE 1. SHOCK PULSE

FIGURE 1

APPENDIX C

DEPLOYABLE BOOM STRUCTURAL CALCULATIONS

EXTENSION ROD ANALYSIS

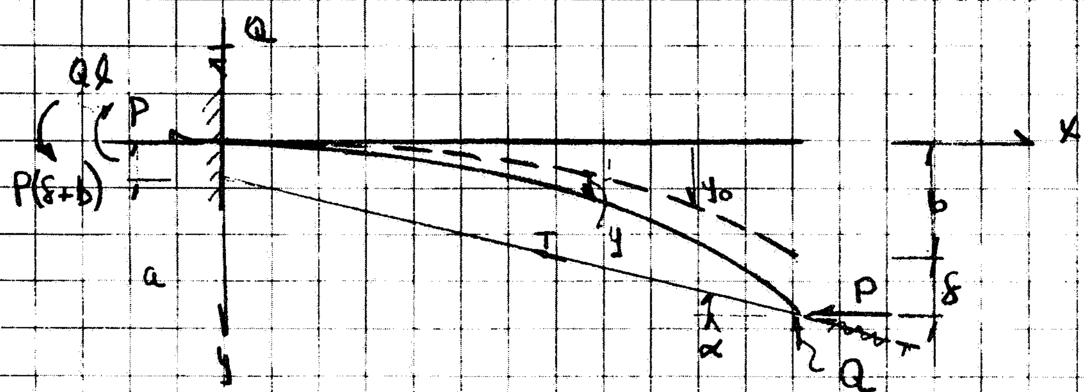

(1) $Q = T \sin\alpha = T\left(\frac{\delta + b - a}{\ell}\right)$

(2) $P = T\cos\alpha \approx T$

ASSUME: $y_0 = kx^2 = \frac{b}{\ell^2}x^2$

(3) $EI\ddot{y} = -M$ WHERE

(4) $M = P(y + y_0) + Q\ell - P(\delta + b) - Qx$

(5) $EI\ddot{y} + Py = -P\frac{b}{\ell^2}x^2 + Qx - Q\ell + P(\delta + b)$

(6) LET $k^2 = \frac{P}{EI}$

(7) $\ddot{y} + k^2 y = -\frac{k^2 b}{\ell^2}x^2 + \frac{Q}{EI}x - \frac{Q\ell}{EI} + k^2(\delta + b)$

(8) $y = A\sin kx + B\cos kx + y_p$

(9) ASSUME $y_p = fx^2 + gx + h$

THEN $\dot{y}_p = 2fx + g$

$\ddot{y}_p = 2f$

EXTENSION ROD ANALYSIS

$$2f + k^2 f x^2 + k^2 g x + k^2 h = -\frac{k^2 b}{\ell^2} x^2 + \frac{Q}{EI} x - \frac{Q\ell}{EI} + k^2(\delta + b)$$

REARRANGING

$$\left[k^2 x^2 f + k^2 x^2 \frac{b}{\ell^2}\right] + \left[k^2 x g - \frac{Q}{EI} x\right] + \left[2f + k^2 h + \frac{Q\ell}{EI} - k^2(\delta + b)\right] = 0$$

FROM ①

$$f = -\frac{b}{\ell^2}$$

FROM ②

$$g = \frac{Q}{P}$$

FROM ③

$$-\frac{2b}{\ell^2} + k^2 h = k^2(\delta + b) - \frac{Q\ell}{EI}$$

OR

$$h = \delta + b + \frac{2b}{k^2 \ell^2} - \frac{Q\ell}{P}$$

THEREFORE (8) BECOMES

$$(10) \quad y = A \sin kx + B \cos kx - \frac{b}{\ell^2} x^2 + \frac{Q}{P} x + \delta + b + \frac{2b}{k^2 \ell^2} - \frac{Q\ell}{P}$$

EXTENSION ROD ANALYSIS

FOR BOUNDARY CONDITIONS:

(11) $\underline{y} = \dot{\underline{y}} = 0$ AT $X = 0$

THEN:

$$0 = B + (\delta + b) + \frac{2b}{k^2 l^2} - \frac{Ql}{P}$$

$$B = \left\{ \frac{Ql}{P} - \delta - b - \frac{2b}{k^2 l^2} \right\}$$

$$\dot{y} = kA \cos kx - kB \sin kx - \frac{2b}{l^2} x + \frac{Q}{P}$$

$$0 = kA + \frac{Q}{P}$$

$$A = -\frac{Q}{kP}$$

THEREFORE THE TOTAL SOLUTION IS:

$$(12) \quad \underline{y} = -\frac{Q}{kP} \sin kx + \left\{ \frac{Ql}{P} - \delta - b - \frac{2b}{k^2 l^2} \right\} \cos kx$$

$$- \frac{b}{l^2} x^2 + \frac{Q}{P} x + \delta + b + \frac{2b}{k^2 l^2} - \frac{Ql}{P}$$

WE ALSO HAVE THE CONDITION $\underline{y} = \delta$ AT $x = l$

$$(12a) \quad \delta = -\frac{Q}{kP} \sin kl - \delta \cos kl + \left[\frac{Ql}{P} - b - \frac{2b}{k^2 l^2} \right] \cos kl - b$$

$$+ \frac{Q}{P} l + \delta + b + \frac{2b}{k^2 l^2} - Ql/P$$

FORM 1-8136 B (9-58)

EXTENSION ROD ANALYSIS

$$(13)\quad \delta = -\frac{Q}{kP}\tan kl + \frac{Ql}{P} - b + \frac{2b}{k^2l^2}\left(\frac{1}{\cos kl} - 1\right)$$

SUBING (1) + (2) INTO (13) GIVES

$$\delta = -\frac{(\delta + b - a)}{kl}\tan kl + \delta + b - a - b + \frac{2b}{k^2l^2}\left(\frac{1-\cos kl}{\cos kl}\right)$$

$$0 = -\delta\tan kl - b\tan kl + a\tan kl - a\,kl$$

$$\frac{2b}{kl}\left(\frac{1-\cos kl}{\cos kl}\right)$$

$$\delta = b\left\{\frac{2(1-\cos kl)}{(\sin kl)kl} - 1\right\} + a\left(1 - \frac{kl}{\tan kl}\right)$$

$$(14)\quad \delta = b\left\{\frac{2(1-\cos kl) - kl\sin kl}{kl\sin kl}\right\} + a\left\{\frac{\tan kl - kl}{\tan kl}\right\}$$

OR

$$(14a)\quad \delta = \frac{b\{2(1-\cos kl) - kl\sin kl\} + a\{kl\cos kl(\tan kl - kl)\}}{(kl)\sin kl}$$

EXTENSION ROD ANALYSIS

FROM EQUATION (14a) WE SEE THAT THE CRITICAL COLUMN LOAD CORRESPONDS TO $\sin kl = 0$

$$kl = n\pi = \pi$$

$$P_{CR} = \frac{\pi^2 EI}{l^2}$$

THIS IS THE CRITICAL LOAD FOR A PIN-ENDED COLUMN —

WE CAN ALSO SEE THE EFFECT OF a ON THE DEFLECTION — i.e. IT WOULD BE ADVANTAGEOUS, IN ORDER TO SATISFY CONDITION 1, TO HAVE A NEGATIVE a.

EXTENSION ROD ANALYSIS

(15) $M = -EI\,y''$

(16) $$y'' = \frac{kQ}{P}\sin kx - k^2\left\{\frac{Ql}{P} - \delta - b - \frac{2b}{k^2l^2}\right\}\cos kx - \frac{2b}{l^2}$$

FOR MAXIMUM BENDING MOMENT

(17) $$\frac{dM}{dx} = 0 = \frac{k^2Q}{P}\cos kx + k^3\left\{\frac{Ql}{P} - \delta - b - \frac{2b}{k^2l^2}\right\}\sin kx$$

$$\tan kx = \frac{-\frac{k^2Q}{P}}{k^3\left\{\frac{Ql}{P} - \delta - b - \frac{2b}{k^2l^2}\right\}}$$

(17a) $$= \frac{-\frac{Q}{P}}{k\left\{\frac{Q}{P}l - \delta - b - \frac{2b}{k^2l^2}\right\}}$$

SUBING (1) AND (2) INTO THE ABOVE

$$\tan kx = \frac{-\frac{1}{l}(\delta + b - a)}{k\left\{\delta + b - a - \delta - b - \frac{2b}{k^2l^2}\right\}}$$

(18) $$\tan kx = \frac{\delta + b - a}{kl\left\{a + \frac{2b}{k^2l^2}\right\}}$$

EXTENSION ROD ANALYSIS

COMBINING (14) AND (18)

$$\tan kx = \frac{b\left\{\frac{2(1-\cos kl)}{kl \sin kl}\right\} - a\left\{\frac{kl}{\tan kl}\right\}}{a\,kl + \frac{2b}{kl}}$$

$$\tan kx = \frac{2b(1-\cos kl) - a(kl)^2 \cos kl}{[a(kl)^2+2b]\sin kl}$$

or

$$x = \frac{1}{k}\tan^{-1}\left\{\frac{2b(1-\cos kl)-a(kl)^2\cos kl}{[a(kl)^2+2b]\sin kl}\right\} \qquad (19)$$

THE APPROPRIATE VALUE OF x ABOVE CAN THE BE SUBSTITUTED INTO EQ'S (15) AND (16) TO GIVE THE MAXIMUM ROD BENDING MOMENT.

$$M_{(ROOT)} = Ta \qquad (20)$$

EXTENSION ROD ANALYSIS

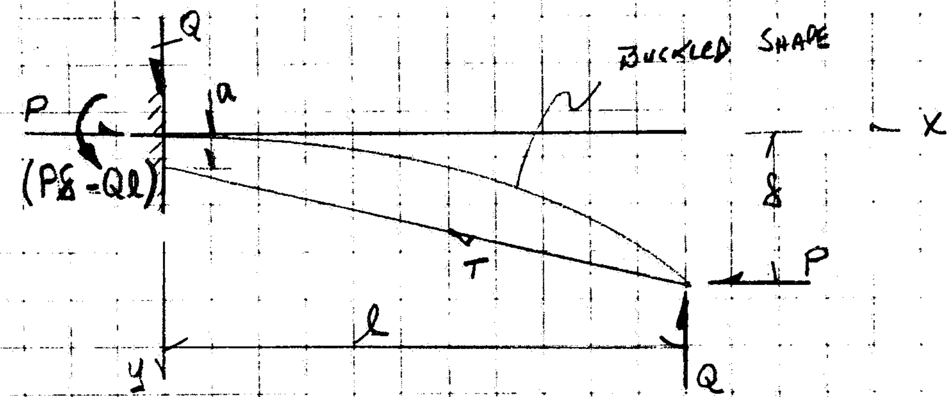

(1) $$EI\,y'' = -M = -[(Q\ell + P\delta) + Py - Qx]$$

$$EI\,y'' + Py = Qx - (Q\ell - P\delta)$$

(2) $$y'' + k^2 y = \frac{Qx}{EI} - \left(\frac{Q\ell}{EI} - k^2\delta\right)$$

(3) $$y = A\sin kx + B\cos kx + y_c$$

(4) $$y_c = ax + b$$

(4a) $$y_c'' = 0$$

AND $$k^2 ax + k^2 b = \frac{Qx}{EI} - \left(\frac{Q\ell}{EI} - k^2\delta\right)$$

$$a = \frac{Q}{k^2 EI} = \frac{Q}{P}$$

$$b = -\left(\frac{Q\ell}{k^2 EI} - \delta\right) = -\left(\frac{Q\ell}{P} - \delta\right)$$

(14) $$y = A\sin kx + B\cos kx + \frac{Q}{P}x - \frac{Q\ell}{P} + \delta$$

FOR BOUNDARY CONDITIONS (6)

EXTENSION ROD ANALYSIS

(15) $0 = B - \frac{Q\ell}{P} + \delta \qquad B = \left(\frac{Q\ell}{P} - \delta\right)$

(16) $\dot{y} = kA\cos kx - kB\sin kx + \frac{Q}{P}$

$0 = kA + \frac{Q}{P} \qquad A = \frac{-Q}{Pk}$

(17) $y = \frac{-Q}{Pk}\sin kx + \left(\frac{Q\ell}{P} - \delta\right)\cos kx + \frac{Q}{P}x - \frac{Q\ell}{P} + \delta$

AT $x = \ell \quad y = \delta$

$\delta = \frac{-Q}{Pk}\sin k\ell + \frac{Q\ell}{P}\cos k\ell - \delta\cos k\ell + \frac{Q\ell}{P} - \frac{Q\ell}{P} + \delta$

$\delta = \frac{-Q}{Pk\cos k\ell}\sin k\ell + \frac{Q\ell}{P}$

(18) $\delta = \frac{-Q}{Pk}\left\{\tan k\ell - k\ell\right\} \qquad P = T, \quad Q = T\left(\frac{\delta - a}{\ell}\right)$

(19) $\delta = a\left\{\frac{\tan k\ell - k\ell}{\tan k\ell}\right\}$

THIS RESULT IS THE SAME AS THAT OF EQUATION FOR $b = 0$

APPENDIX D

STOWED CONFIGURATION STRUCTURAL CALCULATIONS

BY		GENERAL ELECTRIC	PAGE D1
CK.			MODEL
DATE	REV.		REPORT

STRUCTURAL ANALYSIS OF ROLL-UP SOLAR ARRAY SUPPORT STRUCTURE

LOADS OBTAINED FROM DYNAMIC ANALYSIS

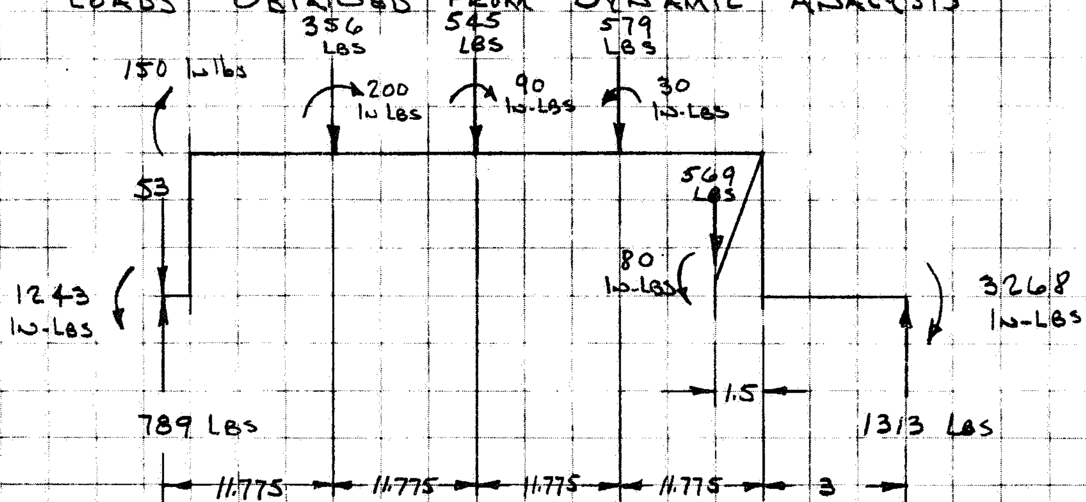

EXTERNAL LOADS ON DRUM & SHAFT

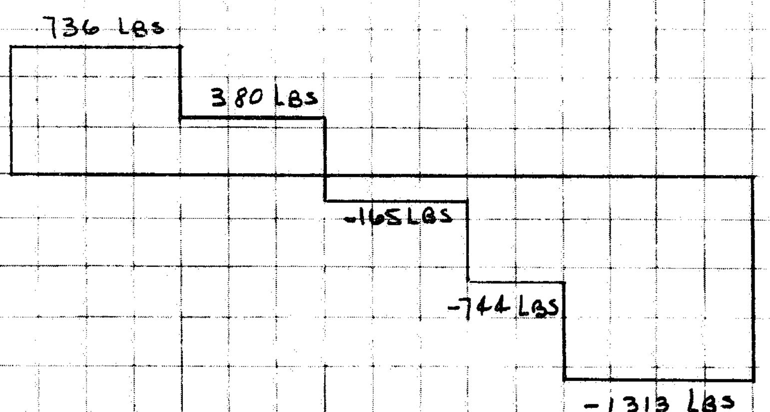

SHEAR DIAGRAM

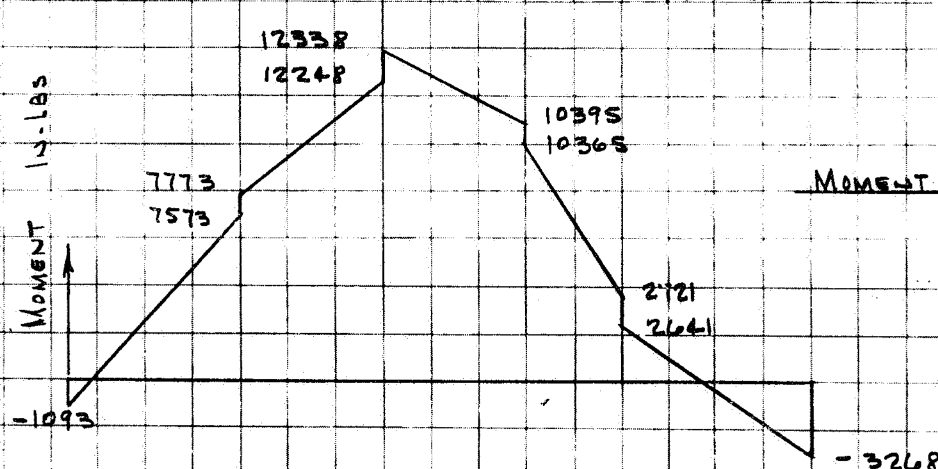

MOMENT DIAGRAM

DRUM ANALYSIS

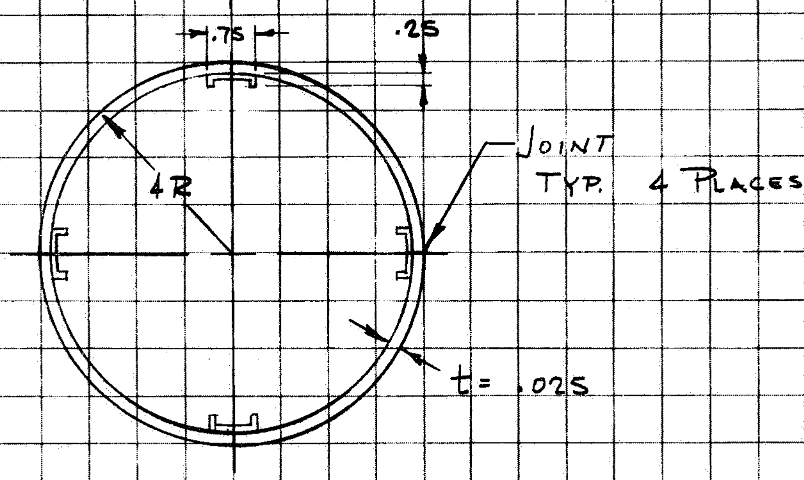

DRUM CROSS-SECTION

MATERIAL

BERYLLIUM CROSS-ROLLED QMV SHEET

F_{TY} = 60,000 PSI

F_{TU} = 78,000 PSI

E = 42.5×10^6 PSI   REF. 1

G = 20×10^6 PSI

F_{BRU} = 1.9 F_{TU} = 148,000 PSI

F_{SU} = .9 F_{TU} = 70,300 PSI

MOMENT OF INERTIA OF CYLINDER

CONSERVATIVELY NEGLECTING THE CHANNELS

$I = \pi R^3 t$

$= .502 \text{ IN}^4$

TWO CONDITIONS ARE ANALYZED

1. MAXIMUM BENDING MOMENT

MAX M = 12338 IN-LBS

$P_{SHEAR} = 0$

$$f_b = \frac{12338(4)}{5.02}$$

$= 9850$ PSI

$f_{b\,ULT} = 1.25\ f_b$

$= 12300$ PSI

$F_{b_{CR}} = C_b E\ t/R$ REF 2 Pg C8.8

ASSUME C_b = COMPRESSIVE BUCKLING COEFF.

$$C = \frac{1}{\sqrt{3(1-\nu^2)}}$$

$\nu = .06$

$C = .578$

$F_{b_{CR}} = .578\,(42.5)10^6\,(.025/4)$

$= 15350$ PSI

$$M.S. = \frac{15.35^K}{12.3^K} - 1 = \underline{\underline{.25}}$$

FORM 1-8136 B (9-58)

2. MAXIMUM TRANSVERSE SHEAR

$P_{SHEAR} = 744$ LBS
$M = 10395$ IN-LBS

$$F_{SCR} = \frac{K_s \pi^2 E}{12(1-\nu^2)} \left(t/L\right)$$ REF 2 PG C8.13

$$Z_L = \frac{L^2}{Rt}\sqrt{1-\nu^2}$$

$= 22100$

$K_t = 850$

$K_s = 1.25\,K_t$

$= 1065$

$$F_{SCR} = \frac{1065\,\pi^2 (42.5)\,10^6}{12(1-.06)^2}\left(\frac{.025}{47}\right)^2$$

$= 10550$ PSI

$$f_s = \frac{V}{\pi R t}$$

$$= \frac{744}{4\pi(.025)}$$

$= 2370$ PSI

$f_{s_{ULT}} = 2970$ $R_s = \frac{2.97}{10.55} = .281$

$$f_b = \frac{10395\,(4)}{5.02}$$

$= 8400$ PSI

$f_{b_{ULT}} = 10500$ PSI $R_b = \frac{10.5}{15.35} = .685$

INTERACTION EQUATION

$R_b^3 + R_s^3 = 1$

$(.685)^3 + (.281)^3 = .342 < 1$ REF 2 PG C8.17

CONSIDER THE SOLAR ARRAY TO ACT AS A BEARING LOAD ON THE CYLINDER DURING VIBRATION.

ASSUME A UNIFORM PRESSURE DISTRIBUTION ON A UNIT LENTH OF THE CYLINDER. SIMPLE SUPPORT IS ASSUMED AT THE CHANNEL SUPPORTS. THIS MAY BE SOMEWHAT UNCONSERVATIVE & DEPENDS ON THE STIFFNESS OF THE CHANNEL - SHEET SECTION; HOWEVER NO END FIXITY IS ASSUMED.

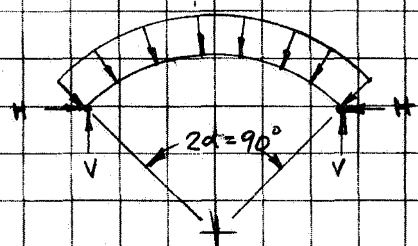

$\alpha = \dfrac{\pi}{4}$

$$p' = \frac{E t^3 \left(\frac{\pi^2}{\alpha^2} - 1\right)}{12 R^3 (1-\nu^2)}$$ REF 3 PAGE 307

$$= \frac{(42.5)10^6 \left(\frac{\pi^2 16}{\pi^2} - 1\right)(.025)^3}{12 (4)^3 (1-.06^2)}$$

$$= 13 \text{ PSI}$$

ASSUMING THE PRESSURE TO ACT ONLY ON ONE HALF OF THE CYLINDER

MAXIMUM INTENSITY OF THE PRESSURE $= \dfrac{579}{11.775(8\pi)}$

$= 1.96$ LBS/IN

ULTIMATE PRESSURE $= 2.45$ LBS/IN

M.S. $= \dfrac{13}{2.45} - 1 =$ HIGH

BY	GENERAL ELECTRIC	PAGE D6
CK.		MODEL
DATE REV.		REPORT

BOND JOINT

$$\text{MAX } f_s = \frac{V}{\pi R t}$$

$$= \frac{744}{4\pi(.025)}$$

$$= 2370 \text{ PSI}$$

$$f_{s_{ULT}} = 2970 \text{ PSI}$$

SHEAR FLOW = 74.5 PPI

THIS SHEAR FLOW HAS TO BE TRANSFERRED ACROSS A BOND JOINT.

ASSUME A 1/4 INCH BOND WIDTH

$$f_{BOND} = 74.5/.25$$

$$= 298 \text{ PSI}$$

$$\text{M.S.} = \frac{2000}{298} - 1 = \underline{\underline{\text{HIGH}}}$$

FORM 1-8136 B (9-58)

END CAP - OUTBOARD

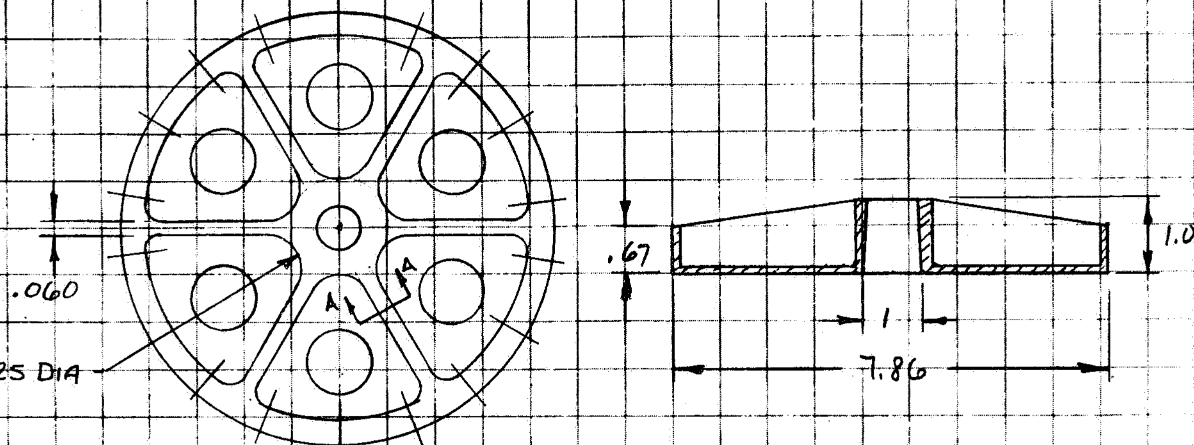

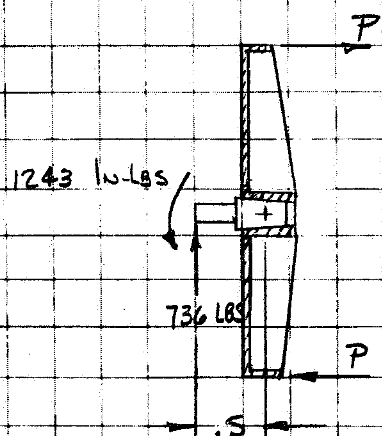

APPLIED LOADS

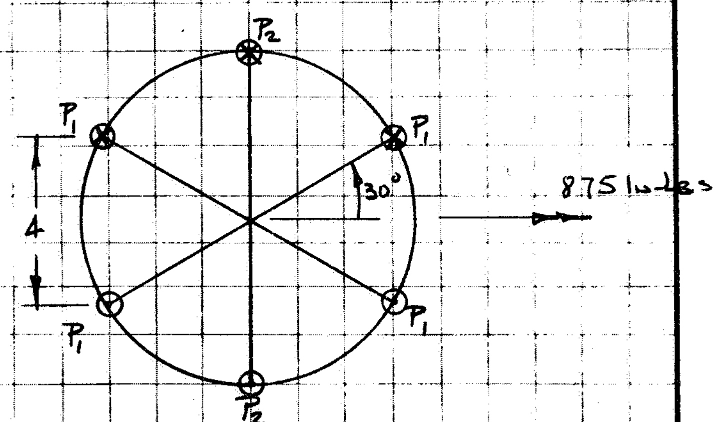

REACTIONS

$$2P_1(4) + 8P_2 = 875$$

$$P_1 = P_2/2$$

$$P_2 = \frac{875}{12}$$

$$= 73 \text{ LBS}$$

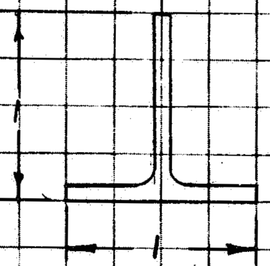

	A	Y	AY	AY^2	I_o
1	.060	.50	.030	.015	.005
2	.056	.03	.00168	.001	–
Σ	.116	$.\overline{273}$	.03168	.016	.005

$$I = .016 + .005 - .116(.273)^2$$
$$= .0124$$

SECTION A-A

MATERIAL

BERYLLIUM S-200C

F_{TU} = 40,000 PSI REF 4

F_{TY} = 30,000 PSI

F_{BRU} = 1.9(40,000) = 76000 PSI

THERE IS AN ADDITIONAL LOAD DUE TO THE TAPERED END PLUG

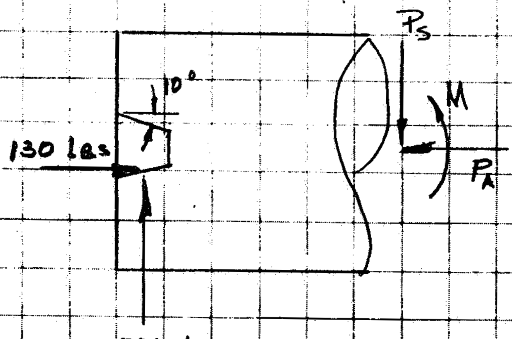

LOAD / RIB = 130/6
= 21.7 LBS

$$f_b = \frac{(73+21.7)(3.5)(.727)}{.0124}$$

$$= 19400 \text{ PSI}$$

$$f_{b_{ULT}} = 24200 \text{ Psi}$$

CRIPPLING

$MAX\ F_{cc} = .8\ F_{cy}$
$= 24000\ PSI$

$f_{cc} = 2/3\ (24200)$
$= 16100\ PSI$

$M.S. = \frac{24^k}{16.1^k} - 1 = .49$

BEARING IN HOLE

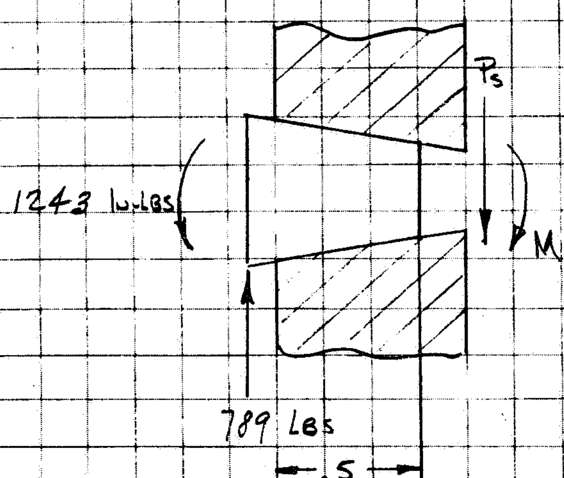

REF 5

$\frac{SL}{M} = \frac{-789(.5)}{1243}$

$= -.276$

$K_1 = 4.9$
$K_2 = 5.5$

$BEARING\ STRESS = \frac{5.5\ (1243)}{(.5)^2\ (.83)}$

$= 33000\ PSI$

$f_{BRU} = 41300\ PSI$

$M.S. = \frac{76^k}{41.3} - 1 = .84$

BY	GENERAL ELECTRIC	PAGE D10
CK.		MODEL
DATE REV.		REPORT

END CAP - INBOARD

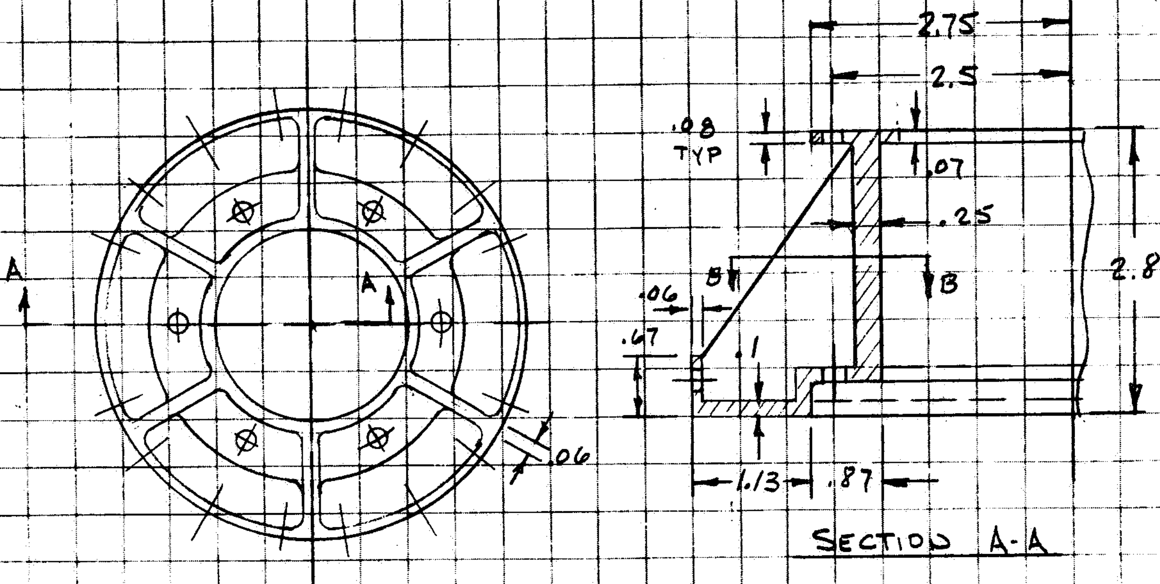

SECTION A-A

MATERIAL

BERYLLIUM S-200-C

$F_{TU} = 40,000$ PSI

$F_{TY} = 30,000$ PSI REF 4

$F_{BRU} = 76,000$ PSI

FROM PAGE 7

$$P_2 = \frac{2721}{12} + 21.7$$
$$= 247.7$$

$$M_{MAX} = 247.7\,(2)$$
$$= 495.4 \text{ IN-LBS}$$

FORM 1-8136 B (9-58)

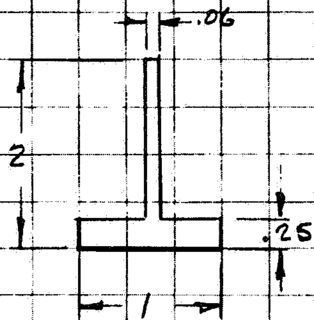

SECTION B-B

	A	Y	AY	AY²	I_o
1	.12	1	.120	.120	.040
2	.235	.125	.029	.0036	.001
Σ	.355	.42	.149	.1236	.041

$$I = .1236 + .041 - .355(.42)^2 = .1026 \text{ IN}^4$$

$$f_b = \frac{\cancel{495.4}(1.58)}{.1026} = 7600 \text{ PSI}$$

$$f_{b_{ULT}} = 9500 \text{ PSI}$$

$$F_{cc} = .8(30,000) = 24000 \text{ PSI MAX}$$

$$f_{cc} = 2/3(9500) = 6340 \text{ PSI}$$

$$M.S. = \frac{24^K}{6.34^K} - 1 = \underline{\text{HIGH}}$$

LUG ANALYSIS

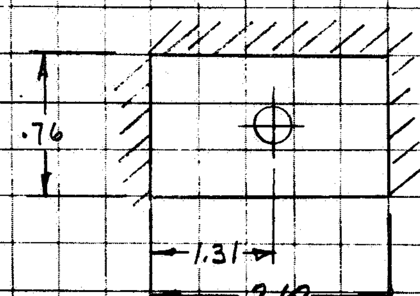

$$M_x = \frac{P}{(2.62 + .76)}(2.62)(.38) = .295 P$$

$$M_y = \frac{P}{3.38}(.76)(1.31) = .295 P$$

$M = .295(2477)$
$= 73$ IN-LBS

$f_b = \dfrac{6(73)}{.76(.25)^2}$

$= 9250$ PSI

$M.S. = \dfrac{30^k}{9.25} - 1 = \text{HIGH}$

BEARING HOUSING

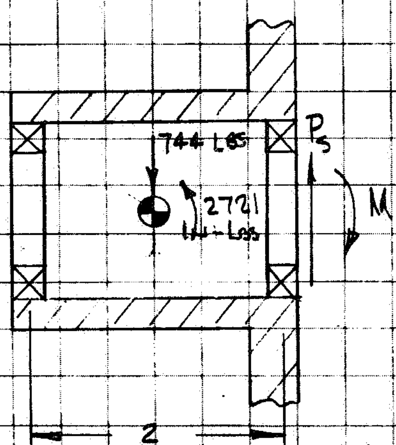

$P_{BRG} = \dfrac{744}{2} + \dfrac{2721}{2}$

$= 1733$ lbs

$P_{ULT} = 2170$ LBS

BEARING HAS A RADIAL LOAD RATING OF 2500 LBS

$M.S. = \dfrac{2500}{2170} - 1 = \underline{\underline{.15}}$

LATERAL LOADING CONDITION (ALONG DRUM CENTERLINE)

ASSUME AN AMPLIFICATION FACTOR OF 15 ALONG CENTERLINE OF DRUM

WEIGHT OF DRUM & SOLAR ARRAY (ONE SIDE) = 25 LBS

THRUST LOAD ON BEARING = 25(4g's)(15) = 1500 LBS.
(ASSUME TOTAL LOAD REACTED BY ONE BEARING)

THRUST RATING OF BEARING = 4680 LBS

$M.S. = \dfrac{4680}{1500} - 1 = \underline{\underline{\text{HIGH}}}$

LEADING EDGE MEMBER
DWG NO. 47E214883

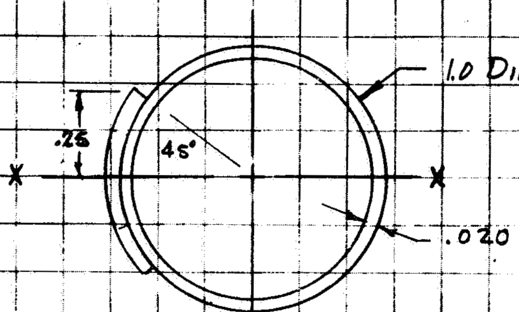

MATERIAL
BERYLLIUM SHEET
$F_{TY} = 60,000$ PSI REF 1
$F_{TU} = 78,000$ PSI

$$I_{xx} = \pi R^3 t + R^3 t (\alpha - \sin\alpha \cos\alpha)$$
$$= R^3 t (\pi + \alpha - \sin\alpha \cos\alpha)$$
$$= (.5)^3 (.020) (\pi + \frac{\pi}{2} - \frac{\pi}{4} \cdot \frac{\pi}{4})$$
$$= .0103 \text{ IN}^4$$

$$A = \pi D t + \frac{\pi}{4} D t$$
$$= .0885 \text{ IN}^2$$

$$WGT = .0885 (47)(.065)$$
$$= .271 \text{ LBS}$$

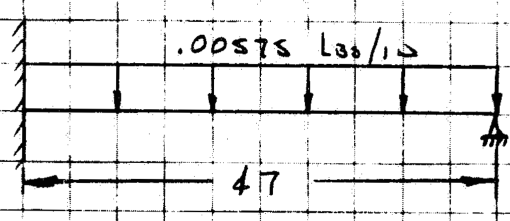

THE ARRAY HAS A PRE-LOAD OF 2 LBS. ASSUME THIS IS AN EQUIVALENT MASS

$$\omega_n = \frac{15.4}{l^2} \left(\frac{EI}{m} \right)^{1/2}$$

$l = 47$ INCHES
$E = 42.5 \times 10^6$ LBS/IN^2
$I = .0103$ IN^4
$m = (2 + .271) / (47)(386)$
$= 1.245 \times 10^{-4}$ LB SEC^2/IN^2

$$\omega_n = \frac{15.4}{(47)^2}\left(\frac{48.5(10^6)(.0103)}{1.245\ (10^{-4})}\right)^{1/2}$$

$$= 414 \text{ RAD/SEC}$$

$$f_N = \omega_n / 2\pi$$
$$= 66 \text{ CPS}$$

DYNAMIC LOADING

ASSUME A MAGNIFICATION FACTOR OF 25 WITH A 4g EXCITATION. THIS APPLIES ONLY TO THE MASS OF THE ROD

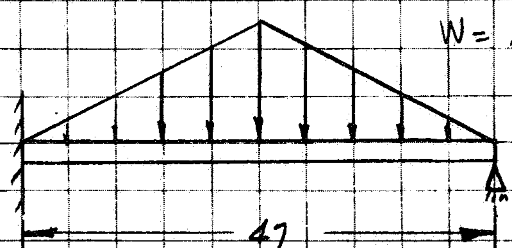

$W = .271 \times 100 + 2 = 29.1$ LBS

$$\text{MAX } M = \frac{5Wl}{32}$$
$$= \frac{5(29.1)(47)}{32}$$
$$= 214 \text{ IN-LBS}$$

$$f_b = \frac{214(.5)}{.0103}$$
$$= 10400 \text{ PSI}$$

$$f_{b_{ULT}} = 1.25\ (10400)$$
$$= 13000$$

$$M.S. = \frac{30^k}{13^k} - 1 = \underline{\underline{HIGH}}$$

SHEAR STRESS IN BOND

MAX $V = 105W/160 = 19.1$ LBS

$q = V/\pi R = 12.2$ LBS/IN

ASSUMING A 1/4 INCH BOND WIDTH

$$f_s = \frac{12.2}{.25} = 48.8 \text{ PSI}$$

M.S. = HIGH

FORM 1-8136 B (9-58)

END SUPPORT - OUTER

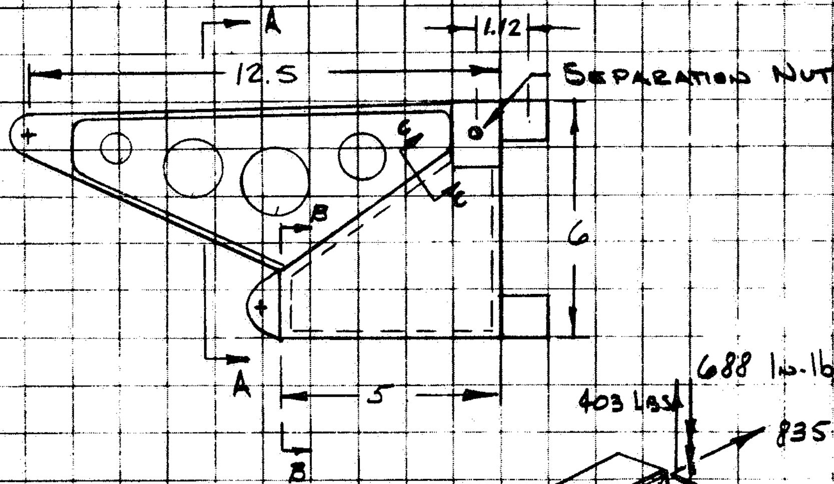

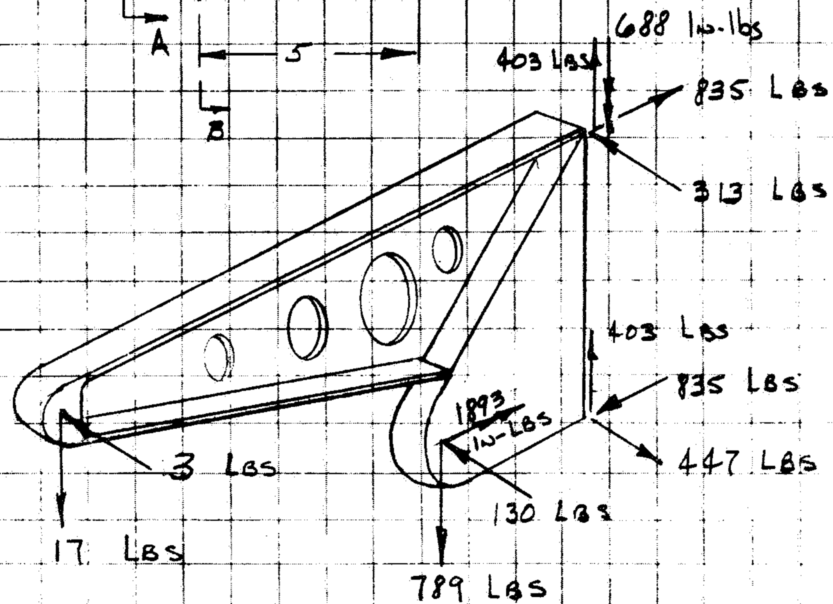

LOADS ACTING ON END SUPPORT

MATERIAL

ALUMINUM 6061-T6

$F_{TU} = 42000$ PSI
$F_{TY} = 35000$ PSI
$F_{SU} = 27000$ PSI
$F_{BRU} = 67000$ PSI

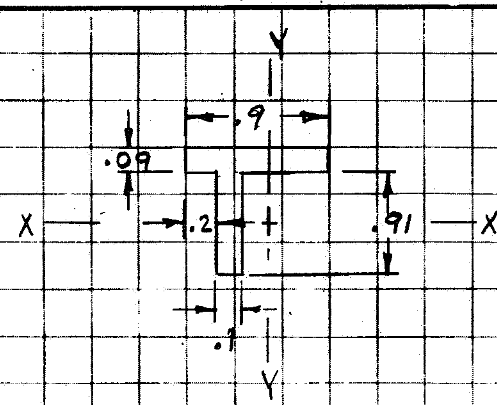

SECTION A-A

	A	X	AX	AX²	I_o
1	.081	.45	.0364	.0164	.00547
2	.091	.25	.0228	.0057	.00008
Σ	.172	.344	.0592	.0221	.00555

$$I_{YY} = .0221 + .00555 - .172(.344)^2$$
$$= .00745 \text{ IN}^4$$

AT SECTION A-A

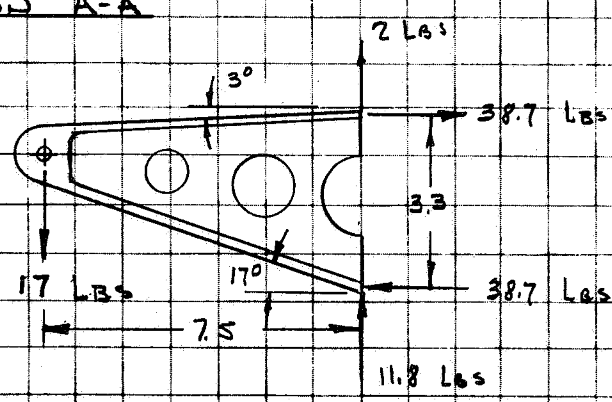

ASSUME THE 3 LB OUT-OF-PLANE LOAD IS REACTED BY THE UPPER EDGE ONLY

$$f = \frac{38.8}{.172} + \frac{3(7.5)(.556)}{.00745}$$
$$= 1905 \text{ PSI}$$

M. S. = HIGH

AT SECTION B-B

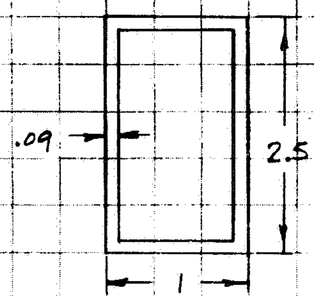

REACTING TORQUE

$$f_s = \frac{1893}{2(.09)(2.5-.09)(1-.09)}$$

REF 3
PAGE 176

$$= 4700 \text{ PSI}$$

$$f_{s_{ULT}} = 5880 \text{ PSI}$$

$$M.S. = \frac{27^K}{5.88^K} - 1 = \underline{HIGH}$$

LUG AT SECTION B-B

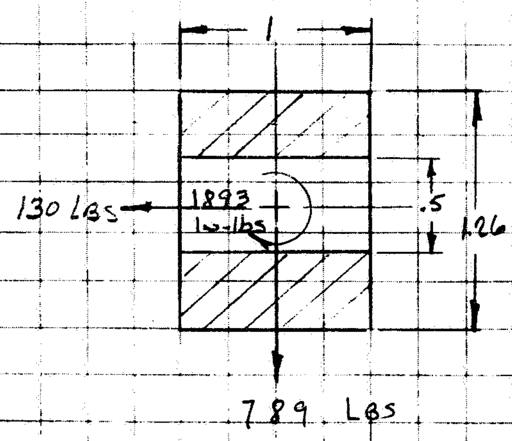

$$\text{MAX SHEAR} = \left[\left(65 + \frac{1893}{.88}\right)^2 + (394.5)^2\right]^{1/2}$$

$$= 2250 \text{ LBS}$$

$$f_s = \frac{2250}{1(.38)}$$

$$= 5750 \text{ PSI}$$

$$f_{s_{ULT}} = 7400 \text{ PSI}$$

$$M.S. = \frac{27^K}{7.4^K} - 1 = \underline{HIGH}$$

SECTION C-C

ALL OF THE OUT-OF-PLANE MOMENTS ARE REACTED BY THE SEPARATION NUT AND UPPER HINGE

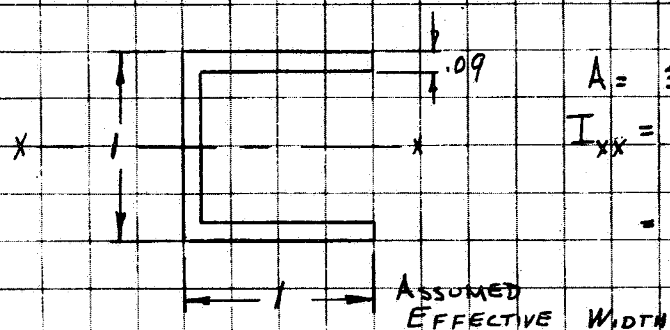

$A = 3(.09) = .27 \text{ IN}^2$

$I_{xx} = \frac{.09(1)^3}{12} + \frac{.09(.9)(.91)^2}{2}$

$= .0411 \text{ IN}^4$

$f_b = \frac{130(6)(.5)}{.0411}$

$= 9500 \text{ PSI}$

TENSION FROM 789 LB LOAD = 192 LBS

$f_T = \frac{192}{.27}$

$= 710 \text{ PSI}$

$f_{ULT} = 1.25(9500 + 710)$
$= 12800 \text{ PSI}$

$M.S. = \frac{42^K}{12.8^K} - 1 = \text{HIGH}$

UPPER HINGE

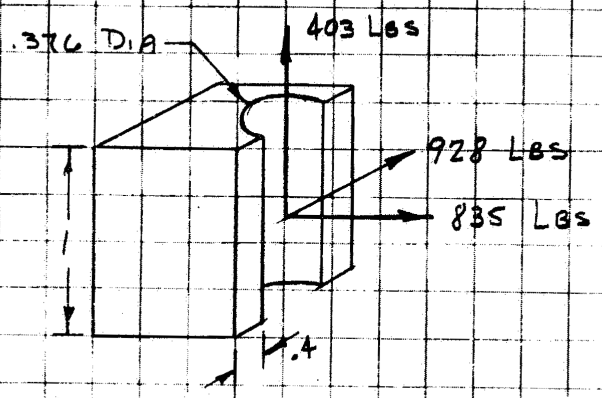

APPLIED LOADS ON HINGE

$$\text{MAX SHEAR} = (928^2 + 403^2)^{1/2}$$
$$= 1012 \text{ LBS}$$

$$f_s = \frac{1012}{1(.08)} =$$
$$= 12650 \text{ PSI}$$

$$f_t = 835/1(.08)$$
$$= 10440 \text{ PSI}$$

$$f_{MAX} = 5220 + \sqrt{(5220)^2 + (12650)^2}$$
$$= 18900 \text{ PSI}$$

$$f_{ULT} = 23600 \qquad M.S. = \frac{42^k}{23.6^k} - 1 = \underline{\underline{.78}}$$

$$\text{MAX } f_s = 13700 \text{ PSI}$$
$$f_{s_{ULT}} = 17100 \text{ PSI} \qquad M.S. = \frac{27^k}{17.1^k} - 1 = \underline{\underline{.58}}$$

$$\text{BEARING LOAD} = (1012^2 + 835^2)^{1/2}$$
$$= 13120 \text{ LBS}$$

$$f_{BRU} = \frac{1.25(13120)}{1(.376)}$$
$$= 43600 \text{ PSI} \qquad M.S. = \frac{67^k}{43.6^k} - 1 = \underline{\underline{.53}}$$

FORM 1-8136 B (9-58)

CENTER SUPPORT STRUCTURE

SUPPORT TUBE & FLANGE

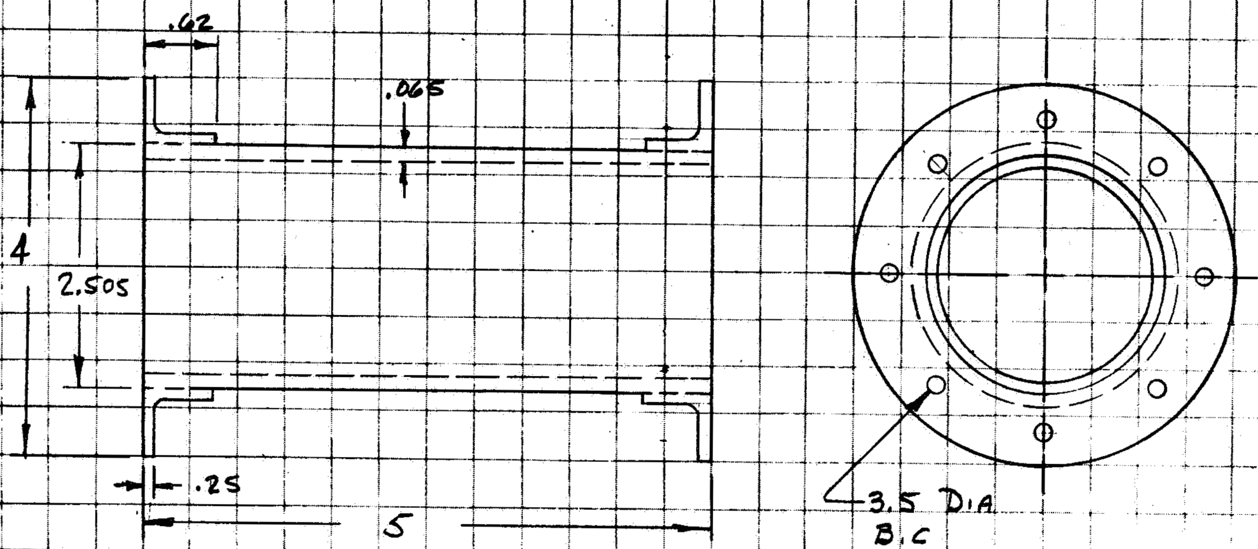

MATERIAL - 6061-T6 ALUMINUM

TUBE

TUBE REACTS 3268 IN-LB

$I_{TUBE} = \pi R^3 t$
$= .398 \text{ IN}^4$

$f_b = \frac{3268(1.25)}{.398}$
$= 10300$ PSI

$f_{ULT} = 12900$ PSI

$D/t = 38.5$

$F_{cc} = 35,000$ PSI

$M.S = \frac{35^K}{12.9^K} - 1$ HIGH

FLANGE

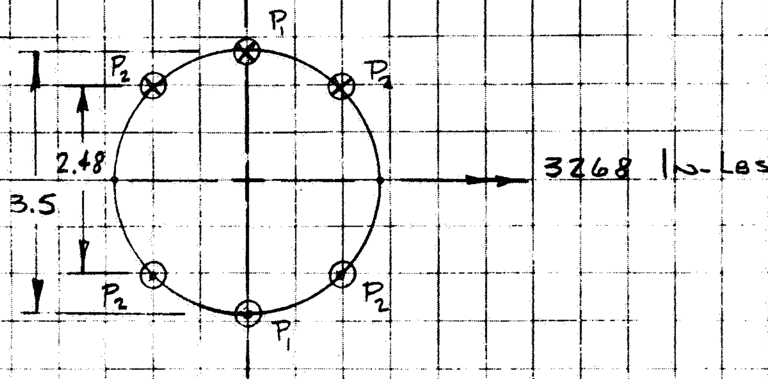

APPLIED LOADS ON FLANGE

$$2P_2(2.48) + 3.5P_1 = 3268$$

$$P_2 = .707\,P_1$$

$$P_1 = \frac{3268}{7}$$
$$= 466 \text{ LBS}$$

$$f = \beta \frac{W}{t^2}$$ REF 3 PAGE 211

$a = 1.75$ IN
$b = 1.25$ IN

$a/b = 1.4$ $\beta = 4.03$

$$f = \frac{4.03\,(466)}{(.25)^2}$$
$$= 30200 \text{ PSI}$$

$f_{ULT} = 37{,}800$

$$M.S. = \frac{42^K}{37.8^K} - 1 = .11$$

SIDE PLATE

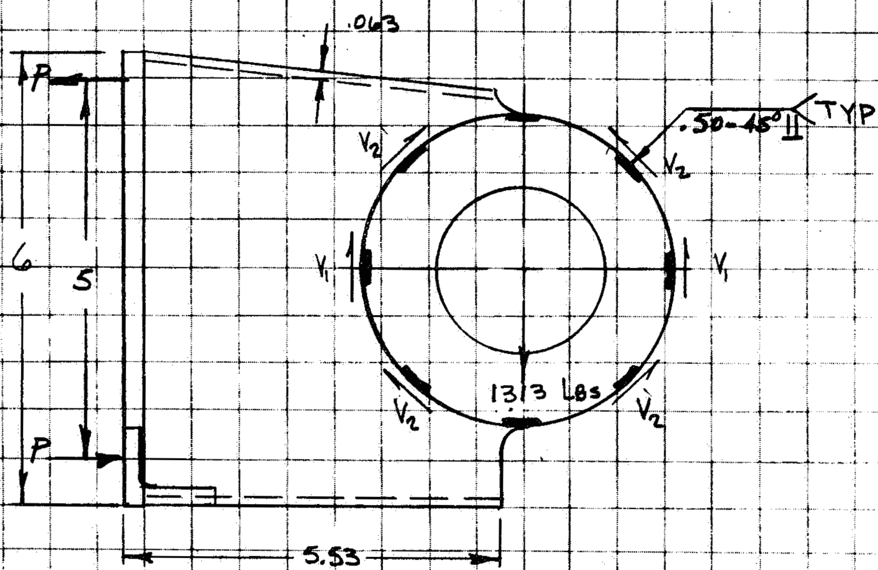

APPLIED LOAD ON SIDE PLATE

ASSUME A $\frac{VQ}{I}$ DISTRIBUTION ON WELD REACTIONS

$$2V_1 + 4V_2 = 1313$$

$$V_2 = .707\ V_1$$

$$V_1 = \frac{1313}{4.83}$$

$$= 272 \text{ LBS}$$

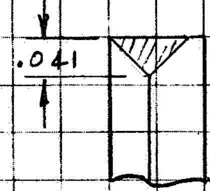

WELD JOINT

$$f_s = \frac{272}{.041(.5)}$$

$$= 13300 \text{ PSI}$$

$$f_{s_{ULT}} = 16600 \text{ PSI}$$

ASSUMING HEAT TREAT AFTER WELDING

$$F_{SU} = 27000 \text{ PSI}$$

$$M.S. = \frac{27}{16.6} - 1 = .63$$

REFERENCES:

1. BERYLLIUM MATERIALS DATA, BRUSH BERYLLIUM CO.
2. BRUHN, E. F., "ANALYSIS AND DESIGN OF FLIGHT VEHICLE STRUCTURES", 1965
3. ROARK, R. J., "FORMULAS FOR STRESS AND STRAIN," McGRAW-HILL
4. AEROSPACE STRUCTURAL METALS HANDBOOK
5. GENERAL ELECTRIC STRUCTURES MANUAL

APPENDIX E

HUNTER STACER TEST RESULTS

As part of the initial deployable boom selection studies two test programs were conducted to determine the mechanical properties of the Hunter STACER rod.

E.1 THERMAL BENDING TEST

A thermal bending test (in air) was conducted by Hunter Spring Corporation to investigate the hypothesis that the thermally induced deflection of a STACER rod would be less than the corresponding deflections of an equivalent solid 304 stainless steel tube. Thermal bending of the deployed boom is an important design consideration. Figure E-1 is a sketch of the test setup showing thermocouple location, heating and cooling system positions, and the position of deflection measurements. The test data are summarized in Table E-1. These data show the thermal bending characteristics of the two types of tubes are similar.

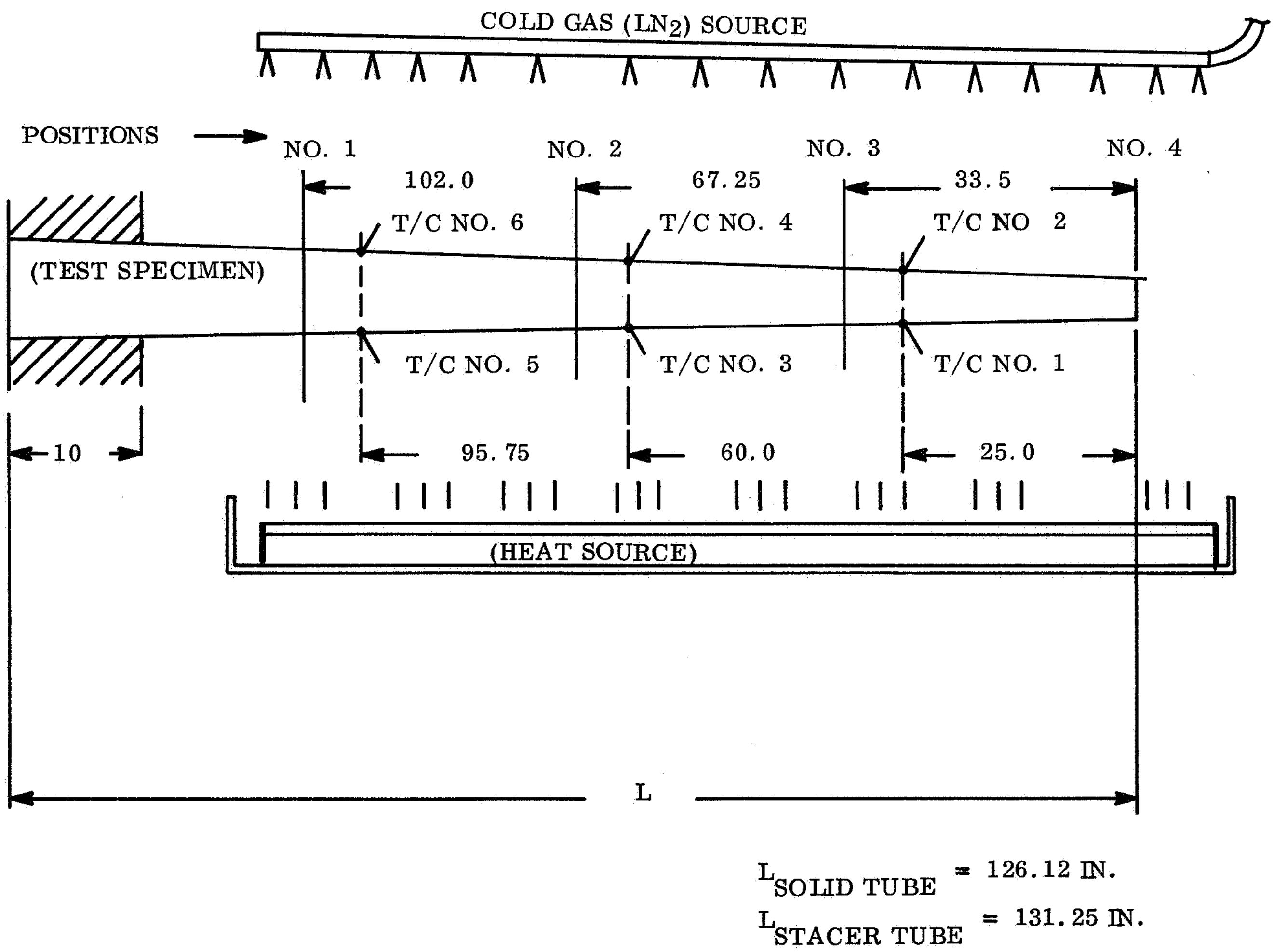

Figure E-1. Hunter STACER Thermal Bending Test Setup

Table E-1. Summary of Test Results

Run	Thermocouple (All temperatures in ^{o}F)						Deflection Measurement Positions				Test Specimen
	1	2	3	4	5	6	1	2	3	4	
1	142	68	169	81	179	77	0.0	0.69	1.70	3.75	Solid 304 S/S Tube
2	170	92	169	92	164	97	0.0	0.53	1.50	2.94	1.12 in. Root Dia x 0.020 in. thick
3	152	37	152	51	146	29	0.02	0.75	2.04	4.19	x 0.63 in. Tip Dia x 126.12 in.
4	147	27	140	35	147	36	0.02	0.88	2.33	4.63	Wt = 2.35 lb
1	200	98	184	85	191	89	0.12	0.75	1.80	3.56	Hunter STACER 301 S/S
2	196	98	185	86	191	86	0.12	0.75	1.80	3.56	Tube 0.006 x 6.0
3	206	100	196	88	204	102	0.12	0.69	1.60	3.19	Strip, 1.12 in. Root Dia.
4	206	102	206	91	207	94	0.12	0.69	1.70	3.34	0.50 in. Tip Dia x 131.25 in.
											Wt = 2.05 lb

E.2 STIFFNESS TEST

The Hunter STACER rod, a spirally wound tapered unit, is not easily analyzed as a structural element; essentially there is no design data available due to the early development stage of this concept. Therefore, a relatively simple stiffness test was performed on a stainless steel sample to satisfy the need for stiffness characteristics for use in analysis. The test sample was typical of the rods being considered for the roll-up solar array application and was subjected to both a pure end moment and a transverse load. The results obtained, though limited in scope and precision, provide data for comparing the stiffness of the STACER rod with other types rods.

The data shown in Table E-2 were obtained by a load test on the rod specimen when supported on floats in a water tank. These data consist of deflections measured at points along the rod length for eight loading conditions: five force couples and three lateral forces applied at the member tip. A sketch of the test specimen showing the stations where deflection measurements were made is shown in Figure E-2. Photographs of the test setup and the method of loading the rod tip are shown as Figures E-3 and E-4, respectively.

Analysis

It was postulated that deflection of the STACER rod acting as a beam would follow the classical beam equation

$$\frac{d^2y}{dx^2} = \frac{-M}{EI}$$

where M is the bending moment and EI is the member stiffness. The purpose of the experiment was to determine the member stiffness of the test specimen and it should be understood that the member stiffness is not necessarily the product of the modulus of elasticity (E) and the moment of inertial of the cross section (I). Given the equation of the elastic curve under the load, the second derivative can be calculated and the local member stiffness calculated.

Table E-2. Measured Rod Deflection - Hunter STACER Stiffness Test (Reference Figure E-2)

No.*	Loading	F (lb)	M (in.-lb)	Deflection 1	2	3	4	5	6	7	8	9	10	11	12	TIP
1	Force couple		50.06	0	0.25	0.50	1.00	1.75	2.50	3.50	4.75	6.25	7.75	9.75	12.75	13.00
2	Force couple		75.09	0	0.50	1.25	1.75	2.50	3.75	5.25	7.00	9.25	11.50	13.75	18.00	19.00
3	Force couple		83.44	0	0.50	1.25	2.00	3.25	4.50	6.50	8.25	10.50	13.50	16.50	20.50	21.50
4	Force couple		61.19	0	0.50	1.25	2.00	3.00	4.25	5.75	7.50	9.25	12.00	14.75	18.25	19.00
5	Force couple		36.16	0	0.50	1.00	1.50	2.00	3.00	4.00	5.50	6.50	8.50	10.50	13.25	13.50
6	Lateral force	0.0975	--	0	0	0.50	0.75	1.00	1.50	2.00	2.50	3.25	4.00	4.75	5.50	--
7	Lateral force	0.2075	--	0	0.75	1.00	1.50	2.25	3.00	4.00	5.00	6.50	7.75	9.25	10.75	--
8	Lateral force	0.3780	--	0	0.75	2.00	2.50	4.00	5.50	7.50	9.00	11.50	14.75	16.50	19.50	--

*Tests are listed in the order they were run. Tests 4 and 5 were unloading.

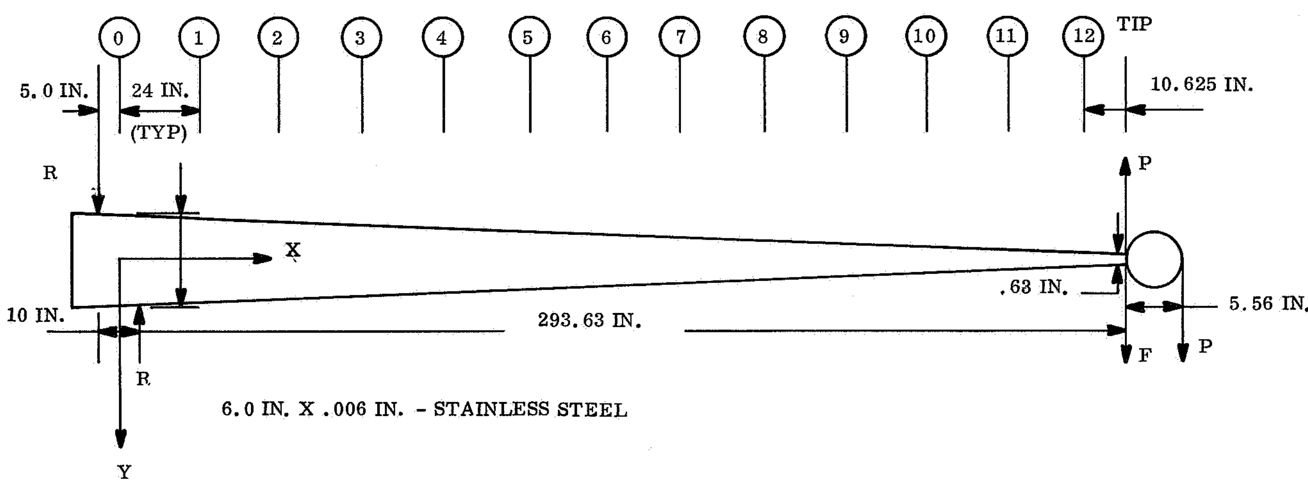

Figure E-2. Hunter STACER Stiffness Test Specimen

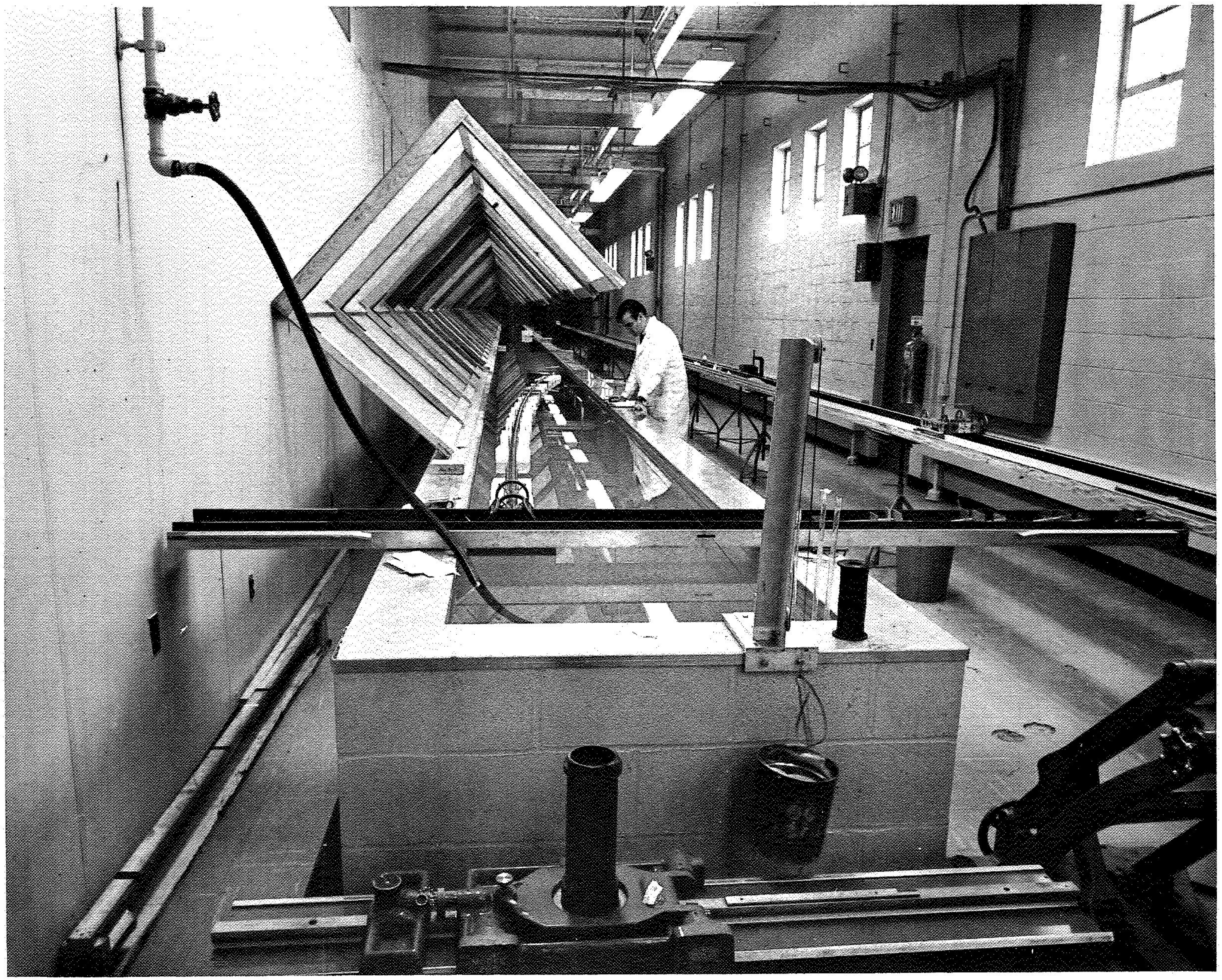

Figure E-3. Hunter STACER Stiffness Test Setup

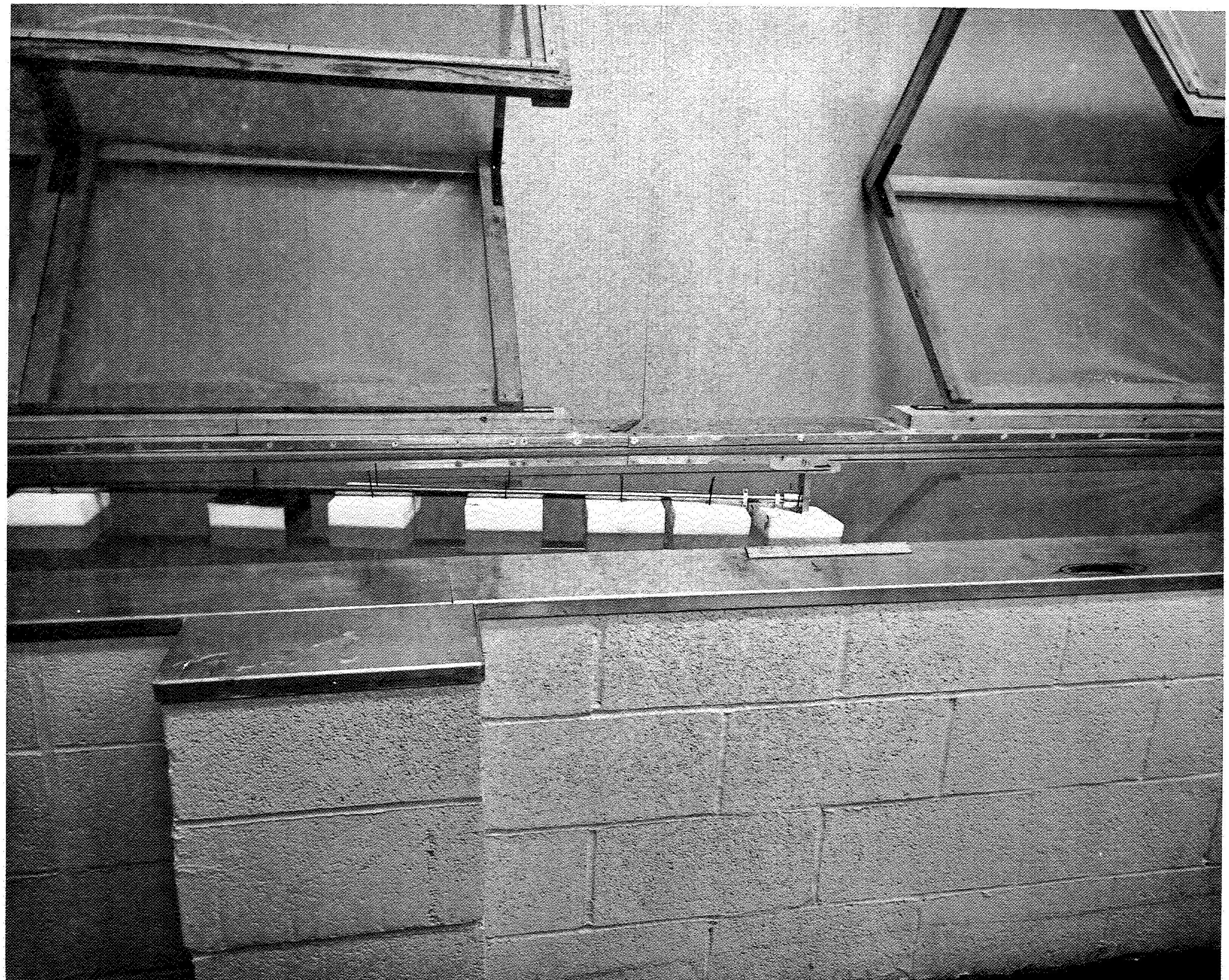

Figure E-4. Hunter STACER Tip Loading Arrangement

A least squares fit of the polynomial

$$y = a + bx + cx^2 + dx^3$$

to the deflection data was selected as the method for obtaining the elastic curve. Arguments that other functions would be better can be made, but the polynomial served the purpose. This has some justification in that the integration of the deflection equation for constant loads and cross sections yields a polynomial.

It would be convenient if the STACER member stiffness were uniquely determined by the cross section and material. However, because of the way the spirally wrapped tube reacts under loads, it is likely that the member stiffness is a function of local deformation, friction, loading history (hysterisis), and possible other factors.

Results

The polynomial curve fits and their associated statistics evaluating the fit are shown on Table E-3. Also shown is the member stiffness corresponding to these deflection curves.

Figures E-5 and E-6, show EI plotted versus length for the eight tests.

Figure E-7 shows the average stiffness obtained from the eight tests. Table E-4 lists the average stiffness EI at several locations along the members length along with the sample standard deviation. For purposes of comparison the stiffness (EI) of a constant thickness tapered tube of equivalent weight is shown on Figure E-7. In this case, a stainless steel tube with 1-3/4 inch and 5/8 inch root and tip diameters and 0.018 inch constant wall thickness will be equal in weight to the STACER rod tested.

Discussion of Results

For the magnitude of deflections measured, the curve fits shown in Table E-3 are reasonably good as illustrated by the mean and variance of the variable n. However, Figures E-5 and E-6 and Table E-4 show considerable variation in the resultant stiffness

Table E-3. Polynomial Curve Fit

Test	a (1×10^{-2})	b (1×10^{-3})	c (1×10^{-5})	d (1×10^{-7})	E (n)	var (n)	EI (x)
1	-4.731	1.964	7.456	2.317	0.1090	0.02030	$\frac{50.06}{2c + 6dx}$
2	-8.525	8.325	7.562	3.754	0.1475	0.02740	$\frac{75.09}{2c + 6dx}$
3	-7.203	3.867	16.952	2.002	0.0848	0.00286	$\frac{83.44}{2c + 6dx}$
4	-12.036	9.044	10.537	2.781	0.1116	0.01520	$\frac{61.19}{2c + 6dx}$
5	-6.587	7.975	5.606	2.478	0.1302	0.02030	$\frac{36.16}{2c + 6dx}$
6	-3.503	0.328	7.664	-0.369	0.0510	0.00238	$\frac{0.0975\,(298.6 - x)}{2c + 6dx}$
7	-1.717	5.959	1.055	0.158	0.0818	0.02190	$\frac{0.2075\,(298.6 - x)}{2c + 6dx}$
8	-8.516	6.974	23.609	-0.843	0.1512	0.02230	$\frac{0.3780\,(298.6 - x)}{2c + 6dx}$

$y = a + bx + cx^2 + dx^3$

$n = y_c - y_o$

y_o - measured deflection at 14 stations along the length

y_c - curve points at 14 stations along the length

$E(n)$ = Mean of $(y_c - y_o)$ for the 14 stations.

$var(n)$ = Variance of $(y_c - y_o)$

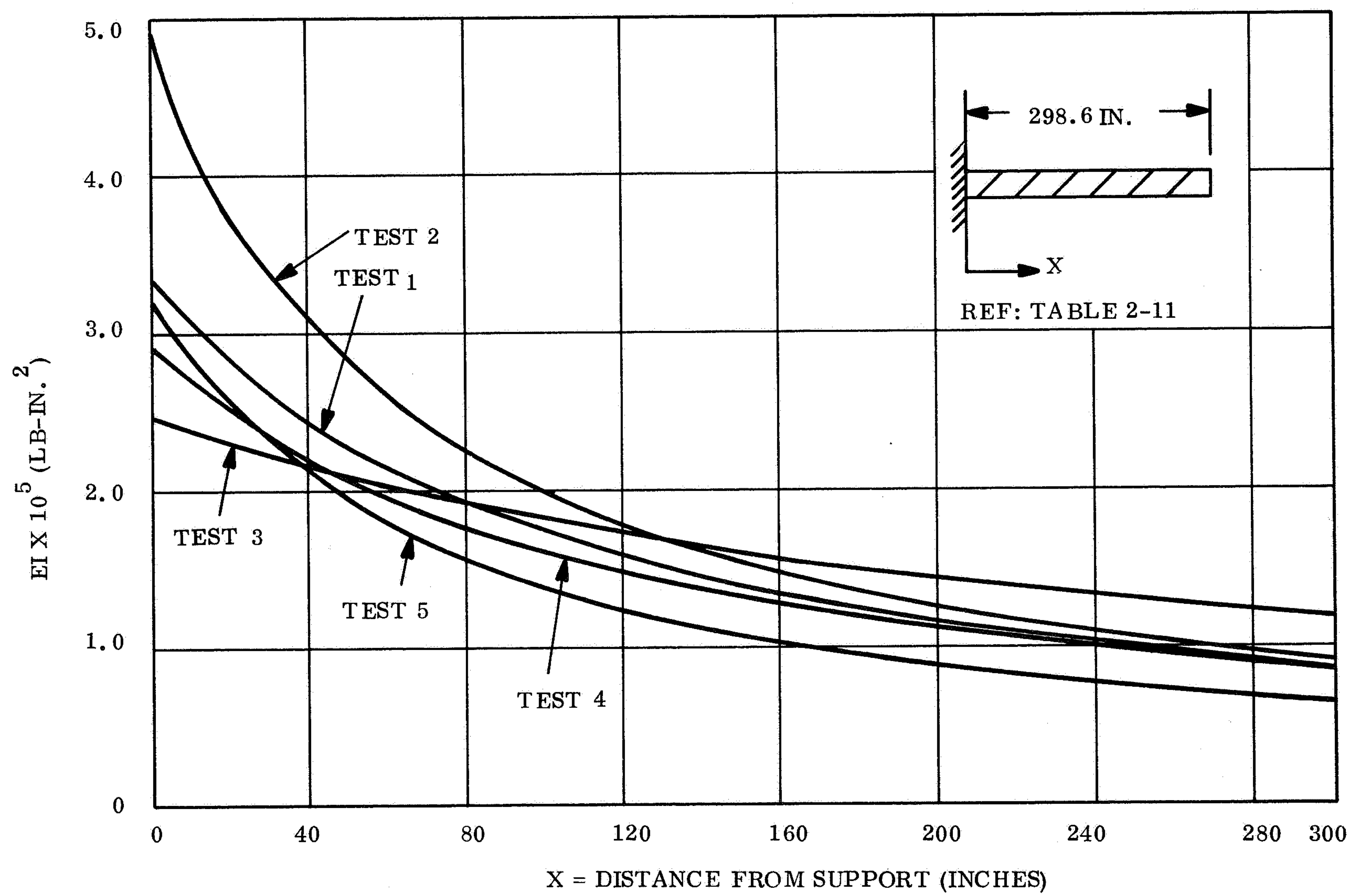

Figure E-5. Stiffness (EI) Versus Length (Tests 1 through 5)

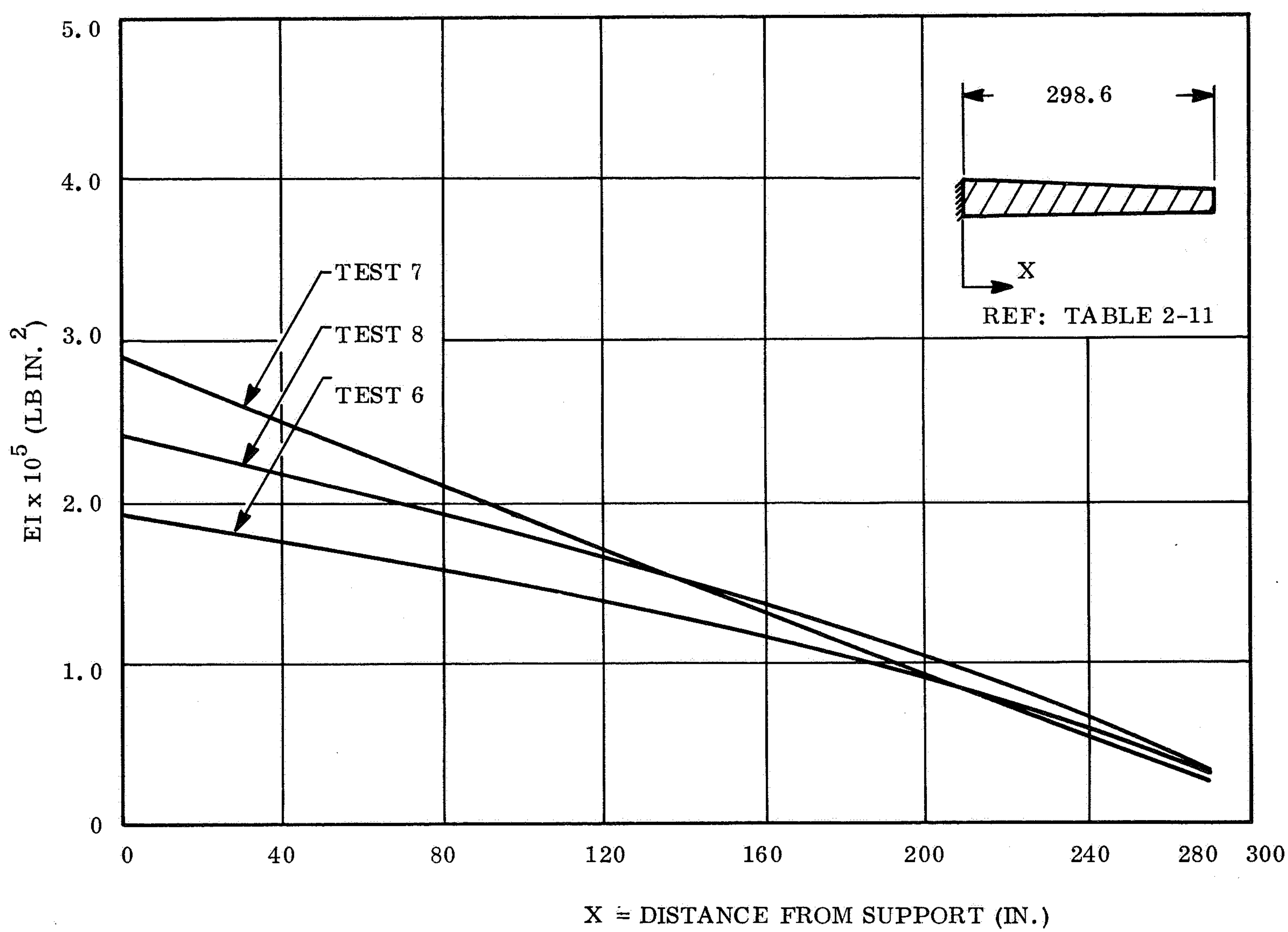

Figure E-6. Stiffness (EI) Versus Length (Tests 6 through 8)

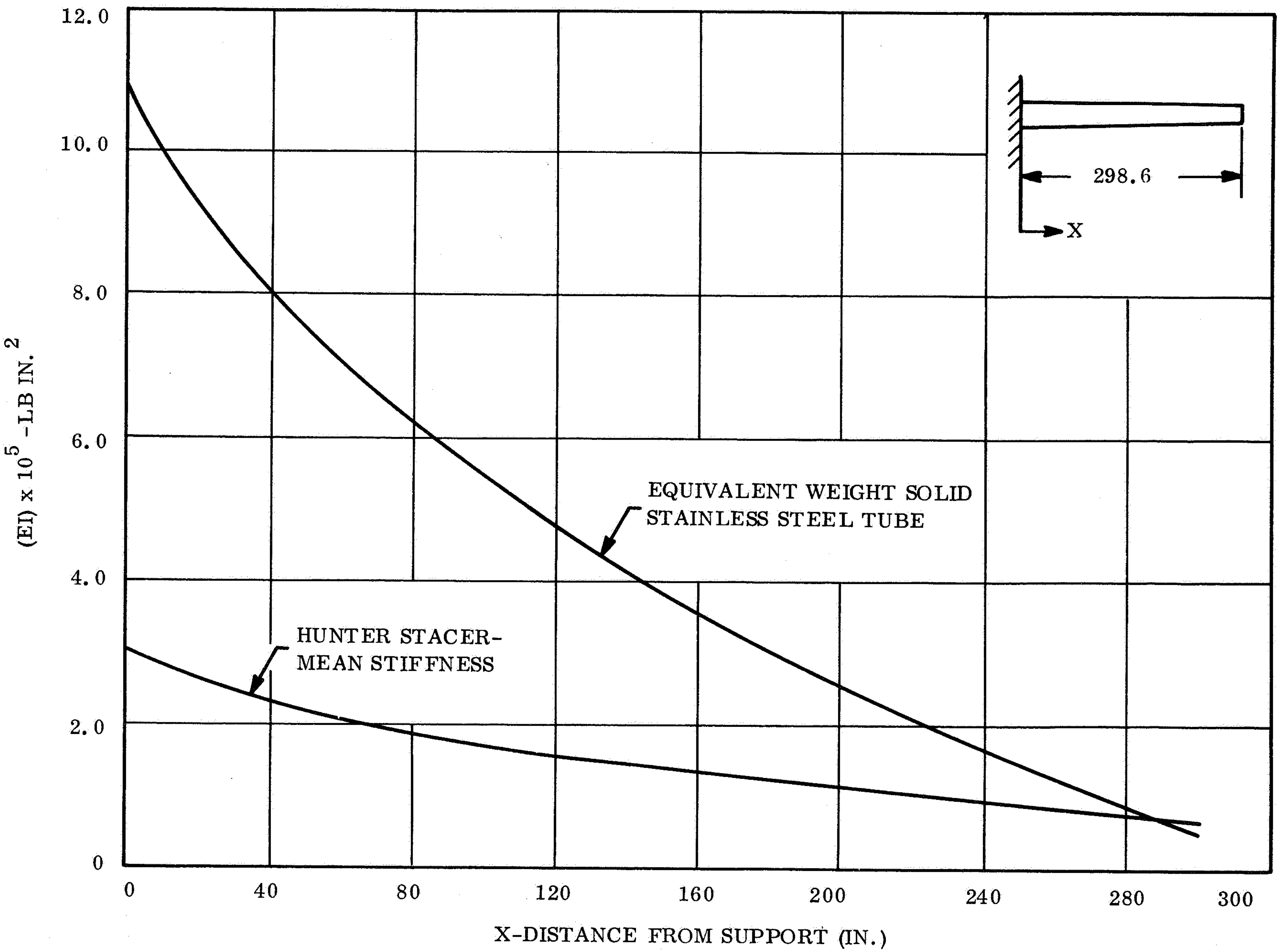

Figure E-7. Mean Stiffness (EI) Versus Length

Table E-4. Mean Stiffness and Standard Deviation

Station (in)	Mean Stiffness* (10^5 - lb-in^2)	Standard Deviation (10^5 - lb-in^2)
0	3.016	0.920
30	2.443	0.477
60	2.069	0.269
90	1.790	0.219
120	1.563	0.183
150	1.367	0.169
180	1.191	0.180
210	1.026	0.220
240	0.868	0.289
270	0.713	0.381

*All 8 tests included in mean.

for the rod. Part of this variation may be attributed to the inaccuracies made in making measurements of load and deflection. Some is probably due to the process of taking the second derivative. Thus, it is difficult from the amount of data taken, to separate experimental error from hysteresis and other effects. The mean stiffness for all tests is shown on Figure E-7.

There seems to be little difference in the results obtained when the member is loaded by lateral forces (Tests 6 to 8) as opposed to bending moments (Tests 1 to 5). Thus, the effects of shear force on the deflection for such a member loaded in this manner may be neglected as in any continuous member of similar dimensions and length.

Figure E-7 shows the stiffness (EI(x)) of an equal total weight stainless steel tapered tube of the same root and tip diameter as the STACER rod tested. The closed tube has greater stiffness at the root and approximately the same as the STACER at the tip. This result is consistent with the configuration of the rod because its tip has more overlap and interwrap friction. It should be noted, at this point, that the aforementioned equal weight closed tube is not necessarily the "equivalent structural tube" for purposes of comparison since its weight distribution has been arbitrarily chosen and as such might be dissimilar to a given STACER rod.

From Tests 4 and 5, it is also evident that this member exhibits hysteresis behavior. This might be expected for the STACER since its deflection under load depends to some extent upon friction between wraps of metal.

These data represent the only structural deflection data available for Hunter STACER rods. Though limited in scope, it provides a basis for structural analysis of this type rod. Caution should be used in applying these data to other STACER rod sizes since it is believed that local member stiffness is significantly affected by the helix angle, local friction, and numerous other effects.